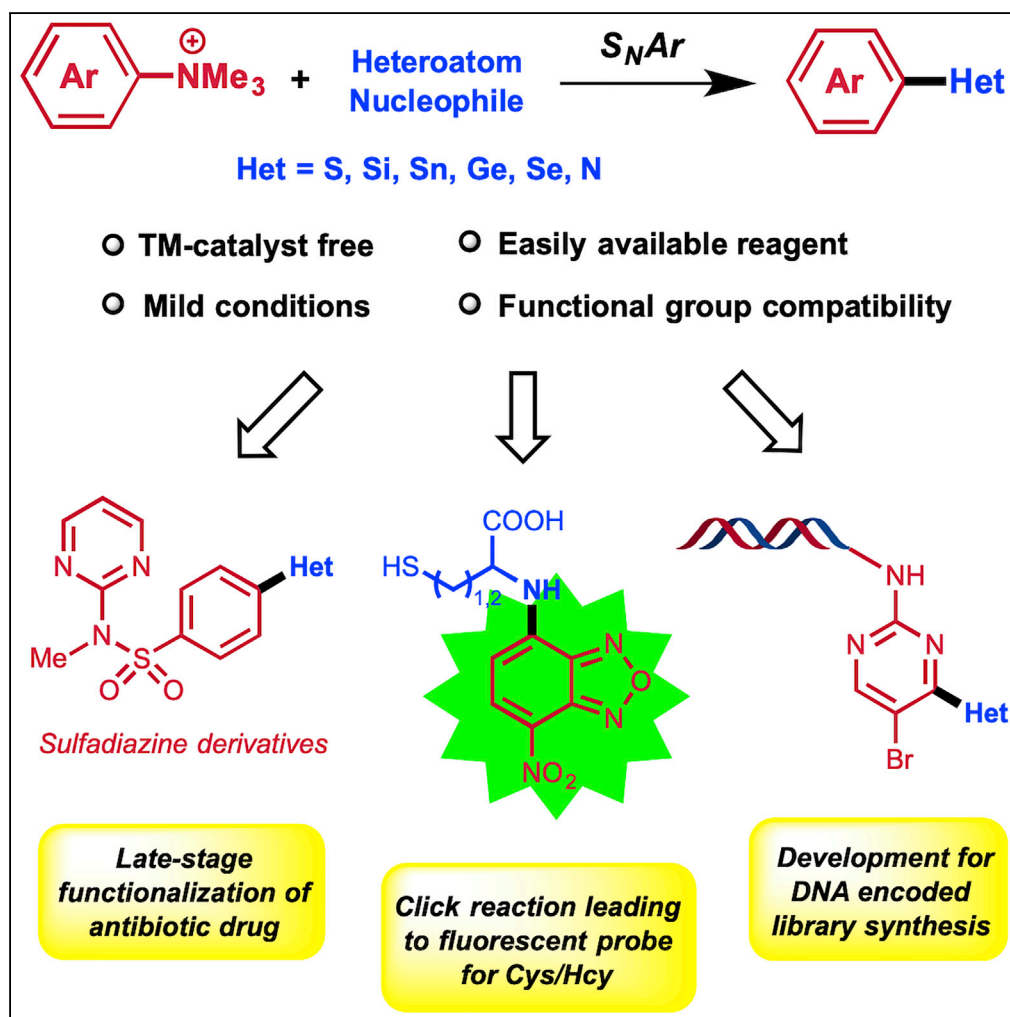


Article

Non-transition Metal-Mediated Diverse Aryl–Heteroatom Bond Formation of Arylammonium Salts



Dong-Yu Wang,
Xin Wen, Chao-
Dong Xiong, ...,
Masanobu
Uchiyama, Xiao-
Jie Lu, Ao Zhang

xjlu@simm.ac.cn (X.-J.L.)
aozhang@simm.ac.cn (A.Z.)

HIGHLIGHTS

An efficient approach to construct various C–heteroatom bonds

Readily accessible ammonium salts as substrates

No request of transition metal catalyst and broad functional group compatibility

Great applicability in late-stage functionalization, fluorescent probe, and DEL

Wang et al., iScience 15, 307–315
May 31, 2019 © 2019 The Author(s).
<https://doi.org/10.1016/j.isci.2019.04.038>



Article

Non-transition Metal-Mediated Diverse Aryl–Heteroatom Bond Formation of Arylammonium Salts

Dong-Yu Wang,¹ Xin Wen,^{1,2} Chao-Dong Xiong,^{1,2} Jian-Nan Zhao,^{1,3} Chun-Yong Ding,^{1,2} Qian Meng,¹ Hu Zhou,^{1,2} Chao Wang,^{4,5} Masanobu Uchiyama,^{4,5} Xiao-Jie Lu,^{1,2,*} and Ao Zhang^{1,2,3,6,*}

SUMMARY

Aryl–heteroatom (C–X) bonds ubiquitously exist in organic, medicinal, and material chemistry, but a universal method to construct diverse C–X bonds is lacking. Here we report our discovery of a convenient and efficient approach to construct various C–X bonds using arylammonium salts as the substrate via an S_NAr process. This strategy features mild reaction condition, no request of transition metal catalyst, and easy formation of various C–X bonds (C–S, C–Si, C–Sn, C–Ge, C–Se, C–N). The method was successfully applied to a late-stage functionalization of an existing antibiotic drug, to a Clickable reaction of NBD-based ammonium salt as turn-on fluorescent probe to recognize L-cysteine and homocysteine, and to the synthesis of a DNA encoded library (DEL) bearing different C–X bonds.

INTRODUCTION

Aryl carbon-heteroatom (C–X) bonds are prevalent in natural and unnatural organic molecules with ample capacities. Some common C–X bonds such as C–O, C–S (Feng et al., 2016), C–N (Ruiz-Castillo and Buchwald, 2016), and C–Si (Franz and Wilson, 2013) bonds are widely embedded in many organic intermediates and therapeutic drugs, whereas the relatively less common C–X bonds such as C–Se (Mugesh et al., 2001), C–Sn (Cordovilla et al., 2015), and C–Ge (Nakamura et al., 2002) bonds generally serve as synthetic precursors for many pharmaceuticals, organic materials, and polymers. In recent years, numerous synthetic methods for C–X bond formations have been developed (Jones et al., 2018; Shen et al., 2014; Liu et al., 2017; Wang et al., 2018a; Hartwig, 2008; Surry and Buchwald, 2008; Bariwal and Van der Eycken, 2013; Cheng and Hartwig, 2015; Zarate and Martin, 2014; Taniguchi and Onami, 2004; Shu et al., 2016; Yoshida, 2016; Gu and Martín, 2017; Komami et al., 2018). Normally, these aryl C–X bonds were formed starting from the same substrate aryl (pseudo)halides through cross-couplings with appropriate heteroatom nucleophiles under transition-metal (TM) catalysis (Scheme 1). However, these methods suffer from limited applications because of several drawbacks, including the additional steps necessary to presynthesize aryl halides, harsh reaction conditions, costive metal catalysts that are either toxic or difficult to remove, especially in the pharmaceutical industry (Wu et al., 2012; Chan et al., 2013). Therefore, it is highly desired to invent a universal method to construct diverse C–X bonds starting from a same substrate (Li et al., 2017; Xu et al., 2016). Ideally, this method should feature (1) using a ubiquitous readily available substrate; (2) wide scope to form various C–X bonds; (3) no TM catalyst needed.

Anilines are one of the most prevalent naturally abundant or readily synthetic accessible reagents in organic synthesis. Therefore, use of anilines, instead of aryl halides, as substrates to undergo the cross-coupling has long been a synthetic aspiration, but only with limited success (Ouyang et al., 2015; Li et al., 2014; Xu et al., 2017), owing to the high inertness of the C–N bond and the high reactivity of the NH₂ group itself. Fortunately, conversion of anilines to the arylammonium species has been reported to enable the TM-catalyzed cross-couplings with appropriate partners (Wenkert et al., 1988; Blakey and MacMillan, 2003; Xie and Wang, 2011; Wang et al., 2016; Zhang et al., 2015; Zhang and Wang, 2014). However, transformations of arylammonium salts through an S_NAr mechanism in the absence of TM catalyst are rare. Limited examples include the fluorination of ammonium salts (Irie et al., 1982) to radiolabel bio-active molecules for positron-emission tomography imaging and the formation of aryl ethers via C–N bond cleavage in the absence of TM catalyst (Wang et al., 2018b). Inspired by these work, we herein describe a universal method to access diverse aryl–heteroatom, especially those uncommon C–Sn/C–Ge/C–Se bonds using aryl ammonium salts as the ubiquitous substrate under mild reaction conditions.

¹CAS Key Laboratory of Receptor Research and the State Key Laboratory of Drug Research, Shanghai Institute of Materia Medica (SIMM), Chinese Academy of Sciences, Shanghai 201203, China

²University of Chinese Academy of Sciences, Beijing 100049, China

³School of Life Science and Technology, ShanghaiTech University, Shanghai 201210, China

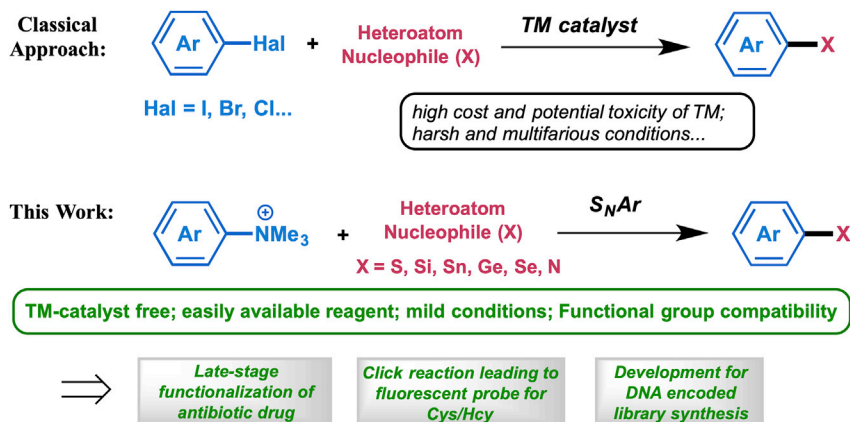
⁴Graduate School of Pharmaceutical Sciences, The University of Tokyo, 7-3-1 Hongo, Bunkyo-ku, Tokyo-to 113-0033, Japan

⁵Cluster of Pioneering Research (CPR), Advanced Elements Chemistry Laboratory, RIKEN, 2-1 Hirosawa, Wako-shi, Saitama 351-0198, Japan

⁶Lead Contact

*Correspondence:
xjlu@simm.ac.cn (X.-J.L.),
aozhang@simm.ac.cn (A.Z.)
<https://doi.org/10.1016/j.isci.2019.04.038>





Scheme 1. Strategies for Diverse Aryl-heteroatom Bond Formation

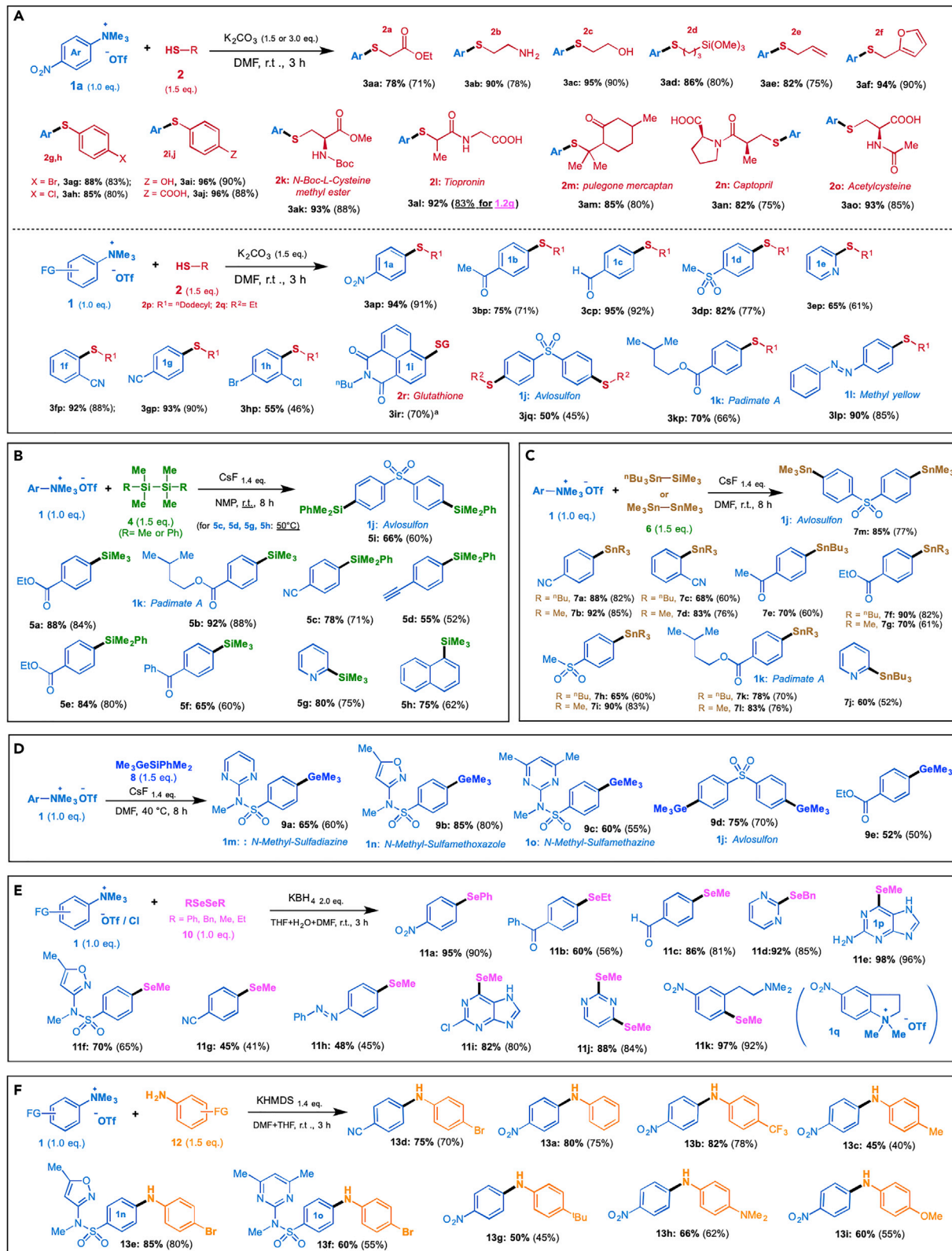
RESULTS AND DISCUSSION

C–X Bond Formation

TM-catalyzed thiolation of aryl halides typically requires the strong base to generate thiolates from thiols and a high temperature or specially designed ligands to avoid the deactivation of TM catalyst by the strong coordination of the thiolates (Feng et al., 2016; Hartwig, 2008). Herein, we report the first example of conversion of aryltrimethylammonium salts to aryl thioethers in the presence of a weak base under room temperature, without the need for any TM catalyst and ligand. In the beginning, we chose the reaction of 4-cyanophenyltrimethylammonium salt with 1-dodecanethiol as the model reaction and optimized the substitution conditions in the absence of TM catalyst (for details, see Table S1). It was found that the best result was obtained by using TfO^- as the counter anion of **1** in DMF with K_2CO_3 as base at room temperature in 3 h without the need of argon protection. We next focused on the synthetic scope and functional group compatibility of the reaction (Scheme 2A). Thiols bearing an ester (**2a**), free amino (**2b**), hydroxyl (**2c, i**), silyl (**2d**), allyl (**2e**), furyl (**2f**), halogen (**2g, h**), or carboxylic (**2j**) group, as well as the sterically congested tertiary thiol (**2m**), were found to proceed the reaction without difficulty, generating the desired thioetheric products in 71%–90% isolated yields. To further evaluate the synthetic applicability of this protocol, we examined reactions of **1a** with several biologically active molecules or their derivatives containing an -SH moiety (**2k–o**). All the reactions occurred smoothly affording corresponding C–S bond-containing products **3ak–3ao** in 75%–88% yields. To illustrate the scalable potential of this method, we conducted the reaction of *Tiopronin* (antidote) derivative **2l** with **1a** on a gram scale, and the product **3al** was obtained in 83% yield after a simple workup procedure.

Meanwhile, the functional group tolerance on the aryl trimethylammonium triflate was also investigated (Scheme 2A). It was found that aryl ammonium salts **1** bearing acyl (**1b**), formyl (**1c**), sulfonyl (**1d**), cyano (**1f, 1g**), halogen (**1h**), ester (**1k**), and heterocycle (**1e**) group reacted without difficulty, providing corresponding C–S bond products in up to 92% yields. It is worth highlighting that ammonium salts **1j–l** derived from the antibiotic drug *Avlosulfon*, sunscreen lotion *Padimate A*, and *Methyl Yellow*, respectively, took part in the C–S bond formation as well to afford the thioetheric products, suggesting the potential use of this reaction in the late-stage functionalization of existing drugs. Interestingly, the tricyclic substrate **1i** prepared from naphthalimide, a well-known fluorophore, was found to readily react with glutathione, providing the corresponding C–S bond product **3ir** in 70% yield. In view of the strong internal charge transfer character of naphthalimides (Zhou et al., 2016) and involvement of glutathione in many biological processes, the current C–S bonding formation process might be used as a biomarker *in vivo*.

Since the C–Si/Sn/Ge bonds belong to the same group in the periodic table of elements, they are widely used in drug design as a bioisosteric replacement of C–C bond or as a precursor for further transformation. Traditional methods to generate Ar–Si/Ge/Sn involved the reaction of Si/Ge/Sn electrophiles with air-sensitive organometallic reagents, alternatively TM-catalyzed C–Si/Ge/Sn coupling reactions at high temperature (McNeill et al., 2007; Komami et al., 2018; Corcoran et al., 2012). We, herein, report an unprecedented silylation, germylation, and stannylation of various ammonium salts via the S_NAr process with stable substrates at low temperature without the need of TM-catalyst. First, we examined the feasibility of C–Si/Sn/Ge bond formation by simply



Scheme 2. Substrate Scope Investigation

(A) Thioesterification reactions. K_2CO_3 : 1.5 eq. (for **2i**, **2j**, **2l**, **2n**, **2o**: 3.0 eq.). ^aFor **3ir**, a mixture of DMF and H_2O was used as the solvent.
(B) Silylation reactions; (C) Stannylation reactions; (D) Germylation reactions; (E) Selenation reactions; (F) Amination reactions. For **11d**, **11e**, **11i** and **11j**, Cl^- was used as the counter anion of **1**. Yields were calculated based on NMR (**bolt**) and isolation (in parentheses).
See also Figures S1–S6.

treating arylammonium salts with appropriate heteroatom nucleophiles. A quick survey of the reaction conditions (for details, see Tables S2 and S3) suggested that the optimum conditions for C–Si/Sn/Ge bond formation are to use CsF as the base, NMP/DMF as the solvent, at room temperature (r.t.) within 8 h. With this result in hand, a small series of arylammonium salts were used to explore the substrate scope. As shown in Scheme 2B–2D, arylammonium salts bearing an ester (**5a**, **5e**, **7f**, **7g**, **9e**), acetylene (**5d**), acyl (**5f**, **7e**), pyridyl (**5g**, **7j**), sulfonyl (**7h**, **7i**), or cyano (**5c**, **7a–d**) substituent went through the reaction very well providing the corresponding C–Si/Sn/Ge bond products in moderate to high yields. Interestingly, 1-naphthyl ammonium salt lacking an electron-withdrawing substituent also participated in the reaction nicely yielding compound **5h** in 75% yield. Padimate A derivatives (**5b**, **7k**, **7l**), Sulfonamides derivatives (**9a–9c**), and the dual functionalized derivatives of the antibiotic drug Avlosulfon (**5i**, **7m**, **9d**) were also easily prepared in moderate to high yields.

Organoselenium compounds have gained more and more interests recently; however, methods to construct C–Se bond are rather limited. To explore the potential of our current method using arylammonium salts to build up C–Se bond, we used RSeSeR ($R = Ph$, Bn , Me , Et) as the selenation source and KBH_4 as the base (for optimization details, see Table S4). As shown in Scheme 2E, arylammonium salts containing a nitro, acyl, formyl, cyano, sulfonyl substituent and purine/pyrimidine derivatives were tolerant in the reaction conditions yielding corresponding C–Se products **11a–j** in up to 96% yields. Meanwhile, the cyclic ammonium salts **1q** prepared from indoline derivative was also suitable substrate, affording the ring-opened product **11k** in 92% yield.

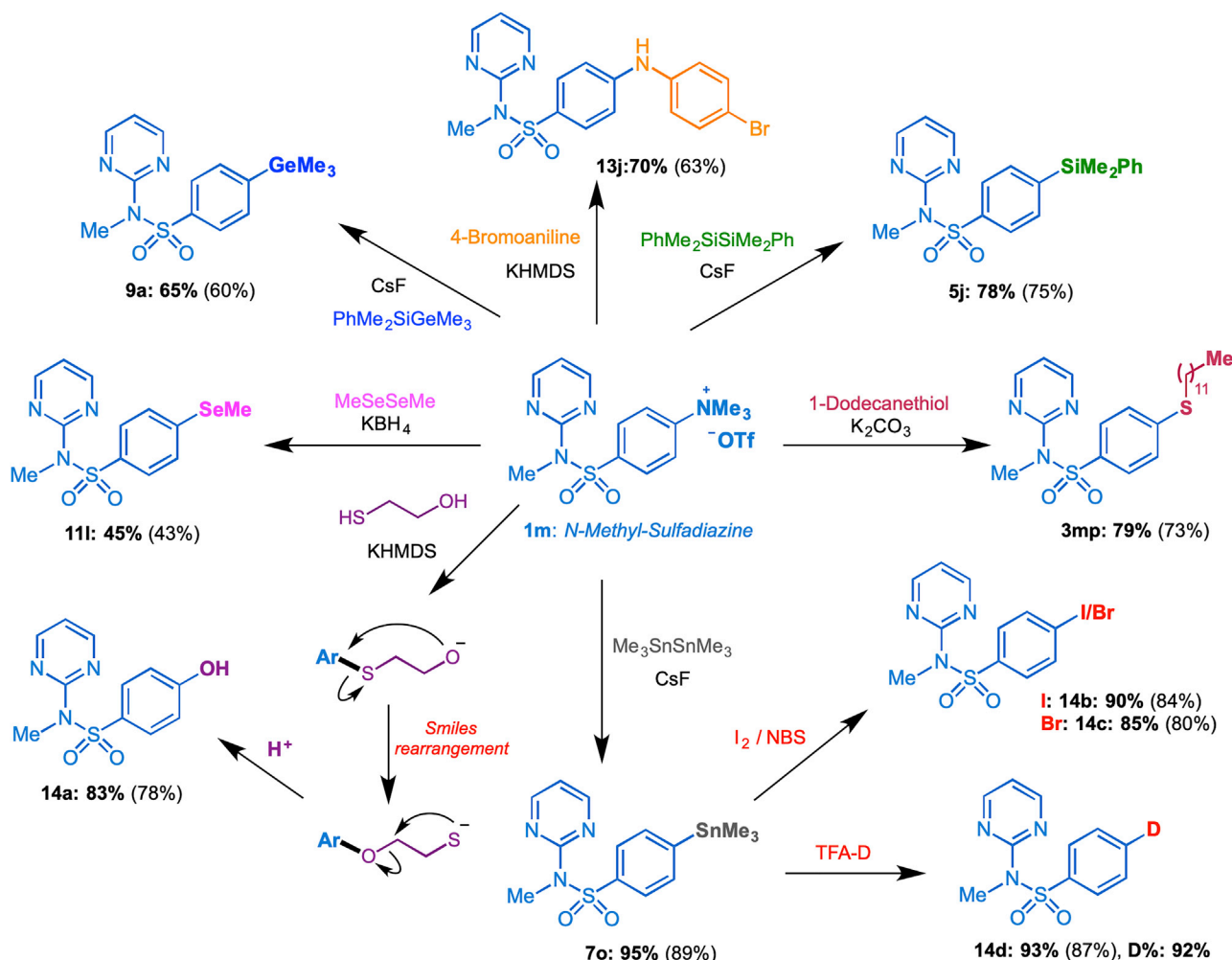
Finally, we decided to explore the feasibility of constructing C–N bond under our S_NAr substitution protocol without the TM-involved catalysis. With this optimized reaction condition in hand (for details, Table S5), we tested the substrate scope by using various arylammonium salts and differently substituted anilines. As shown in Scheme 2F, arylammonium salts with an aminosulfonyl, nitro, or cyano substituent were well tolerant, and the corresponding diaryl amines were obtained in moderate to high yields. Anilines bearing either electron-donating or electron-withdrawing substituents are suitable nucleophiles.

Late-Stage Functionalization of Biologically Active Compounds

To evaluate the utility of our current protocol in the construction of diverse C–X bonds, we conducted a late-stage diversification of the antibiotic drug *Sulfadiazine*. As shown in Scheme 3, *Sulfadiazine* was first converted to the ammonium salt **1m**, which was then subjected to the corresponding C–X bond formation reactions. A small library of sulfadiazine analogues bearing a new C–S (**3mp**), C–Se (**11h**), C–Sn (**7o**), C–Si (**5j**), C–Ge (**9a**), and C–N (**13h**) was conveniently established in moderate to good yields. Interestingly, phenol **14a** bearing a new C–O(H) bond was obtained by treating **1m** with 2-mercptoethan-1-ol in the presence of KHMDS as the base. Likely, a Smiles rearrangement of the initially formed aryl thioether to the aryl ether, followed by elimination of thiirane was involved in the transformation (Boschi et al., 2001). All these products can be used as key intermediates for further functional group transformation. For example, treatment of aryltrimethyltin derivative **7o** with iodine, NBS, or deuterated trifluoroacetic acid provided corresponding iodo-, bromo-, or deuterated derivatives **14b–d** in 80%–87% yields.

Clickable Synthesis of Fluorescent Probes from NBD-Ammonium Salt with Biological Thiols

7-Nitrobenz-2-oxa-1,3-diazole (NBD) moiety has been widely used as a fluorophore in many fluorescent chemosensors because of its emission at longer wavelengths and good cell permeability (Uchiyama et al., 2001). To explore the application of our C–X bond formation protocol, we first prepared C4-ammonium NBD **1r** and tested its sensitivity to various biological thiols, including small-molecule L-cysteine (**Cys**, **2v**), homocysteine (**Hcy**, **2w**), glutathione (**2r**), coenzyme A (**2s**), cyclopeptide (**2t**), as well as bio-macromolecule antibody β -Lactoglobulin (**2u**). As shown in Scheme 4A, all the reactions proceeded very well just by “Clicking” the ammonium salt **1r** with an appropriate thiol in water at r.t. for 20 min, providing corresponding products in moderate to high yields. Notably, the reactions with complex thiols **2r–2u** afforded the expected C–S bond products, whereas reactions with simple thiols **2v–w** gave products bearing a C–N bond. The production of **15e** and **15f** is likely formed through Smiles rearrangement that converted

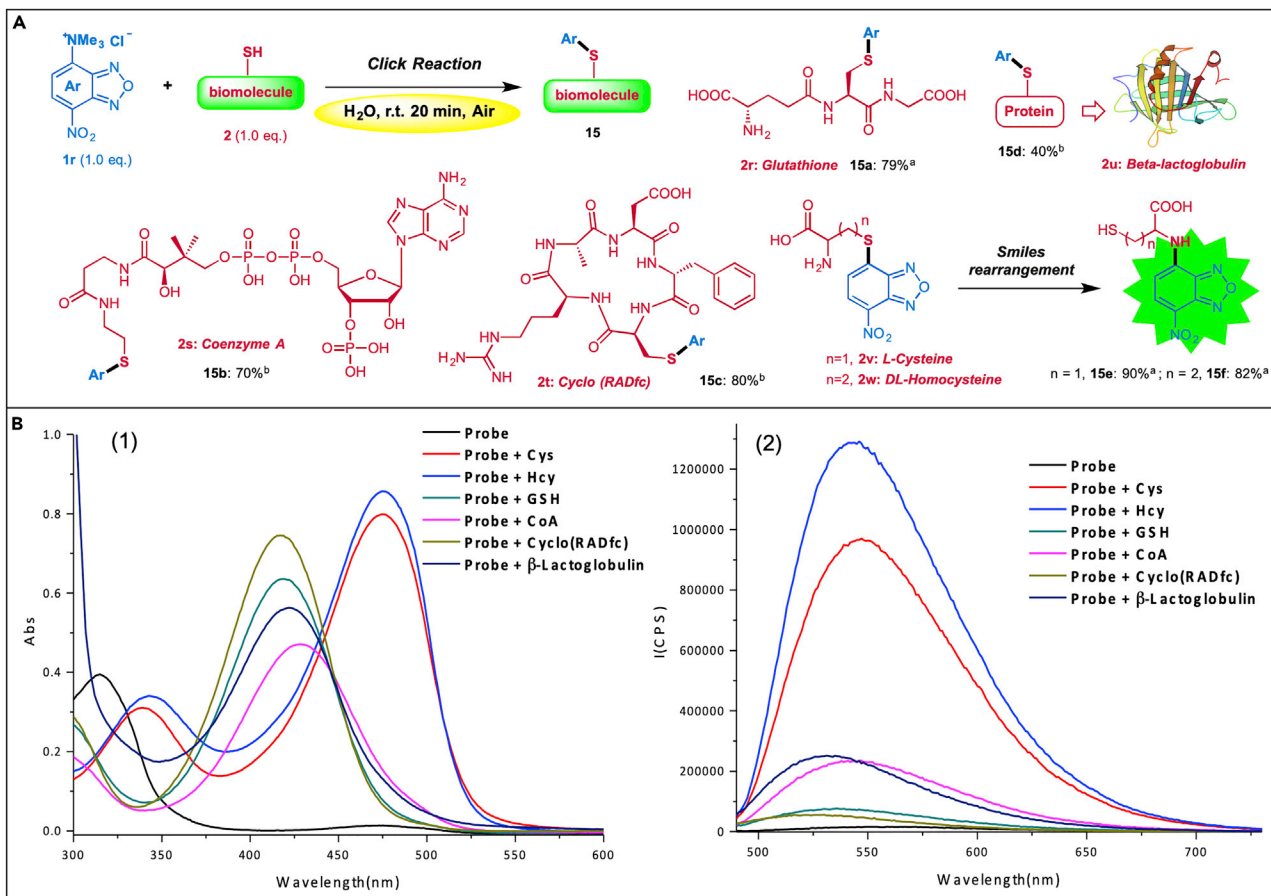


Scheme 3. Late-stage Functionalization of the Antibiotic Drug Sulfadiazine

the initial C–S bond products to the *N*-substituted NBDs. This rearrangement has been further verified by spectroscopic comparison (Wood et al., 2003) (see Figures S7 and S8). In general, the *N*-substituted NBDs have longer-wavelength absorption and stronger fluorescence than the corresponding S-substituted ones (Chen et al., 2016); we then tested the fluorescent properties of these NBD compounds. The absorption and fluorescence emission responses (Scheme 4B) showed that probe 1r was non-fluorescent, whereas treatment of 1r with simple thiols Cys/Hcy induced a dramatic increase of fluorescence intensity at 550 nm. Treatment of 1r with complex thiols 2r, 2s, or 2t showed an absorption maximum at 419, 427, and 417 nm, respectively, and no significant fluorescence response was observed. These results indicated that our NBD probe 1r could specifically recognize and discriminate Cys/Hcy over other more complex bioactive thiols. Since Cys/Hcy play critically important roles in maintaining redox homeostasis in physiological processes (Wood et al., 2003), our NBD-ammonium salt probe and the readily clickable reaction conditions may find use in monitoring biological process *in vivo*.

On-DNA Reaction Development for DNA Encoded Library Synthesis

DNA-encoded library (DEL) is a powerful tool for hit identification in small molecule drug discovery (Goodnow et al., 2017; Mullard, 2016; Buller et al., 2010), and several compounds derived from their original DEL hits have progressed to clinical development (Belyanskaya et al., 2017). The chemical diversity of DEL library is the key to successful discovery of drug-like molecules but is often limited to DNA compatible synthetic reactions (Wang et al., 2014; Satz et al., 2015; Li et al., 2016). Since our C–X bond formation protocol proceeded in mild reaction conditions, it is ideal to be used for the DEL synthesis. 2,4-Dichloropyrimidine



Scheme 4. Clickable Synthesis of Turn-on Fluorescent Probe

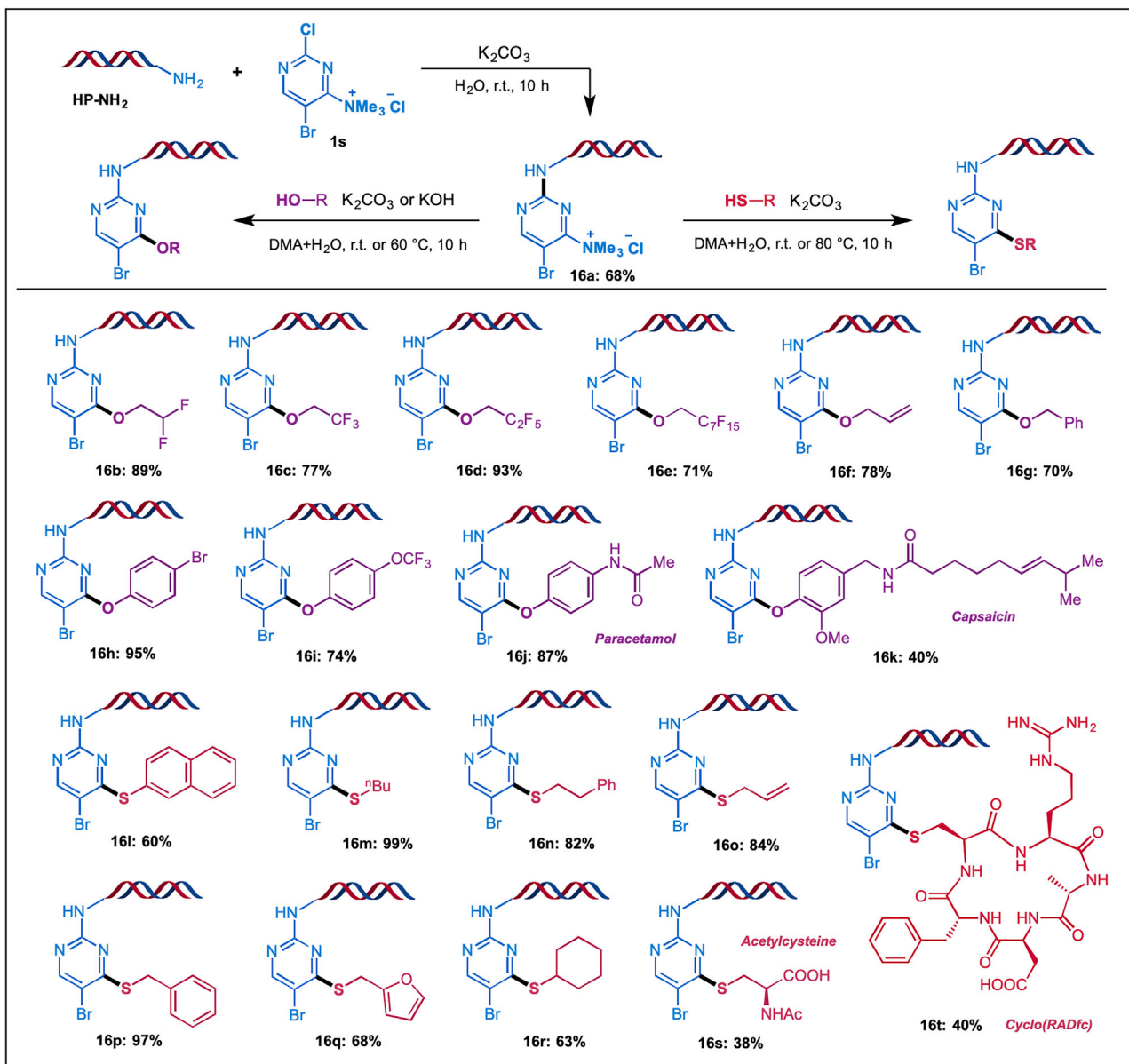
(A) Clickable thioetherification of NBD-ammonium salts with various biological thiols. ^aNMR yield; ^bliquid chromatography-mass spectrometry conversion. (B) Absorption (1) and fluorescence (2) spectra of probe **1r** (50 μM) before (black curve) and after addition of 250 μM Cys (red), Hcy (blue), GSH (green), Coenzyme A (pink), cyclopeptide (brown), and β -Lactoglobulin (purple), respectively, incubated for 30 min in H_2O at 25°C. Excitation wavelength: 480nm. See also Figure S7.

derivatives, a widely used core structure of kinase inhibitors, could be used as valuable building blocks (BB) in the DNA encoded library synthesis (Ding et al., 2016). $\text{S}_{\text{N}}\text{Ar}$ reaction of DNA headpiece (HP, Figure S9) with excessive 2,4-dichloropyrimidine derivatives routinely provides C-4 DNA-conjugated pyrimidine in high regioselectivity (Satz et al., 2015).

In contrast, we developed a novel ammonium building block (**1s**), which could be reacted with HP to give C-2 DNA-conjugated pyrimidine (**16a**) selectively (Scheme 5). By following our protocol, the corresponding C-O/S bond formations occurred smoothly in dilute conditions and provided DNA-conjugated pyrimidines **16b-t** bearing various functional groups (Scheme 5). Several biologically active molecules as well as fluorine-containing functional groups could also be introduced. Alcohol BBs are quite challenging for on-DNA reactions, but our new on-DNA reaction could tolerate a series of alcohol BBs, which significantly increases the diversity of DEL. It is noteworthy that the Br moiety in pyrimidine scaffold might be used for further functionalization through cross-coupling reactions (Ding and Clark, 2015) to provide a more complex compound library with ample chemical diversity. Such novel chemical selectivity brought by **1s** enables the design and synthesis of different types of DNA encoded pyrimidine library that is currently under development for library synthesis.

Conclusion

In summary, we have established a convenient and efficient approach to construct diverse aryl–heteroatom bonds using arylammonium salts as the common substrates via a $\text{S}_{\text{N}}\text{Ar}$ process. This strategy features mild reaction condition, no request of transition metal catalyst, and wide scope for various C-X bonds, especially

**Scheme 5. On-DNA Reaction Development.**

Reactions were carried out in dilute conditions (1 mM). Conversion determined by liquid chromatography-mass spectrometry. See also Figure S10.

those uncommon C–Sn/C–Ge/C–Se formation. The application of this method was exemplified by a late-stage functionalization of an existing antibiotic drug and by a Clickable reaction using NBD-based ammonium salt as a turn-on fluorescent probe for Cys and Hcy. Meanwhile, on-DNA reaction development for DEL was also successfully realized starting from a pyrimidinylammonium salt.

Limitation of Study

Ammonium salts derived from electron-rich anilines (e.g., *p*-R-C₆H₄-NMe₃⁺, R = Me, MeO) showed poor or no reactivity toward heteroatom nucleophiles. Silylation product with acetyl group could not be obtained probably due to the strong basicity of silyl anions.

METHODS

All methods can be found in the accompanying [Transparent Methods supplemental file](#).

SUPPLEMENTAL INFORMATION

Supplemental Information can be found online at <https://doi.org/10.1016/j.isci.2019.04.038>.

ACKNOWLEDGMENTS

This work was supported by grants (to A. Zhang, X.-J. Lu, and D.-Y. Wang.) from the National Natural Science Foundation of China (81773565, 21702216, 21877117, 81430080), the National Program on Key Basic Research Project (973 Program) of China (2015CB910603), the International Cooperative Program (GJHZ1622) and the Key Program of Frontier Science (160621) of the Chinese Academy of Sciences, the Shanghai Commission of Science and Technology (16XD1404600, 14431905300, 14431900400, 18431907100). X.-J. Lu and D.-Y. Wang gratefully acknowledges the support of National Science & Technology Major Project "Key New Drug Creation and Manufacturing Program" China (No. 2018ZX09711002-005, No. 2018ZX09711002-006-003), Sanofi-SIBS 2017 Post-doctoral Fellowship, and China Postdoctoral Science Foundation (2017M621566, 2018T110416). This work was also supported by JSPS Grant-in-Aid for Scientific Research, Japan: No. 17H05430 (to M. Uchiyama), No. 17H06173 (to M. Uchiyama), and No. 18K06544 (to C. Wang).

AUTHOR CONTRIBUTIONS

D.-Y.W. planned, carried out most of experiments, analyzed, and summarized the experiments. X.W. performed the DEL experiment. J.-N.Z., C.-D.X., and C.-Y.D. participated in the experiments or discussions. Q.M. and H.Z. performed biological thiols analysis. C.W. and M.U. conceived and designed the project. X.-J.L. directed the study on DNA encoded library synthesis. A.Z. supervised the whole research and wrote the manuscript with feedback from all authors.

DECLARATION OF INTERESTS

The authors declare no competing interests.

Received: February 18, 2019

Revised: April 1, 2019

Accepted: April 29, 2019

Published: May 31, 2019

REFERENCES

- Bariwal, J., and Van der Eycken, E. (2013). C–N bond forming cross-coupling reactions: an overview. *Chem. Soc. Rev.* 42, 9283.
- Belyanskaya, S.L., Ding, Y., Callahan, J.F., Lazaar, A.L., and Israel, D.I. (2017). Discovering drugs with DNA-encoded library technology: from concept to clinic with an inhibitor of soluble epoxide hydrolase. *ChemBioChem* 18, 837–842.
- Blakey, S.B., and MacMillan, D.W.C. (2003). The first Suzuki cross-couplings of aryltrimethylammonium salts. *J. Am. Chem. Soc.* 125, 6046–6047.
- Boschi, D., Sorba, G., Bertinaria, M., Fruttero, R., Calvino, R., and Gasco, A. (2001). Unsymmetrically substituted furoxans. Part 18.1 Smiles rearrangement in furoxan systems and in related furazans. *J. Chem. Soc. Perkin Trans. 1*, 1751–1757.
- Buller, F., Mannocci, L., Scheuermann, J., and Neri, D. (2010). Drug discovery with DNA-encoded chemical libraries. *Bioconjug. Chem.* 21, 1571–1580.
- Chan, T.L., Wu, Y., Choy, P.Y., and Kwong, F.Y. (2013). A radical process towards the development of transition-metal-free aromatic carbon–carbon bond-forming reactions. *Chem. Eur. J.* 19, 15802–15814.
- Chen, W., Luo, H., Liu, X., Foley, J., and Song, X. (2016). Broadly applicable strategy for the fluorescence based detection and differentiation of glutathione and cysteine/homocysteine: demonstration *in vitro* and *in vivo*. *Anal. Chem.* 88, 3638–3646.
- Cheng, C., and Hartwig, J.F. (2015). Catalytic silylation of unactivated C–H bonds. *Chem. Rev.* 115, 8946–8975.
- Corcoran, E.B., Williams, A.B., and Hanson, R.N. (2012). A synthetic method for palladium-catalyzed stannylation at the 5- and 6-benzo positions of indoles. *Org. Lett.* 14, 4630–4633.
- Cordova, C., Bartolomé, C., Martínez-Illarduya, J.M., and Espinet, P. (2015). The Stille reaction, 38 years later. *ACS Catal.* 5, 3040–3053.
- Ding, Y., and Clark, M.A. (2015). Robust Suzuki–Miyaura cross-coupling on DNA-linked substrates. *ACS Comb. Sci.* 17, 1–4.
- Ding, Y., DeLorey, J.L., and Clark, M.A. (2016). Novel catalyst system for Suzuki–Miyaura coupling of challenging DNA-linked aryl chlorides. *Bioconjug. Chem.* 27, 2597–2600.
- Feng, M., Tang, B., Liang, S., and Jiang, X. (2016). Sulfur containing scaffolds in drugs: synthesis and application in medicinal chemistry. *Curr. Top. Med. Chem.* 16, 1200–1216.
- Franz, A.K., and Wilson, S.O. (2013). Organosilicon molecules with medicinal applications. *J. Med. Chem.* 56, 388–405.
- Goodnow, R.A., Jr., Dumelin, C.E., and Keefe, A.D. (2017). DNA-encoded chemistry: enabling the deeper sampling of chemical space. *Nat. Rev. Drug Discov.* 16, 131–147.
- Gu, Y., and Martín, R. (2017). Ni-catalyzed stannylation of aryl esters via C–O Bond cleavage. *Angew. Chem. Int. Ed.* 56, 3187–3190.
- Hartwig, J.F. (2008). Evolution of a fourth generation catalyst for the amination and thioetherification of aryl halides. *Acc. Chem. Res.* 41, 1534–1544.
- Irie, T., Fukushi, K., Inoue, O., Yamasaki, T., Ido, T., and Nozaki, T. (1982). Preparation of 18F-labeled 6- and 2-fluoro-9-benzylpurine as a potential brain-scanning agent. *Int. J. Appl. Radiat. Isot.* 33, 633–636.

- Jones, K.D., Power, D.J., Bierer, D., Gericke, K.M., and Stewart, S.G. (2018). Nickel phosphite/phosphine-catalyzed C–S cross-coupling of aryl chlorides and thiols. *Org. Lett.* 20, 208–211.
- Komami, N., Matsuoka, K., Yoshino, T., and Matsunaga, S. (2018). Palladium-catalyzed arylation of aryl bromides and aryl triflates using hexamethyldigermane. *Synthesis* 50, 2067–2075.
- Li, Q., Zhang, S.-Y., He, G., Ai, Z., Nack, W.A., and Chen, G. (2014). Copper-catalyzed carboxamide-directed ortho amination of anilines with alkylamines at room temperature. *Org. Lett.* 16, 1764–1767.
- Li, Y., Gabriele, E., Samain, F., Favalli, N., Sladojević, F., Scheuermann, J., and Neri, D. (2016). Optimized reaction conditions for amide bond formation in DNA-encoded combinatorial libraries. *ACS Comb. Sci.* 18, 438–443.
- Li, J.-M., Wang, Y.-H., Yu, Y., Wu, R.-B., Weng, J., and Lu, G. (2017). Copper-catalyzed remote C–H functionalizations of naphthylamides through a coordinating activation strategy and single-electron-transfer (SET) mechanism. *ACS Catal.* 7, 2661–2667.
- Liu, B., Lim, C., and Miyake, G.M. (2017). Visible-light-promoted C–S cross-coupling via intermolecular charge transfer. *J. Am. Chem. Soc.* 139, 13616–13619.
- McNeill, E., Barder, T.E., and Buchwald, S.L. (2007). Palladium-catalyzed silylation of aryl chlorides with hexamethyldisilane. *Org. Lett.* 9, 3785–3788.
- Mugesh, G., du Mont, W.-W., and Sies, H. (2001). Chemistry of biologically important synthetic organoselenium compounds. *Chem. Rev.* 101, 2125–2180.
- Mullard, A. (2016). DNA-encoded drug libraries come of age. *Nat. Biotechnol.* 34, 450–451.
- Nakamura, T., Kinoshita, H., Shinokubo, H., and Oshima, K. (2002). Biaryl synthesis from two different aryl halides with tri(2-furyl)germane. *Org. Lett.* 4, 3165–3167.
- Ouyang, K., Hao, W., Zhang, W., and Xi, Z. (2015). Transition-metal-catalyzed cleavage of C–N single bonds. *Chem. Rev.* 115, 12045–12090.
- Ruiz-Castillo, P., and Buchwald, S.L. (2016). Transition-metal-catalyzed C–S, C–Se, and C–Te bond formation via cross-coupling and atom-economic addition reactions. *Chem. Rev.* 116, 12564–12649.
- Satz, A.L., Cai, J., Chen, Y., Goodnow, R., Gruber, F., Kowalczyk, A., Petersen, A., Naderi-Oboodi, G., Orzechowski, L., and Strelbel, Q. (2015). DNA compatible multistep synthesis and applications to DNA encoded libraries. *Bioconjug. Chem.* 26, 1623–1632.
- Shen, C., Xu, J., Yu, W., and Zhang, P. (2014). A highly active and easily recoverable chitosan@copper catalyst for the C–S coupling and its application in the synthesis of zolimidine. *Green. Chem.* 16, 3007–3012.
- Shu, S., Fan, Z., Yao, Q., and Zhang, A. (2016). Ru(II)-catalyzed direct C(sp²)–H activation/selenylation of arenes with selenyl chlorides. *J. Org. Chem.* 81, 5263–5269.
- Surry, D.S., and Buchwald, S.L. (2008). Biaryl phosphane ligands in palladium-catalyzed amination. *Angew. Chem. Int. Ed.* 47, 6338–6361.
- Taniguchi, N., and Onami, T. (2004). Magnesium-induced copper-catalyzed synthesis of unsymmetrical diaryl chalcogenide compounds from aryl iodide via cleavage of the Se–Se or S–S bond. *J. Org. Chem.* 69, 915–920.
- Uchiyama, S., Santa, T., Okiyama, N., Fukushima, T., and Imai, K. (2001). Fluorogenic and fluorescent labeling reagents with a benzofuran skeleton. *Biomed. Chromatogr.* 15, 295–318.
- Wang, X., Sun, H., Liu, J., Dai, D., Zhang, M., Zhou, H., Zhong, W., and Lu, X. (2014). Ruthenium-promoted C–H activation reactions between DNA-conjugated acrylamide and aromatic acids. *Org. Lett.* 16, 1968–1971.
- Wang, D.-Y., Kawahata, M., Yang, Z.-K., Miyamoto, K., Komagawa, S., Yamaguchi, K., Wang, C., and Uchiyama, M. (2016). Stille coupling via C–N bond cleavage. *Nat. Commun.* 7, 12937.
- Wang, M., Qiao, Z., Zhao, J., and Jiang, X. (2018a). Palladium-catalyzed thiomethylation via a three-component cross-coupling strategy. *Org. Lett.* 20, 6193–6197.
- Wang, D.-Y., Yang, Z.-K., Wang, C., Zhang, A., and Uchiyama, M. (2018b). From anilines to aryl ethers: a facile, efficient, and versatile synthetic method employing mild conditions. *Angew. Chem. Int. Ed.* 57, 3641–3645.
- Wenkert, E., Han, A.-L., and Jenny, C.-J. (1988). Nickel-induced conversion of carbon–nitrogen into carbon–carbon bonds. One-step transformations of aryl, quaternary ammonium salts into alkylarenes and biaryls. *J. Chem. Soc. Chem. Commun.* 975–976.
- Wood, Z.A., Schroder, E., Harris, R.J., and Poole, L.B. (2003). Structure, mechanism and regulation of peroxiredoxins. *Trends Biochem. Sci.* 28, 32–40.
- Wu, Y., Wong, S.M., Mao, F., Chan, T.L., and Kwong, F.Y. (2012). Intramolecular direct C–H bond arylation from aryl chlorides: a transition-metal-free approach for facile access of Phenanthridines. *Org. Lett.* 14, 5306–5309.
- Xie, L., and Wang, Z. (2011). Nickel-catalyzed cross-coupling of aryltrimethylammonium iodides with organozinc reagents. *Angew. Chem. Int. Ed.* 50, 4901–4904.
- Xu, J., Shen, C., Zhu, X., Zhang, P., Ajitha, M.J., Huang, K., An, Z., and Liu, X. (2016). Remote C–H activation of quinolines through copper-catalyzed radical cross-coupling. *Chem. Asian J.* 11, 882–892.
- Xu, J., Qiao, L., Shen, J., Chai, K., Shen, C., and Zhang, P. (2017). Nickel(II)-catalyzed site-selective C–H bond trifluoromethylation of arylamine in water through a coordinating activation strategy. *Org. Lett.* 19, 5661–5664.
- Yoshida, H. (2016). Stannylation reactions under base metal catalysis: some recent. *Synthesis* 48, 2540–2552.
- Zarate, C., and Martin, R. (2014). A mild Ni/Cu-catalyzed silylation via C–O cleavage. *J. Am. Chem. Soc.* 136, 2236–2239.
- Zhang, X.-Q., and Wang, Z.-X. (2014). Nickel-catalyzed cross-coupling of aryltrimethylammonium triflates and amines. *Org. Biomol. Chem.* 12, 1448–1453.
- Zhang, H., Hagihara, S., and Itami, K. (2015). Making dimethylamino a transformable directing group by nickel-catalyzed C–N borylation. *Chem. Eur. J.* 2015, 16796–16800.
- Zhou, P., Yao, J., Hu, G., and Fang, J. (2016). Naphthalimide scaffold provides versatile platform for selective. *ACS Chem. Biol.* 11, 1098–1105.

Supplemental Information

**Non-transition Metal-Mediated Diverse
Aryl–Heteroatom Bond Formation
of Arylammonium Salts**

Dong-Yu Wang, Xin Wen, Chao-Dong Xiong, Jian-Nan Zhao, Chun-Yong Ding, Qian Meng, Hu Zhou, Chao Wang, Masanobu Uchiyama, Xiao-Jie Lu, and Ao Zhang

Supplementary Information

Table of Contents

| | |
|-----|--|
| 1. | General Methods for Experiments |
| 2. | Optimization for Reaction Conditions |
| 3. | Transparent Methods |
| 3.1 | General Procedure for Preparations of Aryltrimethylammonium Salts |
| 3.2 | General Procedure for the Reactions of Aryltrimethylammonium Salts with Thiols |
| 3.3 | General Procedure for the C-Si/Sn/Ge Bond-forming Reaction of Arylammonium Salts |
| 3.4 | General Procedure for the Selenation Reaction of Arylammonium Salts |
| 3.5 | General Procedure for the Amination Reaction of Arylammonium Salts |
| 3.6 | Procedure for the Late-stage Diversification of Pharmaceutical Ammonium Derivative |
| 3.7 | Procedure for Click Reaction of NBD-ammonium Salt and Biological Thiols |
| 3.8 | Procedure for on-DNA Reactions |
| 4. | Copies of NMR Spectrums for All Compounds |
| 5. | Copies of MS Spectrums for Compounds in Fig 5 and Fig 6 |
| 6. | Reference |

1. General Methods for Experiments

All solvents and chemical reagents were obtained from commercial sources such as *Strem Chemicals*, *Adamas-beta*, *Sigma-Aldrich*, *J&K*, *Accela* and *TCI*, which were used without further purification. ^1H and ^{13}C NMR spectra were recorded with tetramethylsilane as an internal reference. Low and high-resolution mass spectra were recorded on EI-TOF (electrospray ionization-time of flight) or ESI-TOF. Normal-phase column chromatography was performed with silica gel 60 (230–400 mesh) from Merck and thin-layer chromatography was carried out on 0.25 mm Merck silica gel plates (60F-254). DNA headpiece HP-NH2 (5'-/5phos/GAGTCA/iSp9/iUniAmM/iSp9/TGACTCCC-3') was obtained from Biosearch Technologies, Novato, CA.

2. Optimization for Reaction Conditions

Table S1. Screening of Thioetherification Conditions, related to **Scheme 2a**.

The reaction scheme shows the thioetherification of a substituted benzene ring. The starting materials are a benzene ring with a cyanide group (NC) and a trimethylsilyl ether group (-XMe₃⁺) reacting with a thiol (HS-X₁₁-Me) in the presence of a base (n eq) in a solvent at room temperature for 3 hours. The product is a substituted benzene ring with a cyanide group and a thiomethyl group (-S-X₁₁-Me).

| Entry | X | Base | n | solvent | NMR Yield |
|-------|-----------------|------------------------------------|-----|---------|-----------|
| 1 | OTf | NaO <i>t</i> Bu | 2.0 | DMF | 46% |
| 2 | OTf | KO <i>t</i> Bu | 2.0 | DMF | 90% |
| 3 | OTf | KHMDS | 2.0 | DMF+THF | 87% |
| 4 | OTf | K ₂ CO ₃ | 2.0 | DMF | 98% |
| 5 | I | K ₂ CO ₃ | 2.0 | DMF | 90% |
| 6 | BF ₄ | K ₂ CO ₃ | 2.0 | DMF | 85% |
| 7 | OTf | Li ₂ CO ₃ | 2.0 | DMF | trace |
| 8 | OTf | Na ₂ CO ₃ | 2.0 | DMF | 35% |
| 9 | OTf | Cs ₂ CO ₃ | 2.0 | DMF | 93% |
| 10 | OTf | K ₃ PO ₄ | 2.0 | DMF | 82% |
| 11 | OTf | K ₂ CO ₃ | 2.0 | THF | 88% |
| 12 | OTf | K ₂ CO ₃ | 2.0 | DMSO | 45% |
| 13 | OTf | K ₂ CO ₃ | 2.0 | DMA | 78% |
| 14 | OTf | K ₂ CO ₃ | 2.0 | NMP | 53% |
| 15 | OTf | K ₂ CO ₃ | 2.0 | DCM | 38% |
| 16 | OTf | K ₂ CO ₃ | 1.5 | DMF | 96% |
| 17 | OTf | K ₂ CO ₃ | 1.1 | DMF | 80% |
| 18 | OTf | KO <i>t</i> Bu (with 2.0eq. TEMPO) | 1.5 | DMF | 92% |

Table S2. Screening of Silylation Conditions, related to **Scheme 2b**.

| | | NMR yield | | |
|-------|-------------------------|-----------|--------------------|-------|
| Entry | Base | n | solvent | NMR |
| 1 | KO <i>i</i> Bu | 2.0 | NMP | 0% |
| 2 | KF | 2.0 | NMP | 25% |
| 3 | KOAc | 2.0 | NMP | 0% |
| 4 | NaOEt | 2.0 | NMP | 0% |
| 5 | TBAF | 2.0 | NMP | 32% |
| 6 | CsF | 2.0 | DMF | 65% |
| 7 | CsF | 2.0 | DMSO | 42% |
| 8 | CsF | 2.0 | CH ₃ CN | trace |
| 9 | CsF | 2.0 | DCM | trace |
| 10 | CsF | 1.5 | NMP | 88% |
| 11 | CsF | 1.1 | NMP | 55% |
| 12 | CsF (with 2.0eq. TEMPO) | 1.5 | NMP | 72% |

Table S3. Screening of Stannylation Conditions, related to **Scheme 2c**.

| | | NMR Yield | | |
|-------|-------------------------|-----------|--------------------|-----------|
| Entry | Base | n | solvent | NMR Yield |
| 1 | KF | 2.0 | DMF | 83% |
| 2 | CsF | 2.0 | DMF | 92% |
| 3 | NaOMe | 2.0 | DMF | 76% |
| 4 | TBAF | 2.0 | DMF | 80% |
| 5 | CsF | 2.0 | THF | 75% |
| 6 | CsF | 2.0 | DMSO | 47% |
| 7 | CsF | 2.0 | CH ₃ CN | 62% |
| 8 | CsF | 2.0 | NMP | 83% |
| 9 | CsF | 1.5 | DMF | 90% |
| 10 | CsF | 1.1 | DMF | 77% |
| 11 | CsF (with 2.0eq. TEMPO) | 1.5 | DMF | 85% |

Table S4. Screening of Selenation Conditions, related to **Scheme 2e**.

| Entry | Base | n | m | solvent | NMR Yield |
|-------|-------------------------------|-----|-----|--------------------------------|-----------|
| 1 | $\text{KO}^\ddagger\text{Bu}$ | 1.5 | 1.5 | DMF | 0% |
| 2 | NaH | 1.5 | 1.5 | DMF | trace |
| 3 | KH | 1.5 | 1.5 | DMF | 65% |
| 4 | KHMDS | 1.5 | 1.5 | DMF+THF | trace |
| 5 | NaBH_4 | 1.5 | 3.0 | THF+ H_2O +DMF | 80% |
| 6 | KBH_4 | 1.5 | 3.0 | THF+ H_2O +DMF | 98% |
| 7 | KBH_4 | 1.0 | 2.0 | THF+ H_2O +DMF | 95% |
| 8 | KBH_4 | 0.6 | 1.2 | THF+ H_2O +DMF | 55% |

Table S5. Screening of Amination Conditions, related to **Scheme 2f**.

| Entry | Base | n | solvent | NMR Yield |
|-------|-------------------------------|-----|---------|-----------|
| 1 | $\text{KO}^\ddagger\text{Bu}$ | 2.0 | DMF | 15% |
| 2 | K_2CO_3 | 2.0 | DMF | 0% |
| 3 | Cs_2CO_3 | 2.0 | DMF | 0% |
| 4 | KH | 2.0 | DMF | 35% |
| 5 | KOH | 2.0 | DMF | 40% |
| 6 | KHMDS | 2.0 | DMF | 83% |
| 7 | KHMDS | 2.0 | DMSO | 42% |
| 8 | KHMDS | 1.5 | DMF | 80% |
| 9 | KHMDS | 1.1 | DMF | 56% |

3. Transparent Methods

3.1 General Procedure for Preparations of Aryltrimethylammonium Salts.

3.1.1 Preparations of ArNMe_3OTf : To a stirred solution of N,N -dimethylaniline (10 mmol) in CH_2Cl_2 (10 mL) was added dropwise methyl trifluoromethanesulfonate (1.24 mL, 11.0 mmol, 1.1 equiv.) at 25°C. The resulting solution was stirred for 4 h or 12 h at room temperature (r.t.). For some anilines bearing strong electron-withdrawing groups, the reactions may need heating up to 70 °C in MeCN in stead of CH_2Cl_2 . Solvent was then removed in

vacuum and the residue was washed with Et₂O, dried under vacuum to give a white solid. (Wang et al., 2016)

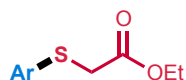
3.1.2 Preparations of ArNMe₃Cl: To a stirred solution of aryl chloride (10 mmol) in CH₂Cl₂ (10 mL) was added dropwise NMe₃ (2M in THF, 6 mL, 12.0 mmol, 1.2 equiv.; For **1s**, 0.7 equiv.) at 25°C. The resulting solution was stirred for 2 h at room temperature (r.t.). Solvent was then removed in vacuum and the residue was washed with Et₂O, dried under vacuum to give a white solid.

3.2 General Procedure for the Reactions of Aryltrimethylammonium Salts with Thiols (Fig. S1)

A flask was charged with aryltrimethylammonium triflates (0.2 mmol), thiols (0.3 mmol), K₂CO₃ (0.3 or 0.6 mmol) and DMF (3 mL). The reaction mixture was stirred at r.t. for 3 h to give a colorless or (pale) yellow suspended solution. Then water (30 mL) was added to remove DMF. The aqueous layer was extracted with ethyl acetate (3 x 10 mL). The combined organic layer was dried over Na₂SO₄, filtered and concentrated. The residue was purified on column chromatography or preparative TLC (silica gel) or preparative HPLC (for **3ir**) to give the product and NMR yields with mesitylene as an internal standard.



Fig.S1, related to Scheme 2a.



3aa: White solid, isolated yield 71%; ¹H NMR (300 MHz, CDCl₃) δ 8.15 (d, *J* = 8.9 Hz, 2H), 7.42 (d, *J* = 8.9 Hz, 2H), 4.22 (q, *J* = 7.1 Hz, 2H), 3.77 (s, 2H), 1.28 (d, *J* = 7.1 Hz, 3H). ¹³C NMR (126 MHz, CDCl₃) δ 168.60, 145.73, 145.46, 126.89, 124.07, 62.14, 34.67, 14.10.; All spectral data match those previously reported. (Nagao et al., 2006)



3ab: Yellow solid, isolated yield 78%; ¹H NMR (300 MHz, CDCl₃) δ 8.13 (d, *J* = 9.0 Hz, 2H), 7.37 (d, *J* = 8.9 Hz, 2H), 3.14 (t, *J* = 6.0 Hz, 2H), 3.04 (t, *J* = 5.9 Hz, 2H), 1.52 (s, 2H). ¹³C NMR (126 MHz, CDCl₃) δ 146.94, 145.24, 126.63, 124.02, 40.68, 36.12. HRMS (EI) *m/z*: calcd for C₈H₁₀N₂O₂S [M⁺] 198.0458, found 198.0462.



3ac: Yellow solid, isolated yield 90%; ¹H NMR (300 MHz, CDCl₃) δ 8.13 (d, *J* = 9.0 Hz, 2H), 7.40 (d, *J* = 9.0 Hz, 2H), 3.89 (t, *J* = 6.1 Hz, 2H), 3.25 (t, *J* = 6.1 Hz, 2H), 2.04 (s, 1H). ¹³C NMR (126 MHz, CDCl₃) δ 146.30, 145.41, 126.88, 124.04, 60.54, 35.12.; All spectral data match those previously reported. (Irie et al., 1980)

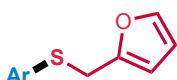


3ad: Colorless oil, isolated yield 80%; ¹H NMR (300 MHz, CDCl₃) δ 8.11 (d, *J* = 9.0 Hz, 2H), 7.32 (d, *J* = 9.0 Hz,

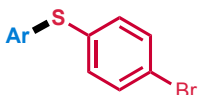
2H), 3.57 (s, 9H), 3.07 – 3.01 (m, 2H), 1.83 (dt, J = 15.2, 7.7 Hz, 2H), 0.85 – 0.77 (m, 2H). ^{13}C NMR (126 MHz, CDCl_3) δ 147.85, 144.92, 126.12, 123.94, 50.61, 34.47, 22.28, 8.69. HRMS (EI) m/z : calcd for $\text{C}_{12}\text{H}_{19}\text{NO}_5\text{SSi} [\text{M}^+]$ 317.0748, found 317.0760.



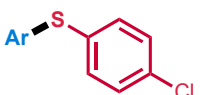
3ae: Yellow solid, isolated yield 75%; ^1H NMR (300 MHz, CDCl_3) δ 8.11 (d, J = 9.1 Hz, 2H), 7.34 (d, J = 9.1 Hz, 2H), 5.89 (ddt, J = 16.7, 10.1, 6.5 Hz, 1H), 5.26 (ddd, J = 13.5, 11.2, 1.1 Hz, 2H), 3.68 (d, J = 6.5 Hz, 2H). ^{13}C NMR (126 MHz, CDCl_3) δ 146.83, 145.23, 131.96, 126.81, 123.86, 119.04, 35.21.; All spectral data match those previously reported. (Pace et al., 2012)



3af: Colorless oil, isolated yield 90%; ^1H NMR (500 MHz, CDCl_3) δ 8.12 (d, J = 9.0 Hz, 2H), 7.39 (d, J = 9.1 Hz, 2H), 7.36 (dd, J = 1.9, 0.8 Hz, 1H), 6.31 (dd, J = 3.2, 1.9 Hz, 1H), 6.24 (dd, J = 3.2, 0.8 Hz, 1H), 4.24 (s, 2H). ^{13}C NMR (126 MHz, CDCl_3) δ 149.04, 145.79, 145.11, 142.23, 126.83, 123.52, 110.29, 108.11, 29.18.



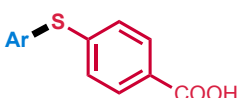
3ag: White solid, isolated yield 83%; ^1H NMR (600 MHz, CDCl_3) δ 8.08 (d, J = 9.0 Hz, 2H), 7.57 (d, J = 8.5 Hz, 2H), 7.39 (d, J = 8.5 Hz, 2H), 7.19 (d, J = 9.0 Hz, 2H). ^{13}C NMR (151 MHz, CDCl_3) δ 146.86, 145.07, 135.43, 132.69, 129.31, 126.52, 123.63.; All spectral data match those previously reported. (Taniguchi et al., 2017)



3ah: White solid, isolated yield 80%; ^1H NMR (300 MHz, CDCl_3) δ 8.08 (d, J = 9.1 Hz, 2H), 7.45 (q, J = 8.6 Hz, 4H), 7.21 – 7.15 (m, 2H). ^{13}C NMR (126 MHz, CDCl_3) δ 147.59, 145.66, 136.08, 135.84, 130.29, 129.20, 127.00, 124.17.; All spectral data match those previously reported. (Taniguchi et al., 2017)

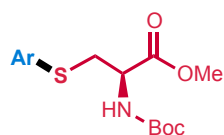


3ai: White solid, isolated yield 90%; ^1H NMR (300 MHz, CDCl_3) δ 8.04 (d, J = 9.0 Hz, 2H), 7.44 (d, J = 8.7 Hz, 2H), 7.10 (d, J = 9.0 Hz, 2H), 6.94 (d, J = 8.7 Hz, 2H), 5.53 (s, 1H). ^{13}C NMR (126 MHz, CDCl_3) δ 157.37, 150.07, 144.96, 137.38, 125.57, 123.96, 120.29, 117.19.; All spectral data match those previously reported. (Tian et al., 2014)

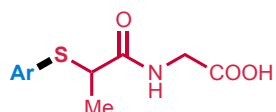


3aj: Yellow solid, isolated yield 88%; ^1H NMR (300 MHz, DMSO) δ 8.19 (d, J = 9.0 Hz, 2H), 8.00 (d, J = 8.2 Hz, 2H), 7.61 (d, J = 8.3 Hz, 2H), 7.47 (d, J = 9.0 Hz, 2H). ^{13}C NMR (126 MHz, DMSO) δ 166.58, 145.85, 144.77, 136.88, 132.45, 131.03, 130.71, 129.09, 124.48. HRMS (ESI) m/z : calcd for $\text{C}_{13}\text{H}_8\text{NO}_4\text{S} [\text{M}-\text{H}]^-$ 274.0180, found

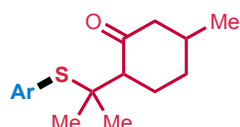
274.0182.



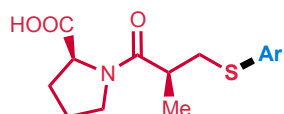
3ak: White solid, isolated yield 88%; ^1H NMR (600 MHz, CDCl_3) δ 8.12 (d, $J = 8.8$ Hz, 2H), 7.43 (d, $J = 8.8$ Hz, 2H), 5.34 (d, $J = 6.7$ Hz, 1H), 4.65 (dd, $J = 11.7, 4.9$ Hz, 1H), 3.70 (s, 3H), 3.57 (dd, $J = 14.0, 4.8$ Hz, 1H), 3.44 (dd, $J = 14.0, 4.8$ Hz, 1H), 1.41 (s, 9H). ^{13}C NMR (151 MHz, CDCl_3) δ 170.52, 154.88, 145.61, 127.60, 123.97, 80.52, 53.16, 52.79, 35.01, 28.21. HRMS (EI) m/z : calcd for $\text{C}_{15}\text{H}_{20}\text{N}_2\text{O}_6\text{S}$ [M^+] 356.1037, found 356.1043.



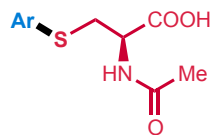
3al: White solid, isolated yield 83%; ^1H NMR (300 MHz, DMSO) δ 12.61 (s, 1H), 8.61 (t, $J = 5.8$ Hz, 1H), 8.13 (d, $J = 9.1$ Hz, 2H), 7.55 (d, $J = 9.1$ Hz, 2H), 4.29 (q, $J = 7.0$ Hz, 1H), 3.79 (dd, $J = 5.9, 2.2$ Hz, 2H), 1.46 (d, $J = 7.0$ Hz, 3H). ^{13}C NMR (126 MHz, DMSO) δ 171.44, 171.39, 146.23, 145.43, 128.20, 124.35, 44.28, 41.39, 18.53. HRMS (ESI) m/z : calcd for $\text{C}_{11}\text{H}_{13}\text{N}_2\text{O}_5\text{S}$ [$\text{M}+\text{H}]^+$ 285.0540, found 285.0544.



3am: White solid, isolated yield 80%; ^1H NMR (300 MHz, CDCl_3) δ 8.17 (d, $J = 8.9$ Hz, 2H), 7.65 (d, $J = 8.9$ Hz, 2H), 2.66 (d, $J = 13.2$ Hz, 1H), 2.40 – 2.26 (m, 2H), 1.97 (d, $J = 11.7$ Hz, 3H), 1.64 (dd, $J = 13.1, 3.1$ Hz, 2H), 1.43 (d, $J = 11.1$ Hz, 6H), 1.02 (d, $J = 6.0$ Hz, 3H). ^{13}C NMR (126 MHz, CDCl_3) δ 209.98, 148.02, 141.38, 137.50, 123.39, 57.98, 52.93, 52.26, 36.75, 34.54, 29.78, 28.20, 24.67, 22.19. HRMS (EI) m/z : calcd for $\text{C}_{16}\text{H}_{21}\text{NO}_3\text{S}$ [M^+] 307.1237, found 307.1236.

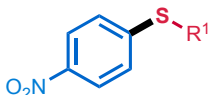


3an: Colorless oil, isolated yield 75%; ^1H NMR (300 MHz, CDCl_3) δ 8.14 (d, $J = 8.6$ Hz, 2H), 7.35 (d, $J = 8.6$ Hz, 2H), 4.56 (d, $J = 5.5$ Hz, 1H), 3.59 – 3.51 (m, 1H), 3.42 (dd, $J = 12.6, 8.9$ Hz, 2H), 3.10 (dd, $J = 13.0, 5.3$ Hz, 1H), 2.92 (dd, $J = 14.5, 6.0$ Hz, 1H), 2.01 (s, 2H), 1.33 (d, $J = 6.8$ Hz, 3H). ^{13}C NMR (126 MHz, CDCl_3) δ 175.45, 172.92, 146.58, 145.38, 126.55, 124.10, 59.72, 47.66, 38.11, 35.16, 27.72, 24.80, 17.53. HRMS (ESI) m/z : calcd for $\text{C}_{15}\text{H}_{19}\text{N}_2\text{O}_5\text{S}$ [$\text{M}+\text{H}]^+$ 339.1009, found 339.1007.

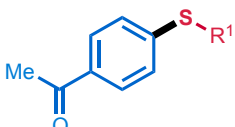


3ao: Colorless oil, isolated yield 85%; ^1H NMR (500 MHz, DMSO) δ 12.99 (s, 1H), 8.42 (d, $J = 8.0$ Hz, 1H), 8.14 (d, $J = 9.1$ Hz, 2H), 7.54 (d, $J = 9.1$ Hz, 2H), 4.47 (td, $J = 8.4, 4.9$ Hz, 1H), 3.54 (dd, $J = 13.6, 5.0$ Hz, 1H), 3.33 (d, $J = 5.1$ Hz, 1H), 1.83 (s, 3H). ^{13}C NMR (126 MHz, DMSO) δ 171.55, 169.52, 146.60, 144.68, 126.62, 123.95,

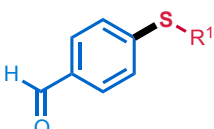
51.15, 32.73, 22.29. HRMS (ESI) m/z : calcd for $C_{11}H_{11}N_2O_5S$ [M-H]⁻ 283.0394, found 283.0393.



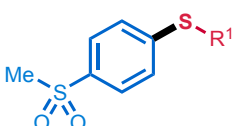
3ap: White solid, isolated yield 91%; ¹H NMR (300 MHz, CDCl₃) δ 8.10 (d, J = 9.0 Hz, 2H), 7.30 (d, J = 9.0 Hz, 2H), 3.04 – 2.96 (m, 2H), 1.76 – 1.65 (m, 2H), 1.50 – 1.40 (m, 2H), 1.25 (s, 16H), 0.87 (t, J = 6.7 Hz, 3H). ¹³C NMR (151 MHz, CDCl₃) δ 148.16, 144.72, 125.86, 123.84, 31.85, 29.57, 29.50, 29.41, 29.29, 29.06, 28.82, 28.41, 22.64, 14.07.; All spectral data match those previously reported. (Kondoh et al., 2006)



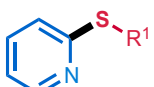
3bp: White solid, isolated yield 71%; ¹H NMR (300 MHz, CDCl₃) δ 7.85 (d, J = 8.7 Hz, 2H), 7.29 (d, J = 8.6 Hz, 2H), 3.02 – 2.94 (m, 2H), 2.57 (s, 3H), 1.74 – 1.65 (m, 2H), 1.44 (s, 2H), 1.25 (s, 16H), 0.87 (t, J = 6.7 Hz, 3H). ¹³C NMR (126 MHz, CDCl₃) δ 197.15, 145.03, 133.75, 128.74, 126.28, 32.01, 31.92, 29.63, 29.63, 29.57, 29.48, 29.34, 29.15, 28.90, 28.76, 26.41, 22.69, 14.11.; All spectral data match those previously reported. (Xu et al., 2013)



3cp: Colorless oil, isolated yield 92%; ¹H NMR (300 MHz, CDCl₃) δ 9.91 (s, 1H), 7.75 (d, J = 8.6 Hz, 2H), 7.34 (d, J = 8.3 Hz, 2H), 3.03 – 2.96 (m, 2H), 1.70 (dd, J = 15.0, 7.6 Hz, 2H), 1.52 – 1.41 (m, 2H), 1.25 (s, 16H), 0.87 (t, J = 6.6 Hz, 3H). ¹³C NMR (126 MHz, CDCl₃) δ 191.18, 147.17, 133.13, 130.00, 126.31, 31.92, 31.84, 29.63, 29.63, 29.56, 29.48, 29.34, 29.14, 28.91, 28.66, 22.69, 14.12.; All spectral data match those previously reported. (Kondoh et al., 2006)

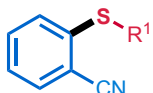


3dp: White solid, isolated yield 77%; ¹H NMR (300 MHz, CDCl₃) δ 7.80 (d, J = 8.7 Hz, 2H), 7.36 (d, J = 8.7 Hz, 2H), 3.03 (s, 3H), 2.99 (t, J = 7.4 Hz, 2H), 1.75 – 1.65 (m, 2H), 1.45 (s, 2H), 1.25 (s, 16H), 0.87 (t, J = 6.7 Hz, 3H). ¹³C NMR (126 MHz, CDCl₃) δ 146.43, 136.45, 127.67, 126.66, 44.67, 31.96, 31.91, 29.62, 29.56, 29.47, 29.34, 29.13, 28.88, 28.58, 22.69, 14.11. HRMS (EI) m/z : calcd for $C_{19}H_{23}O_2S_2$ [M⁺] 356.1838, found 356.1834.

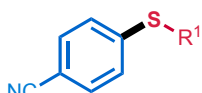


3ep: Colorless oil, isolated yield 61%; ¹H NMR (300 MHz, CDCl₃) δ 8.42 (ddd, J = 5.0, 1.8, 0.9 Hz, 1H), 7.46 (ddd, J = 8.1, 7.4, 1.9 Hz, 1H), 7.16 (dt, J = 8.1, 1.0 Hz, 1H), 6.95 (ddd, J = 7.3, 4.9, 1.1 Hz, 1H), 3.21 – 3.09 (m, 2H), 1.69 (dd, J = 15.1, 7.5 Hz, 2H), 1.48 – 1.40 (m, 2H), 1.25 (s, 16H), 0.88 (t, J = 6.6 Hz, 3H). ¹³C NMR (151 MHz, CDCl₃) δ 159.65, 149.42, 135.75, 122.11, 119.12, 31.91, 30.14, 29.65, 29.62, 29.59, 29.51, 29.33, 29.31, 29.20,

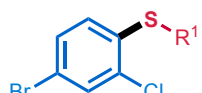
28.96, 22.68, 14.11.; All spectral data match those previously reported. (Kanemura et al., 2008)



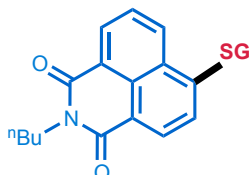
3fp: Colorless oil, isolated yield 88%; ^1H NMR (300 MHz, CDCl_3) δ 7.60 (d, $J = 7.7$ Hz, 1H), 7.49 (t, $J = 7.7$ Hz, 1H), 7.39 (d, $J = 8.0$ Hz, 1H), 7.24 (d, $J = 9.3$ Hz, 1H), 3.00 (t, $J = 7.4$ Hz, 2H), 1.74 – 1.59 (m, 2H), 1.44 (s, 2H), 1.25 (s, 16H), 0.87 (t, $J = 6.5$ Hz, 3H). ^{13}C NMR (126 MHz, CDCl_3) δ 142.31, 133.65, 132.73, 128.66, 125.69, 117.19, 113.38, 33.56, 31.92, 29.63, 29.56, 29.46, 29.34, 29.12, 28.82, 28.77, 22.69, 14.12. HRMS (EI) m/z : calcd for $\text{C}_{19}\text{H}_{29}\text{NS} [\text{M}^+]$ 303.2015, found 303.2022.



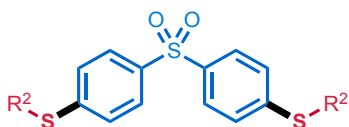
3gp: White solid, isolated yield 90%; ^1H NMR (300 MHz, CDCl_3) δ 7.52 (d, $J = 8.7$ Hz, 2H), 7.28 (d, $J = 8.7$ Hz, 2H), 3.01 – 2.92 (m, 2H), 1.75 – 1.62 (m, 2H), 1.49 – 1.37 (m, 2H), 1.25 (s, 16H), 0.87 (t, $J = 6.6$ Hz, 3H). ^{13}C NMR (126 MHz, CDCl_3) δ 145.35, 132.19, 126.68, 118.97, 107.91, 31.92, 29.62, 29.55, 29.46, 29.34, 29.12, 28.87, 28.57, 22.69, 14.11.; All spectral data match those previously reported. (Kondoh et al., 2006)



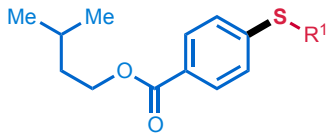
3hp: Colorless oil, isolated yield 46%; ^1H NMR (500 MHz, CDCl_3) δ 7.51 (d, $J = 2.1$ Hz, 1H), 7.33 (dd, $J = 8.5, 2.1$ Hz, 1H), 7.10 (d, $J = 8.5$ Hz, 1H), 2.92 – 2.88 (m, 2H), 1.67 (dt, $J = 15.0, 7.4$ Hz, 2H), 1.48 – 1.41 (m, 2H), 1.26 (s, 16H), 0.88 (t, $J = 7.0$ Hz, 3H). ^{13}C NMR (126 MHz, CDCl_3) δ 136.02, 133.94, 132.12, 130.14, 128.89, 118.54, 32.55, 31.92, 29.63, 29.56, 29.46, 29.34, 29.15, 28.91, 28.50, 22.69, 14.12.



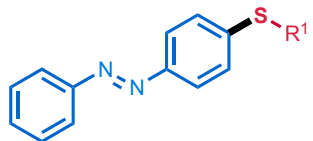
3ir: Yellow solid, isolated yield 70%; ^1H NMR (500 MHz, D_2O) δ 7.88 – 7.78 (m, 2H), 7.67 (d, $J = 7.7$ Hz, 1H), 7.29 (t, $J = 7.3$ Hz, 1H), 7.19 (d, $J = 7.6$ Hz, 1H), 4.74 – 4.69 (m, 1H), 3.83 – 3.74 (m, 3H), 3.71 – 3.64 (m, 2H), 3.59 (d, $J = 9.5$ Hz, 1H), 3.35 (s, 1H), 2.54 – 2.43 (m, 2H), 2.10 – 2.01 (m, 2H), 1.57 (s, 2H), 1.43 (dd, $J = 13.8, 6.7$ Hz, 2H), 1.02 (t, $J = 7.1$ Hz, 3H). ^{13}C NMR (126 MHz, D_2O) δ 176.01, 175.56, 174.92, 170.97, 164.30, 164.17, 143.71, 131.29, 130.27, 129.95, 127.83, 126.50, 125.99, 123.38, 120.52, 117.24, 54.42, 52.36, 43.41, 40.44, 33.28, 31.63, 30.10, 29.47, 27.12, 19.91, 13.17. HRMS (ESI) m/z : calcd for $\text{C}_{26}\text{H}_{31}\text{N}_4\text{O}_8\text{S} [\text{M}+\text{H}]^+$ 559.1857, found 559.1848.



3jq: White solid, isolated yield 45%; ^1H NMR (300 MHz, CDCl_3) δ 7.78 (d, $J = 8.7$ Hz, 4H), 7.30 (d, $J = 8.7$ Hz, 4H), 2.99 (q, $J = 7.4$ Hz, 4H), 1.35 (t, $J = 7.4$ Hz, 6H). ^{13}C NMR (126 MHz, CDCl_3) δ 145.33, 137.81, 127.84, 126.72, 26.05, 13.79. HRMS (EI) m/z : calcd for $\text{C}_{16}\text{H}_{18}\text{O}_2\text{S}_3 [\text{M}^+]$ 338.0463, found 338.0458.



3kp: White solid, isolated yield 66%; ^1H NMR (300 MHz, CDCl_3) δ 7.92 (d, $J = 8.6$ Hz, 2H), 7.27 (d, $J = 8.4$ Hz, 2H), 4.33 (t, $J = 6.7$ Hz, 2H), 3.01 – 2.92 (m, 2H), 1.79 (dt, $J = 13.3, 6.7$ Hz, 1H), 1.71 – 1.59 (m, 4H), 1.44 (s, 2H), 1.25 (s, 16H), 0.97 (d, $J = 6.5$ Hz, 6H), 0.88 (t, $J = 6.7$ Hz, 3H). ^{13}C NMR (126 MHz, CDCl_3) δ 166.40, 144.29, 129.83, 126.90, 126.30, 63.52, 37.42, 32.10, 31.89, 29.61, 29.61, 29.55, 29.46, 29.32, 29.13, 28.88, 28.76, 25.21, 22.67, 22.51, 14.10. HRMS (EI) m/z : calcd for $\text{C}_{24}\text{H}_{40}\text{O}_2\text{S} [\text{M}^+]$ 392.2744, found 392.2748.



3lp: Yellow solid, isolated yield 85%; ^1H NMR (300 MHz, CDCl_3) δ 7.94 – 7.81 (m, 4H), 7.56 – 7.44 (m, 3H), 7.39 (d, $J = 8.6$ Hz, 2H), 3.01 (t, $J = 7.4$ Hz, 2H), 1.70 (dd, $J = 14.8, 7.5$ Hz, 2H), 1.45 (d, $J = 5.6$ Hz, 2H), 1.27 (s, 16H), 0.89 (t, $J = 6.5$ Hz, 3H). ^{13}C NMR (126 MHz, CDCl_3) δ 152.69, 150.18, 141.86, 130.76, 129.05, 127.56, 123.33, 122.73, 32.67, 31.90, 29.63, 29.62, 29.56, 29.48, 29.33, 29.15, 28.89, 22.68, 14.11. HRMS (EI) m/z : calcd for $\text{C}_{24}\text{H}_{34}\text{N}_2\text{S} [\text{M}^+]$ 382.2437, found 382.2435.

3.3 General Procedure for the C-Si/Sn/Ge Bond-forming Reaction of Arylammonium Salts (Fig. S2, S3, S4)

A Schlenk tube was charged with aryltrimethylammonium triflate (0.2 mmol), Si/Sn/Ge reagents (0.3 mmol), CsF (0.28 mmol), and DMF (3 mL) under a argon atmosphere. The reaction mixture was stirred at r.t. or 50°C for 8 hours to give a colorless or (pale) yellow transparent solution (slightly suspended for some cases). Then water (30 mL) was added to remove DMF. The aqueous layer was extracted with ethyl acetate (3 x 10 mL). The combined organic layer was dried over Na_2SO_4 , filtered and concentrated. The residue was purified on column chromatography or preparative TLC (silica gel) to give the product and NMR yields with mesitylene as an internal standard.

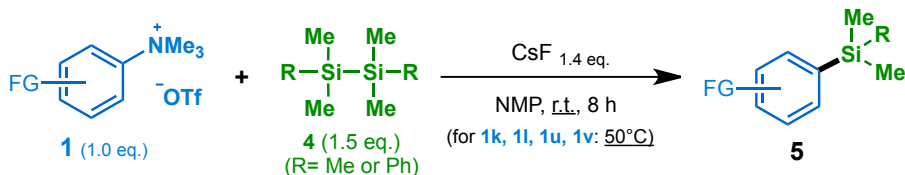
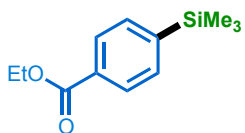
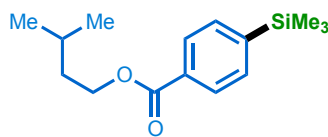


Fig.S2, related to Scheme 2b.

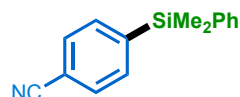


5a: Colorless oil, isolated yield 84%; ^1H NMR (300 MHz, CDCl_3) δ 8.01 (d, $J = 8.1$ Hz, 2H), 7.60 (d, $J = 8.1$ Hz, 2H), 4.39 (q, $J = 7.1$ Hz, 2H), 1.40 (t, $J = 7.1$ Hz, 3H), 0.29 (s, 9H). ^{13}C NMR (151 MHz, CDCl_3) δ 166.82, 146.70, 133.27, 130.67, 128.49, 60.91, 14.37, -1.29.; All spectral data match those previously reported. (Tobisu et al.,

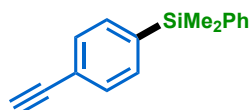
2008)



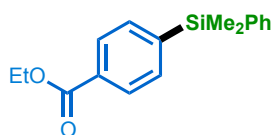
5b: Colorless oil, isolated yield 88%; ^1H NMR (300 MHz, CDCl_3) δ 8.00 (d, $J = 8.2$ Hz, 2H), 7.59 (d, $J = 8.2$ Hz, 2H), 4.36 (t, $J = 6.7$ Hz, 2H), 1.81 (dt, $J = 13.6, 6.5$ Hz, 1H), 1.66 (q, $J = 6.7$ Hz, 2H), 0.97 (d, $J = 6.5$ Hz, 6H), 0.29 (s, 9H). ^{13}C NMR (126 MHz, CDCl_3) δ 166.87, 146.71, 133.27, 130.67, 128.47, 63.59, 37.44, 25.25, 22.54, -1.31.



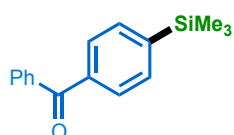
5c: Colorless oil, isolated yield 71%; ^1H NMR (500 MHz, CDCl_3) δ 7.61 (s, 4H), 7.50 (dd, $J = 7.7, 1.7$ Hz, 2H), 7.43 – 7.35 (m, 3H), 0.58 (s, 6H). ^{13}C NMR (126 MHz, CDCl_3) δ 145.41, 136.48, 134.62, 134.11, 131.04, 129.65, 128.09, 118.97, 112.71, -2.74. All spectral data match those previously reported. (Guo et al., 2015)



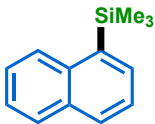
5d: Colorless oil, isolated yield 52%; ^1H NMR (500 MHz, CDCl_3) δ 7.50 (dd, $J = 7.6, 1.8$ Hz, 2H), 7.47 (d, $J = 1.5$ Hz, 4H), 7.39 – 7.34 (m, 3H), 3.09 (s, 1H), 0.55 (s, 6H). ^{13}C NMR (126 MHz, CDCl_3) δ 139.55, 137.60, 134.12, 134.01, 131.25, 129.26, 127.88, 122.68, 83.70, 77.66, -2.56. HRMS (EI) m/z : calcd for $\text{C}_{16}\text{H}_{16}\text{Si} [\text{M}^+]$ 236.1016, found 236.1009.



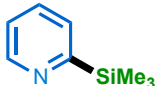
5e: Colorless oil, isolated yield 80%; ^1H NMR (300 MHz, CDCl_3) δ 8.01 (d, $J = 7.9$ Hz, 2H), 7.60 (d, $J = 7.9$ Hz, 2H), 7.55 – 7.47 (m, 2H), 7.37 (d, $J = 5.9$ Hz, 3H), 4.38 (d, $J = 7.1$ Hz, 2H), 1.39 (t, $J = 7.1$ Hz, 3H), 0.58 (s, 6H). ^{13}C NMR (126 MHz, CDCl_3) δ 166.76, 144.51, 137.40, 134.15, 134.14, 130.96, 129.36, 128.53, 127.94, 60.95, 14.35, -2.55.; All spectral data match those previously reported. (Hamze et al., 2006)



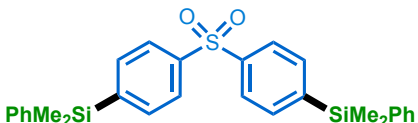
5f: Colorless oil, isolated yield 60%; ^1H NMR (500 MHz, CDCl_3) δ 7.81 (dd, $J = 8.3, 1.3$ Hz, 2H), 7.76 (d, $J = 8.2$ Hz, 2H), 7.64 (d, $J = 8.2$ Hz, 2H), 7.59 (t, $J = 7.4$ Hz, 1H), 7.48 (t, $J = 7.6$ Hz, 2H), 0.32 (s, 9H). ^{13}C NMR (126 MHz, CDCl_3) δ 196.88, 146.29, 137.69, 137.63, 133.16, 132.38, 130.07, 129.00, 128.24, -1.30. All spectral data match those previously reported. (McNeill et al., 2007)



5g: Colorless oil, isolated yield 75%; ^1H NMR (500 MHz, CDCl_3) δ 8.16 (d, $J = 8.0$ Hz, 1H), 7.90 (dd, $J = 7.8, 5.9$ Hz, 2H), 7.75 (d, $J = 6.8$ Hz, 1H), 7.52 (ddd, $J = 21.9, 15.0, 6.7$ Hz, 3H), 0.53 (s, 9H). ^{13}C NMR (126 MHz, CDCl_3) δ 138.12, 136.89, 133.41, 133.15, 129.71, 129.11, 128.12, 125.56, 125.26, 125.08, 0.24.; All spectral data match those previously reported. (Tobisu et al., 2008)



5h: Colorless oil, isolated yield 62%; ^1H NMR (400 MHz, CDCl_3) δ 8.77 (d, $J = 4.5$ Hz, 1H), 7.58 (td, $J = 7.6, 1.7$ Hz, 1H), 7.50 (d, $J = 7.5$ Hz, 1H), 7.19 (ddd, $J = 7.5, 4.9, 1.4$ Hz, 1H), 0.32 (s, 9H). ^{13}C NMR (126 MHz, CDCl_3) δ 167.89, 149.60, 133.63, 128.31, 122.28, -2.25. All spectral data match those previously reported. (Chau et al., 2008)



5i: Colorless oil, isolated yield 60%; ^1H NMR (500 MHz, CDCl_3) δ 7.88 (d, $J = 8.3$ Hz, 4H), 7.62 (d, $J = 8.3$ Hz, 4H), 7.48 (dd, $J = 7.8, 1.6$ Hz, 4H), 7.41 – 7.33 (m, 6H), 0.55 (s, 12H). ^{13}C NMR (126 MHz, CDCl_3) δ 145.70, 141.92, 136.51, 134.86, 134.06, 129.57, 128.02, 126.54, -2.73. HRMS (EI) m/z : calcd for $\text{C}_{28}\text{H}_{30}\text{O}_2\text{Si}_2\text{S} [\text{M}^+]$ 486.1500, found 486.1503.

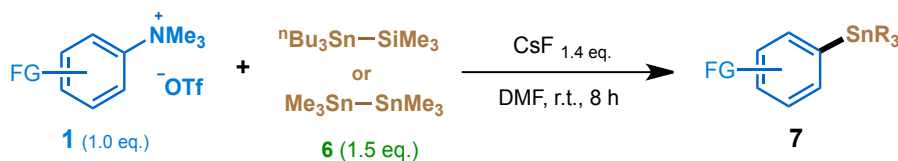
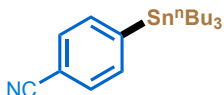
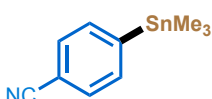


Fig.S3, related to **Scheme 2c**.



7a: Colorless oil, isolated yield 82%; ^1H NMR (300 MHz, CDCl_3) δ 7.87 (d, $J = 7.5$ Hz, 2H), 7.58 (d, $J = 7.6$ Hz, 2H), 2.59 (s, 3H), 1.59 – 1.48 (m, 6H), 1.33 (dd, $J = 14.6, 7.3$ Hz, 6H), 1.20 – 0.98 (m, 6H), 0.88 (t, $J = 7.2$ Hz, 9H). ^{13}C NMR (126 MHz, CDCl_3) δ 198.66, 150.30, 136.64, 136.59, 127.10, 29.04, 27.33, 26.55, 13.66, 9.68.; All spectral data match those previously reported. (Komeyama et al., 2015)



7b: Colorless oil, isolated yield 85%; ^1H NMR (300 MHz, CDCl_3) δ 7.66 – 7.50 (m, 4H), 0.33 (s, 9H). ^{13}C NMR (126 MHz, CDCl_3) δ 150.28, 136.31, 130.87, 119.13, 111.85, -9.49.; All spectral data match those previously

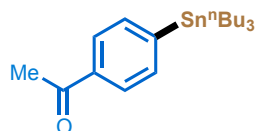
reported. (Chen et al., 2016)



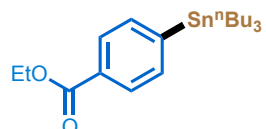
7c: Colorless oil, isolated yield 60%; ^1H NMR (300 MHz, CDCl_3) δ 7.65 (d, $J = 7.7$ Hz, 1H), 7.57 – 7.43 (m, 2H), 7.36 (td, $J = 7.5, 1.5$ Hz, 1H), 1.63 – 1.48 (m, 6H), 1.41 – 1.26 (m, 6H), 1.26 – 1.17 (m, 6H), 0.89 (t, $J = 7.3$ Hz, 9H). ^{13}C NMR (126 MHz, CDCl_3) δ 148.37, 136.96, 132.89, 131.37, 128.27, 120.60, 120.28, 28.98, 27.23, 13.63, 10.05.; All spectral data match those previously reported. (Shirakawa et al., 2003)



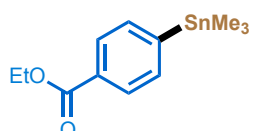
7d: Colorless oil, isolated yield 76%; ^1H NMR (300 MHz, CDCl_3) δ 7.66 (ddd, $J = 7.6, 1.3, 0.7$ Hz, 1H), 7.60 – 7.47 (m, 2H), 7.39 (td, $J = 7.5, 1.6$ Hz, 1H), 0.44 (s, 9H). ^{13}C NMR (126 MHz, CDCl_3) δ 148.03, 136.40, 132.79, 131.51, 128.59, 120.31, 120.03, -9.02.; All spectral data match those previously reported. (Chen et al., 2016)



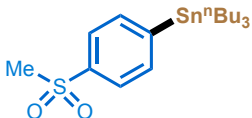
7e: Colorless oil, isolated yield 60%; ^1H NMR (300 MHz, CDCl_3) δ 7.56 (s, 4H), 1.51 (d, $J = 7.7$ Hz, 6H), 1.32 (d, $J = 7.2$ Hz, 6H), 1.19 – 0.99 (m, 6H), 0.88 (t, $J = 7.2$ Hz, 9H). ^{13}C NMR (126 MHz, CDCl_3) δ 150.37, 136.89, 130.73, 119.26, 111.57, 28.98, 27.30, 13.64, 9.75.; All spectral data match those previously reported. (Komeyama et al., 2015)



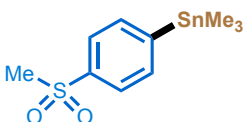
7f: Colorless oil, isolated yield 82%; ^1H NMR (300 MHz, CDCl_3) δ 7.96 (d, $J = 8.0$ Hz, 2H), 7.54 (d, $J = 8.0$ Hz, 2H), 4.37 (q, $J = 7.1$ Hz, 2H), 1.63 – 1.47 (m, 6H), 1.35 (dd, $J = 16.0, 7.3$ Hz, 10H), 1.14 – 1.01 (m, 5H), 0.88 (s, 9H). ^{13}C NMR (126 MHz, CDCl_3) δ 167.10, 149.49, 136.39, 129.93, 128.35, 60.83, 29.04, 27.33, 14.36, 13.66, 9.66.; All spectral data match those previously reported. (Reed et al., 2012)



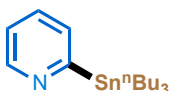
7g: Colorless oil, isolated yield 61%; ^1H NMR (300 MHz, CDCl_3) δ 7.98 (d, $J = 8.1$ Hz, 2H), 7.57 (d, $J = 8.1$ Hz, 2H), 4.38 (q, $J = 7.1$ Hz, 2H), 1.39 (t, $J = 7.1$ Hz, 3H), 0.32 (s, 9H). ^{13}C NMR (126 MHz, CDCl_3) δ 166.94, 149.44, 135.72, 130.16, 128.47, 60.85, 14.33, -9.55.; All spectral data match those previously reported. (Chen et al., 2016)



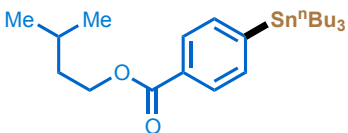
7h: Colorless oil, isolated yield 60%; ^1H NMR (300 MHz, CDCl_3) δ 7.85 (d, J = 8.1 Hz, 2H), 7.67 (d, J = 8.1 Hz, 2H), 3.05 (s, 3H), 1.59 – 1.46 (m, 6H), 1.33 (dq, J = 14.2, 7.1 Hz, 6H), 1.15 – 1.04 (m, 6H), 0.89 (t, J = 7.3 Hz, 9H). ^{13}C NMR (126 MHz, CDCl_3) δ 151.36, 140.01, 137.16, 125.88, 44.50, 28.98, 27.30, 13.63, 9.79. All spectral data match those previously reported. (Tang et al., 2010)



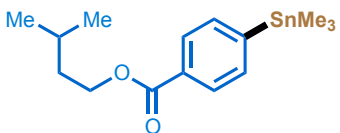
7i: Colorless oil, isolated yield 83%; ^1H NMR (300 MHz, CDCl_3) δ 7.87 (d, J = 8.2 Hz, 2H), 7.70 (d, J = 8.2 Hz, 2H), 3.04 (s, 3H), 0.35 (s, 9H). ^{13}C NMR (126 MHz, CDCl_3) δ 151.29, 140.30, 136.60, 126.06, 44.53, -9.45. HRMS (EI) m/z : calcd for $\text{C}_{10}\text{H}_{16}\text{O}_2\text{SSn} [\text{M}^+]$ 319.9888, found 319.9896.



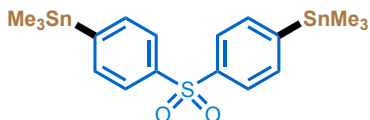
7j: Colorless oil, isolated yield 52%; ^1H NMR (600 MHz, CDCl_3) δ 8.73 (ddd, J = 4.9, 1.6, 1.0 Hz, 1H), 7.49 (td, J = 7.5, 1.8 Hz, 1H), 7.40 (d, J = 7.4 Hz, 1H), 7.11 (ddd, J = 7.6, 4.9, 1.4 Hz, 1H), 1.59 – 1.52 (m, 6H), 1.33 (dq, J = 14.6, 7.3 Hz, 6H), 1.14 – 1.10 (m, 6H), 0.88 (t, J = 7.3 Hz, 9H). ^{13}C NMR (151 MHz, CDCl_3) δ 174.09, 150.51, 133.24, 132.36, 121.97, 29.06, 27.33, 13.66, 9.76. All spectral data match those previously reported. (Fargeas et al., 2003)



7k: Colorless oil, isolated yield 70%; ^1H NMR (500 MHz, CDCl_3) δ 7.95 (d, J = 8.1 Hz, 2H), 7.55 (d, J = 8.1 Hz, 2H), 4.34 (t, J = 6.7 Hz, 2H), 1.85 – 1.75 (m, 1H), 1.66 (q, J = 6.8 Hz, 2H), 1.52 (dd, J = 15.7, 8.1 Hz, 5H), 1.37 – 1.28 (m, 7H), 1.14 – 1.02 (m, 6H), 0.97 (d, J = 6.6 Hz, 6H), 0.88 (t, J = 7.3 Hz, 9H). ^{13}C NMR (126 MHz, CDCl_3) δ 167.12, 149.47, 136.38, 129.93, 128.33, 63.49, 37.45, 29.04, 27.33, 25.22, 22.53, 13.66, 9.66. HRMS (EI) m/z : calcd for $\text{C}_{24}\text{H}_{42}\text{O}_2\text{Sn} [\text{M}^+]$ 482.2201, found 482.2197.



7l: Colorless oil, isolated yield 76%; ^1H NMR (300 MHz, CDCl_3) δ 7.97 (d, J = 8.1 Hz, 2H), 7.57 (d, J = 8.1 Hz, 2H), 4.35 (t, J = 6.7 Hz, 2H), 1.79 (tt, J = 12.9, 6.4 Hz, 1H), 1.66 (q, J = 6.7 Hz, 2H), 0.97 (d, J = 6.5 Hz, 6H), 0.31 (s, 9H). ^{13}C NMR (126 MHz, CDCl_3) δ 167.01, 149.46, 135.76, 130.22, 128.50, 63.57, 37.45, 25.26, 22.53, -9.55. HRMS (EI) m/z : calcd for $\text{C}_{15}\text{H}_{24}\text{O}_2\text{Sn} [\text{M}^+]$ 356.0793, found 356.0793.



7m: Colorless oil, isolated yield 77%; ^1H NMR (300 MHz, CDCl_3) δ 7.86 (d, J = 8.2 Hz, 4H), 7.62 (d, J = 8.2 Hz, 4H), 0.30 (s, 18H). ^{13}C NMR (151 MHz, CDCl_3) δ 150.43, 141.45, 136.46, 126.33, -9.52. All spectral data match those previously reported. (Jeon et al., 2014)

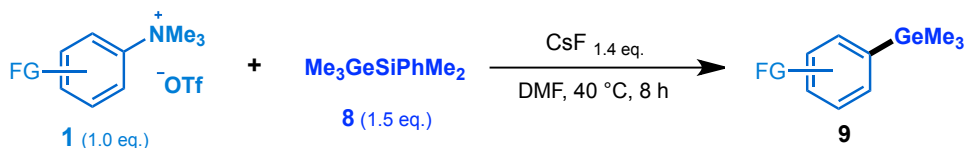
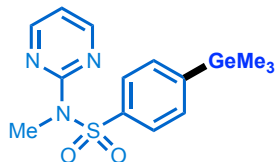


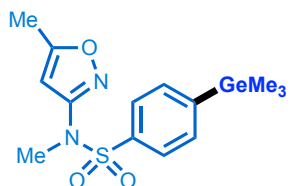
Fig.S4, related to **Scheme 2d.**

Procedure for the Preparation of $\text{Me}_3\text{GeSiPhMe}_2$:

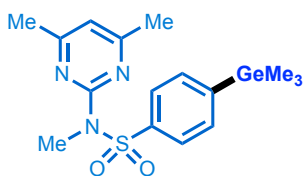
To a solution of naphthalene (0.4 mmol) in THF (16 mL), were added lithium clippings (24 mmol). The resulting mixture started turning dark green and was stirred at room temperature for 1 h under an argon atmosphere. Then chlorodimethylphenylsilane (4 mmol) was added dropwise and the mixture was stirred at room temperature for 3 h. The resulting solution was added into a stirred solution of Me_3GeCl (4 mmol) in THF at 0°C. The reaction was stirred at room temperature for 8 h followed by extraction with hexane and H_2O . The organic phase was washed with brine and dried over Na_2SO_4 . The residue was purified on column chromatography to give the product **8** as colorless oil: isolated yield 78%; ^1H NMR (300 MHz, CDCl_3) δ 7.49 – 7.41 (m, 2H), 7.39 – 7.29 (m, 3H), 0.39 (s, 6H), 0.15 (s, 9H). ^{13}C NMR (126 MHz, CDCl_3) δ 139.25, 133.64, 128.53, 127.78, -3.09, -3.39.



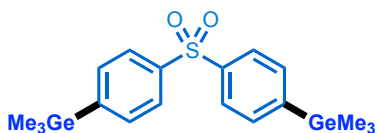
9a: Colorless oil, isolated yield 60%; ^1H NMR (300 MHz, CDCl_3) δ 8.47 (d, J = 4.8 Hz, 2H), 8.02 (d, J = 8.3 Hz, 2H), 7.58 (d, J = 8.3 Hz, 2H), 6.88 (t, J = 4.8 Hz, 1H), 3.68 (s, 3H), 0.40 (s, 9H). ^{13}C NMR (126 MHz, CDCl_3) δ 158.78, 157.46, 149.73, 140.12, 132.97, 127.28, 115.38, 34.23, -1.91. HRMS (EI) m/z : calcd for $\text{C}_{14}\text{H}_{19}\text{N}_3\text{O}_2\text{GeS} [\text{M}^+]$ 367.0404, found 367.0404.



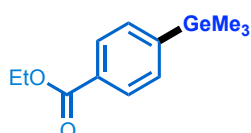
9b: Colorless oil, isolated yield 80%; ^1H NMR (400 MHz, CDCl_3) δ 7.66 (d, J = 8.3 Hz, 2H), 7.58 (d, J = 8.3 Hz, 2H), 6.51 (s, 1H), 3.26 (s, 3H), 2.38 (s, 3H), 0.40 (s, 9H). ^{13}C NMR (126 MHz, CDCl_3) δ 170.33, 160.86, 150.80, 136.55, 133.79, 126.05, 97.58, 35.12, 12.67, -1.96. HRMS (EI) m/z : calcd for $\text{C}_{13}\text{H}_{17}\text{O}_3\text{N}_2\text{GeS} [\text{M}-\text{CH}_3]^+$ 355.0166, found 355.0136.



9c: Colorless oil, isolated yield 55%; ^1H NMR (400 MHz, CDCl_3) δ 8.04 (d, $J = 8.3$ Hz, 2H), 7.56 (d, $J = 8.3$ Hz, 2H), 6.57 (s, 1H), 3.66 (s, 3H), 2.31 (s, 6H), 0.39 (s, 9H). ^{13}C NMR (126 MHz, CDCl_3) δ 167.24, 158.20, 149.33, 140.59, 132.59, 127.74, 114.45, 33.85, 23.62, -1.89. HRMS (ESI) m/z : calcd for $\text{C}_{16}\text{H}_{24}\text{N}_3\text{O}_2\text{SGe} [\text{M}+\text{H}]^+$ 396.0801, found 396.0811.



9d: Colorless oil, isolated yield 70%; ^1H NMR (500 MHz, CDCl_3) δ 7.88 (d, $J = 8.2$ Hz, 4H), 7.59 (d, $J = 8.2$ Hz, 4H), 0.38 (s, 18H). ^{13}C NMR (126 MHz, CDCl_3) δ 150.14, 141.47, 133.76, 126.58, -1.95. HRMS (EI) m/z : calcd for $\text{C}_{17}\text{H}_{21}\text{O}_2\text{Ge}_2\text{S} [\text{M}-\text{CH}_3]^+$ 436.9680, found 436.9686.



9e: Colorless oil, isolated yield 50%; ^1H NMR (400 MHz, CDCl_3) δ 7.99 (d, $J = 8.0$ Hz, 2H), 7.55 (d, $J = 8.0$ Hz, 2H), 4.37 (q, $J = 7.1$ Hz, 2H), 1.39 (t, $J = 7.1$ Hz, 3H), 0.40 (s, 9H). ^{13}C NMR (126 MHz, CDCl_3) δ 166.89, 149.20, 132.91, 130.25, 128.60, 60.87, 14.34, -1.90. All spectral data match those previously reported. (Komami et al., 2018)

3.4 General Procedure for the Selenation Reaction of Arylammonium Salts (Fig. S5)

A flask was charged with RSeSeR (0.2 mmol) and 1mL THF, KBH_4 (0.4 mmol) in 1mL H_2O was added. The reaction mixture was stirred at r.t. for 10 minutes and then aryltrimethylammonium triflates (0.2 mmol) in 1mL DMF was added. After 3 h, the water (30 mL) was added to remove DMF. The aqueous layer was extracted with ethyl acetate (3 x 10 mL). The combined organic layer was dried over Na_2SO_4 , filtered and concentrated. The residue was purified on column chromatography or preparative TLC (silica gel) to give the product and NMR yields with mesitylene as an internal standard.

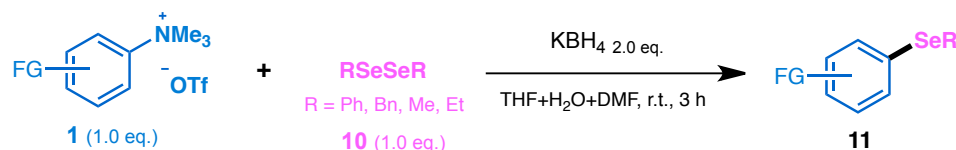
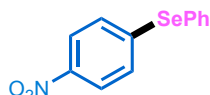
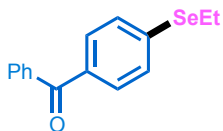


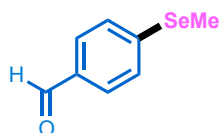
Fig.S5, related to Scheme 2e.



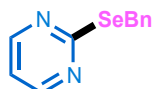
11a: Yellow oil, isolated yield 90%; ^1H NMR (500 MHz, CDCl_3) δ 8.03 (d, $J = 9.0$ Hz, 2H), 7.64 (dd, $J = 8.1, 1.4$ Hz, 2H), 7.42 (dt, $J = 14.2, 7.0$ Hz, 3H), 7.36 (d, $J = 9.0$ Hz, 2H). ^{13}C NMR (126 MHz, CDCl_3) δ 146.22, 143.94, 135.89, 130.06, 129.74, 129.39, 127.24, 123.98.; All spectral data match those previously reported. (Maity et al., 2017)



11b: Colorless oil, isolated yield 56%; ^1H NMR (400 MHz, CDCl_3) δ 7.80 (d, $J = 7.7$ Hz, 2H), 7.72 (d, $J = 7.3$ Hz, 2H), 7.61 (t, $J = 7.4$ Hz, 1H), 7.52 (dd, $J = 15.6, 7.7$ Hz, 4H), 3.06 (q, $J = 7.1$ Hz, 2H), 1.53 (t, $J = 7.2$ Hz, 3H). ^{13}C NMR (151 MHz, CDCl_3) δ 196.08, 138.04, 137.64, 135.15, 132.32, 130.57, 130.16, 129.89, 128.28, 20.58, 15.19. HRMS (EI) m/z : calcd for $\text{C}_{15}\text{H}_{14}\text{OSe} [\text{M}^+]$ 290.0204, found 290.0196.



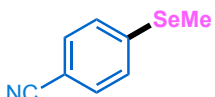
11c: Colorless oil, isolated yield 81%; ^1H NMR (500 MHz, CDCl_3) δ 9.93 (s, 1H), 7.73 (d, $J = 8.3$ Hz, 2H), 7.49 (d, $J = 8.3$ Hz, 2H), 2.42 (s, 3H). ^{13}C NMR (126 MHz, CDCl_3) δ 191.45, 142.40, 133.95, 129.95, 128.85, 6.43.; All spectral data match those previously reported. (Sugiura et al., 1990)



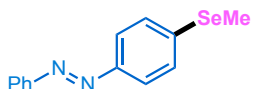
11d: Colorless oil, isolated yield 85%; ^1H NMR (400 MHz, CDCl_3) δ 8.54 (d, $J = 4.8$ Hz, 2H), 7.45 (d, $J = 7.5$ Hz, 2H), 7.31 (dd, $J = 12.6, 5.7$ Hz, 2H), 7.27 – 7.21 (m, 1H), 7.03 (t, $J = 4.2$ Hz, 1H), 4.49 (s, 2H). ^{13}C NMR (151 MHz, CDCl_3) δ 170.72, 157.24, 138.58, 129.06, 128.48, 126.93, 117.27, 30.32.; All spectral data match those previously reported. (Ma et al., 2017)



11f: Colorless oil, isolated yield 65%; ^1H NMR (400 MHz, CDCl_3) δ 7.56 (d, $J = 8.5$ Hz, 2H), 7.43 (d, $J = 8.5$ Hz, 2H), 6.48 (s, 1H), 3.25 (s, 3H), 2.38 (d, $J = 2.0$ Hz, 6H). ^{13}C NMR (126 MHz, CDCl_3) δ 170.39, 160.79, 141.28, 133.69, 129.11, 127.39, 97.60, 35.15, 12.68, 6.54. HRMS (ESI) m/z : calcd for $\text{C}_{15}\text{H}_{19}\text{N}_2\text{O}_5\text{S} [\text{M}+\text{H}]^+$ 339.1009, found 339.1007. HRMS (ESI) m/z : calcd for $\text{C}_{12}\text{H}_{15}\text{N}_2\text{O}_3\text{SSe} [\text{M}+\text{H}]^+$ 346.9969, found 346.9973.



11g: Colorless oil, isolated yield 41%; ^1H NMR (500 MHz, CDCl_3) δ 7.49 (d, $J = 8.5$ Hz, 2H), 7.43 (d, $J = 8.5$ Hz, 2H), 2.40 (s, 3H). ^{13}C NMR (126 MHz, CDCl_3) δ 140.28, 132.17, 129.19, 118.90, 108.98, 6.58. All spectral data match those previously reported. (Lewis et al., 1987)



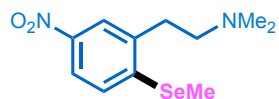
11h: Yellow solid, isolated yield 45%; ^1H NMR (400 MHz, CDCl_3) δ 7.91 (d, $J = 7.2$ Hz, 2H), 7.83 (d, $J = 8.4$ Hz, 2H), 7.56 – 7.45 (m, 5H), 2.43 (s, 3H). ^{13}C NMR (126 MHz, CDCl_3) δ 152.23, 150.35, 136.38, 130.44, 129.29, 128.65, 122.92, 122.34, 6.46. HRMS (ESI) m/z : calcd for $\text{C}_{13}\text{H}_{13}\text{N}_2\text{Se} [\text{M}+\text{H}]^+$ 277.0244, found 277.0249.



11i: White solid, isolated yield 80%; ^1H NMR (400 MHz, DMSO) δ 13.75 (s, 1H), 8.52 (s, 1H), 2.55 (s, 3H). ^{13}C NMR (126 MHz, DMSO) δ 174.33, 152.18, 144.70, 129.62, 123.99. HRMS (ESI) m/z : calcd for $\text{C}_{15}\text{H}_{19}\text{N}_2\text{O}_5\text{S} [\text{M}+\text{H}]^+$ 339.1009, found 339.1007. HRMS (ESI) m/z : calcd for $\text{C}_6\text{H}_6\text{ClN}_4\text{Se} [\text{M}+\text{H}]^+$ 248.9446, found 248.9451.



11j: Colorless oil, isolated yield 84%; ^1H NMR (400 MHz, CDCl_3) δ 8.00 (d, $J = 5.3$ Hz, 1H), 6.97 (d, $J = 5.3$ Hz, 1H), 2.45 (d, $J = 1.9$ Hz, 6H). ^{13}C NMR (126 MHz, CDCl_3) δ 169.84, 168.20, 154.00, 117.84, 6.79, 5.27. All spectral data match those previously reported. (Dhau et al., 2014)



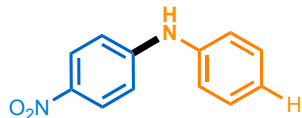
11k: Yellow oil, isolated yield 92%; ^1H NMR (500 MHz, CDCl_3) δ 8.03 – 7.94 (m, 2H), 7.35 (d, $J = 8.6$ Hz, 1H), 2.93 – 2.87 (m, 2H), 2.62 – 2.57 (m, 2H), 2.41 (s, 3H), 2.32 (s, 6H). ^{13}C NMR (126 MHz, CDCl_3) δ 145.83, 143.75, 140.41, 127.48, 123.43, 121.60, 58.82, 45.37, 33.25, 6.74. HRMS (ESI) m/z : calcd for $\text{C}_{11}\text{H}_{17}\text{N}_2\text{O}_2\text{Se} [\text{M}+\text{H}]^+$ 289.0455, found 289.0448.

3.5 General Procedure for the Amination Reaction of Arylammonium Salts (Fig. S6)

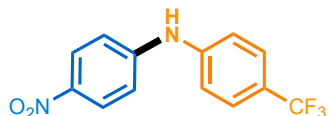
A Schlenk tube was charged with ArNH_2 (0.3 mmol), KHMDS (0.28 mL, 1M in THF) and DMF (3mL). The reaction mixture was stirred at r.t. for 5 minutes and then aryltrimethylammonium triflates (0.2 mmol) was added. After 3 h, the water (30 mL) was added to remove DMF. The aqueous layer was extracted with ethyl acetate (3×10 mL). The combined organic layer was dried over Na_2SO_4 , filtered and concentrated. The residue was purified on column chromatography or preparative TLC (silica gel) to give the product and NMR yields with mesitylene as an internal standard.



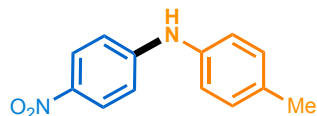
Fig.S6, related to **Scheme 2f**.



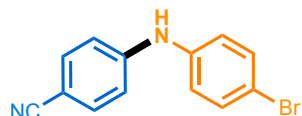
13a: Yellow oil, isolated yield 75%; ^1H NMR (500 MHz, CDCl_3) δ 8.12 (d, $J = 9.2$ Hz, 2H), 7.39 (dd, $J = 8.4, 7.5$ Hz, 2H), 7.23 – 7.19 (m, 2H), 7.17 (t, $J = 7.4$ Hz, 1H), 6.94 (d, $J = 9.2$ Hz, 2H), 6.31 (s, 1H). ^{13}C NMR (126 MHz, CDCl_3) δ 150.16, 139.77, 139.48, 129.72, 126.22, 124.65, 121.91, 113.67.; All spectral data match those previously reported. (Ding et al., 2017)



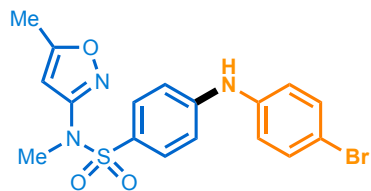
13b: Yellow oil, isolated yield 78%; ^1H NMR (500 MHz, CDCl_3) δ 8.17 (d, $J = 9.1$ Hz, 2H), 7.62 (d, $J = 8.4$ Hz, 2H), 7.27 (d, $J = 8.4$ Hz, 2H), 7.09 (d, $J = 9.2$ Hz, 2H), 6.47 (s, 1H). ^{13}C NMR (126 MHz, CDCl_3) δ 148.29, 143.18, 141.02, 127.01 (q, $^3J_{\text{C-F}} = 3.7$ Hz), 126.13, 125.40 (q, $^2J_{\text{C-F}} = 33.0$ Hz), 124.05 (q, $^1J_{\text{C-F}} = 271.4$ Hz), 119.59, 115.31. HRMS (EI) m/z : calcd for $\text{C}_{13}\text{H}_9\text{N}_2\text{O}_2\text{F}_3$ [M^+] 282.0611, found 282.0606.



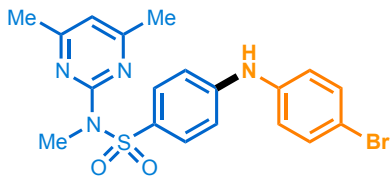
13c: White solid, isolated yield 40%; ^1H NMR (300 MHz, CDCl_3) δ 8.10 (d, $J = 9.1$ Hz, 2H), 7.20 (d, $J = 8.1$ Hz, 2H), 7.11 (d, $J = 8.3$ Hz, 2H), 6.86 (d, $J = 9.2$ Hz, 2H), 6.22 (s, 1H), 2.36 (s, 3H). ^{13}C NMR (126 MHz, CDCl_3) δ 150.83, 139.48, 136.73, 134.86, 130.31, 126.28, 122.71, 113.22, 20.93.; All spectral data match those previously reported. (Fors et al., 2009)



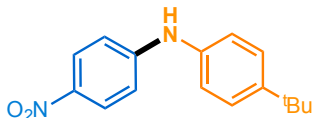
13d: Colorless oil, isolated yield 70%; ^1H NMR (400 MHz, CDCl_3) δ 7.49 (d, $J = 8.8$ Hz, 2H), 7.45 (d, $J = 8.8$ Hz, 2H), 7.05 (d, $J = 8.8$ Hz, 2H), 6.96 (d, $J = 8.8$ Hz, 2H), 6.07 (s, 1H). ^{13}C NMR (126 MHz, CDCl_3) δ 147.42, 139.25, 133.85, 132.66, 122.56, 119.65, 116.29, 115.28, 102.28. All spectral data match those previously reported. (Miti et al., 2011)



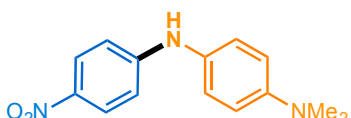
13e: Colorless oil, isolated yield 80%; ^1H NMR (400 MHz, CDCl_3) δ 7.55 (d, $J = 8.8$ Hz, 2H), 7.44 (d, $J = 8.7$ Hz, 2H), 7.03 (d, $J = 8.7$ Hz, 2H), 6.93 (d, $J = 8.9$ Hz, 2H), 6.49 (d, $J = 0.7$ Hz, 1H), 6.11 (s, 1H), 3.24 (s, 3H), 2.37 (d, $J = 0.5$ Hz, 3H). ^{13}C NMR (126 MHz, CDCl_3) δ 170.21, 161.05, 148.39, 139.14, 132.65, 129.33, 126.67, 122.81, 116.47, 114.78, 97.69, 35.02, 12.67. HRMS (ESI) m/z : calcd for $\text{C}_{17}\text{H}_{17}\text{N}_3\text{O}_3\text{SBr}$ [$\text{M}+\text{H}]^+$ 422.0169, found 422.0177.



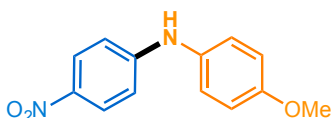
13f: Colorless oil, isolated yield 55%; ^1H NMR (400 MHz, CDCl_3) δ 7.95 (d, $J = 8.9$ Hz, 2H), 7.42 (d, $J = 8.8$ Hz, 2H), 7.04 – 6.99 (m, 2H), 6.95 (d, $J = 8.9$ Hz, 2H), 6.57 (s, 1H), 6.07 (s, 1H), 3.64 (s, 3H), 2.32 (s, 6H). ^{13}C NMR (126 MHz, CDCl_3) δ 167.17, 158.31, 147.32, 139.71, 132.55, 131.06, 130.92, 122.10, 115.71, 114.26, 114.10, 33.82, 23.69. HRMS (ESI) m/z : calcd for $\text{C}_{19}\text{H}_{20}\text{N}_4\text{O}_2\text{BrS} [\text{M}+\text{H}]^+$ 447.0485, found 447.0482.



13g: Yellow oil, isolated yield 45%; ^1H NMR (400 MHz, CDCl_3) δ 8.10 (d, $J = 9.2$ Hz, 2H), 7.41 (d, $J = 8.5$ Hz, 2H), 7.15 (d, $J = 8.5$ Hz, 2H), 6.90 (d, $J = 9.2$ Hz, 2H), 6.27 (s, 1H), 1.34 (s, 9H). ^{13}C NMR (126 MHz, CDCl_3) δ 150.63, 148.00, 139.45, 136.67, 126.56, 126.24, 122.03, 113.30, 34.48, 31.34. All spectral data match those previously reported. (Kayama et al., 2016)



13h: Yellow solid, isolated yield 62%; ^1H NMR (400 MHz, DMSO) δ 9.02 (s, 1H), 8.02 (d, $J = 9.2$ Hz, 2H), 7.08 (d, $J = 8.6$ Hz, 2H), 6.79 (dd, $J = 15.7, 7.7$ Hz, 4H), 2.89 (s, 6H). ^{13}C NMR (126 MHz, DMSO) δ 152.74, 147.92, 136.62, 128.58, 126.35, 124.22, 113.30, 111.94, 40.41. All spectral data match those previously reported. (Novak et al., 1989)



13i: Yellow solid, isolated yield 55%; ^1H NMR (400 MHz, CDCl_3) δ 8.08 (d, $J = 9.2$ Hz, 2H), 7.16 (d, $J = 8.8$ Hz, 2H), 6.93 (d, $J = 8.9$ Hz, 2H), 6.76 (d, $J = 9.2$ Hz, 2H), 6.18 (s, 1H), 3.83 (s, 3H). ^{13}C NMR (126 MHz, CDCl_3) δ 157.43, 151.69, 139.09, 131.97, 126.30, 125.49, 114.95, 112.60, 55.53. All spectral data match those previously reported. (McNulty et al., 2007)

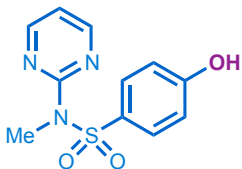
3.6 Procedure for the Late-stage Diversification of Pharmaceutical Ammonium Derivative (Fig. 4)

Various aryl-heteroatom bonds formation products **3mp**, **5j**, **7o**, **9a**, **11h**, **13h** were prepared following a similar procedure above. **14b**, **14c**, **14d** were prepared with previously reported methods. (Lang et al., 2009)

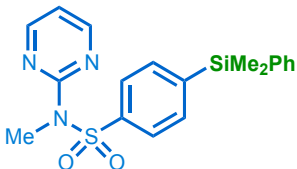
Procedure for the Preparation of 14a: A flask was charged with aryltrimethylammonium triflates (0.2 mmol), 2-mercaptoethanol (0.3 mmol), KHMS (0.6 mmol, 2M in THF) and DMF (3 mL). The reaction mixture was stirred at r.t. for 3 h to give a yellow suspended solution. Then 1M HCl (30 mL) was added and the aqueous layer was extracted with ethyl acetate (3 x 10 mL). The combined organic layer was dried over Na_2SO_4 , filtered and concentrated. The residue was purified on column chromatography to give the product and NMR yields with mesitylene as an internal standard.



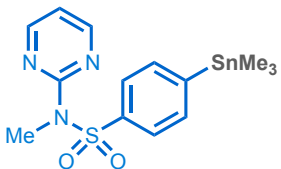
3mp: Colorless oil, isolated yield 73%; ^1H NMR (300 MHz, CDCl_3) δ 8.46 (d, $J = 4.8$ Hz, 2H), 7.94 (d, $J = 8.5$ Hz, 2H), 7.28 (d, $J = 8.8$ Hz, 2H), 6.88 (t, $J = 4.8$ Hz, 1H), 3.67 (s, 3H), 2.96 (t, $J = 7.4$ Hz, 2H), 1.68 (dt, $J = 14.8, 7.2$ Hz, 2H), 1.48 – 1.36 (m, 2H), 1.25 (s, 16H), 0.87 (t, $J = 6.5$ Hz, 3H). ^{13}C NMR (126 MHz, CDCl_3) δ 158.71, 157.44, 145.16, 136.23, 128.77, 125.87, 115.37, 34.15, 32.01, 31.91, 29.62, 29.56, 29.47, 29.33, 29.13, 28.89, 28.63, 22.69, 14.11. HRMS (EI) m/z : calcd for $\text{C}_{23}\text{H}_{36}\text{N}_3\text{O}_2\text{S}_2$ [M $^+$] 450.2243, found 450.2268.



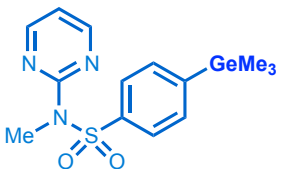
14a: Colorless oil, isolated yield 78%; ^1H NMR (300 MHz, CDCl_3) δ 8.45 (d, $J = 4.8$ Hz, 2H), 7.97 – 7.90 (m, 2H), 6.90 – 6.83 (m, 3H), 3.65 (s, 3H). ^{13}C NMR (126 MHz, CDCl_3) δ 160.23, 158.69, 157.48, 131.33, 130.86, 115.39, 115.25, 34.20. HRMS (ESI) m/z : calcd for $\text{C}_{11}\text{H}_{12}\text{N}_3\text{O}_3\text{S}$ [M+H] $^+$ 266.0594, found 266.0594.



5j: Colorless oil, isolated yield 75%; ^1H NMR (300 MHz, CDCl_3) δ 8.46 (d, $J = 4.8$ Hz, 2H), 8.02 (d, $J = 8.3$ Hz, 2H), 7.62 (d, $J = 8.3$ Hz, 2H), 7.52 – 7.44 (m, 2H), 7.40 – 7.32 (m, 3H), 6.88 (t, $J = 4.8$ Hz, 1H), 3.68 (s, 3H), 0.57 (s, 6H). ^{13}C NMR (126 MHz, CDCl_3) δ 158.76, 157.47, 145.15, 140.86, 136.78, 134.14, 129.53, 128.01, 127.19, 115.44, 34.25, -2.63. HRMS (EI) m/z : calcd for $\text{C}_{19}\text{H}_{22}\text{N}_3\text{O}_2\text{SSi}$ [M $^+$] 384.1197, found 384.1195.



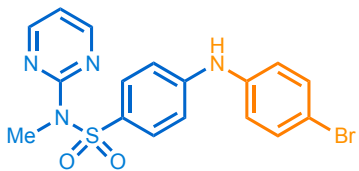
7o: Colorless oil, isolated yield 43%; ^1H NMR (300 MHz, CDCl_3) δ 8.46 (d, $J = 4.8$ Hz, 2H), 7.99 (d, $J = 7.4$ Hz, 2H), 7.60 (d, $J = 7.4$ Hz, 2H), 6.87 (t, $J = 4.8$ Hz, 1H), 3.68 (s, 3H), 0.31 (s, 9H). ^{13}C NMR (126 MHz, CDCl_3) δ 158.77, 157.46, 150.06, 140.10, 135.72, 127.10, 115.39, 34.23, -9.46. HRMS (EI) m/z : calcd for $\text{C}_{14}\text{H}_{20}\text{O}_2\text{N}_3\text{SnS}$ [M $^+$] 414.0293, found 414.0300.



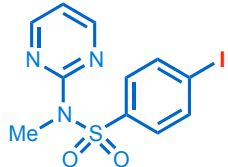
9a: Colorless oil, isolated yield 60%; ^1H NMR (300 MHz, CDCl_3) δ 8.47 (d, $J = 4.8$ Hz, 2H), 8.02 (d, $J = 8.3$ Hz, 2H), 7.58 (d, $J = 8.3$ Hz, 2H), 6.88 (t, $J = 4.8$ Hz, 1H), 3.68 (s, 3H), 0.40 (s, 9H). ^{13}C NMR (126 MHz, CDCl_3) δ 158.78, 157.46, 149.73, 140.12, 132.97, 127.28, 115.38, 34.23, -1.91. HRMS (EI) m/z : calcd for $\text{C}_{14}\text{H}_{19}\text{N}_3\text{O}_2\text{GeS}$ $[\text{M}^+]$ 367.0404, found 367.0404.



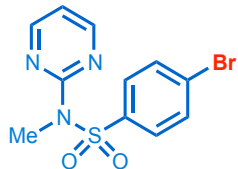
11h: Colorless oil, isolated yield 43%; ^1H NMR (400 MHz, CDCl_3) δ 8.45 (d, $J = 4.8$ Hz, 2H), 7.92 (d, $J = 8.4$ Hz, 2H), 7.42 (d, $J = 8.5$ Hz, 2H), 6.88 (t, $J = 4.8$ Hz, 1H), 3.67 (s, 3H), 2.38 (s, 3H). ^{13}C NMR (126 MHz, CDCl_3) δ 158.67, 157.46, 140.03, 137.37, 128.73, 128.39, 115.43, 34.16, 6.54. HRMS (ESI) m/z : calcd for $\text{C}_{12}\text{H}_{14}\text{N}_3\text{O}_2\text{SSe}$ $[\text{M}+\text{H}]^+$ 343.9972, found 343.9994.



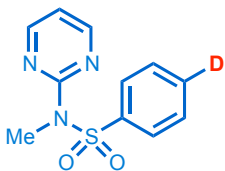
13h: Colorless oil, isolated yield 63%; ^1H NMR (400 MHz, CDCl_3) δ 8.46 (d, $J = 4.8$ Hz, 2H), 7.92 (d, $J = 8.9$ Hz, 2H), 7.43 (d, $J = 8.8$ Hz, 2H), 7.03 (d, $J = 8.7$ Hz, 2H), 6.95 (d, $J = 8.9$ Hz, 2H), 6.87 (t, $J = 4.8$ Hz, 1H), 3.65 (s, 3H). ^{13}C NMR (126 MHz, CDCl_3) δ 158.85, 157.42, 147.64, 139.53, 132.57, 130.66, 130.33, 122.34, 115.95, 115.19, 114.27, 34.16. HRMS (ESI) m/z : calcd for $\text{C}_{17}\text{H}_{16}\text{N}_4\text{O}_2\text{SBr}$ $[\text{M}+\text{H}]^+$ 419.0172, found 419.0169.



14b: Colorless oil, isolated yield 84%; ^1H NMR (400 MHz, CDCl_3) δ 8.46 (d, $J = 4.8$ Hz, 2H), 7.84 (d, $J = 8.8$ Hz, 2H), 7.79 (d, $J = 8.8$ Hz, 2H), 6.90 (s, 1H), 3.67 (s, 3H). ^{13}C NMR (126 MHz, CDCl_3) δ 158.51, 157.48, 140.12, 137.68, 129.81, 115.62, 100.38, 34.15. HRMS (ESI) m/z : calcd for $\text{C}_{11}\text{H}_{11}\text{N}_3\text{O}_2\text{SI}$ $[\text{M}+\text{H}]^+$ 375.9611, found 375.9618.



14c: Colorless oil, isolated yield 80%; ^1H NMR (400 MHz, CDCl_3) δ 8.46 (d, $J = 4.8$ Hz, 2H), 7.94 (d, $J = 8.7$ Hz, 2H), 7.62 (d, $J = 8.8$ Hz, 2H), 6.90 (t, $J = 4.8$ Hz, 1H), 3.67 (s, 3H). ^{13}C NMR (151 MHz, CDCl_3) δ 158.50, 157.53, 139.38, 131.74, 130.01, 127.94, 115.69, 34.20. HRMS (ESI) m/z : calcd for $\text{C}_{11}\text{H}_{11}\text{N}_3\text{O}_2\text{SBr}$ $[\text{M}+\text{H}]^+$ 327.9750, found 327.9751.



14d: Colorless oil, isolated yield 87%; ^1H NMR (500 MHz, CDCl_3) δ 8.45 (d, $J = 4.8$ Hz, 2H), 8.07 (d, $J = 8.5$ Hz, 2H), 7.48 (d, $J = 8.3$ Hz, 2H), 6.87 (t, $J = 4.8$ Hz, 1H), 3.69 (s, 3H). ^{13}C NMR (126 MHz, CDCl_3) δ 158.71, 157.45, 140.43, 128.45, 128.34, 128.32, 115.44, 34.19. HRMS (ESI) m/z : calcd for $\text{C}_{11}\text{H}_{11}\text{N}_3\text{O}_2\text{SD} [\text{M}+\text{H}]^+$ 251.0708, found 251.0712.

3.7 Procedure for Click Reaction of NBD-ammonium Salt and Biological Thiols (Fig. 5)

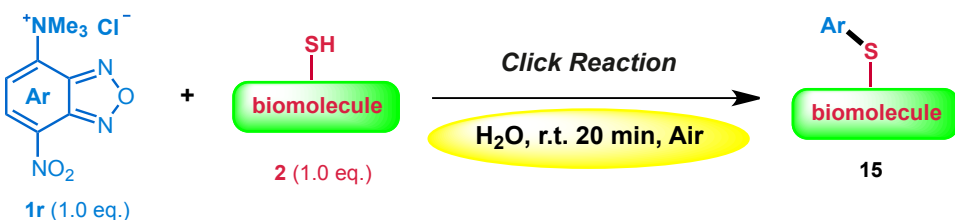


Fig.S7, related to **Scheme 4a**.

3.7.1 An open-air vial was charged with NBD-ammonium salt **1r** (0.01 mmol; for **15d**: 0.005 mmol), biological thiols (0.01 mmol; for **15d**: 0.005 mmol) and H_2O (1 mL). The reaction mixture was stirred at r.t. for 20 minutes and then determined by LCMS.

3.7.2 An open-air vial was charged with NBD-ammonium salt **1r** (0.05 mmol), biological thiols (**2r**, **2v**, **2w**) (0.05 mmol) and D_2O (0.5 mL). The reaction mixture was stirred at r.t. for 20 minutes and then was analyzed by ^1H -NMR in DMSO-d_6 - D_2O (4:1, v/v). When Cys or Hcy was the reactant, the H^{a} and H^{b} protons of the product NBD moiety showed upfield shifts, especially for H^{a} , which were different from NBD-SR (GSH as reactant) was being formed. (Chen et al., 2016) (**Fig. S8**)

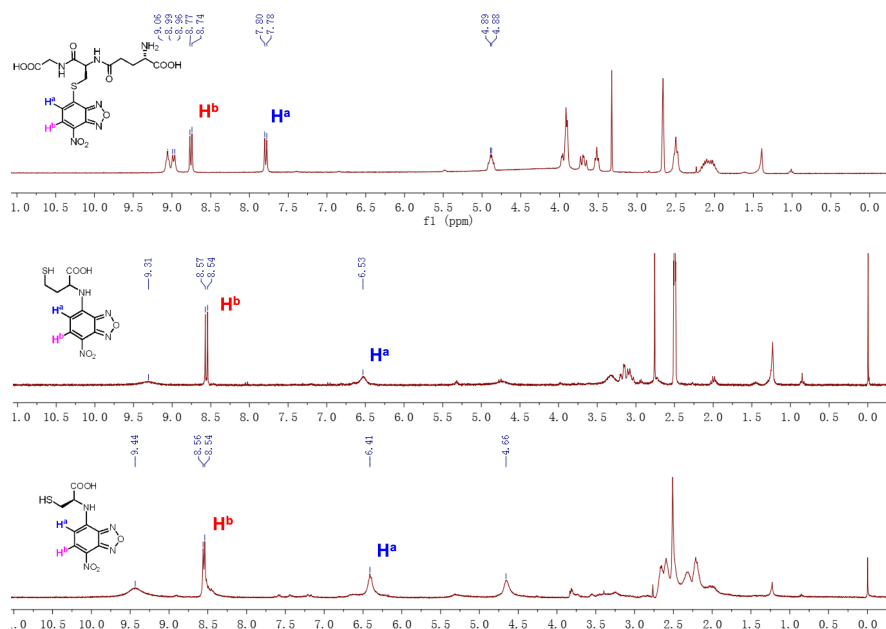


Fig.S8, related to Scheme 4a.

3.7.3 For the procedure of fluorescence measurement: stock solutions of probe (**1r**) and biological thiols were freshly prepared in H₂O prior to each experiment. 5eq. biological thiols (250μM) were added to separate portions of the probe (50μM) solution and mixed thoroughly. The reaction mixture was shaken uniformly before absorption and fluorescence spectra were measured.

3.8 Procedure for on-DNA Reactions

3.8.1 Headpiece Structure (Fig. S9)

DNA headpiece HP-NH₂ (5'-/5phos/GAGTCA/iSp9/iUniAmM/iSp9/TGACTCCC-3', Figure 1) was obtained from Biosearch Technologies, Novato, CA.

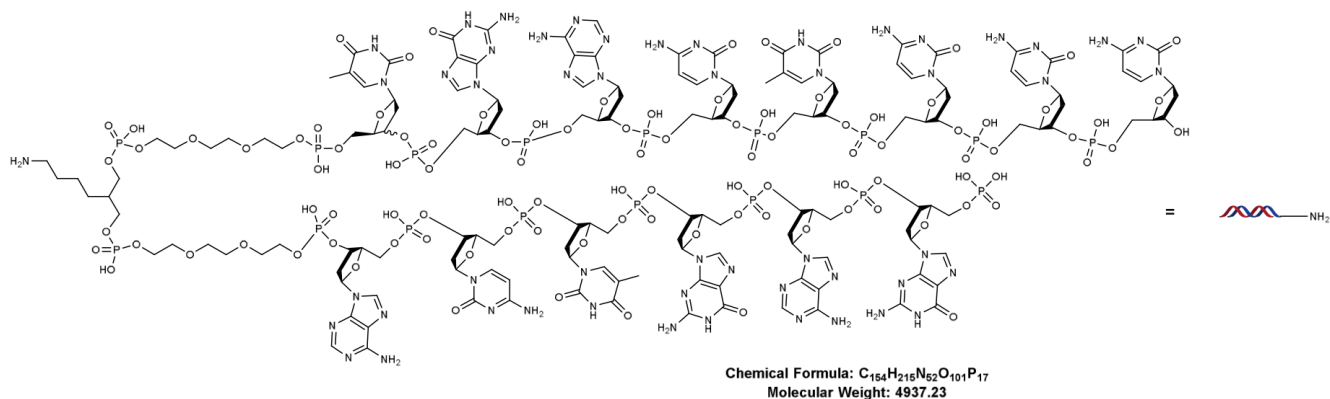


Fig.S9, related to Scheme 5.

3.8.2 Preparation of HP-Ar-N⁺Me₃Cl⁻

Materials

Headpiece: 2 mM in water

B: 200 mM in water

K₂CO₃: 200 mM in water

Procedure

- 1) To the headpiece in H₂O (100 nmol, 50 μL), was added 100 eq. of K₂CO₃ (in 50 μL H₂O) and 60 eq. of ammonium salt **1s** (in 30 μL H₂O). The mixture was vortexed.
- 2) React at room temperature for 10 h.
- 3) Add 5 M NaCl solution (10 % by volume) and cold ethanol (2.5 times by volume, ethanol stored at -20°C). The mixture was stored at a -80°C freezer for more than 30 minutes.
- 4) Centrifuge the sample for around 30 minutes at 4°C in a microcentrifuge at 10000 rpm. The above supernatant was removed and the pellet (precipitate) was cooled in liquid nitrogen and then placed on a lyophilizer. After lyophilization, the dry pellet was recovered.
- 5) To gain a higher yield, the dry pellet was solute in water (50 μL), then repeat step 1-4.

Molecular Weight: 5151.65

68% conversion determined by LCMS.

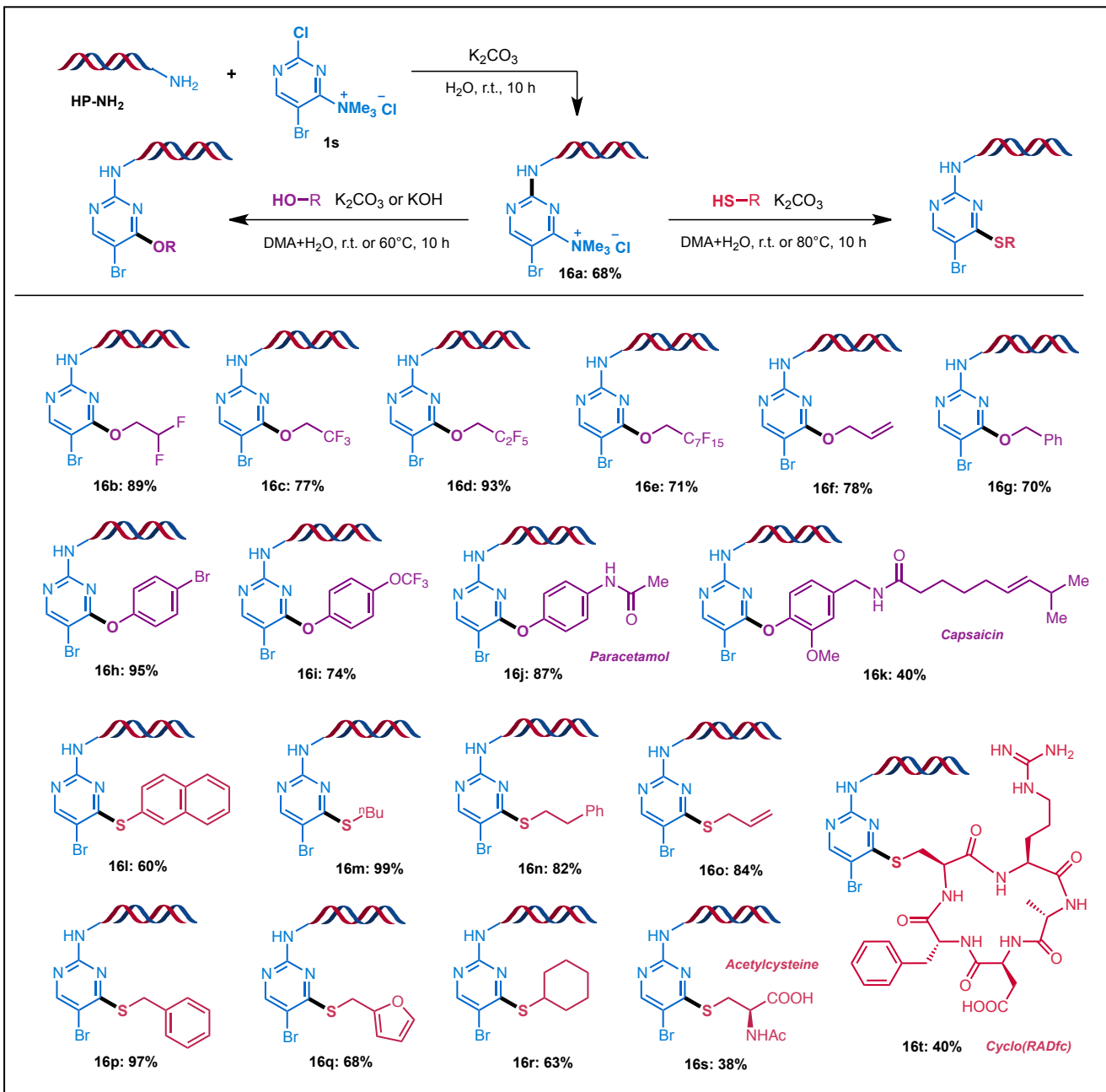


Fig.S10, related to **Scheme 5**.

3.8.3 C–O bond formations of arylammonium salts on DNA

Materials

16a: 1 mM in water

ROH: 200 mM in DMA

K₂CO₃ (or **KOH**): 1M in water

Procedure

- 1) To **16a** solution (5 nmol, 5 µL), was added 35µL H₂O, 1000 eq. of ROH (25 µL) and 1000 eq. of K₂CO₃ (for

16c–f, 16i–k) or KOH (for **16b, 16g–h**) (5 μ L). The mixture was vortexed.

2) React at room temperature (or 60°C for **16h–k**) for 10 h.

3) Add 5 M NaCl solution (10 % by volume) and cold ethanol (2.5 times by volume, ethanol stored at -20°C). The mixture was stored at a -80°C freezer for more than 30 minutes.

4) Centrifuge the sample for around 30 minutes at 4 °C in a microcentrifuge at 10000 rpm. The above supernatant was removed and the pellet (precipitate) was cooled in liquid nitrogen and then placed on a lyophilizer. After lyophilization, the dry pellet was recovered.

Conversion determined by LCMS.

3.8.4 C–S bond formations of arylammonium salts on DNA

Materials

16a: 1 mM in water

RSH: 200 mM in DMA

K₂CO₃: 200 mM in water

Procedure

1) To **16a** solution (5 nmol, 5 μ L), was added 35 μ L H₂O, 1000 eq. of RSH (25 μ L) and 200 eq. of K₂CO₃ (5 μ L). The mixture was vortexed.

2) React at room temperature (or 80°C for **16s, 16t**) for 10 h.

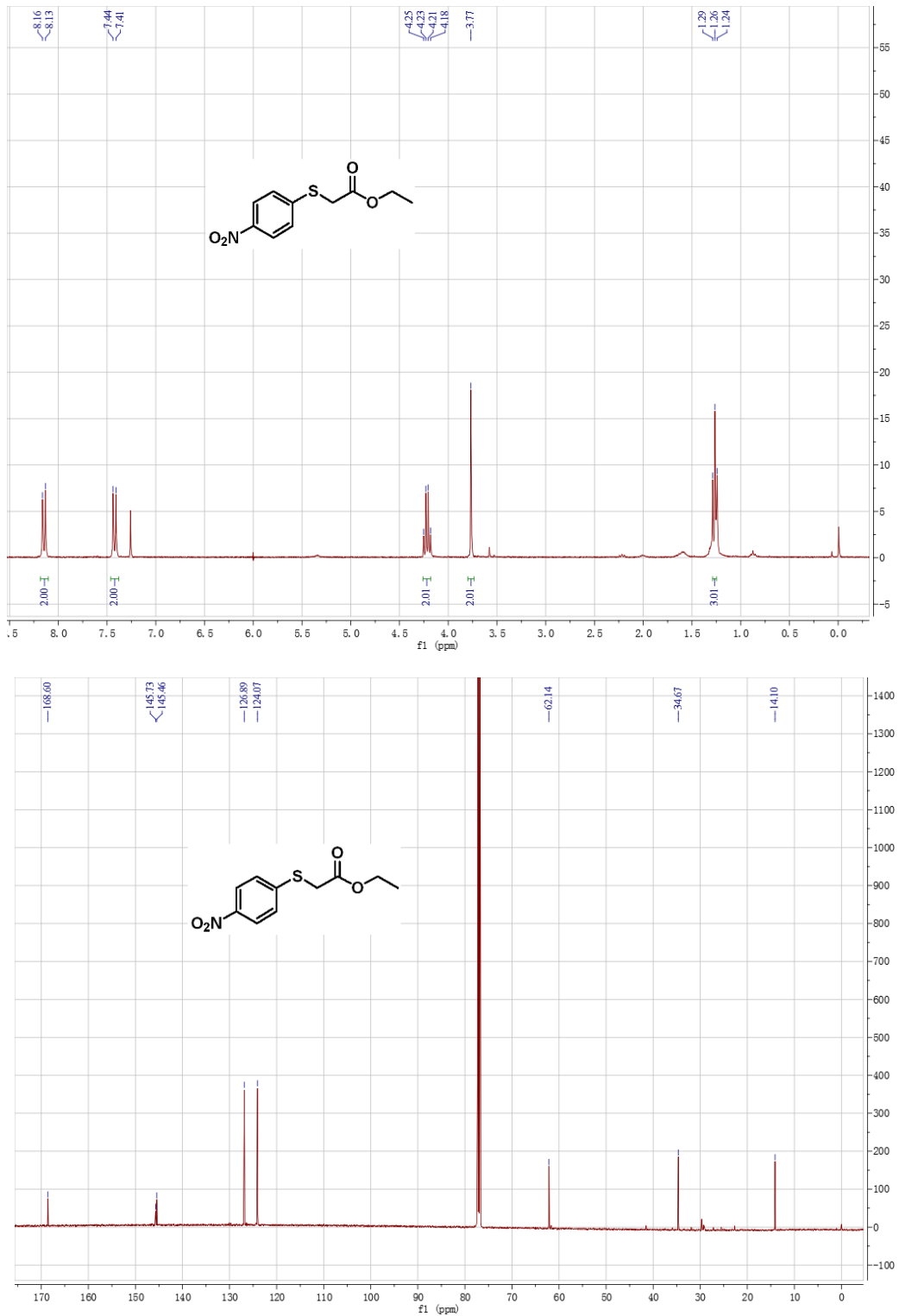
3) Add 5 M NaCl solution (10 % by volume) and cold ethanol (2.5 times by volume, ethanol stored at -20°C). The mixture was stored at a -80°C freezer for more than 30 minutes.

4) Centrifuge the sample for around 30 minutes at 4 °C in a microcentrifuge at 10000 rpm. The above supernatant was removed and the pellet (precipitate) was cooled in liquid nitrogen and then placed on a lyophilizer. After lyophilization, the dry pellet was recovered.

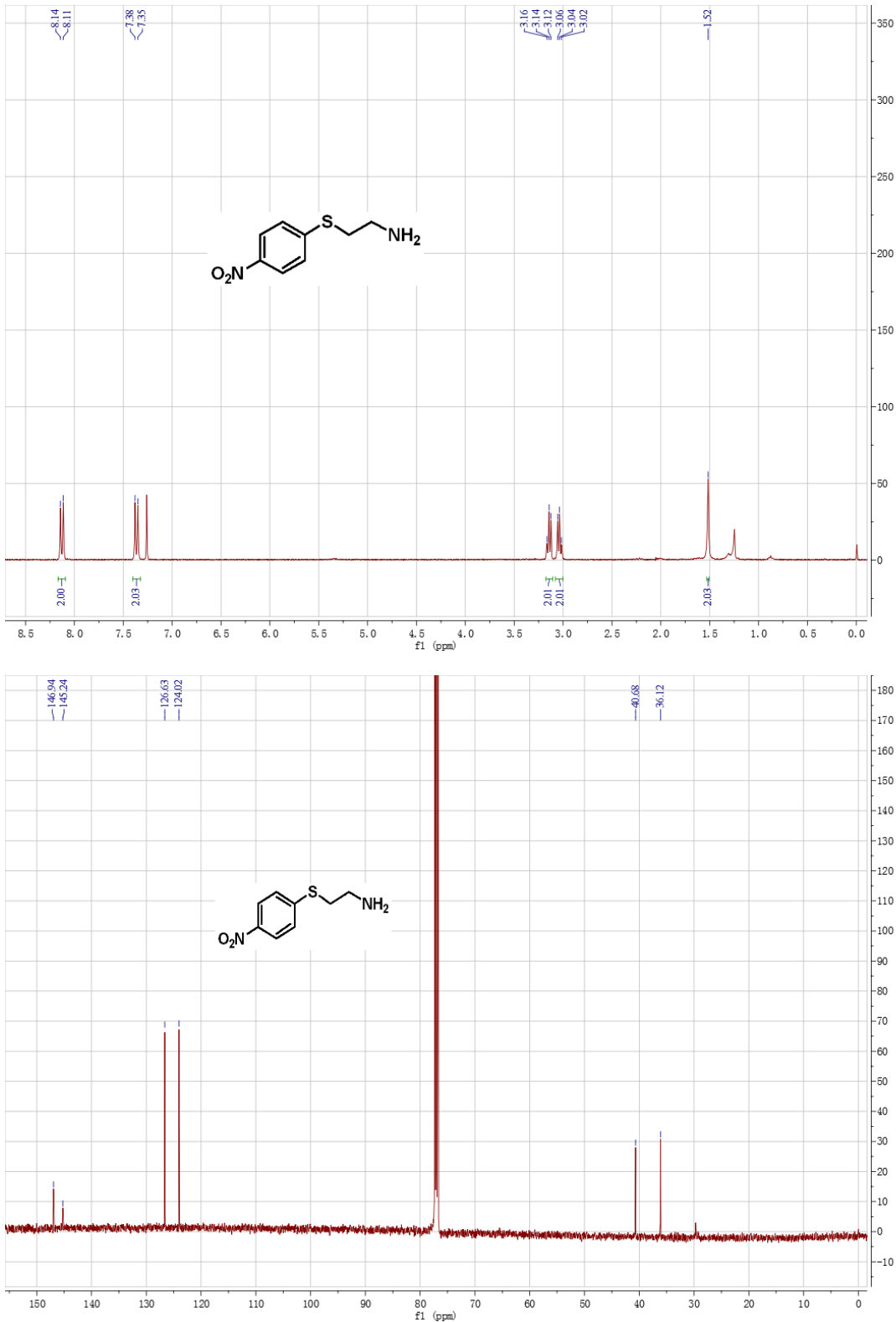
Conversion determined by LCMS.

4. Copies of NMR Spectrums for All Compounds

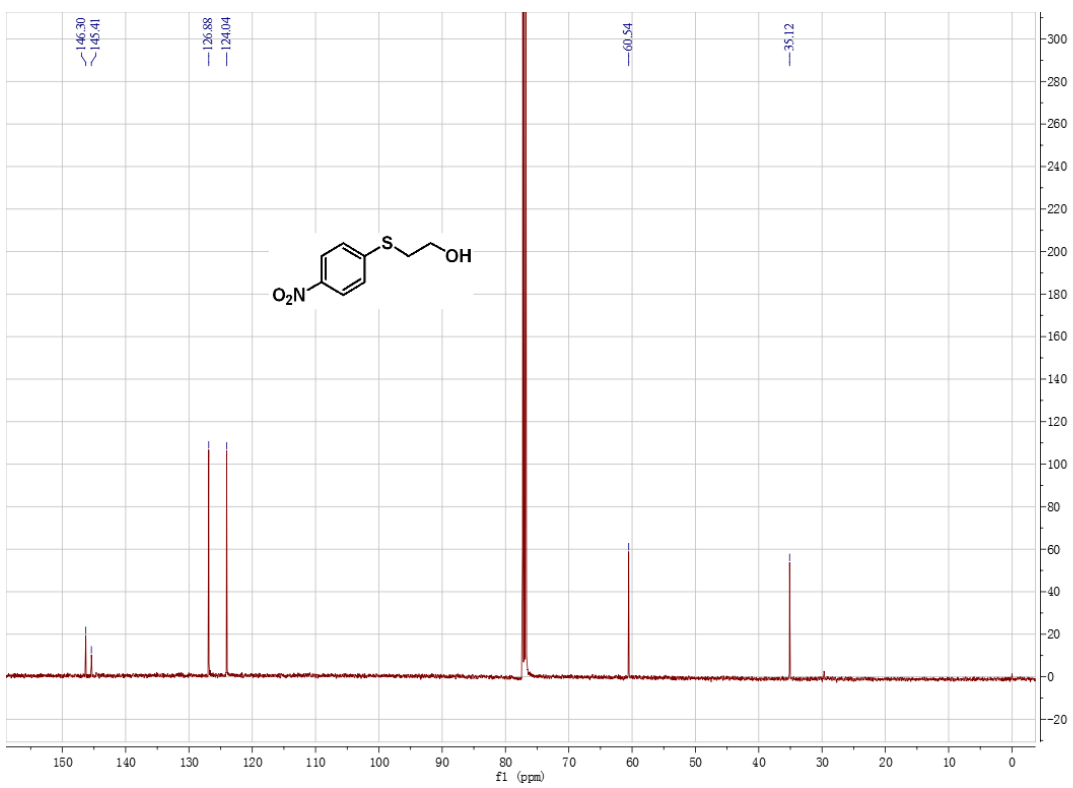
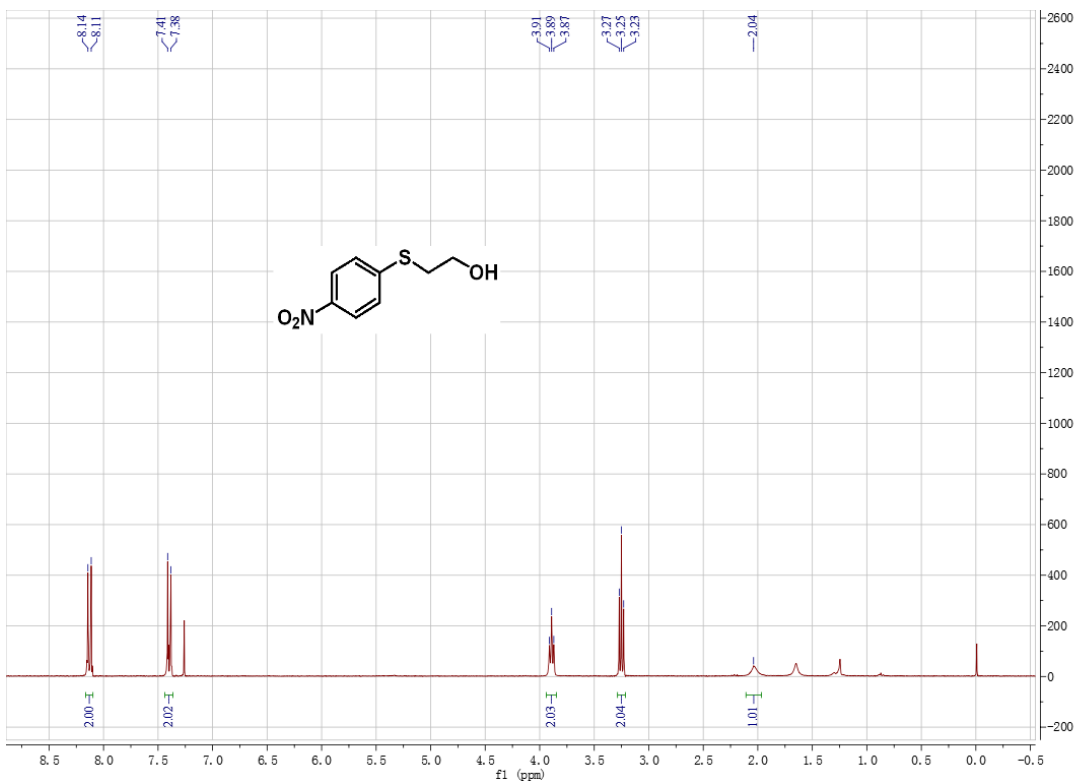
Compound 3aa



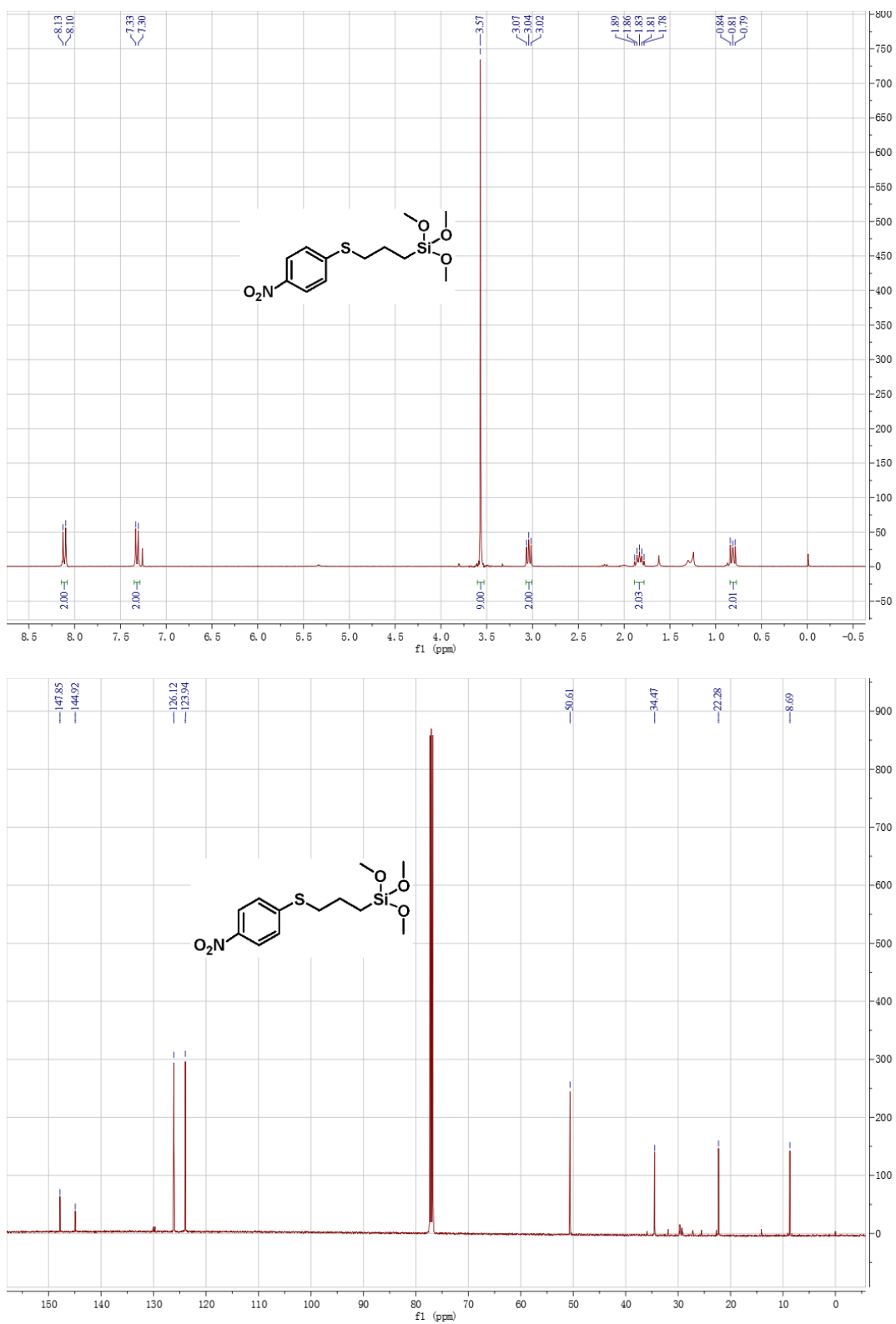
Compound 3ab



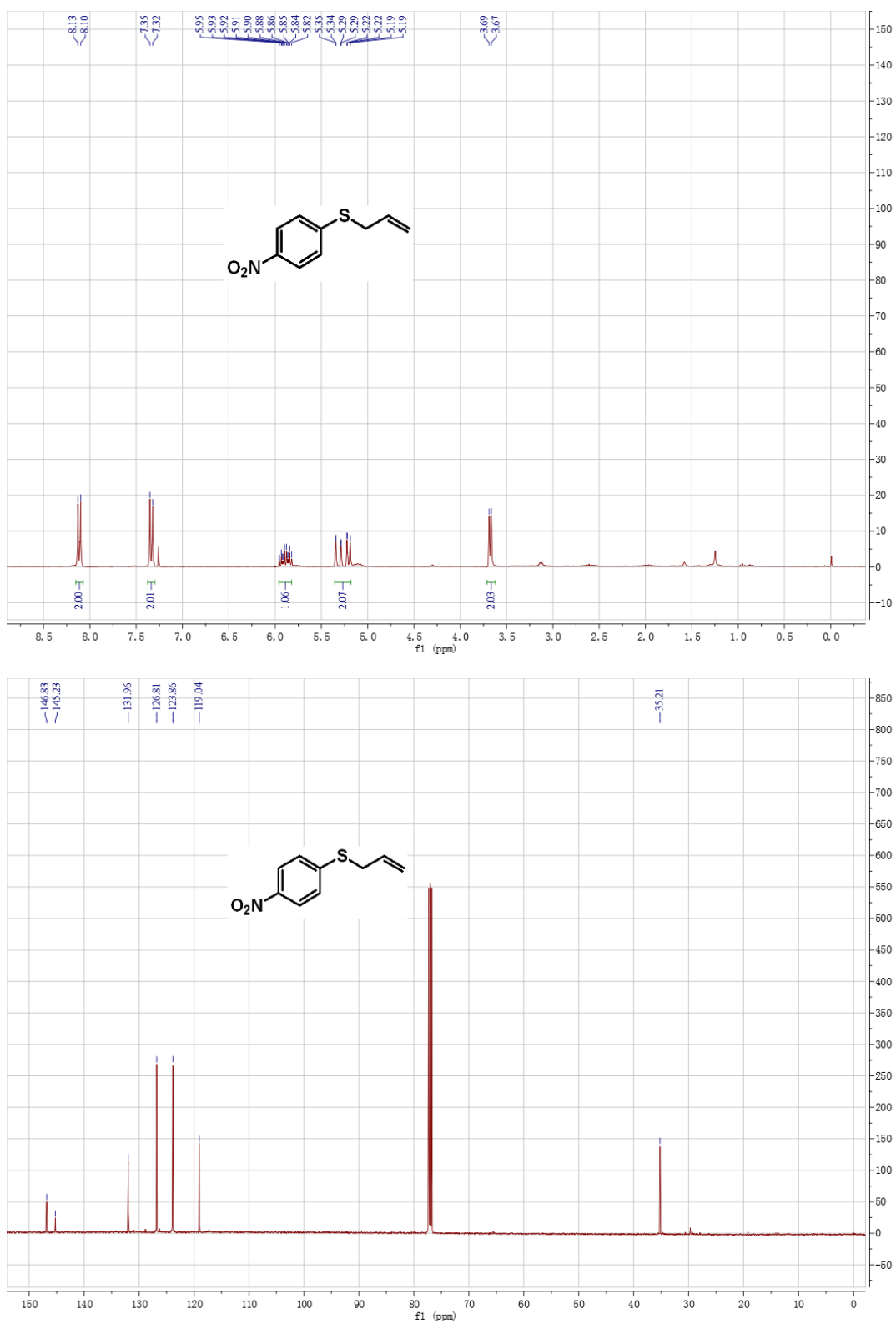
Compound 3ac



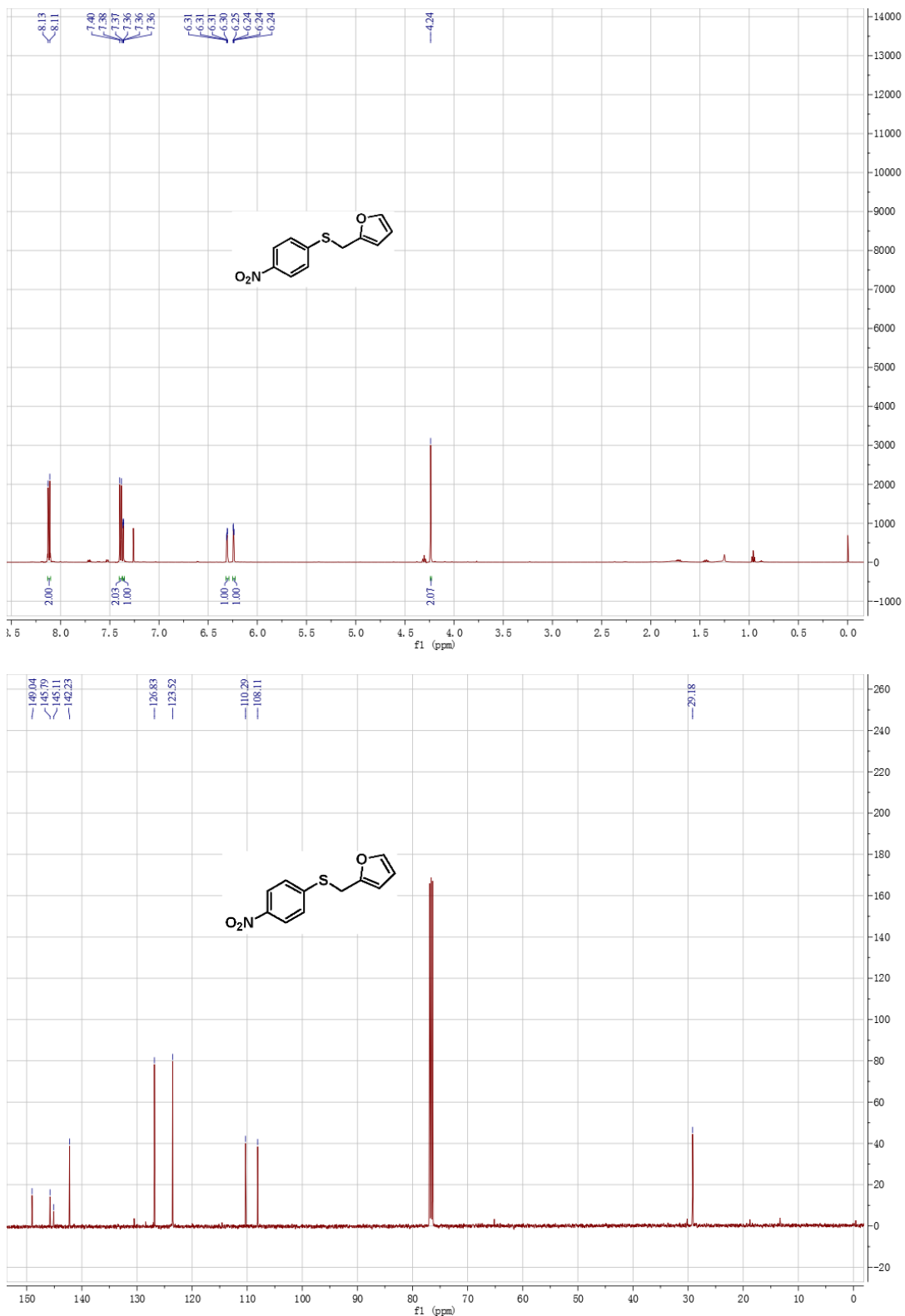
Compound 3ad



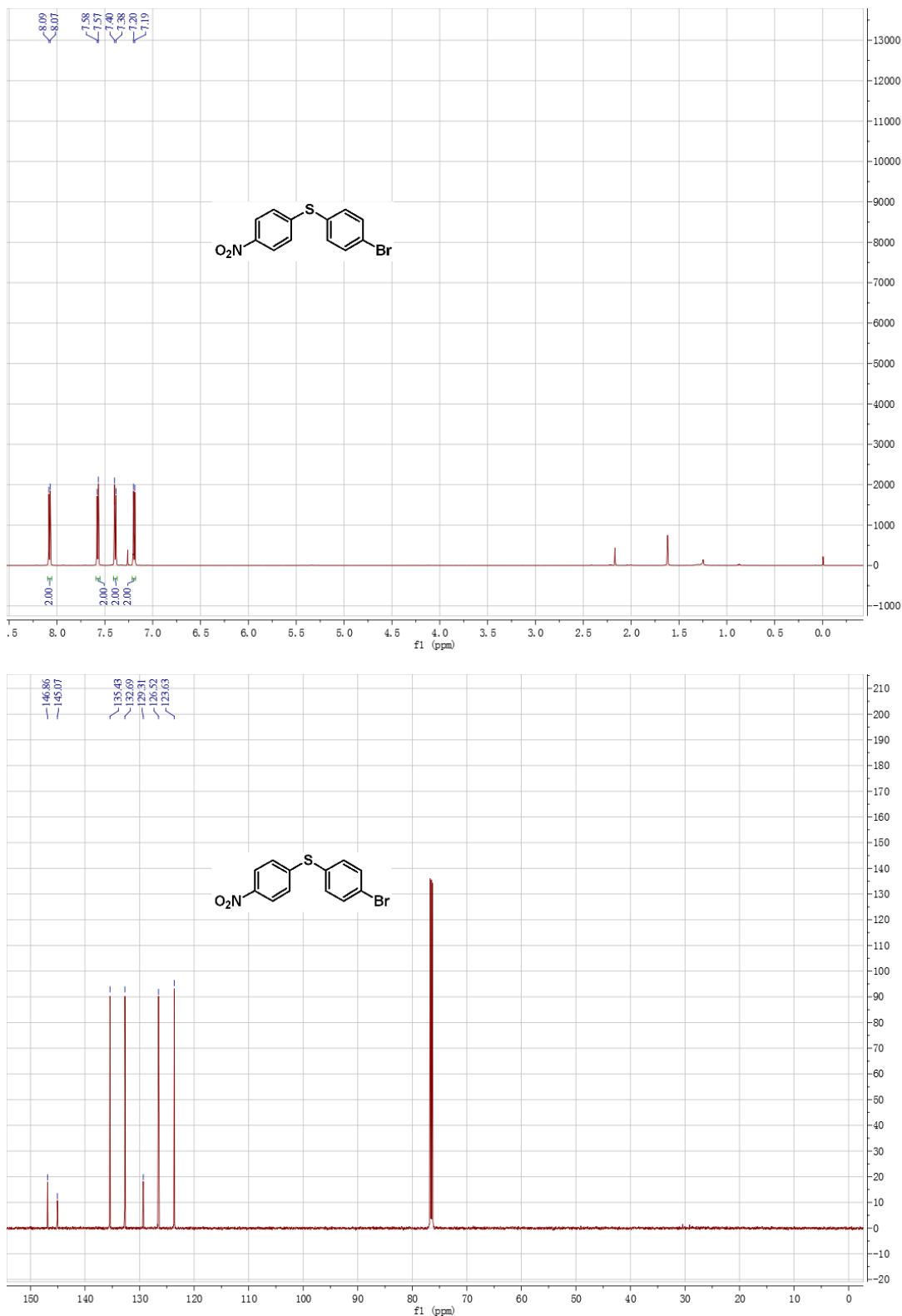
Compound 3ae



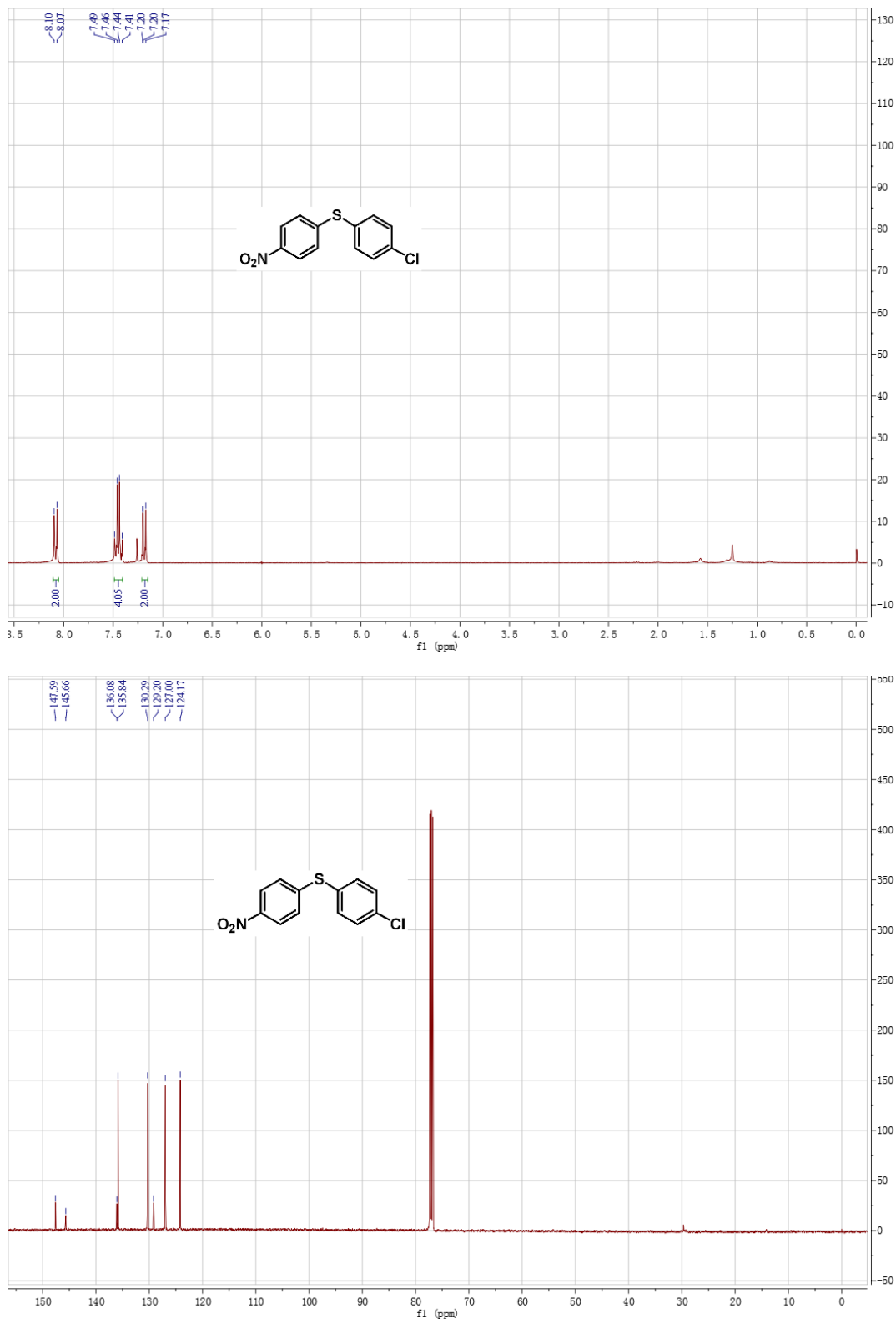
Compound 3af



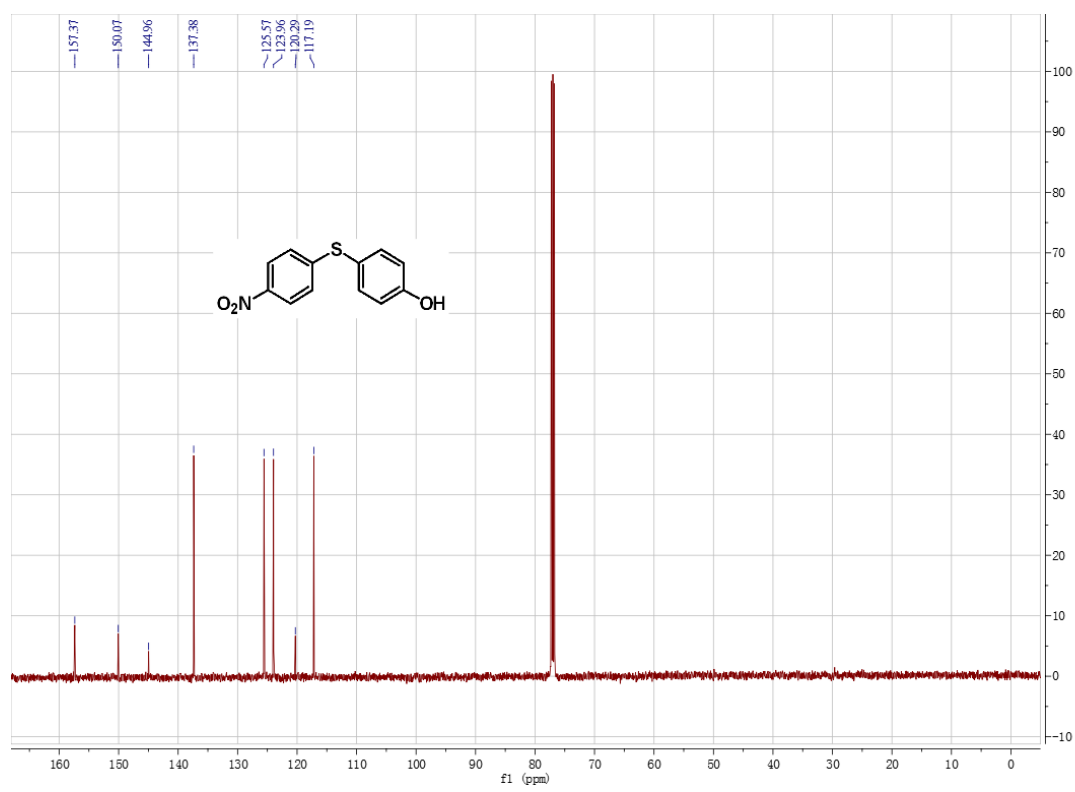
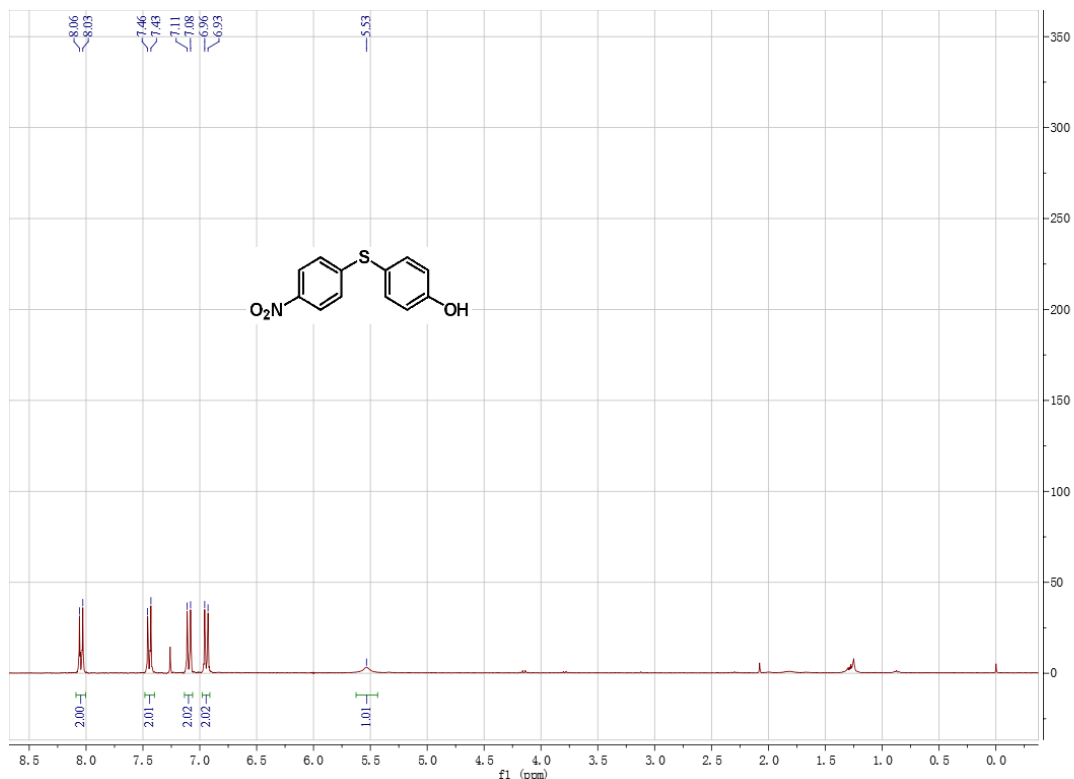
Compound 3ag



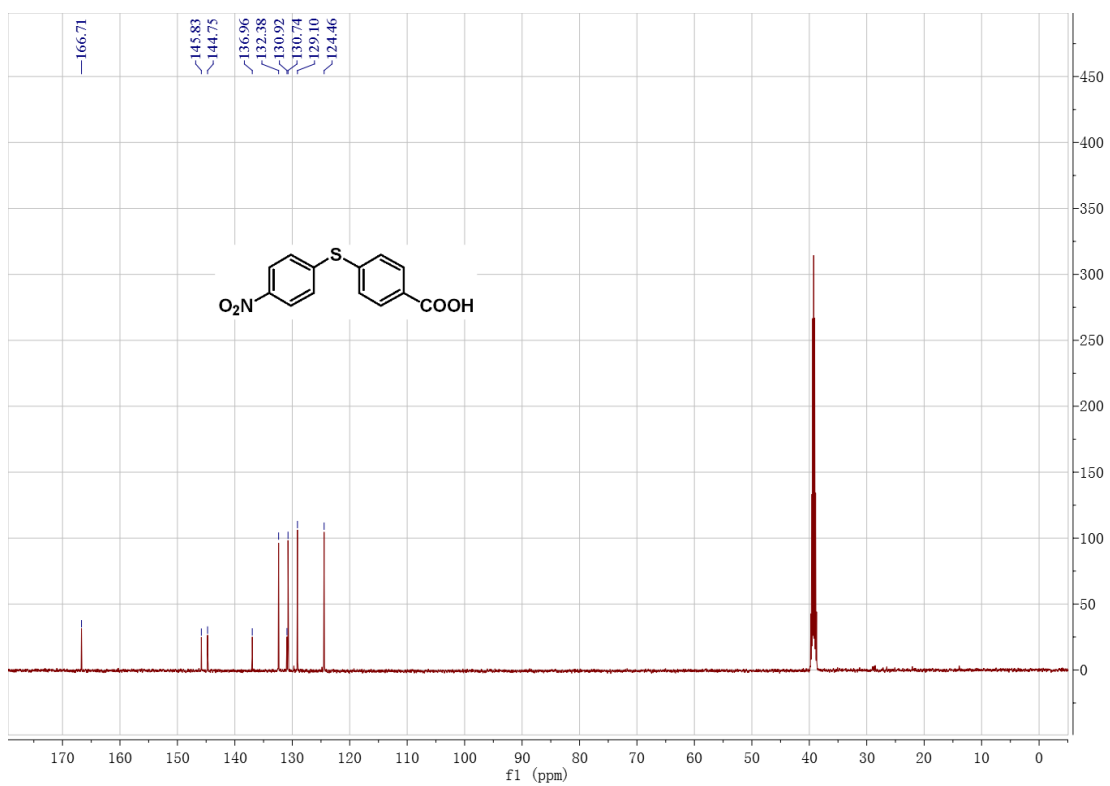
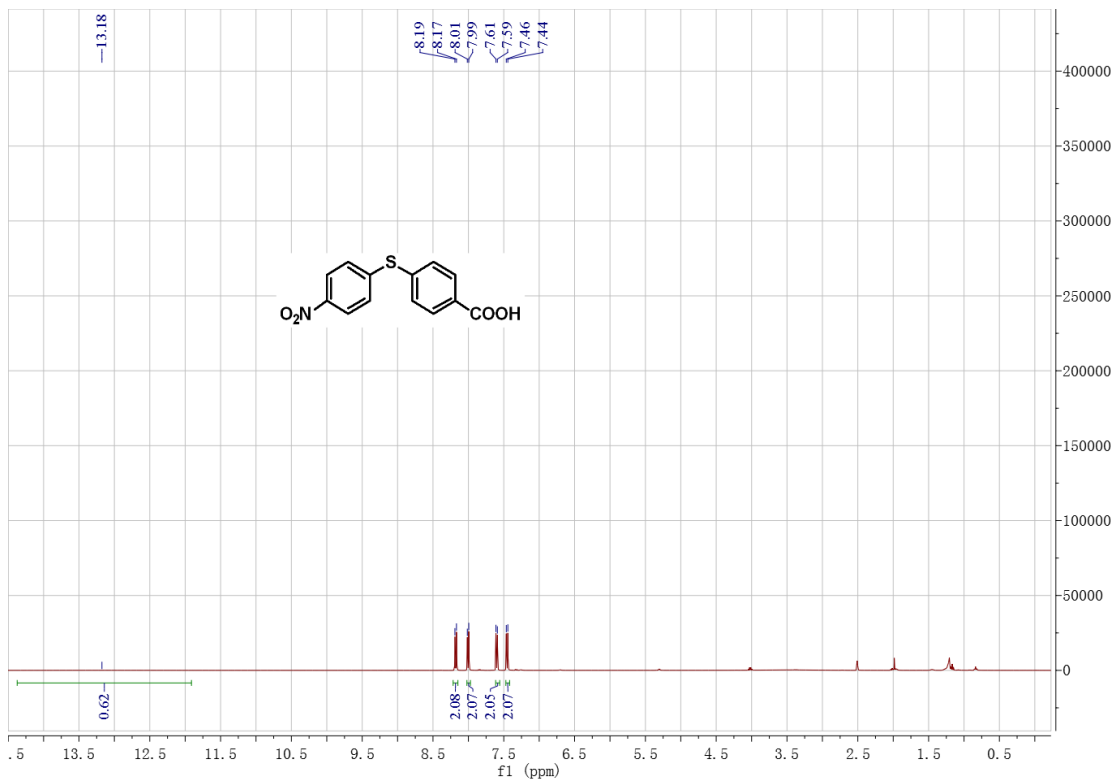
Compound 3ah



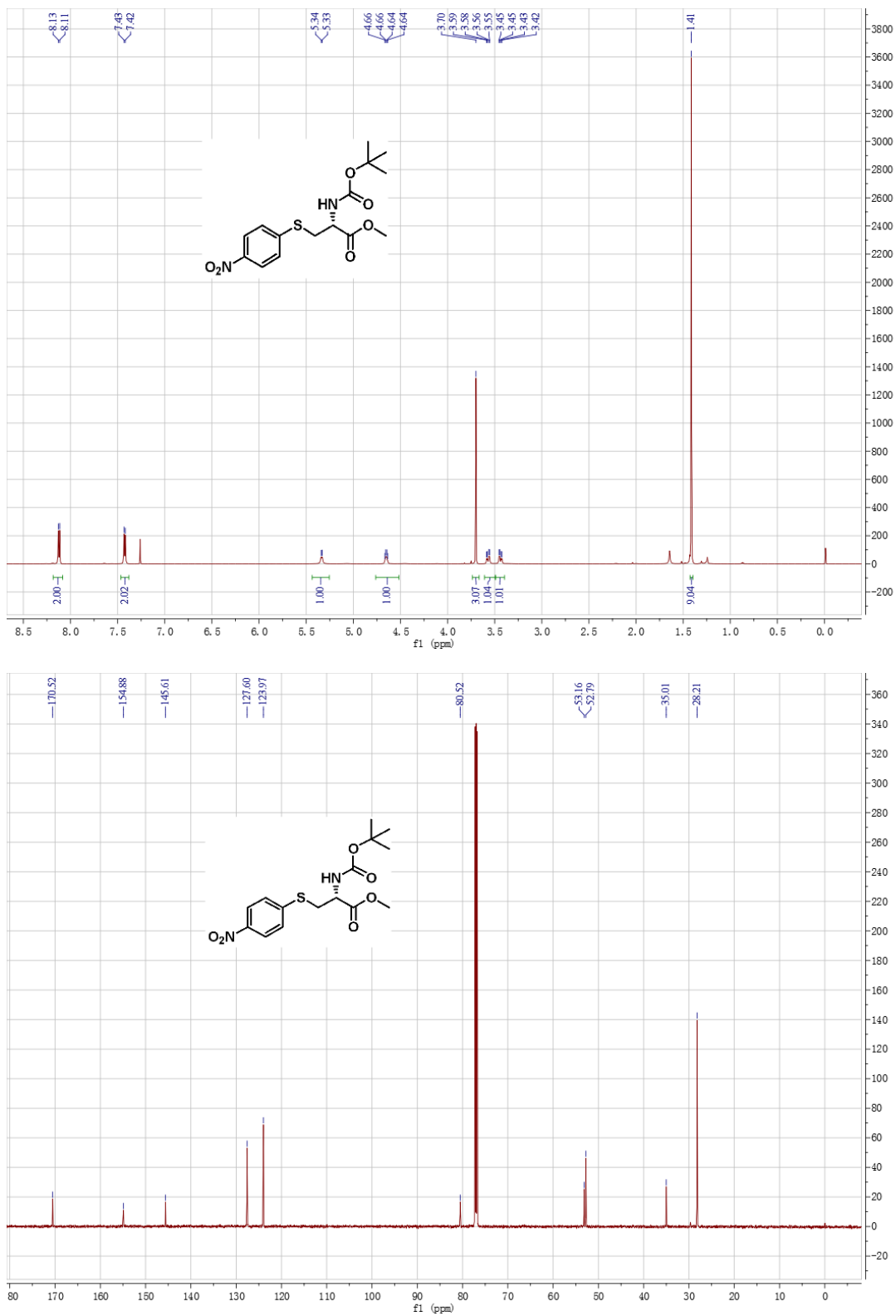
Compound 3ai



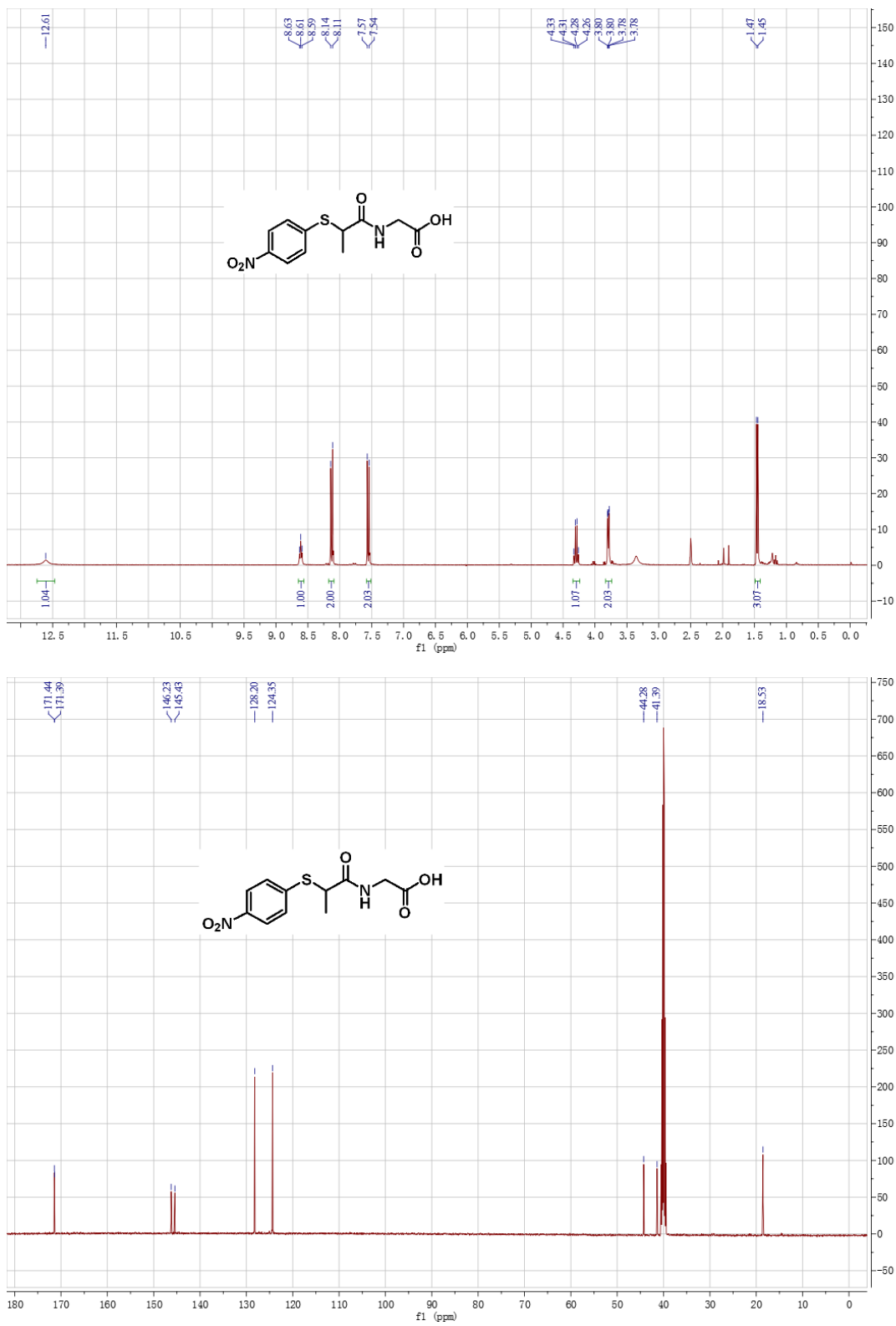
Compound 3aj



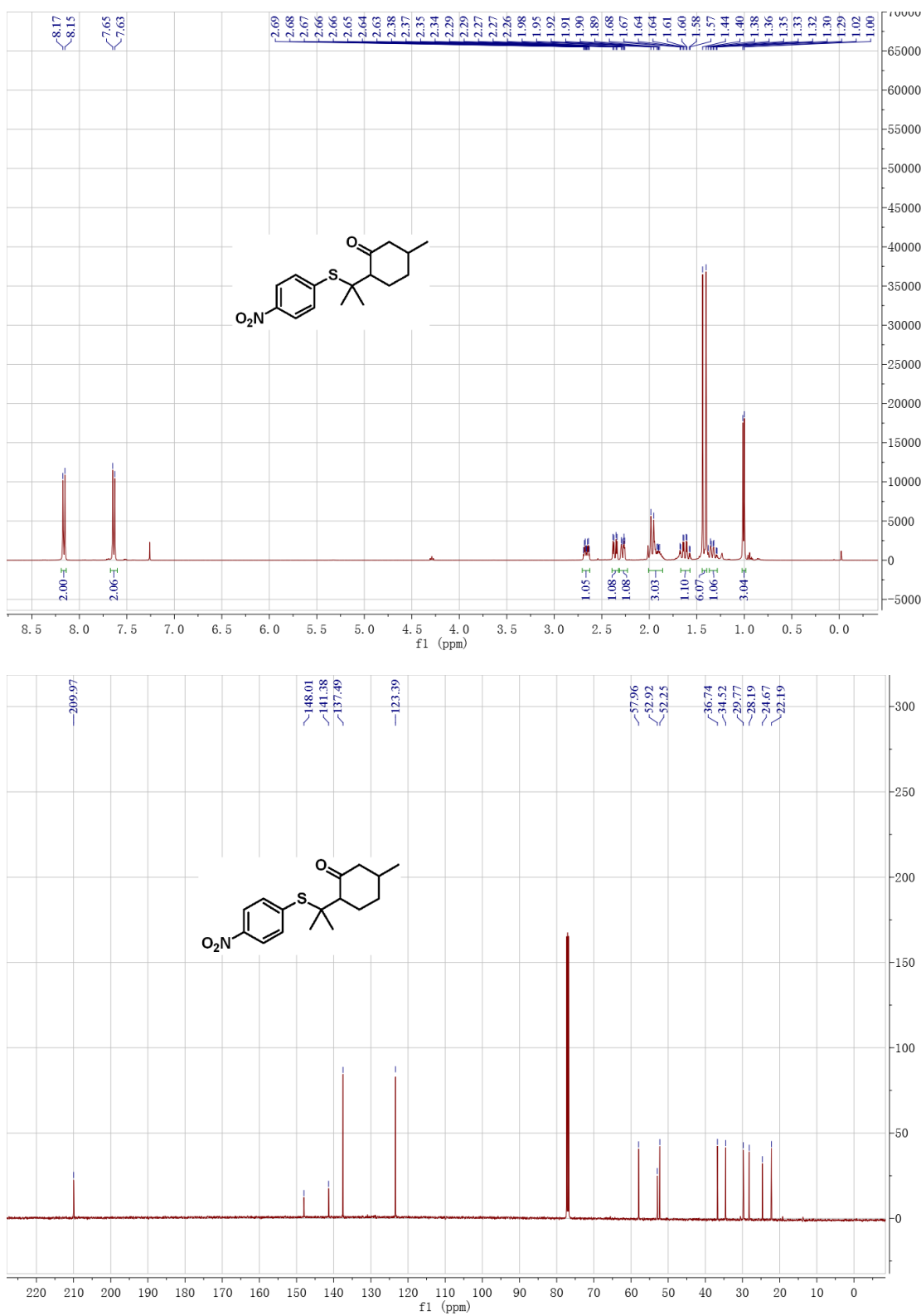
Compound 3ak



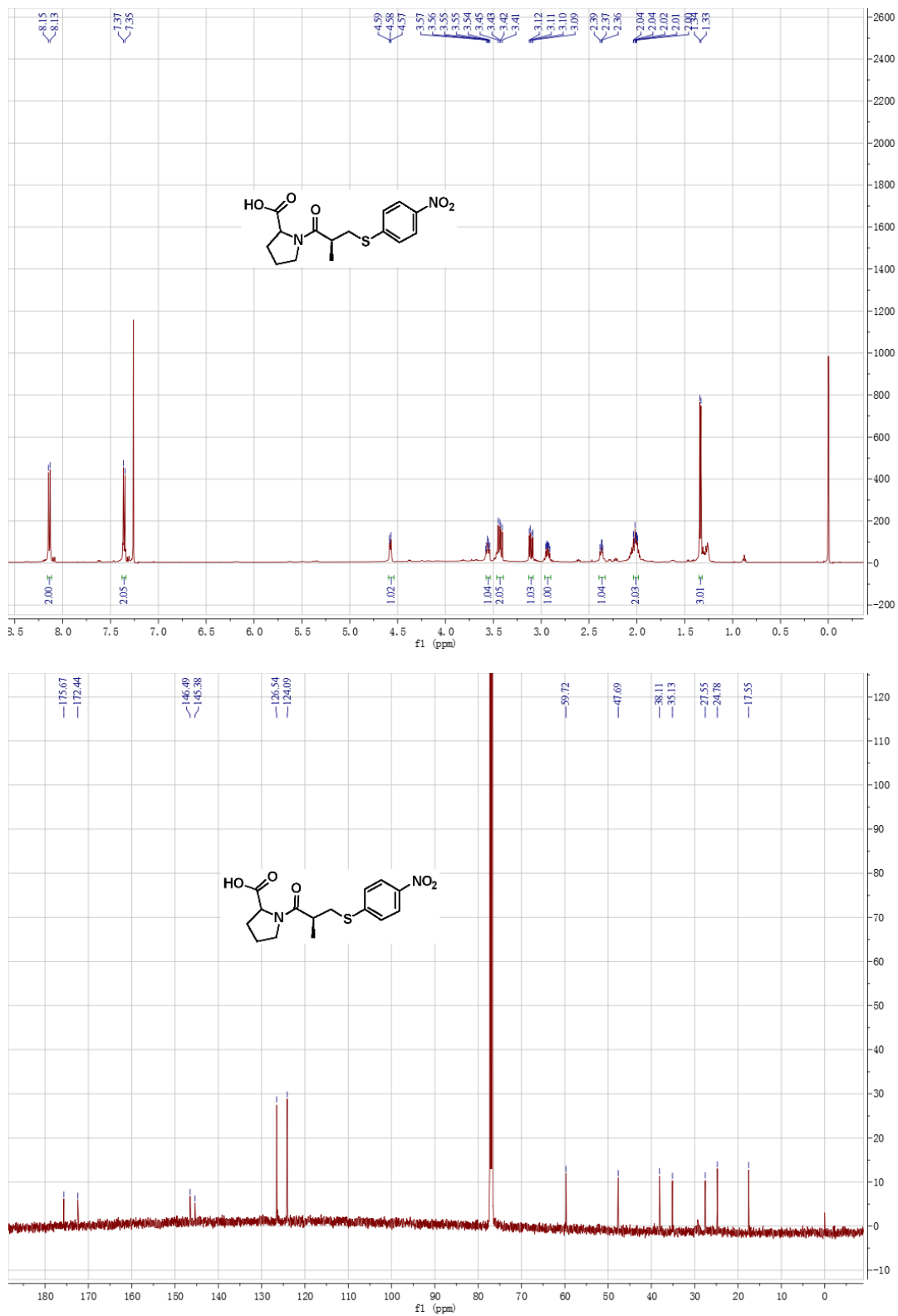
Compound 3al



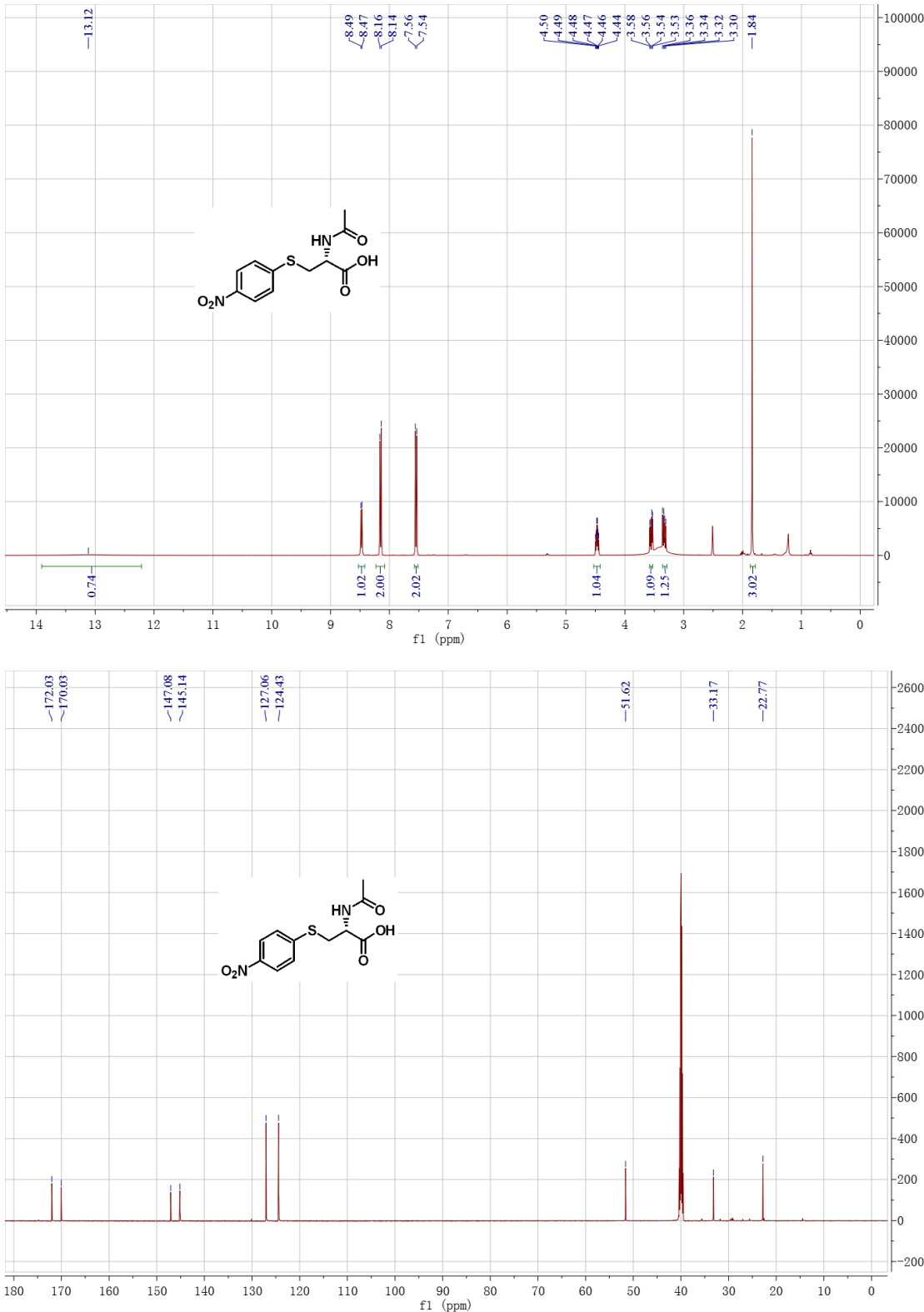
Compound 3am



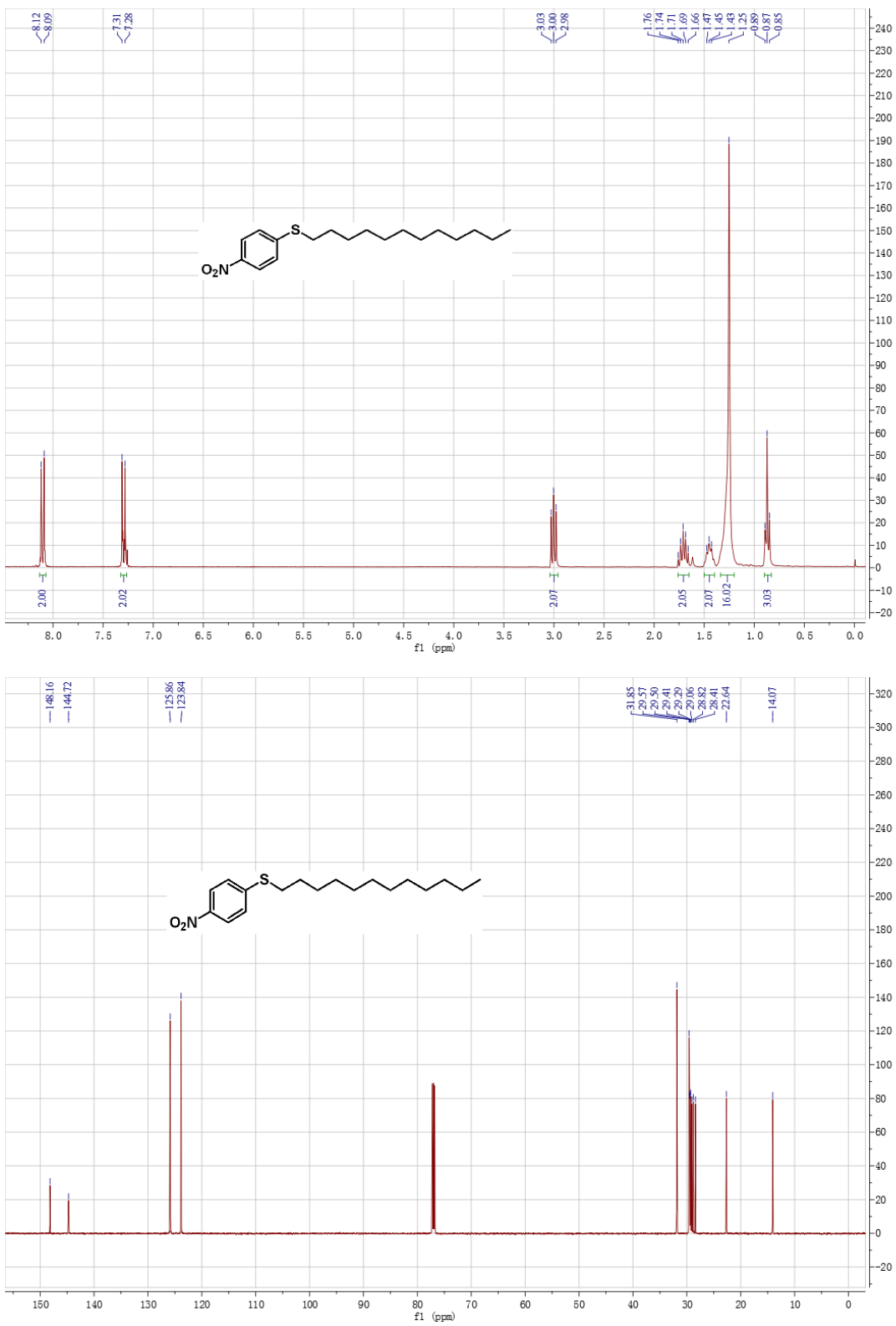
Compound 3an



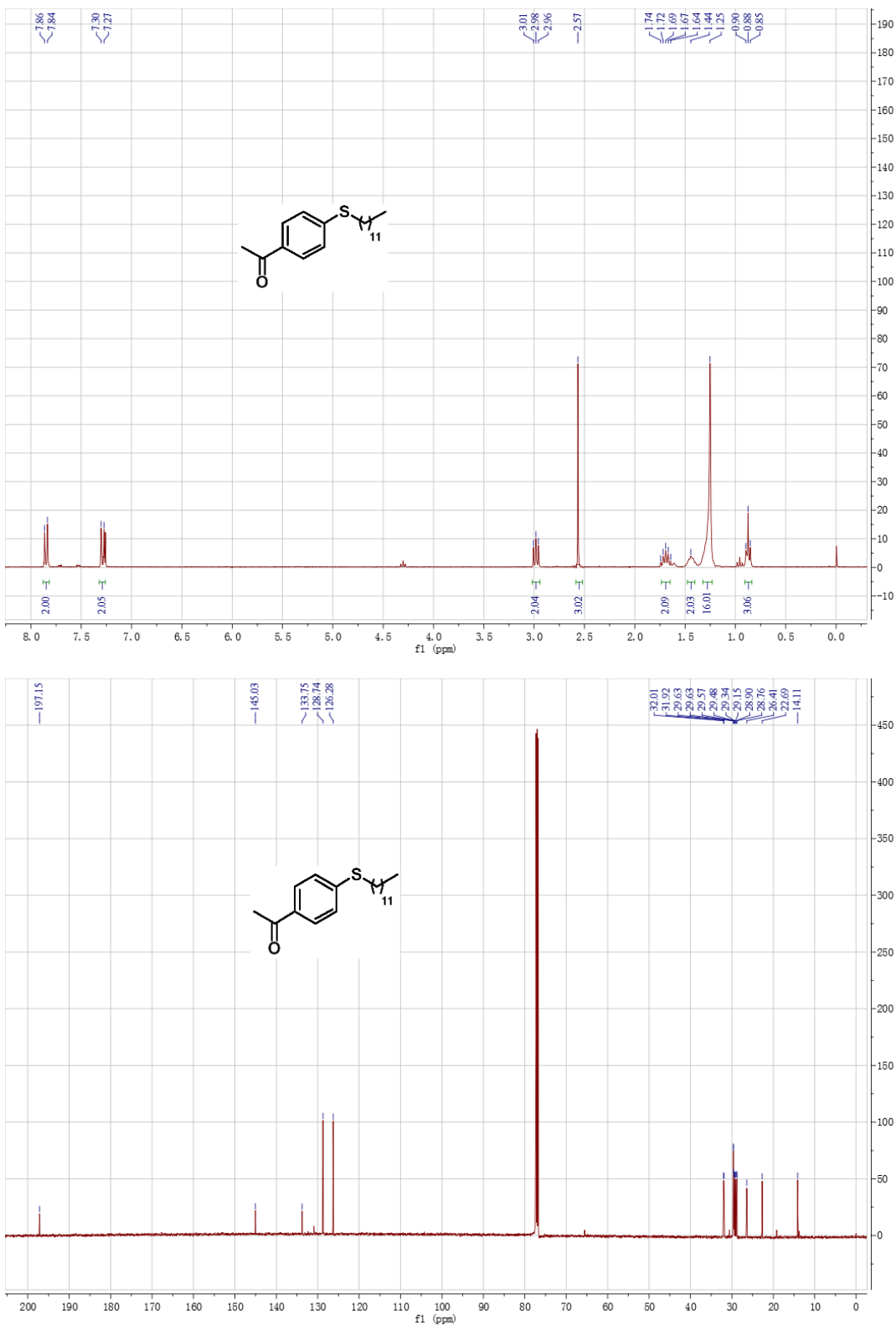
Compound 3ao



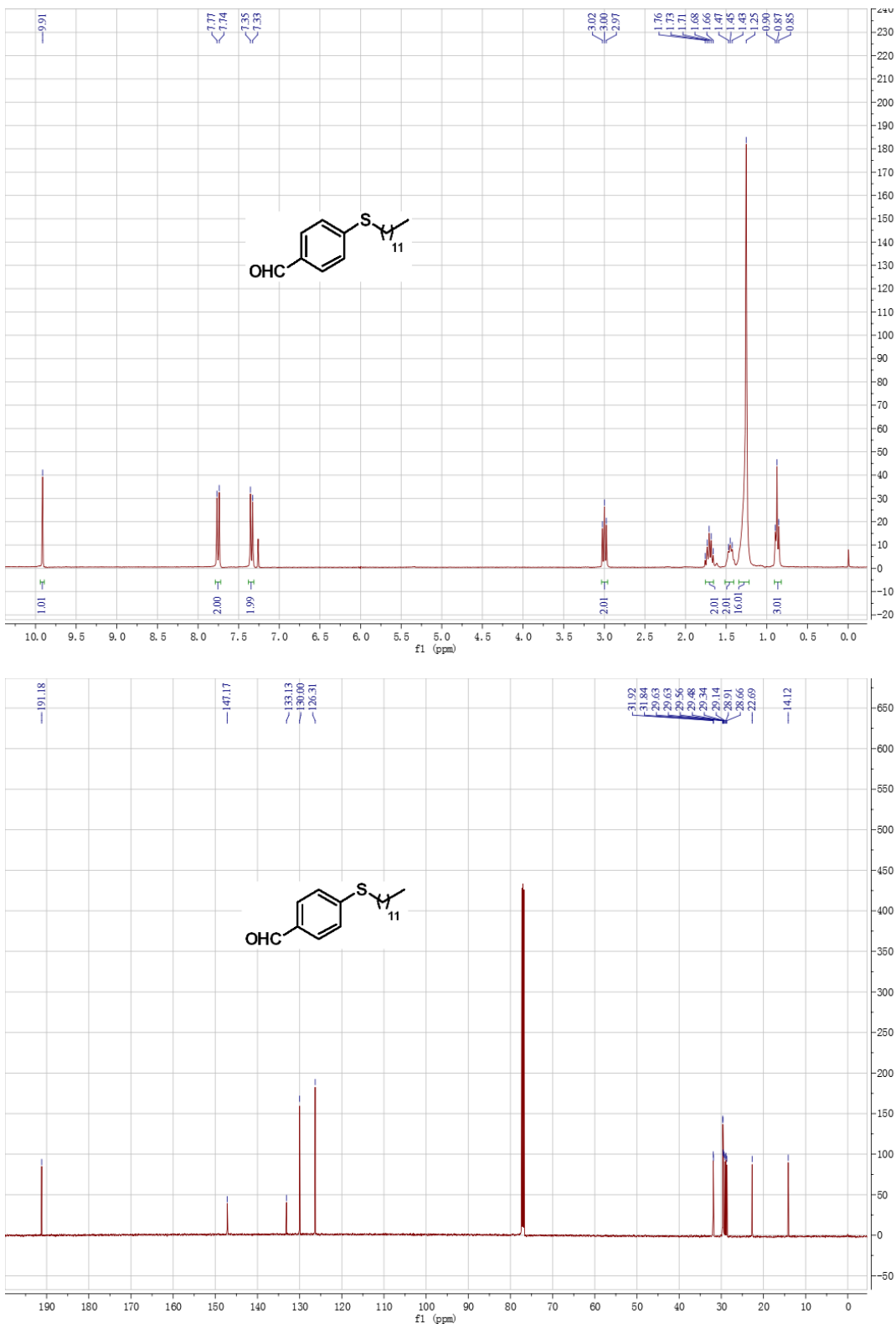
Compound 3ap



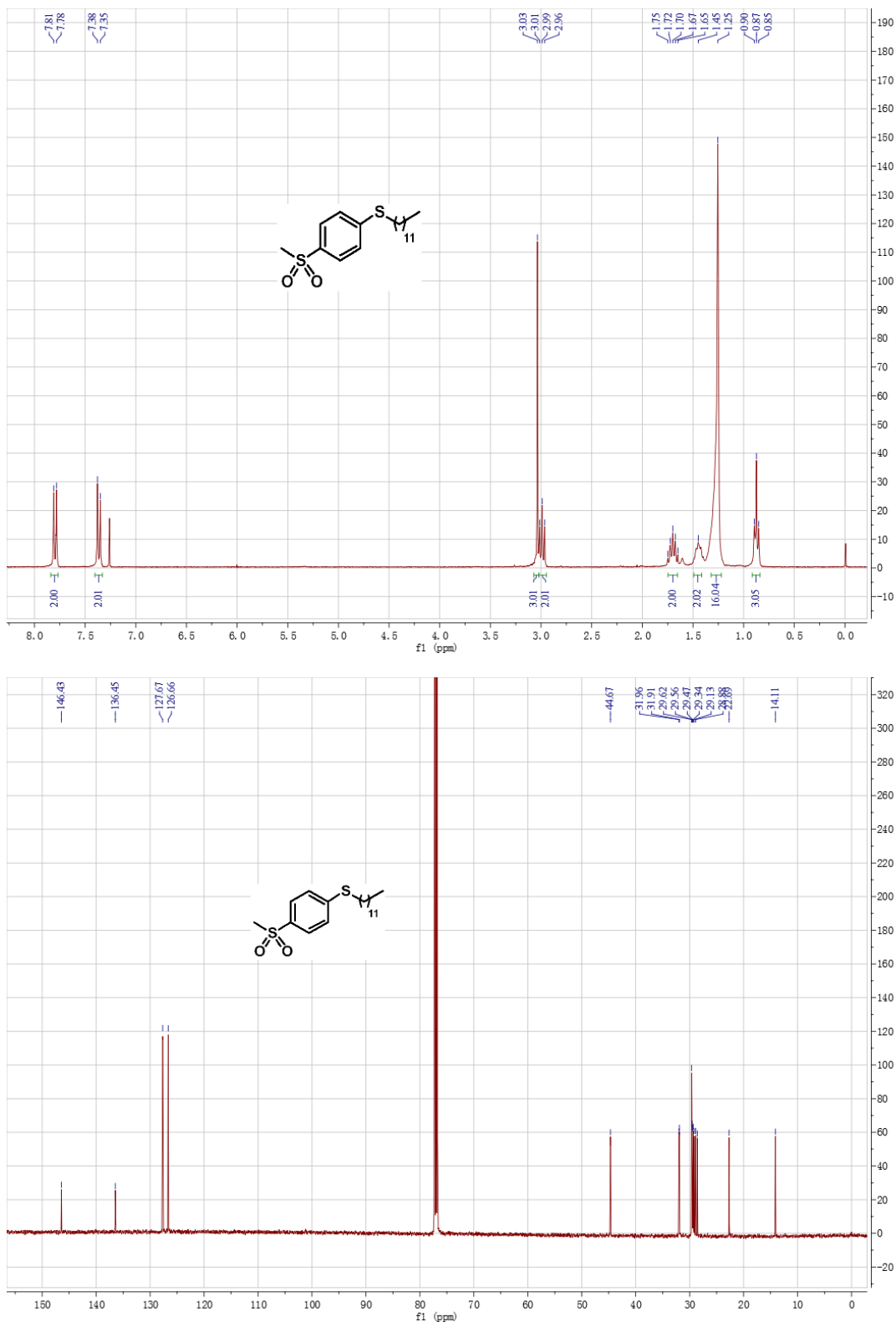
Compound 3bp



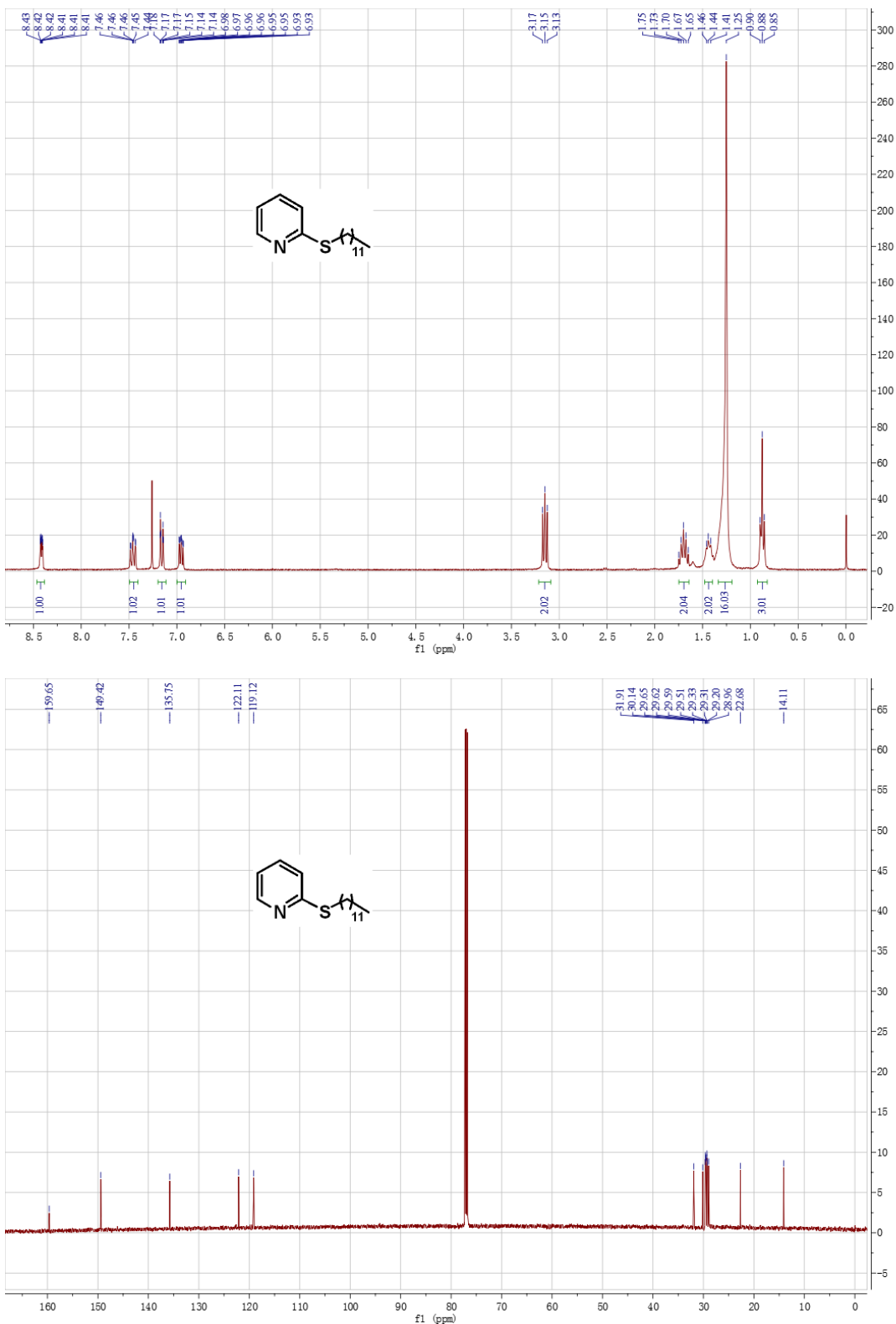
Compound 3cp



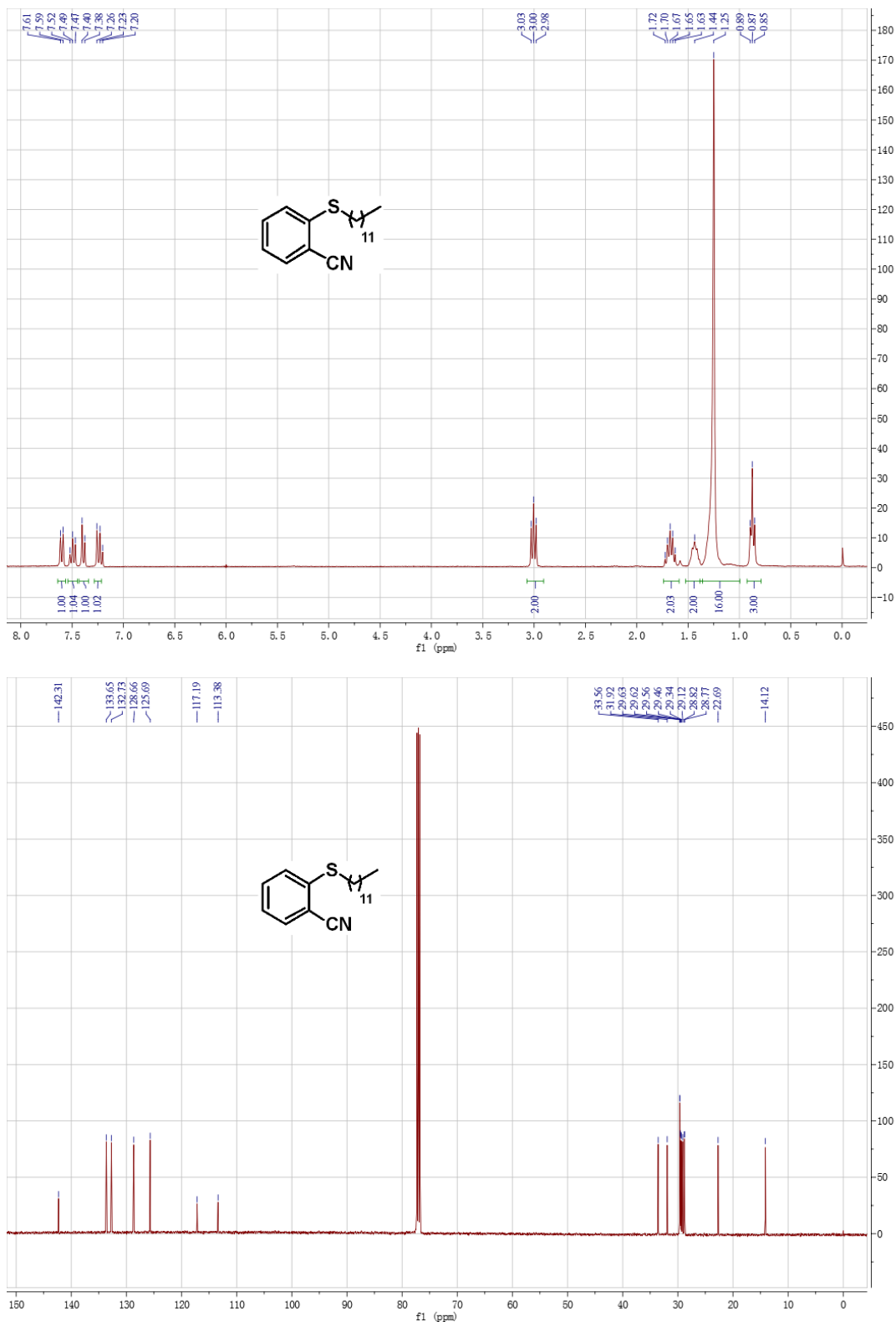
Compound 3dp



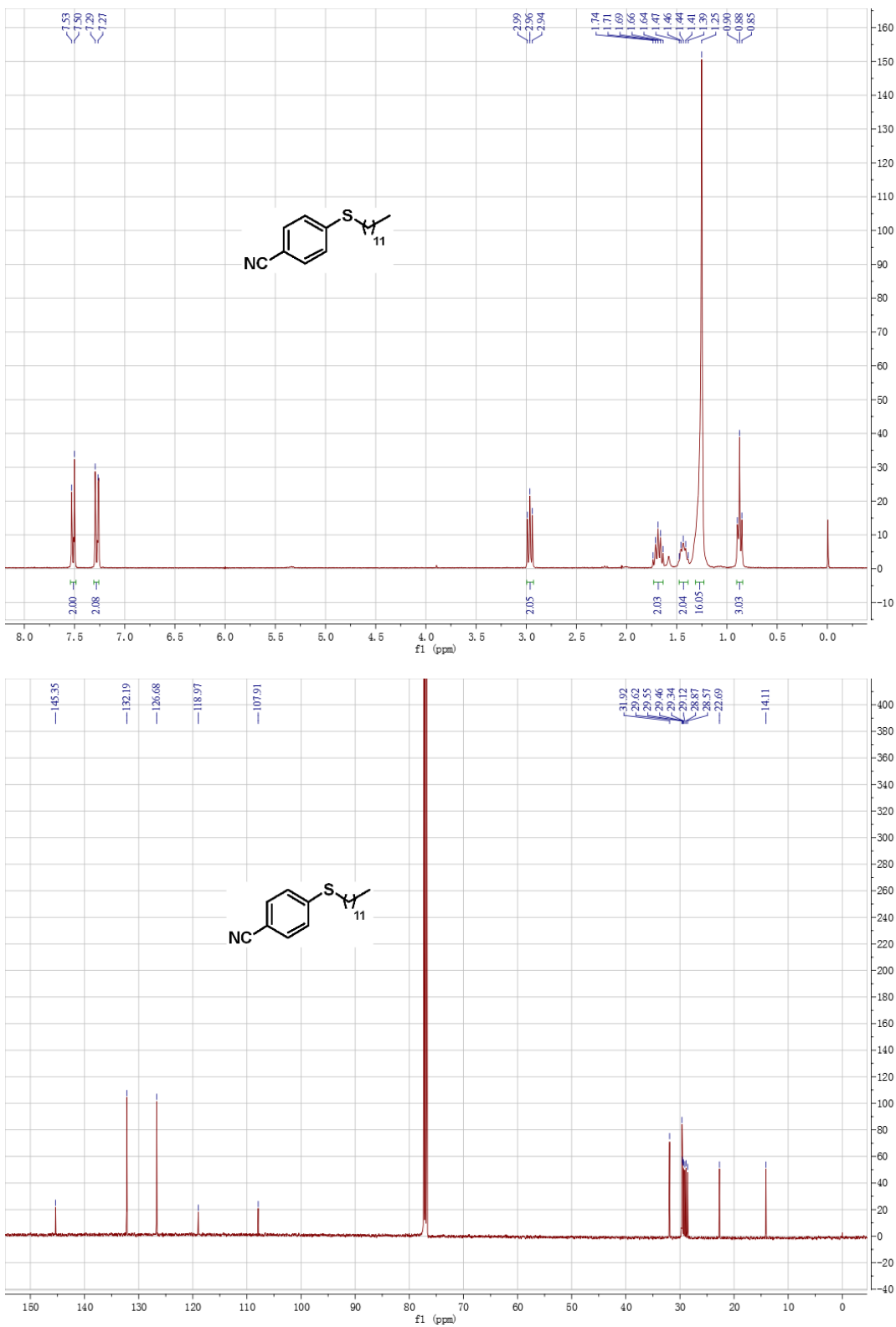
Compound 3ep



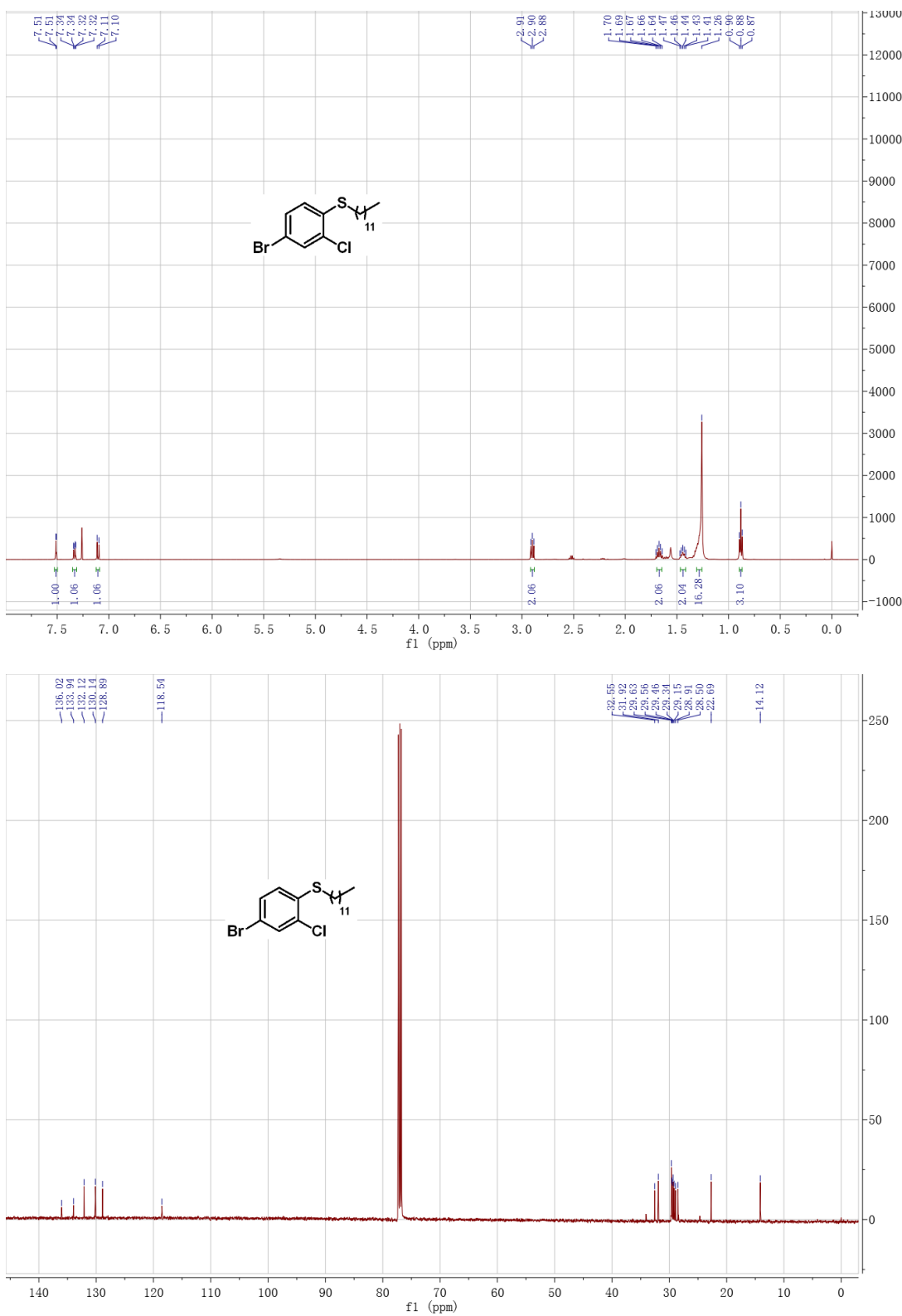
Compound 3fp



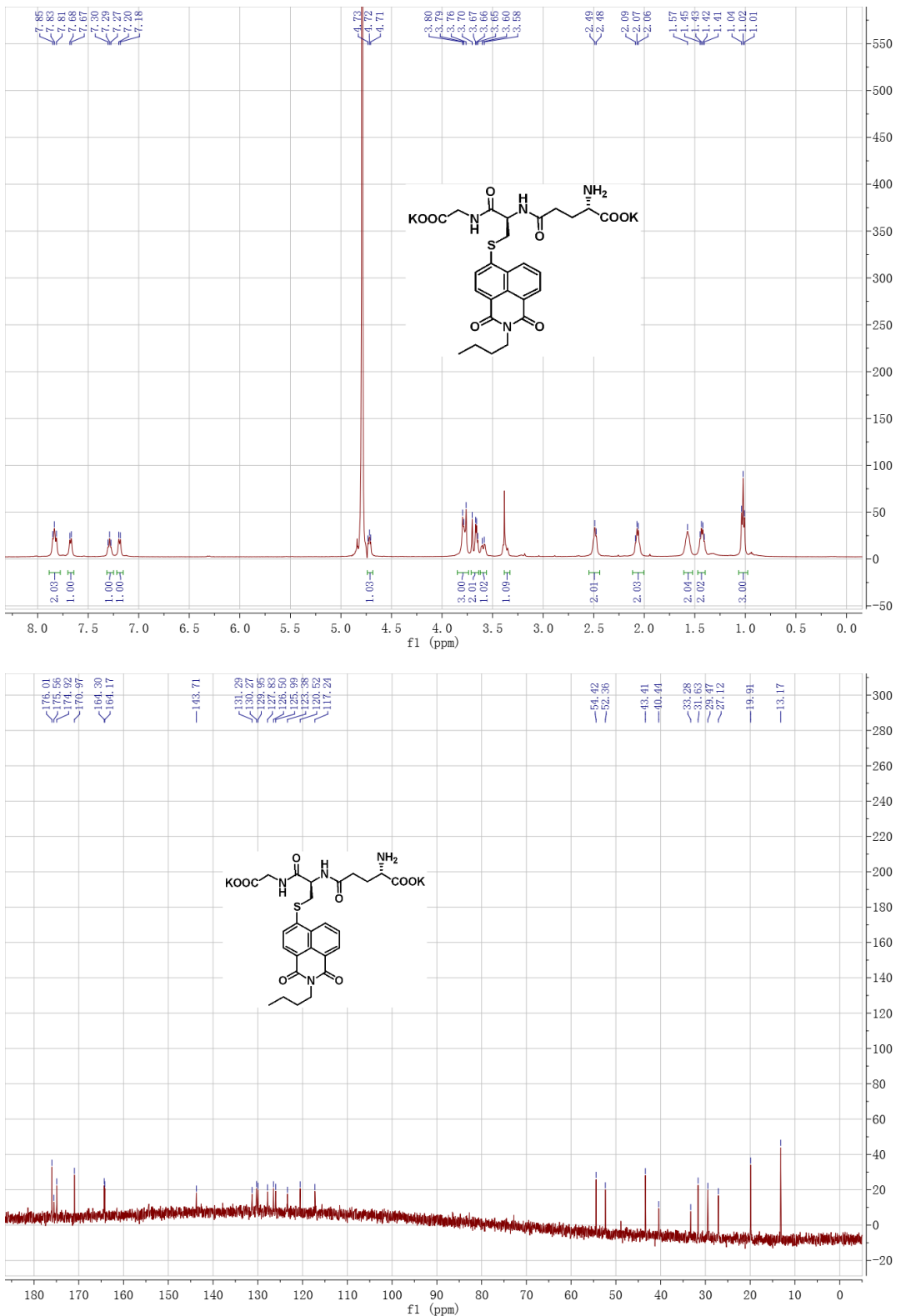
Compound 3gp



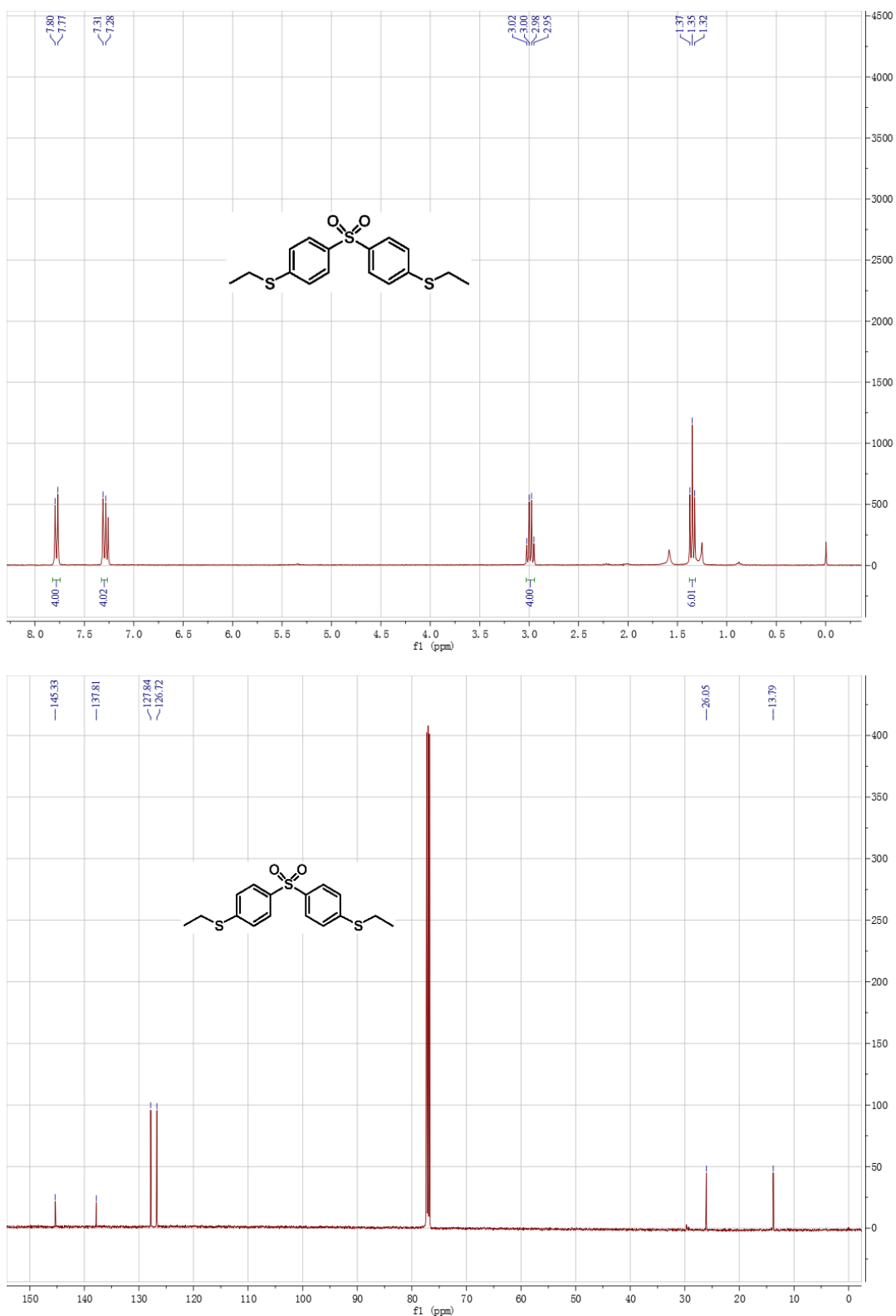
Compound 3hp



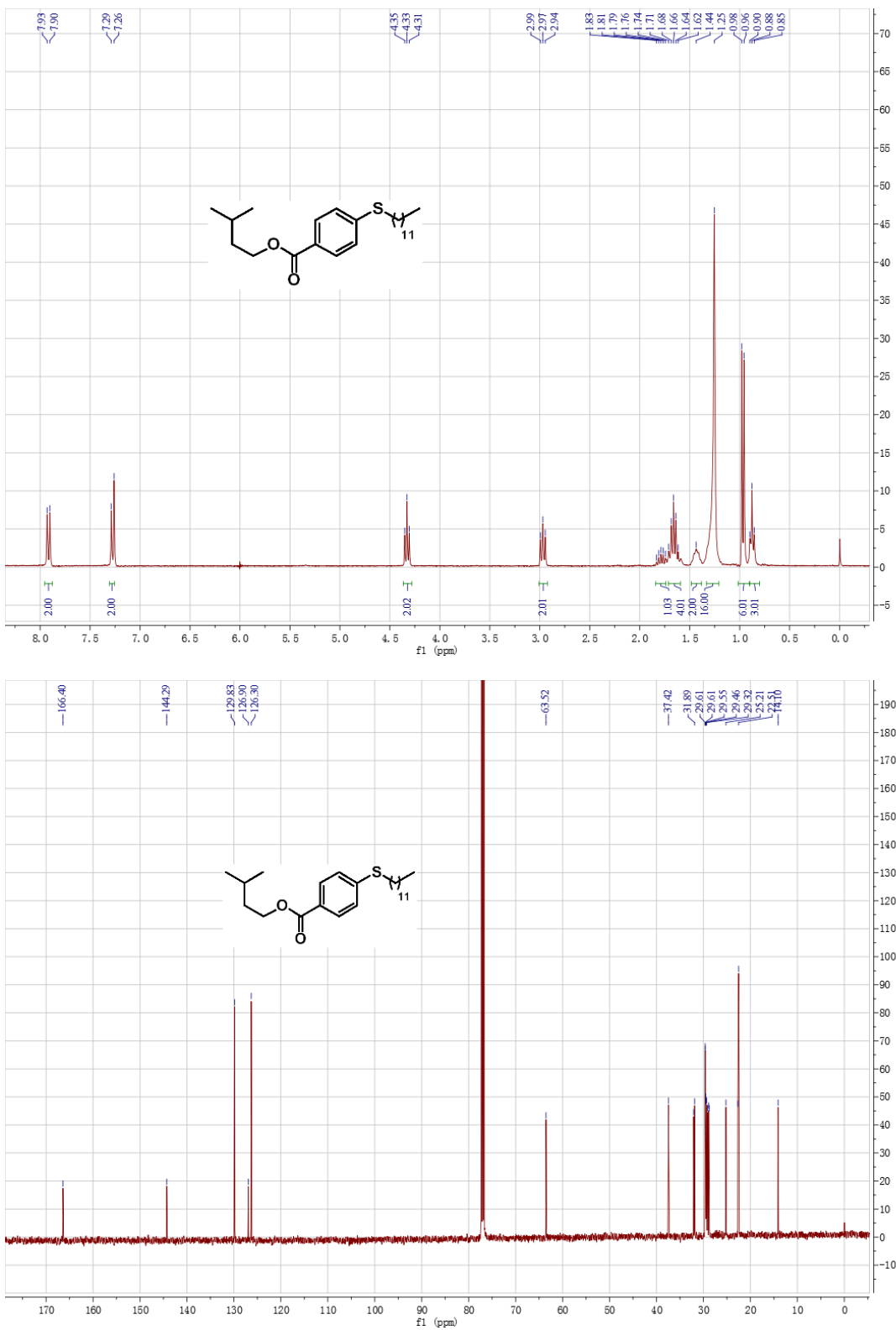
Compound 3ir



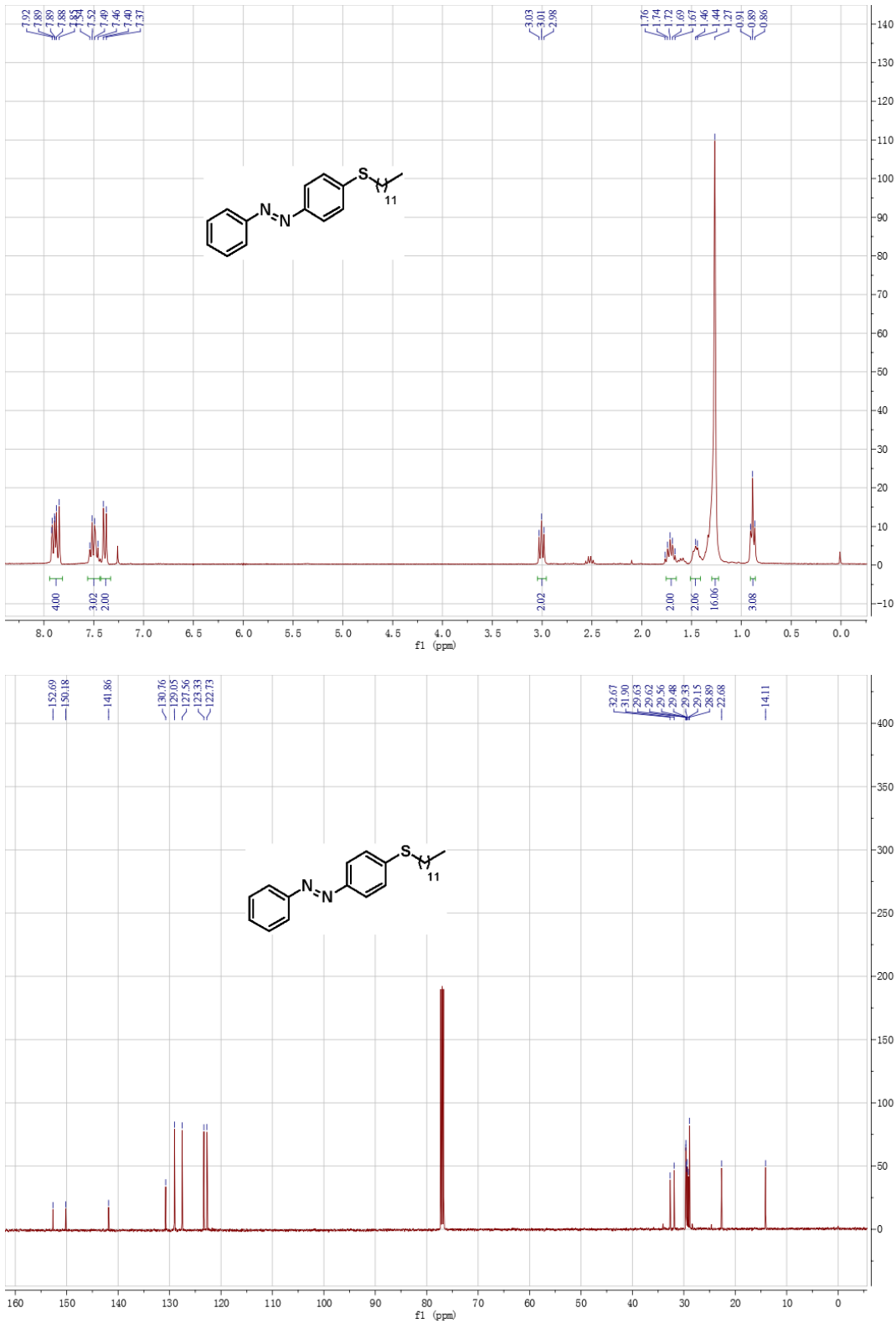
Compound 3jq



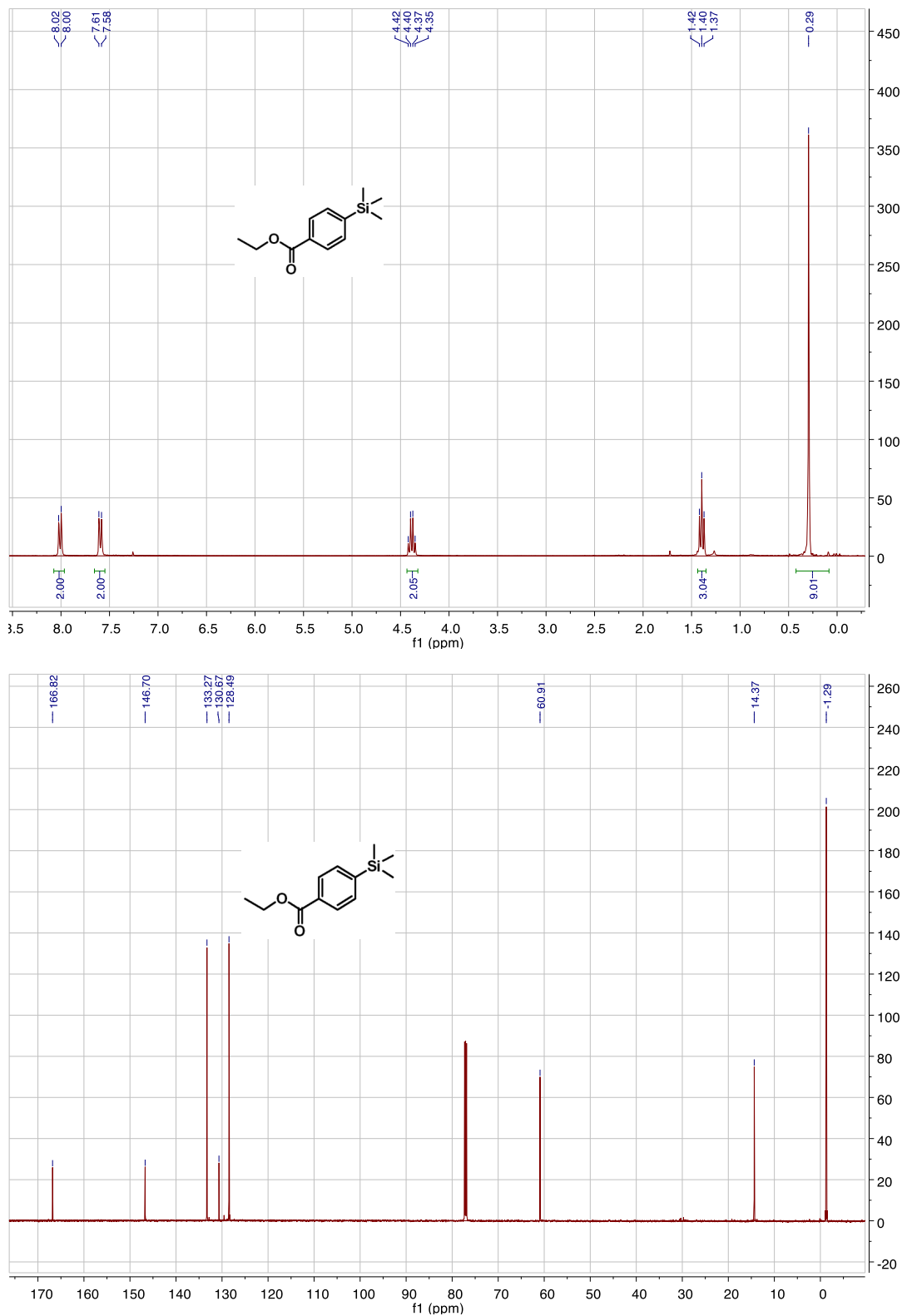
Compound 3kp



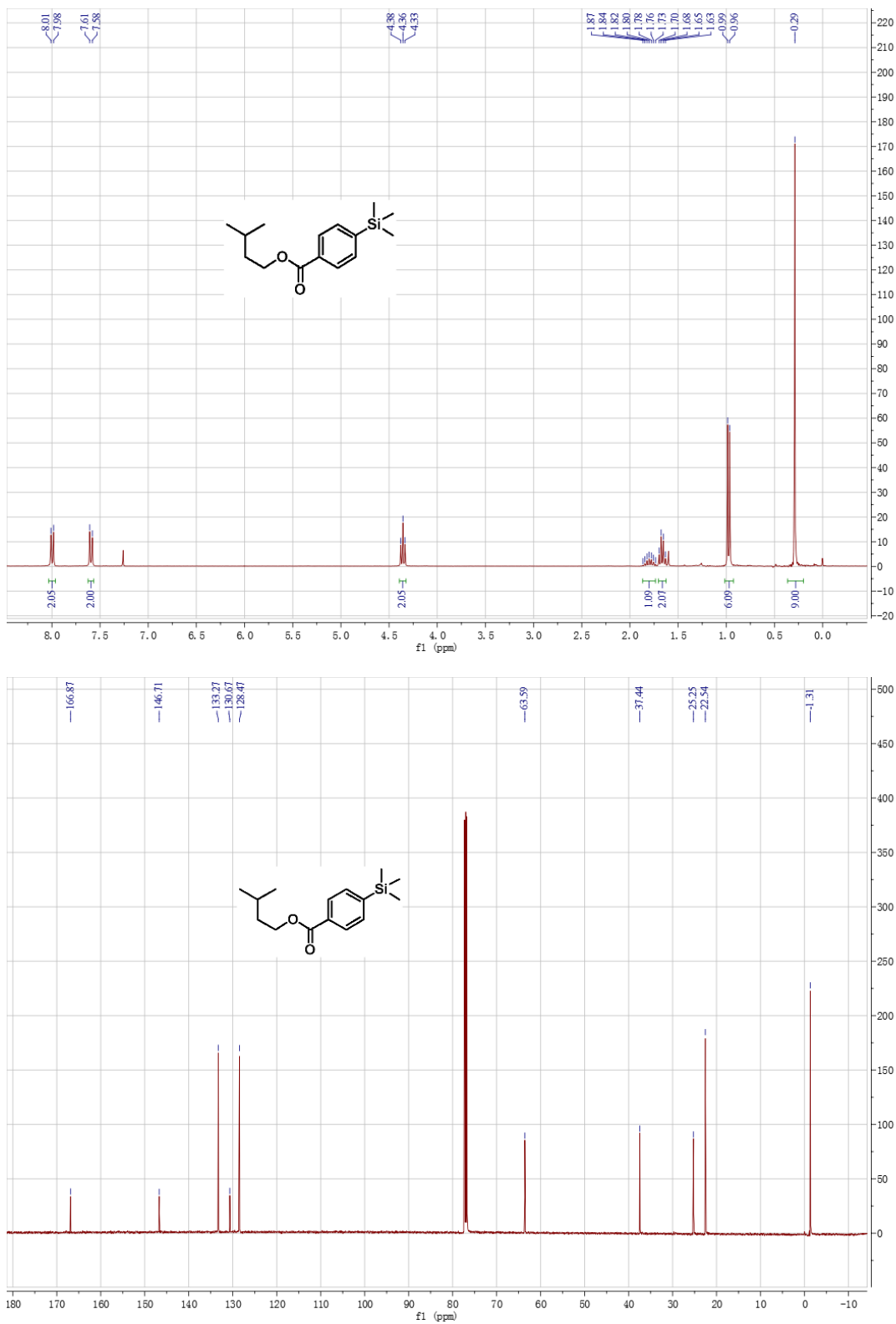
Compound 3Ip



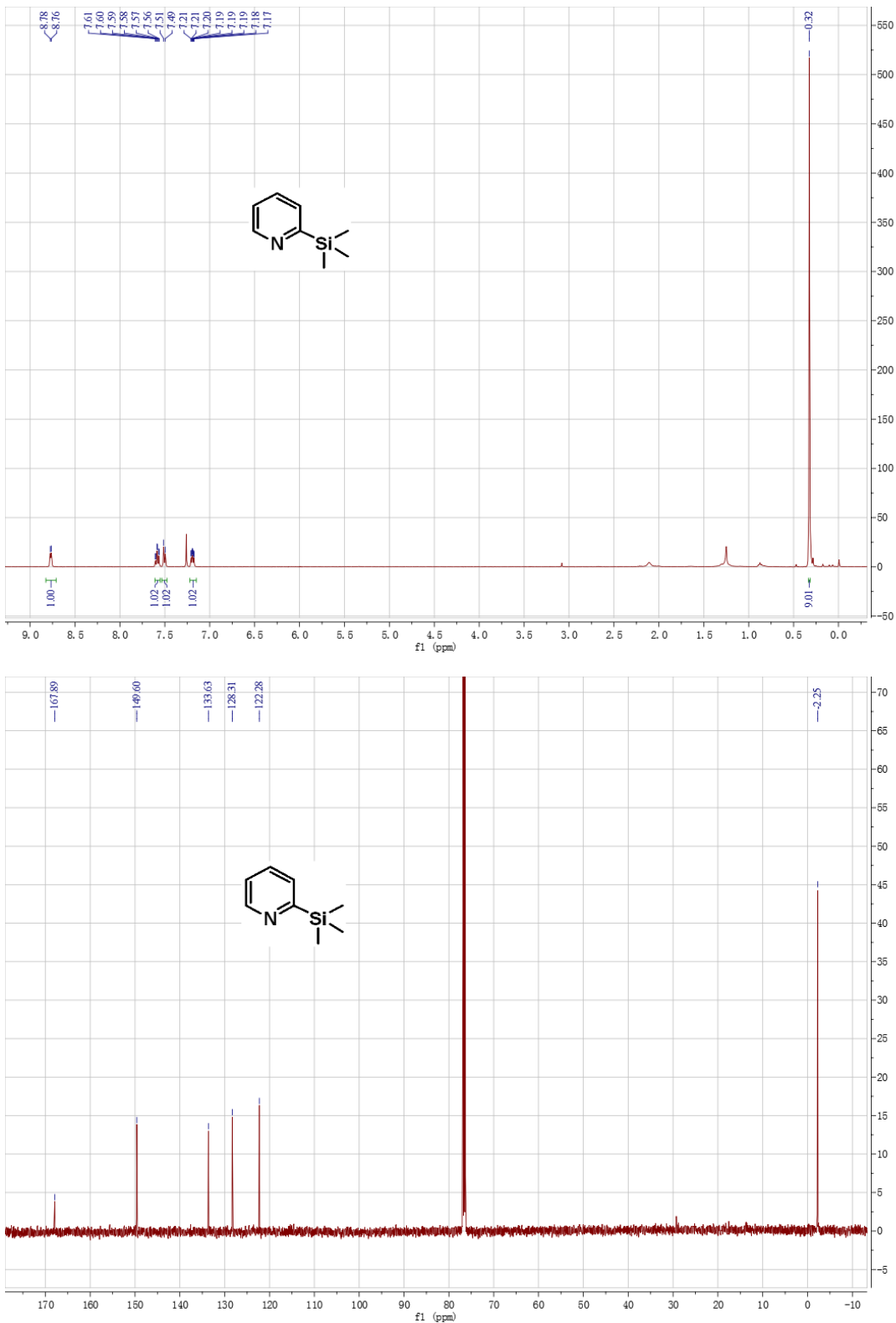
Compound 5a



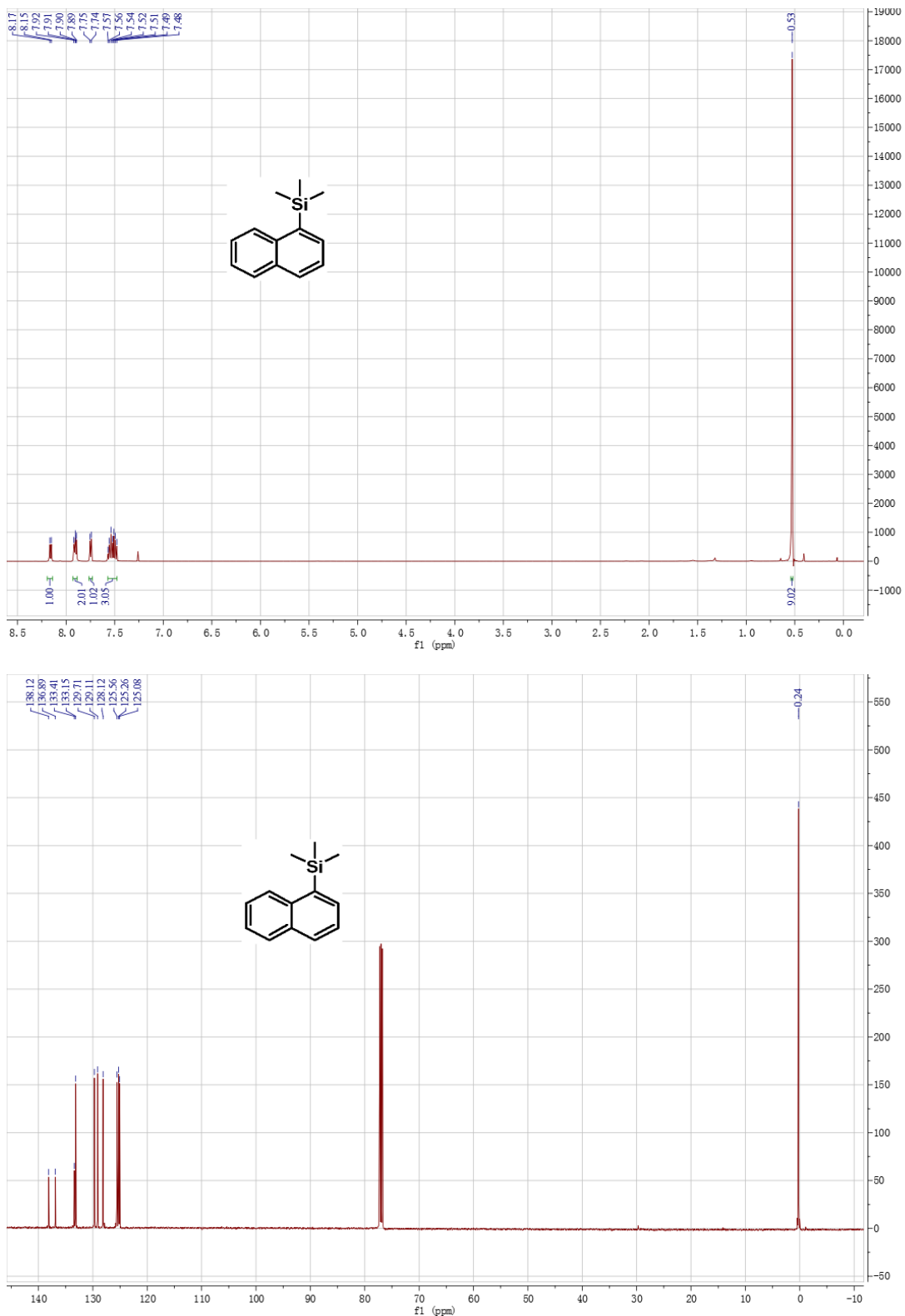
Compound 5b



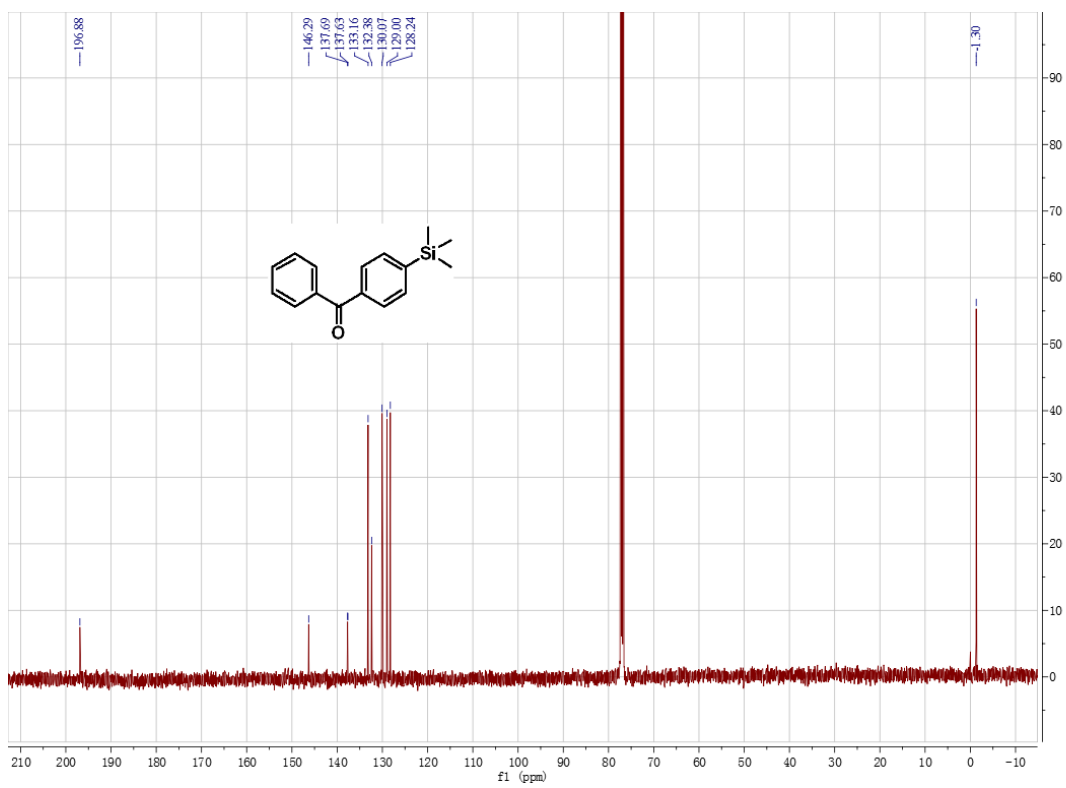
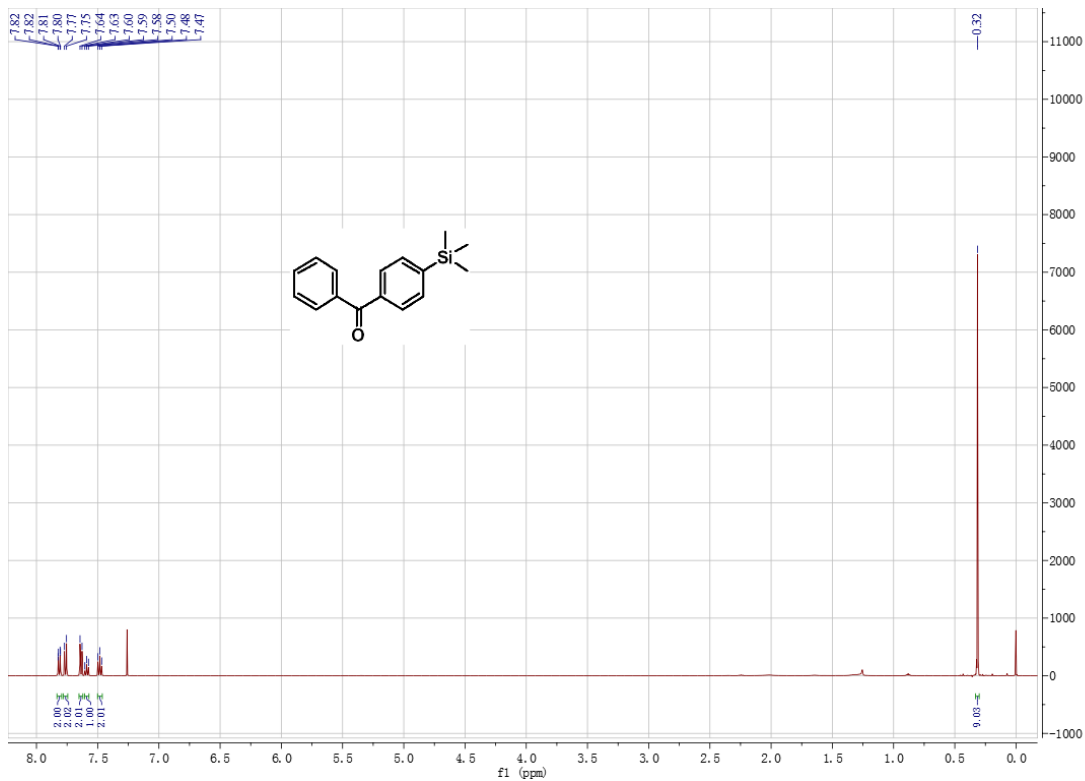
Compound 5h



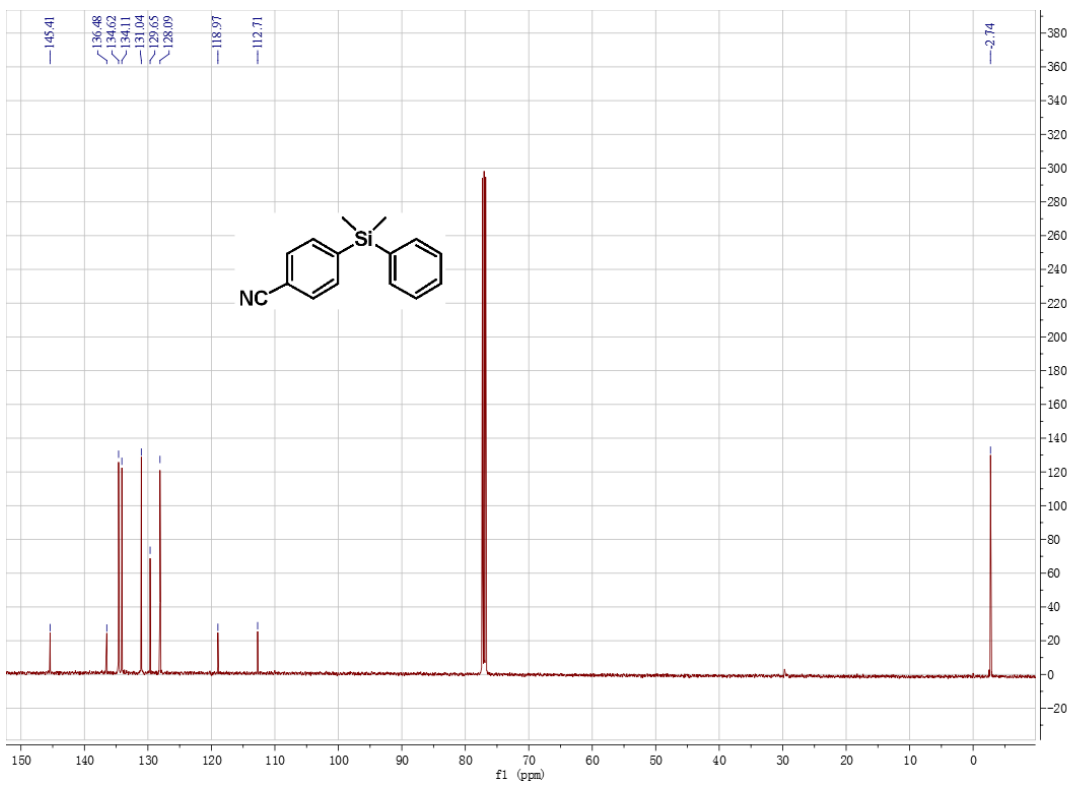
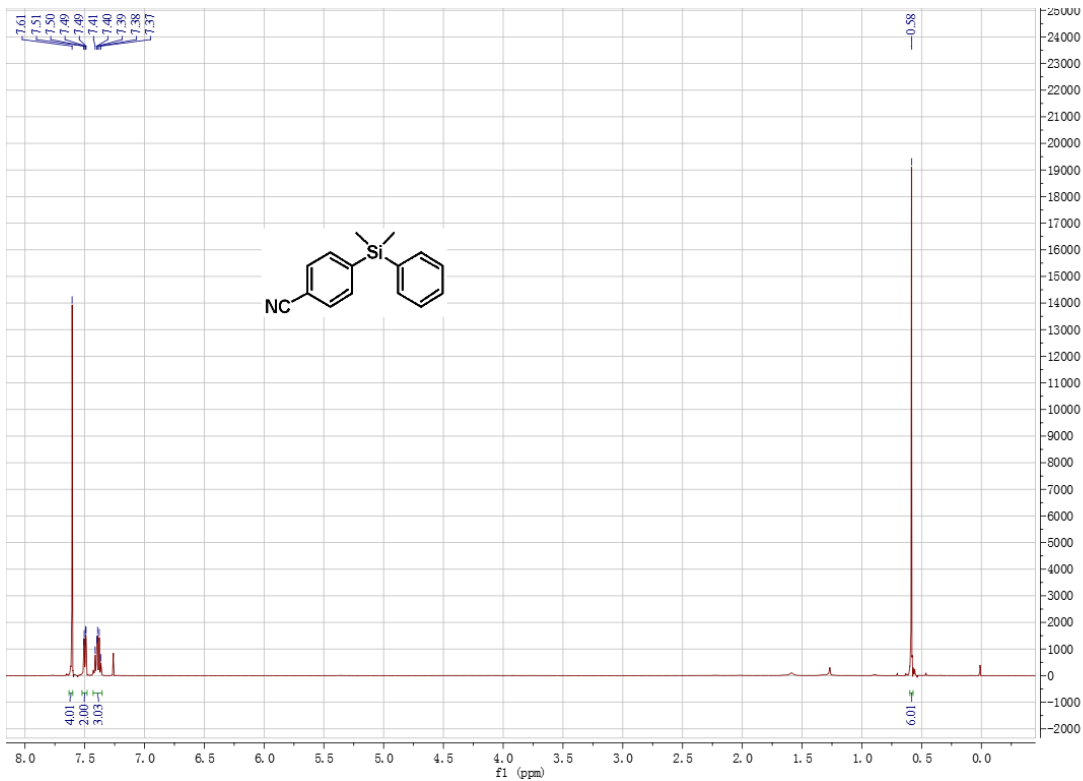
Compound 5g



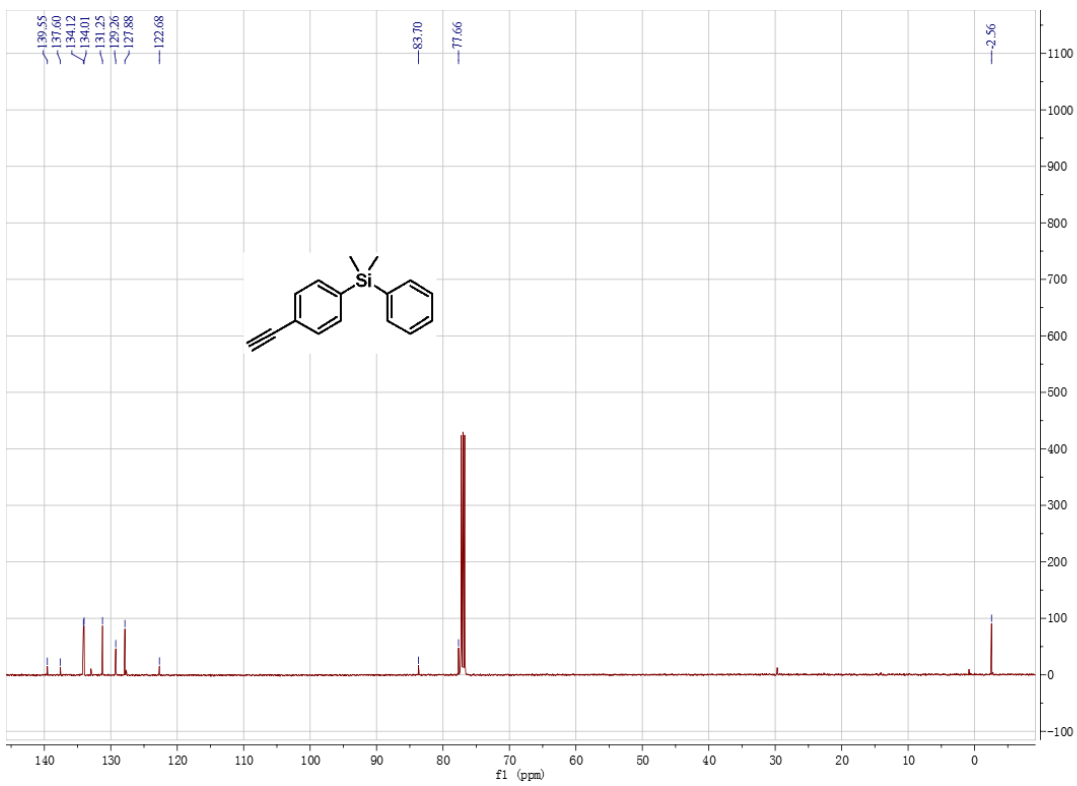
Compound 5f



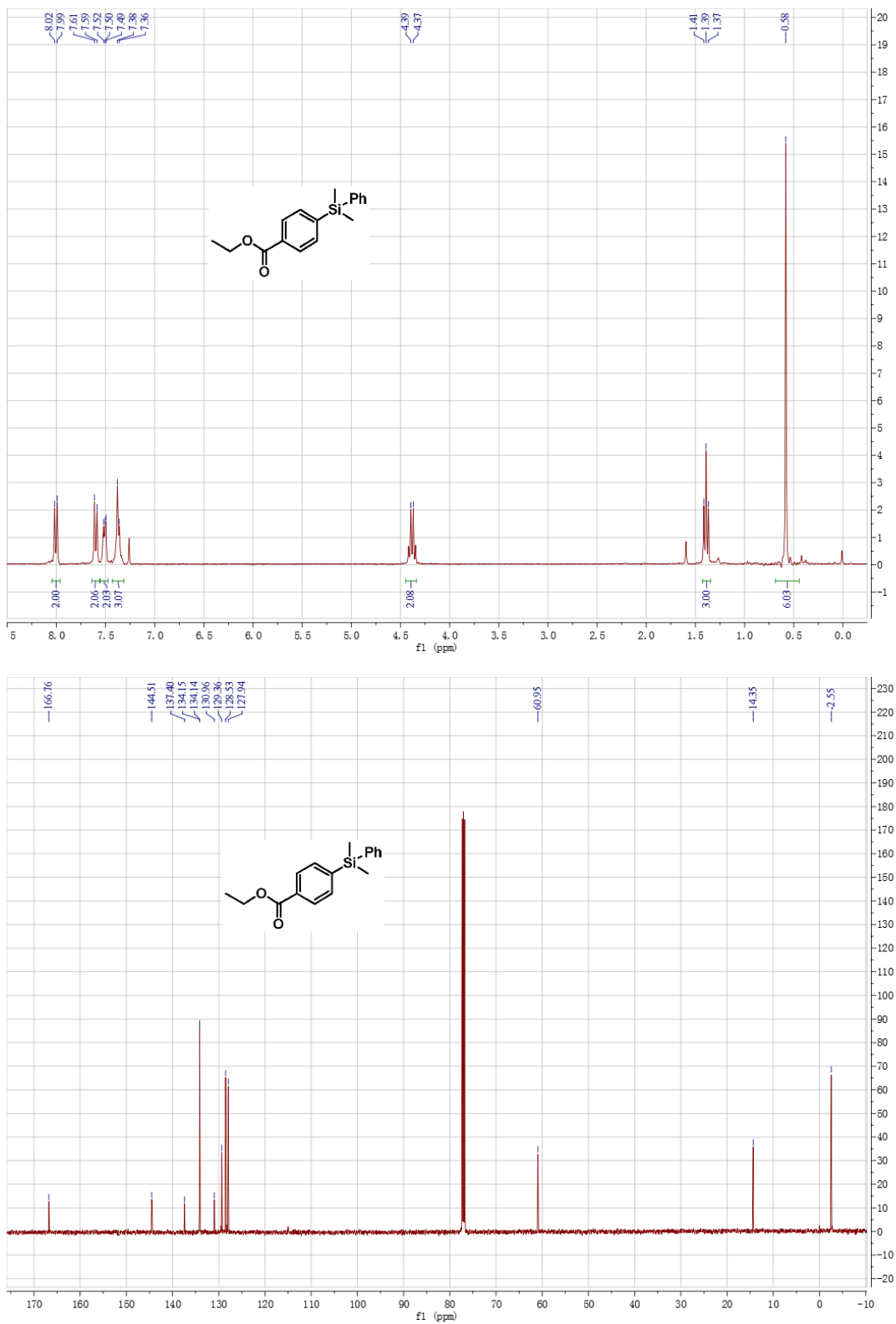
Compound 5c



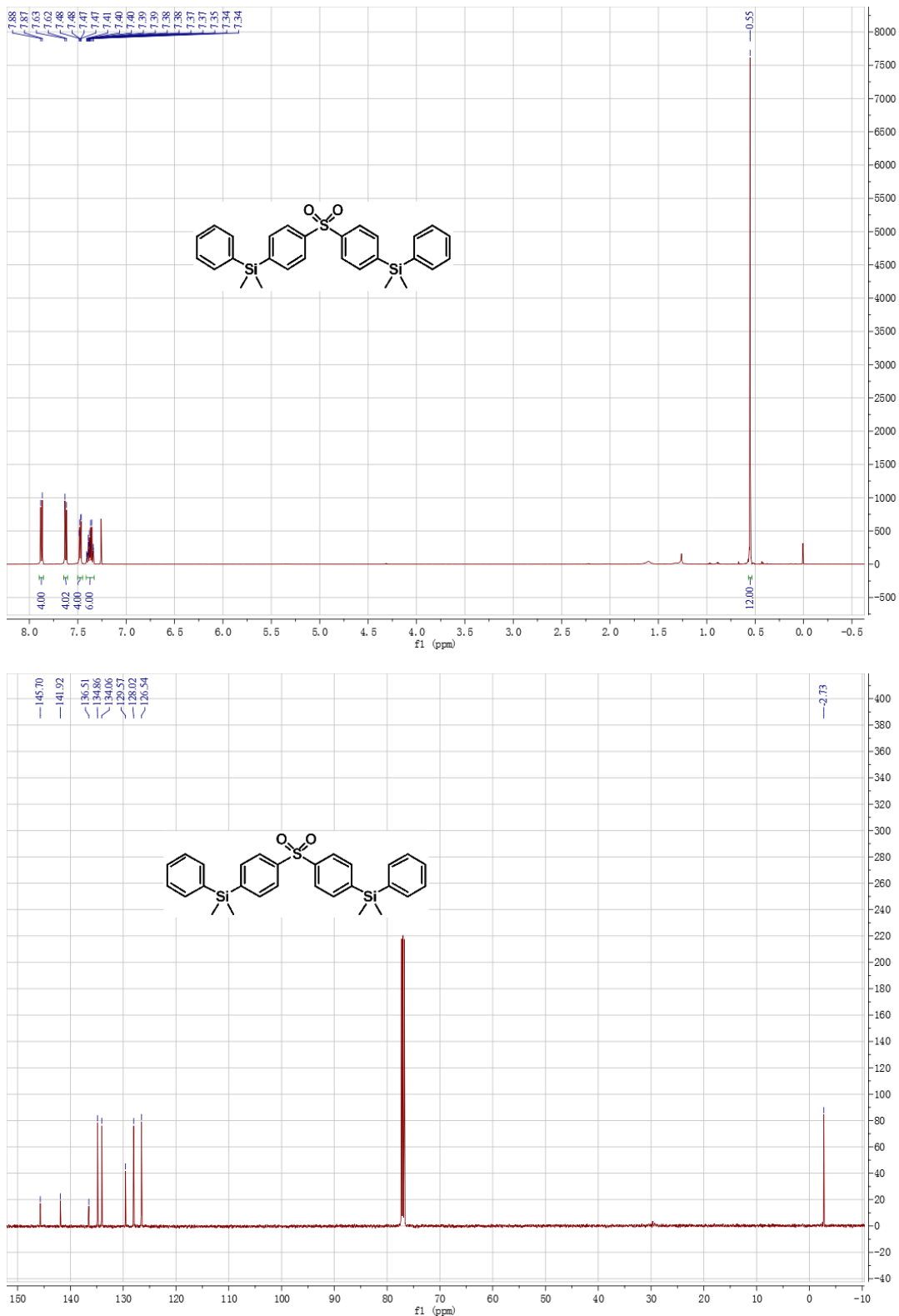
Compound 5d



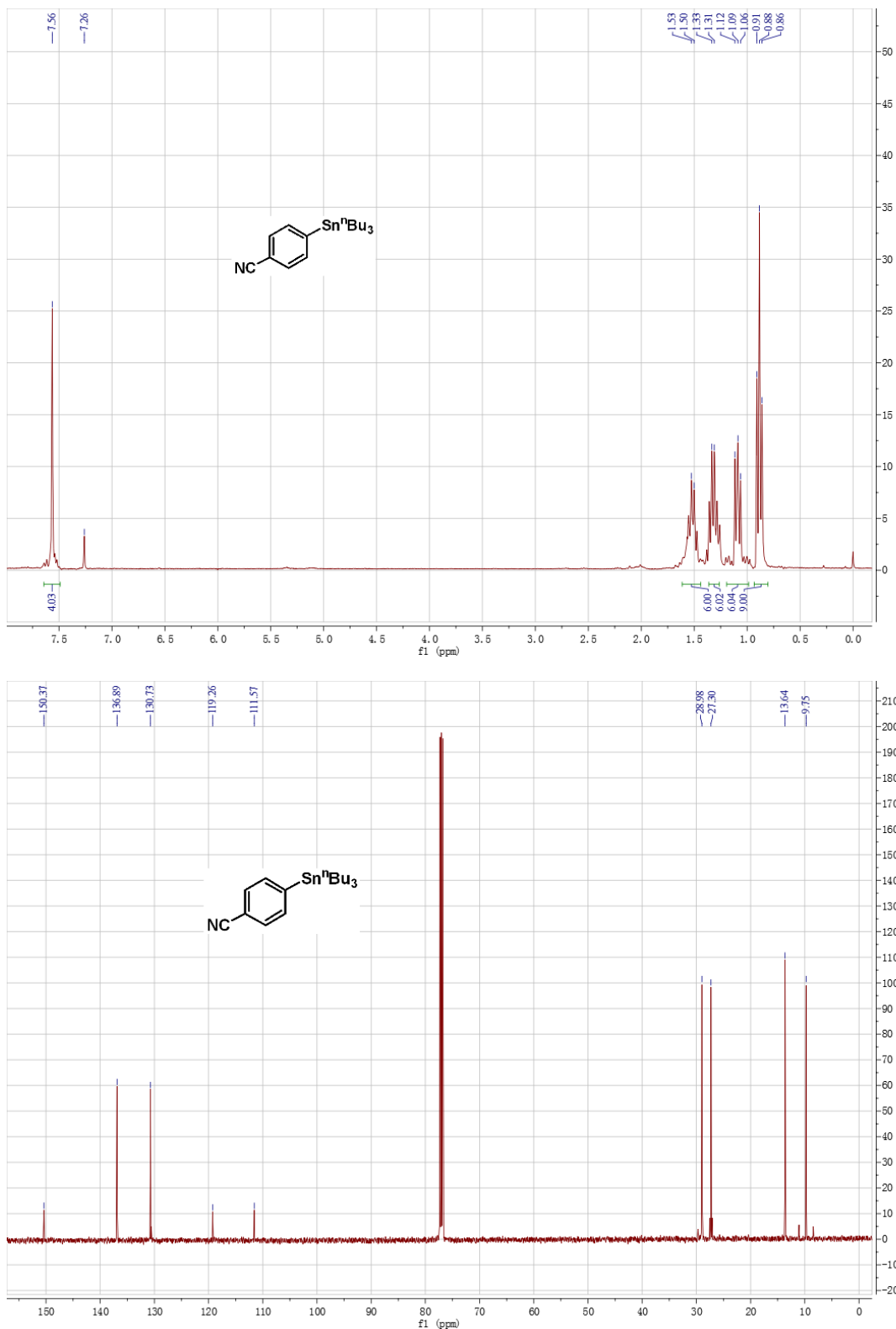
Compound 5e



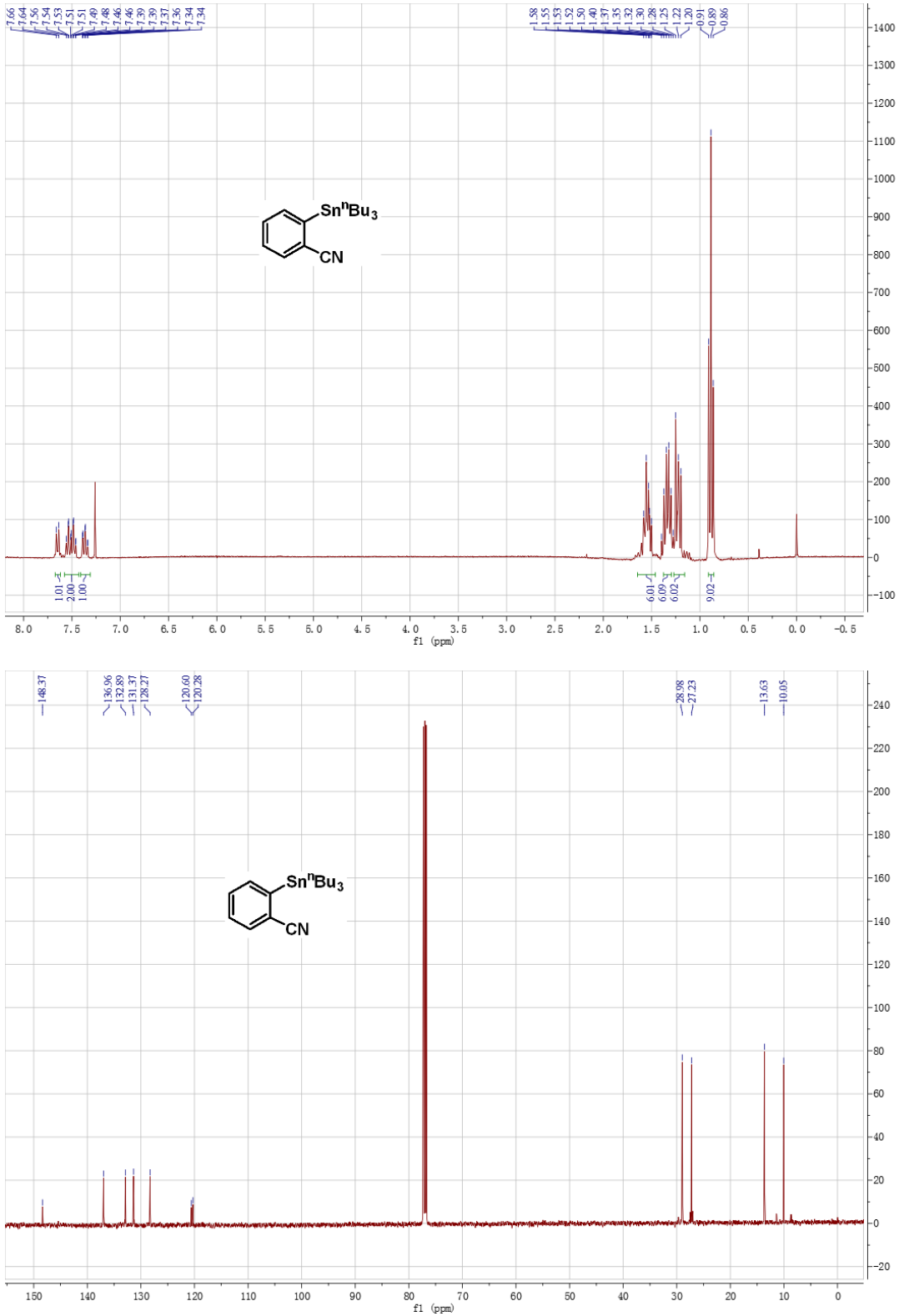
Compound 5i



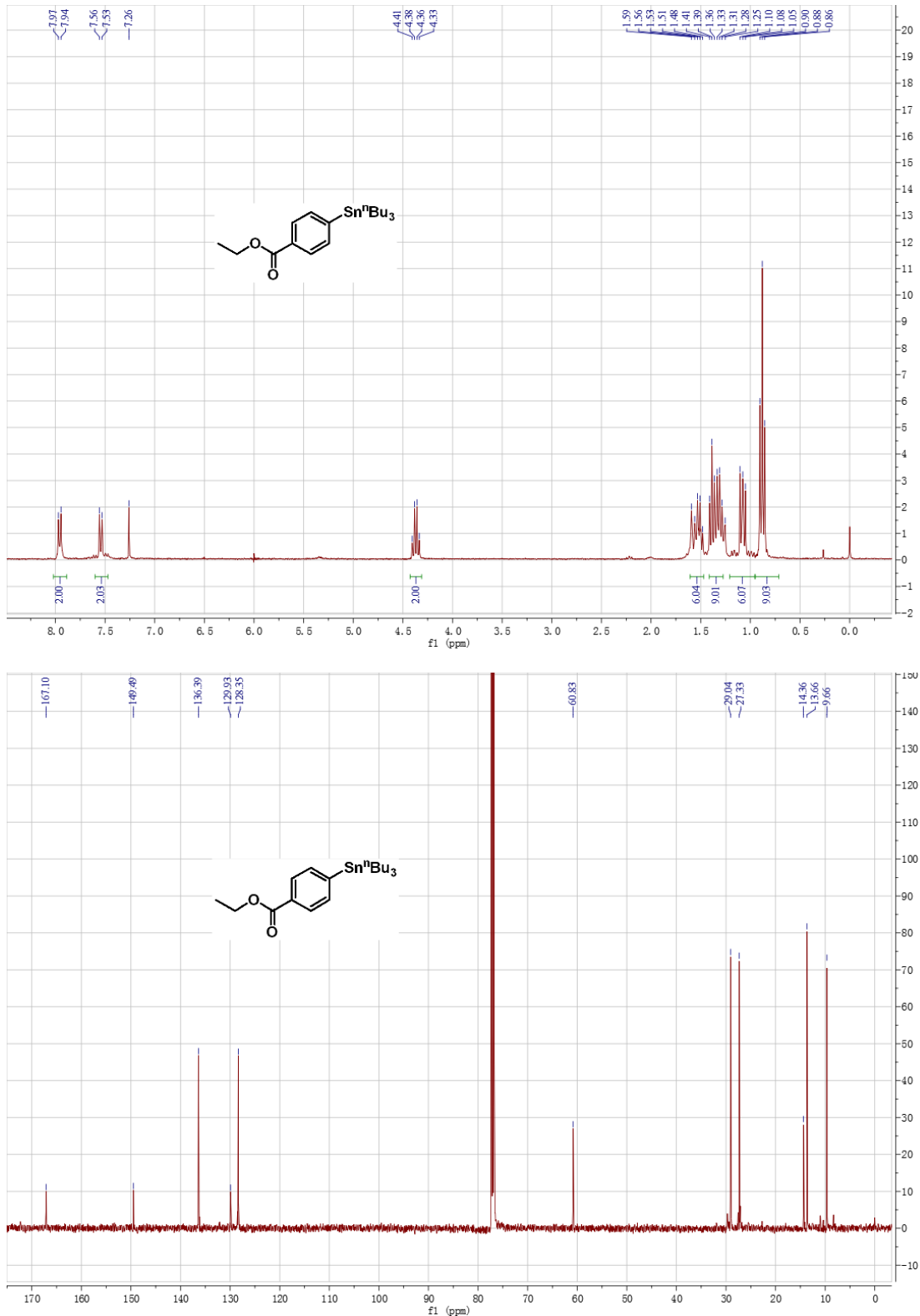
Compound 7a



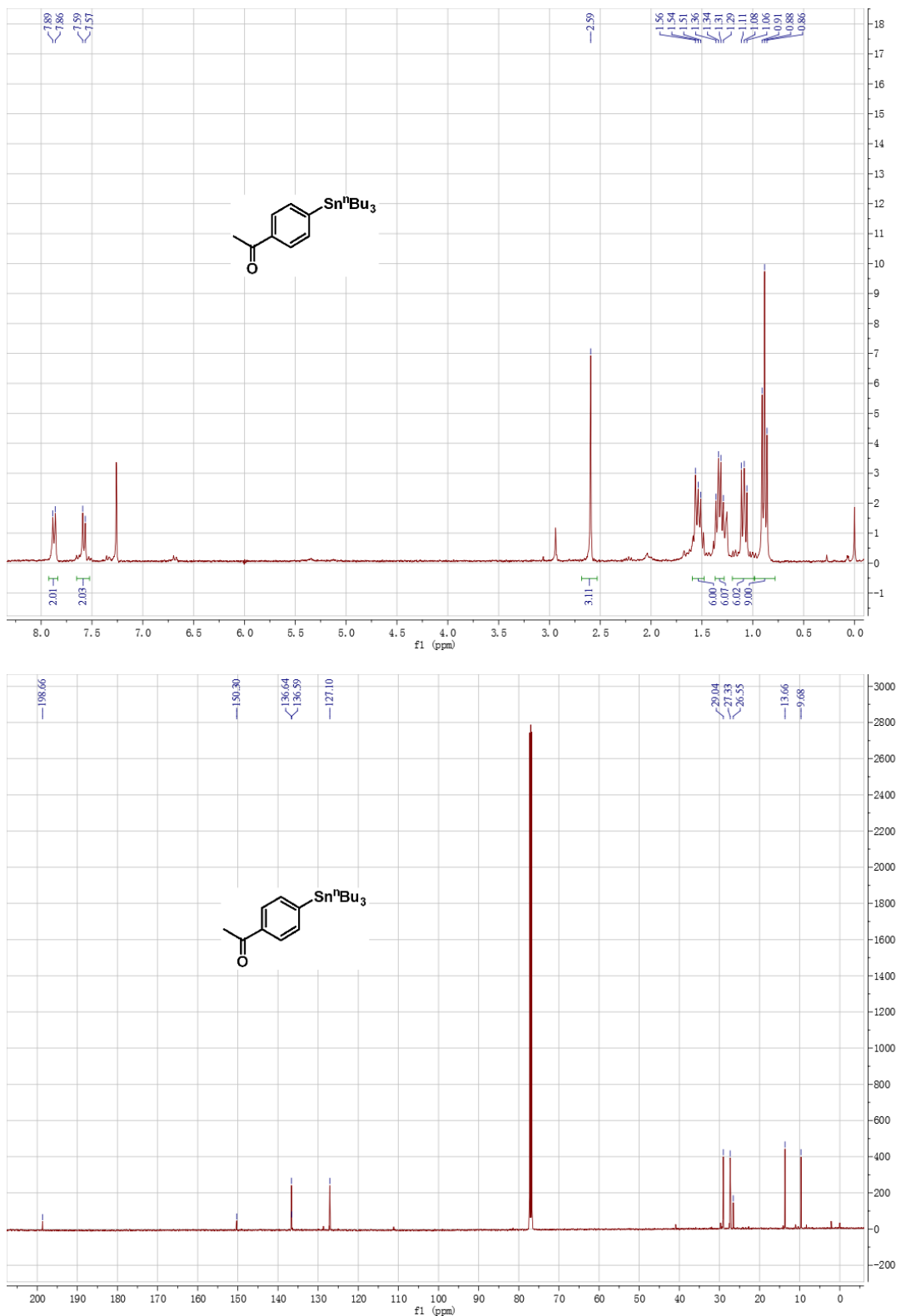
Compound 7c



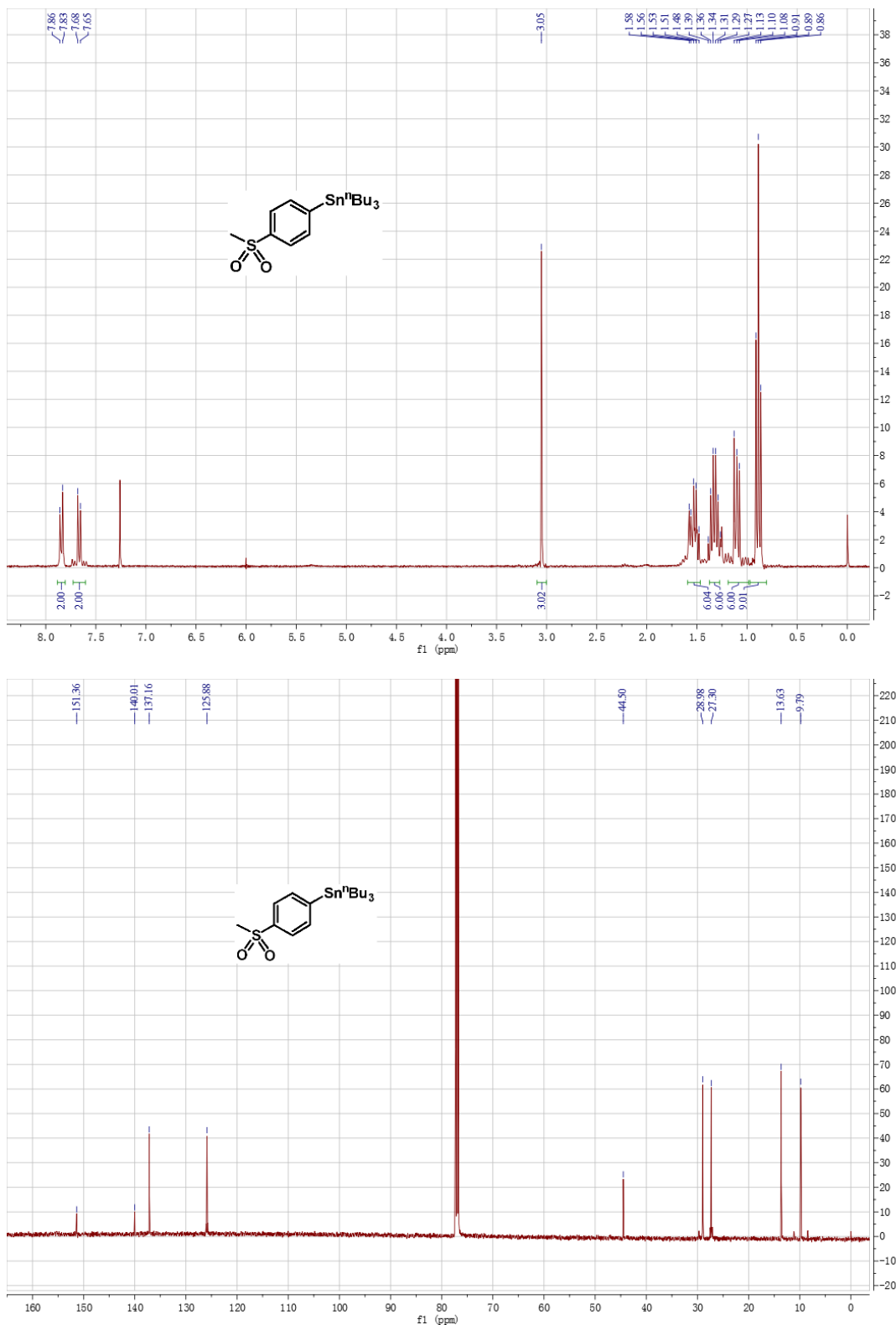
Compound 7f



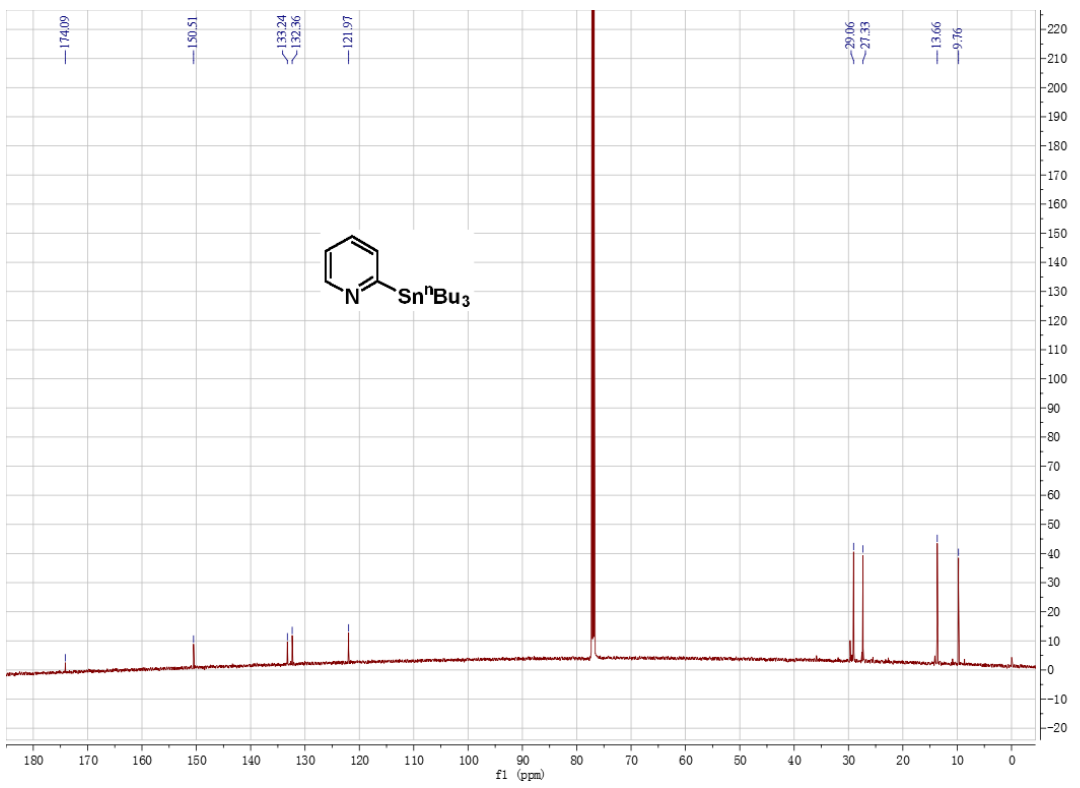
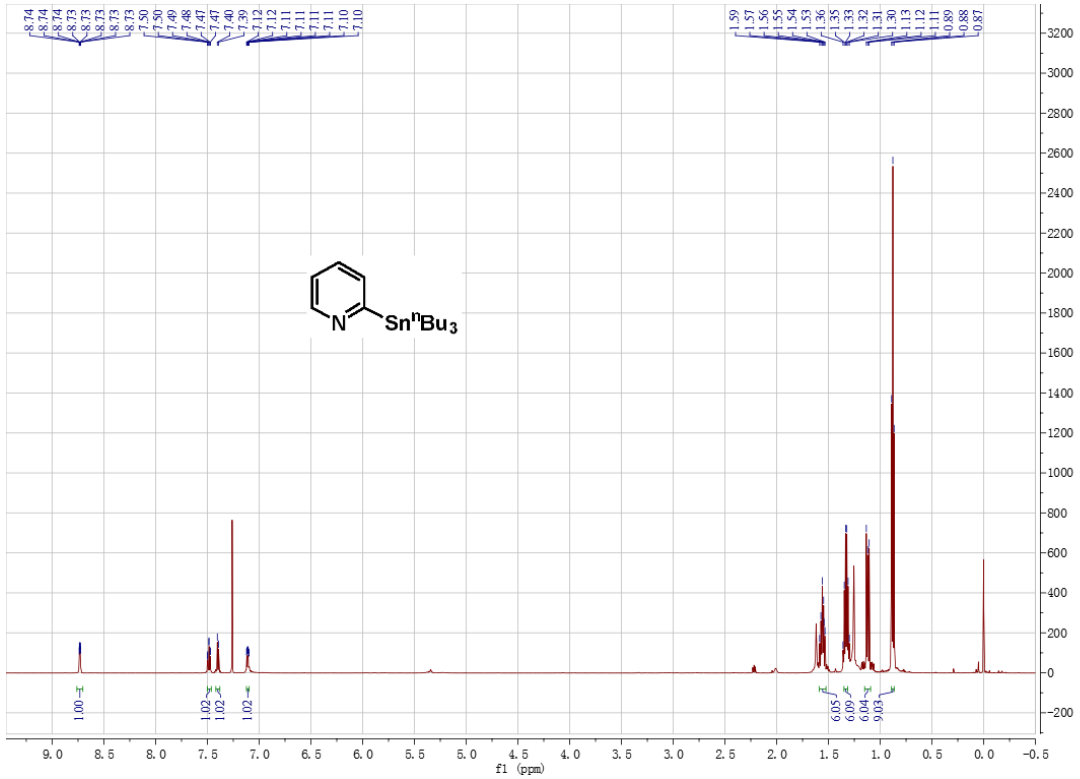
Compound 7e



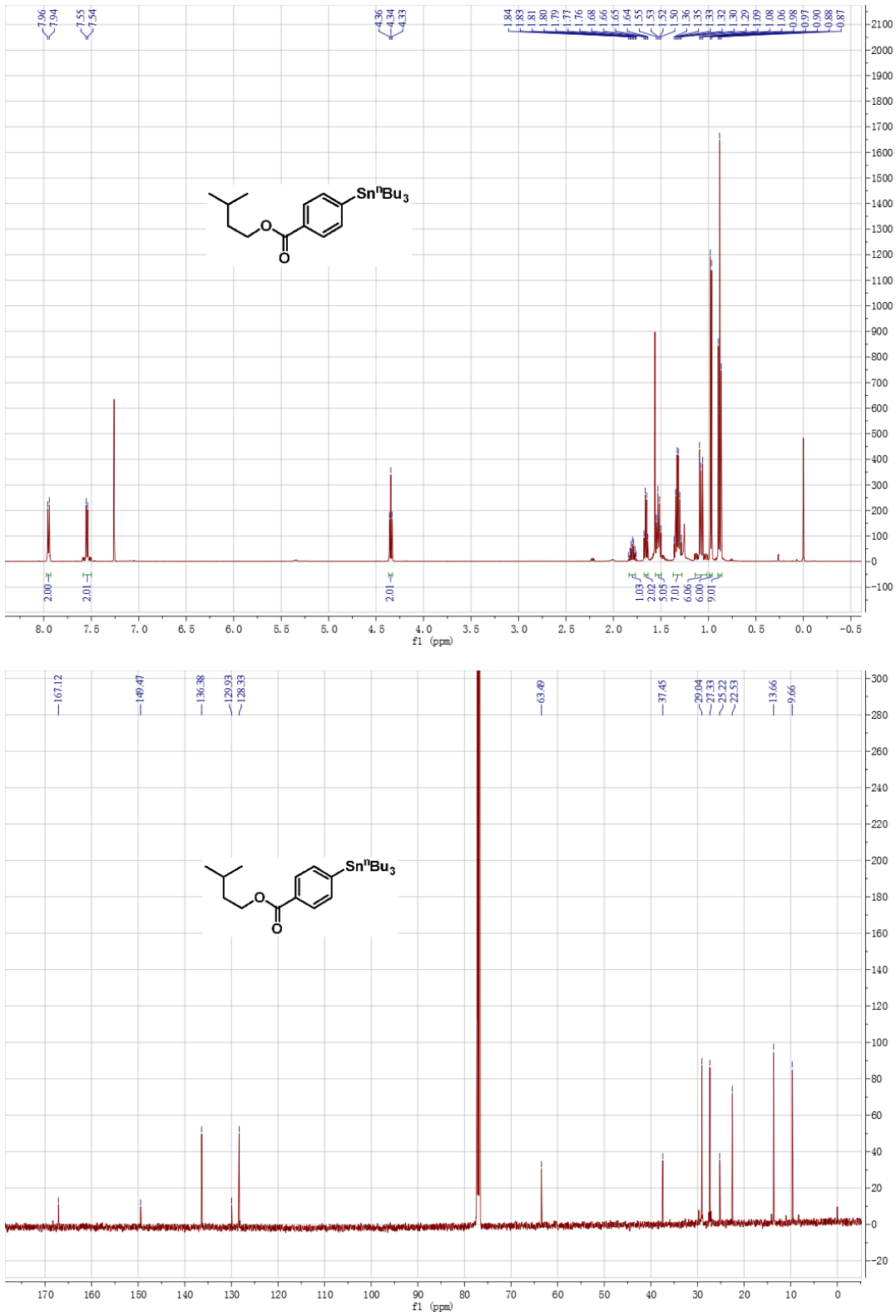
Compound 7h



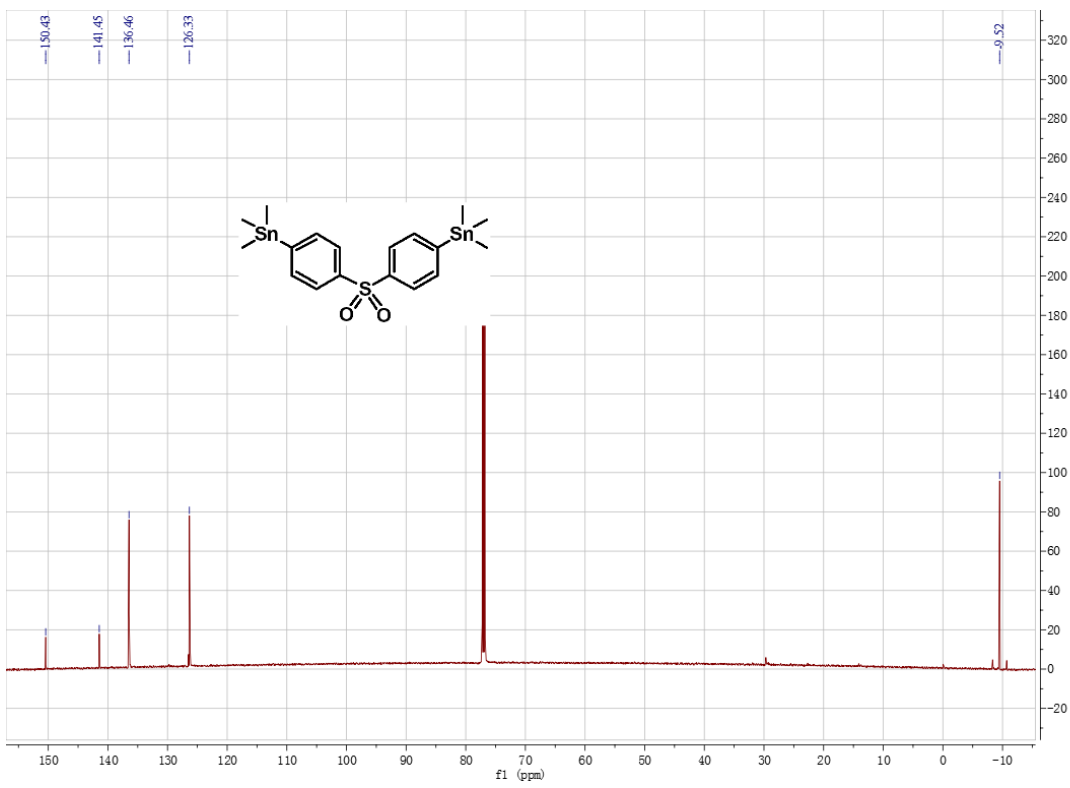
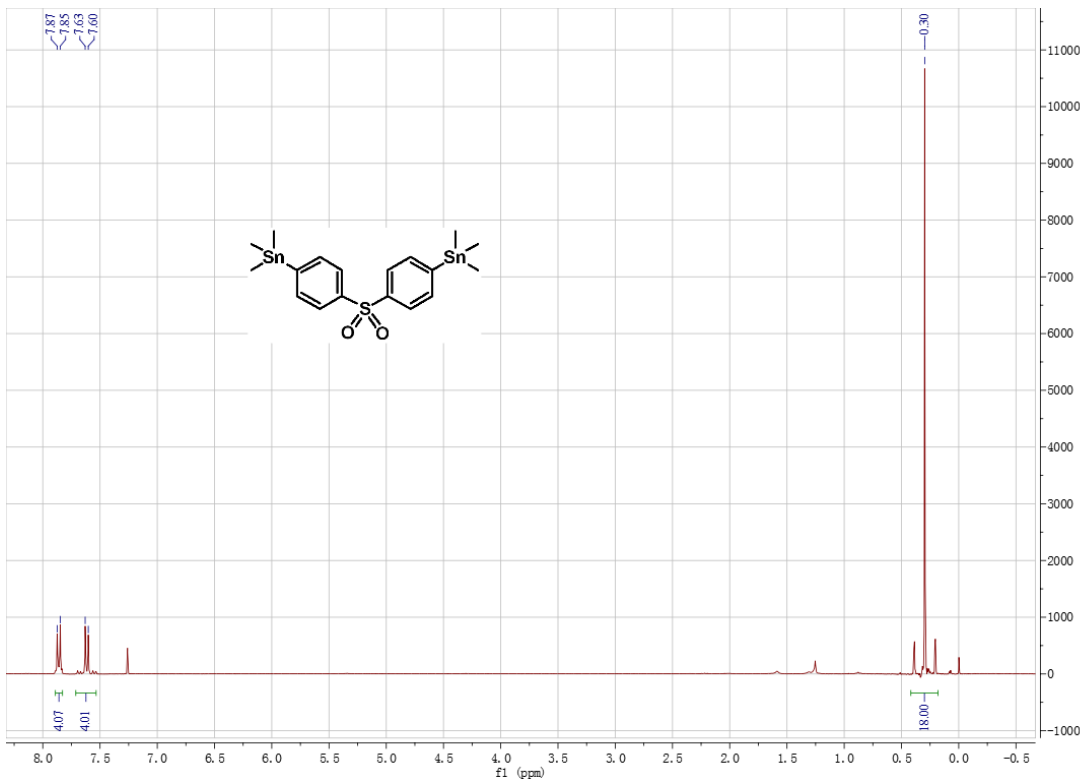
Compound 7j



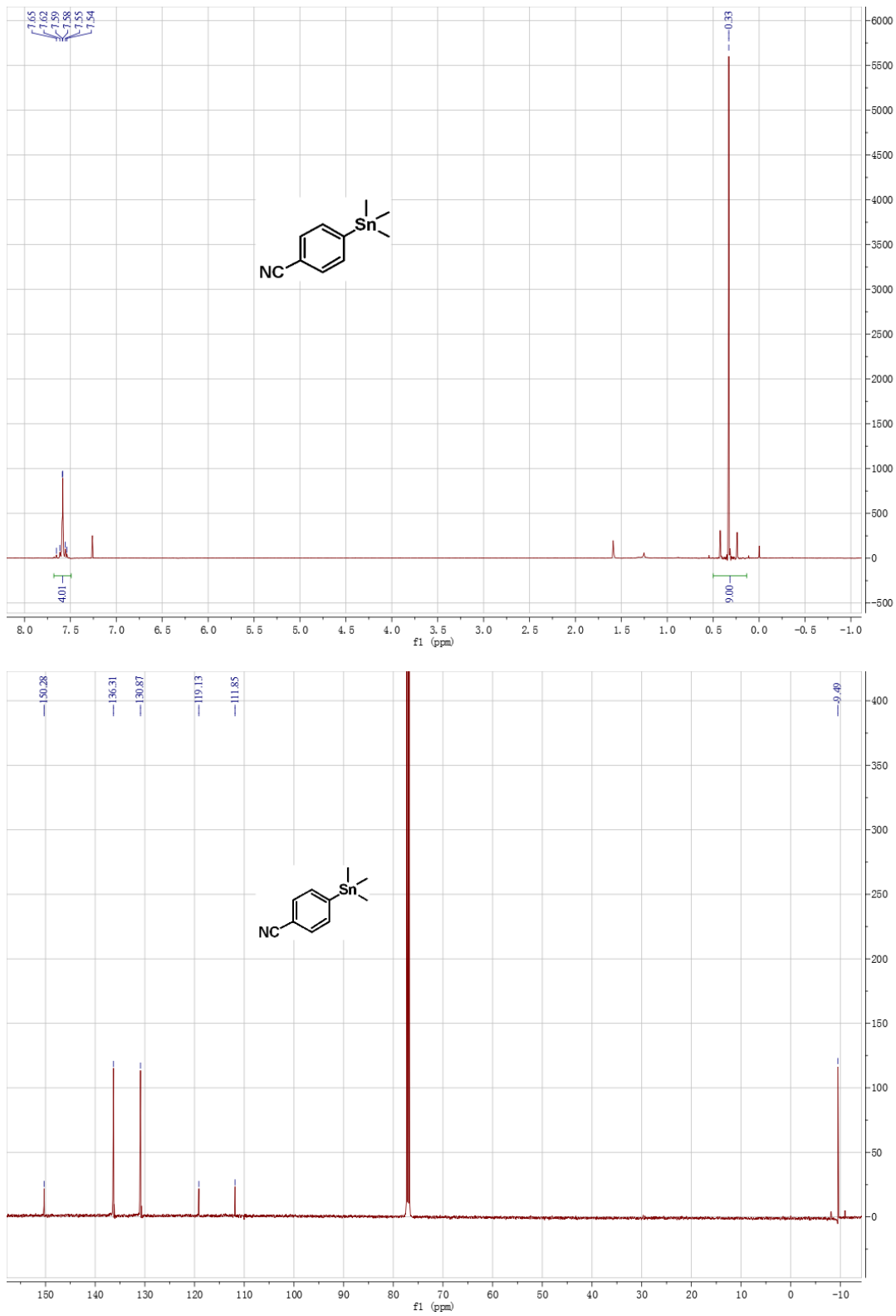
Compound 7k



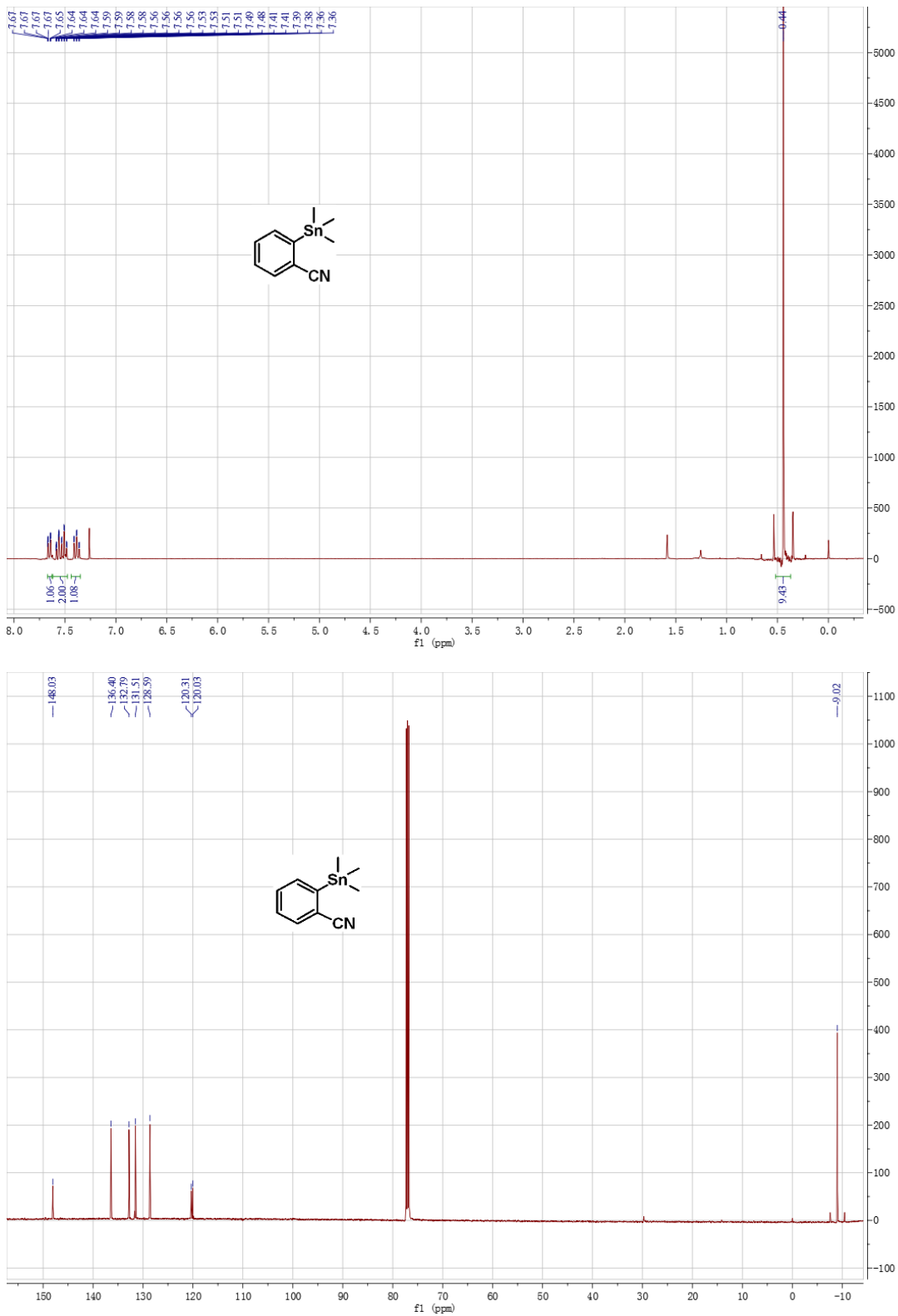
Compound 7m



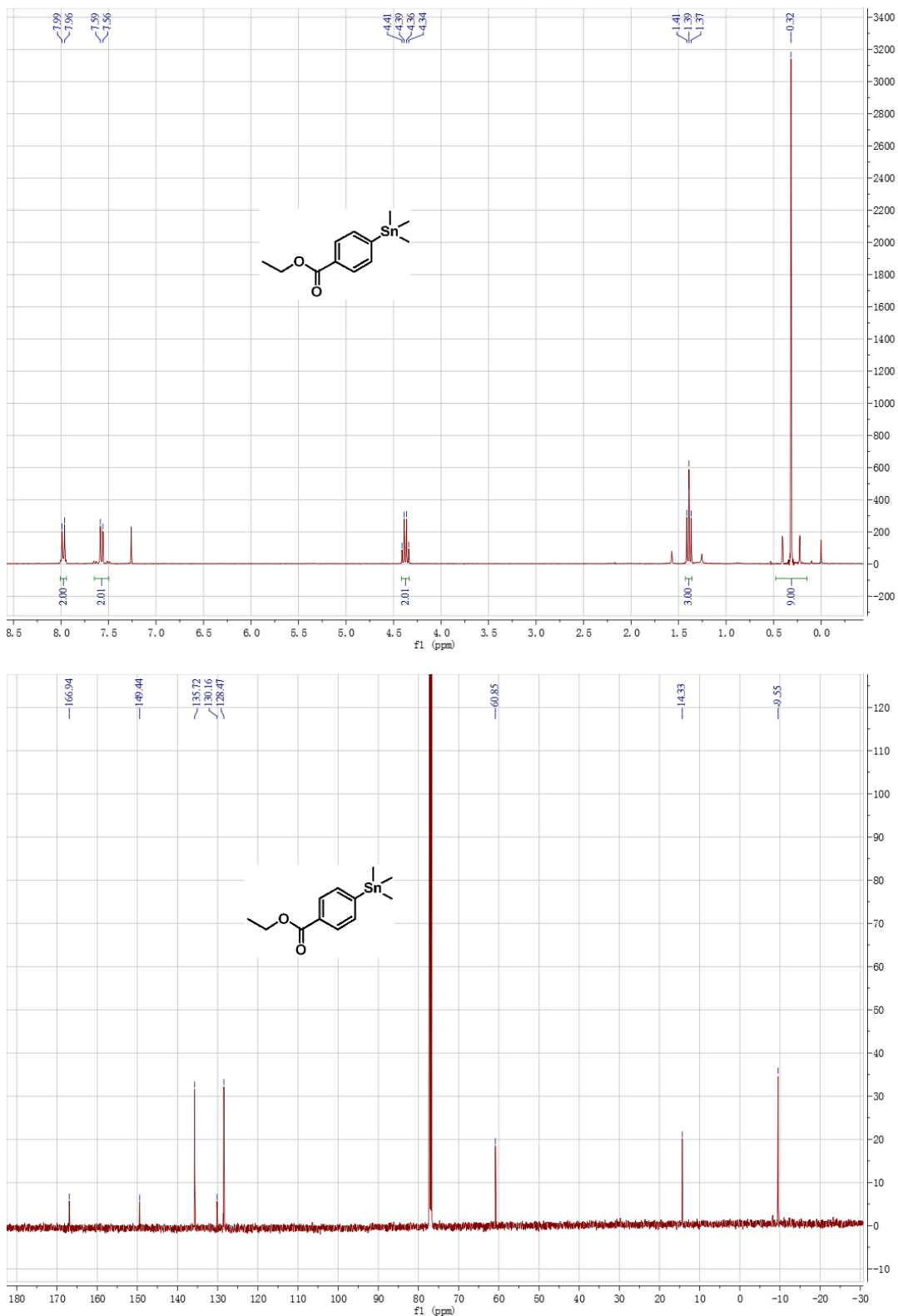
Compound 7b



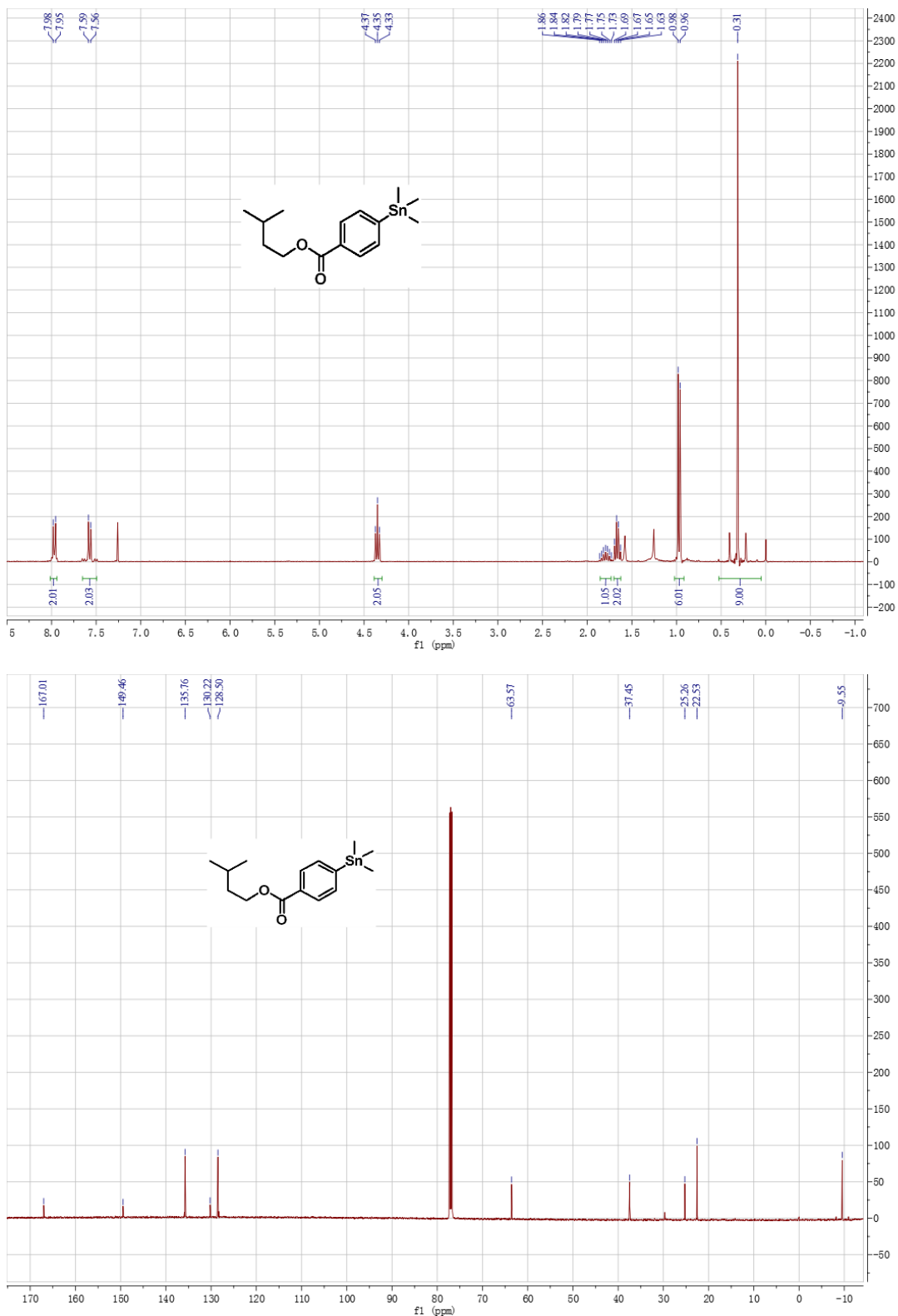
Compound 7d



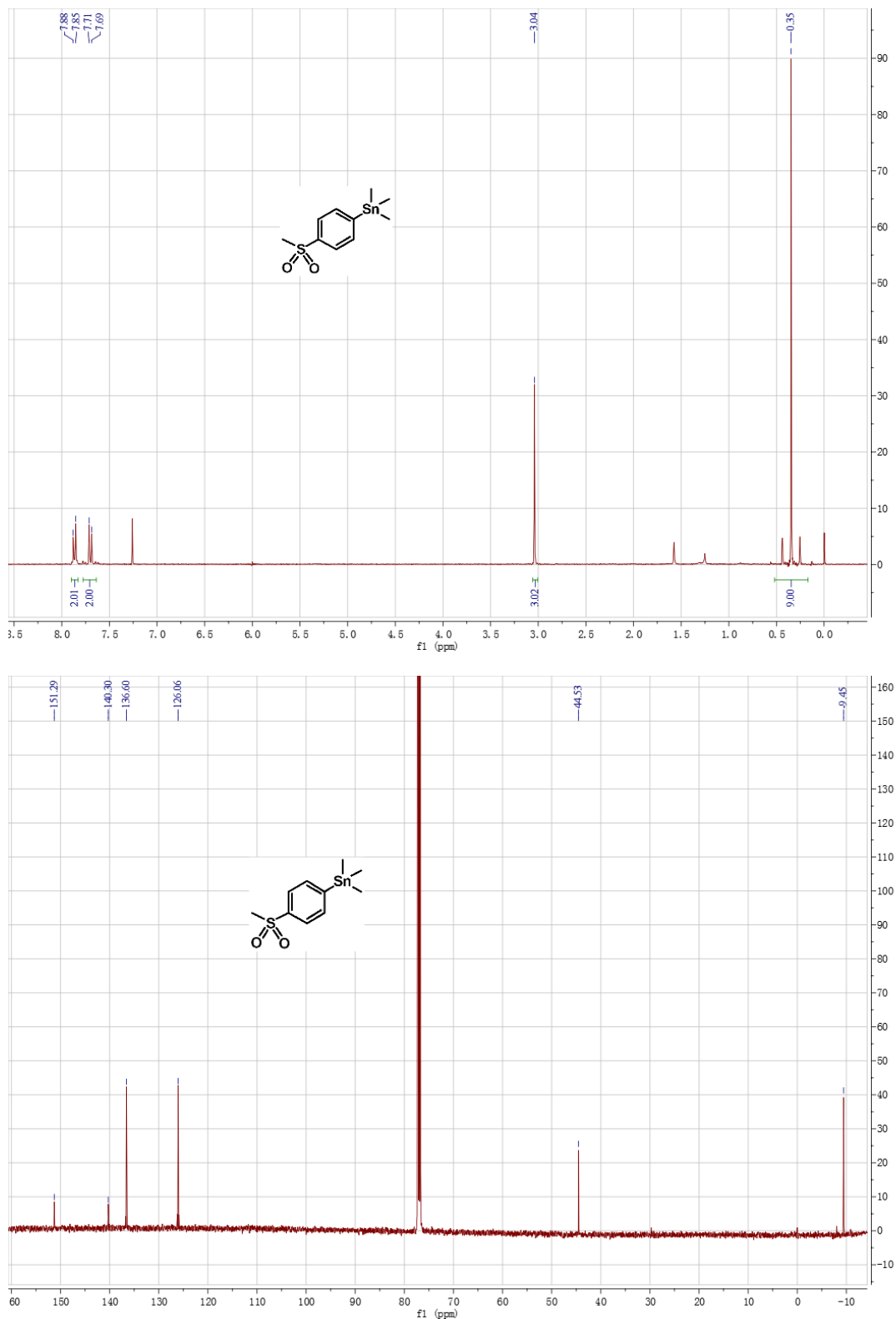
Compound 7g



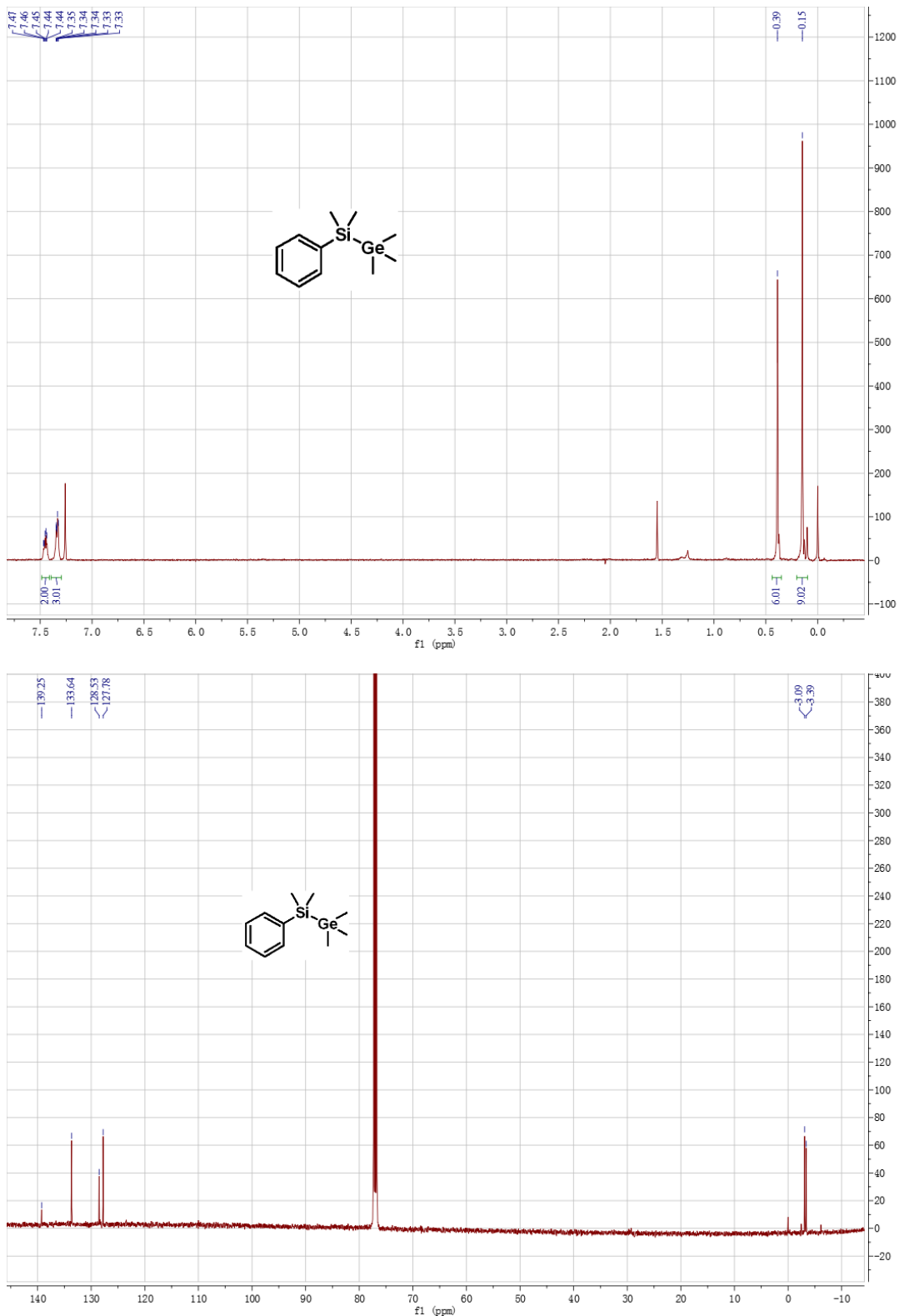
Compound 7I



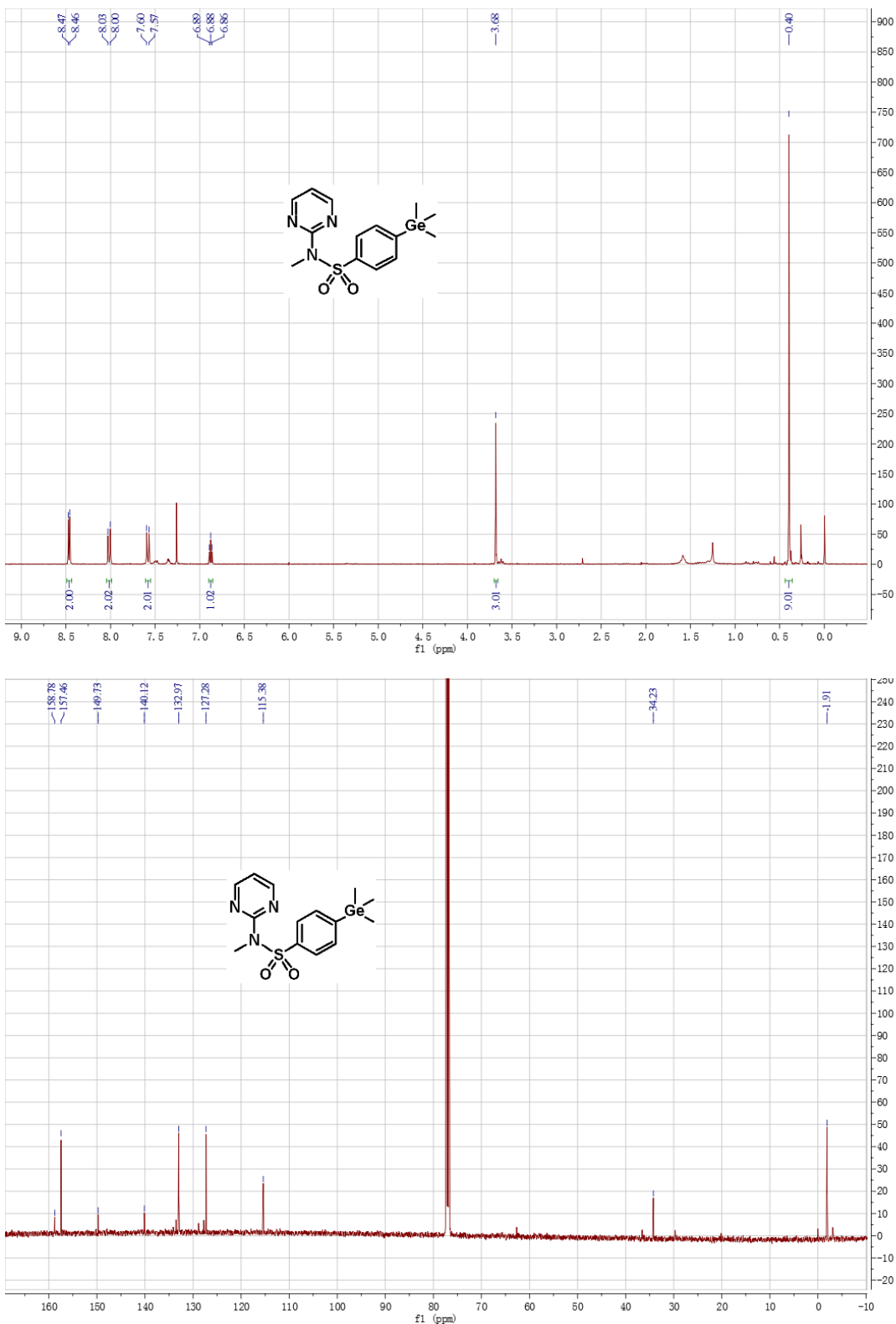
Compound 7i



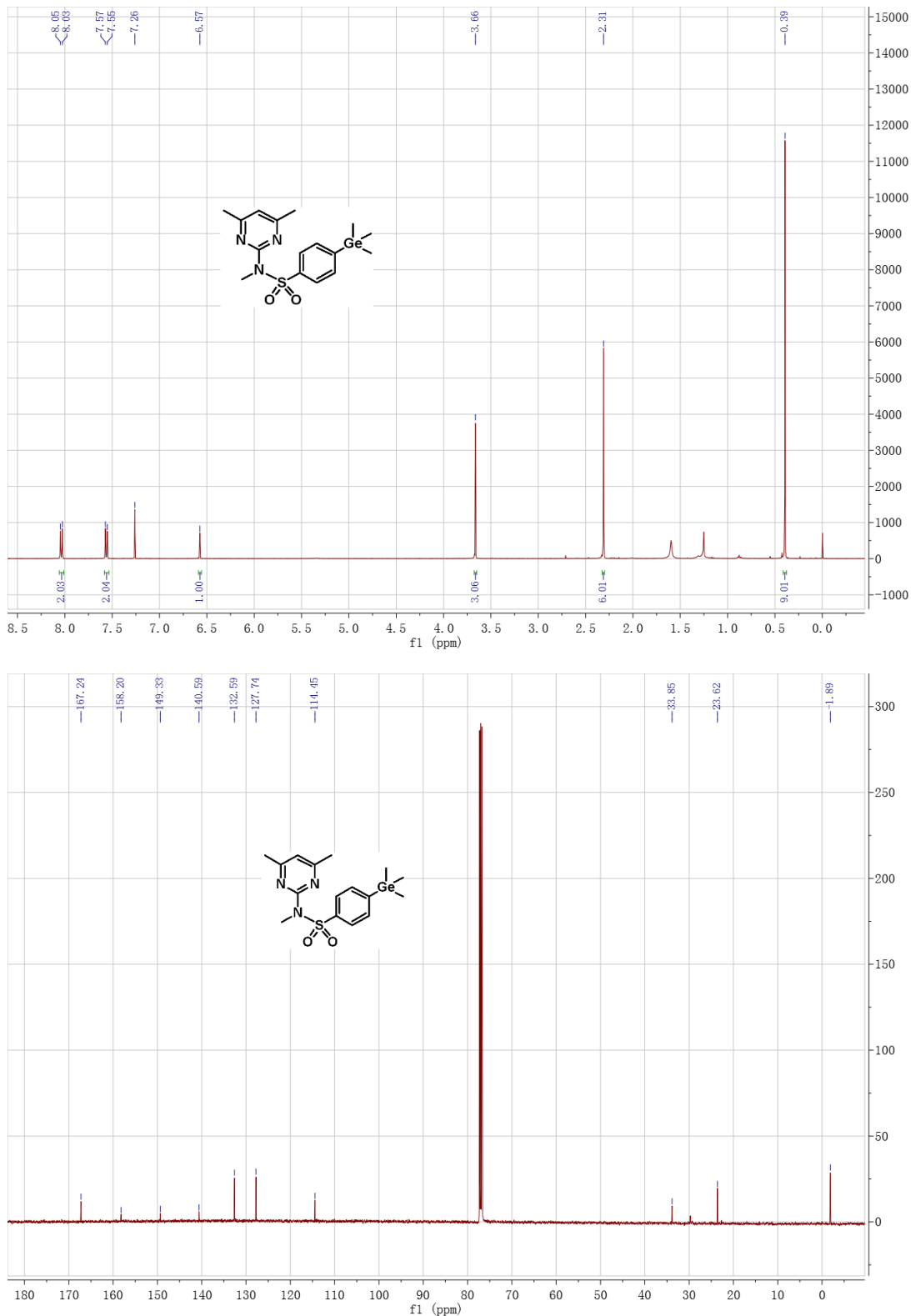
Compound 8



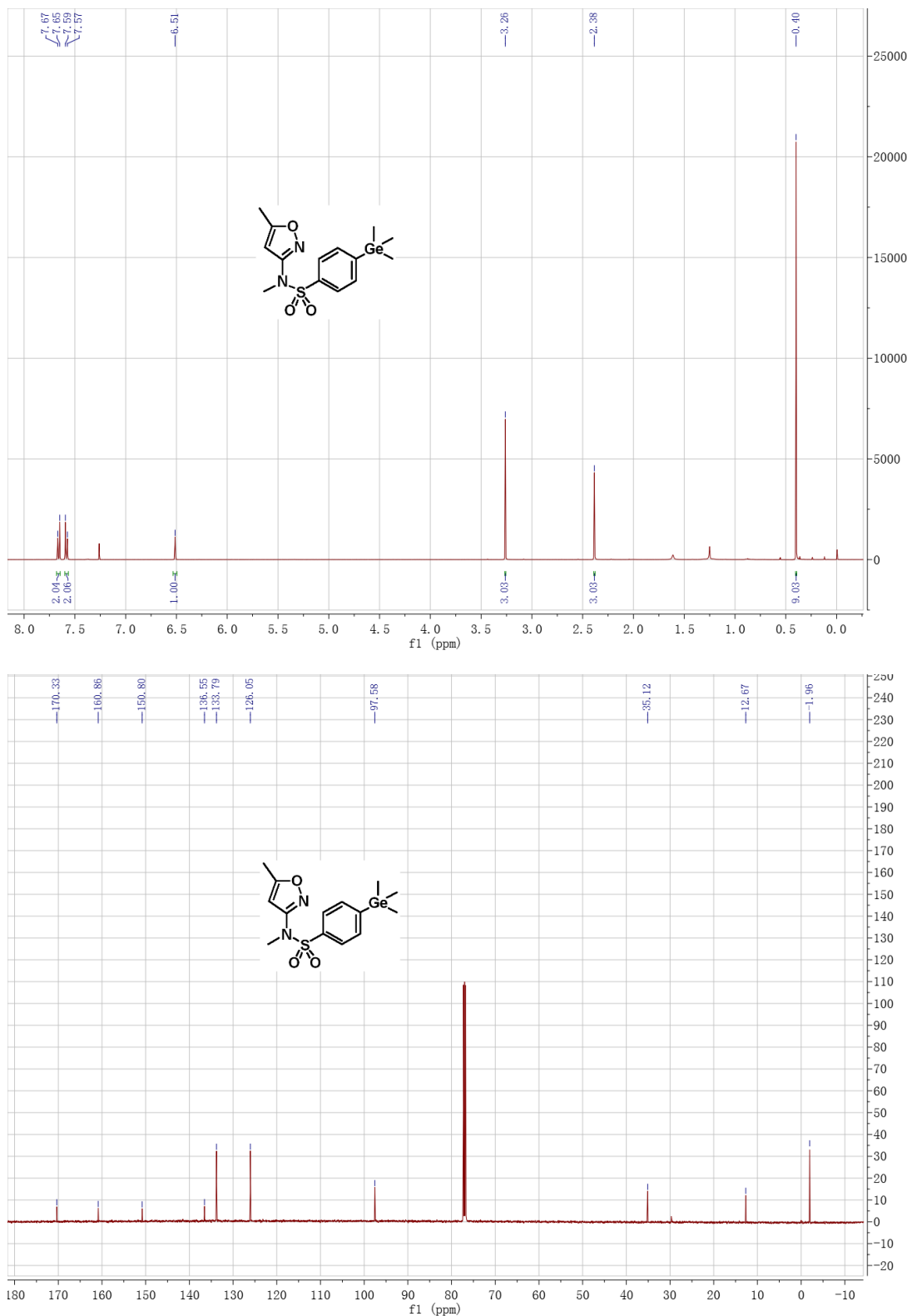
Compound 9a



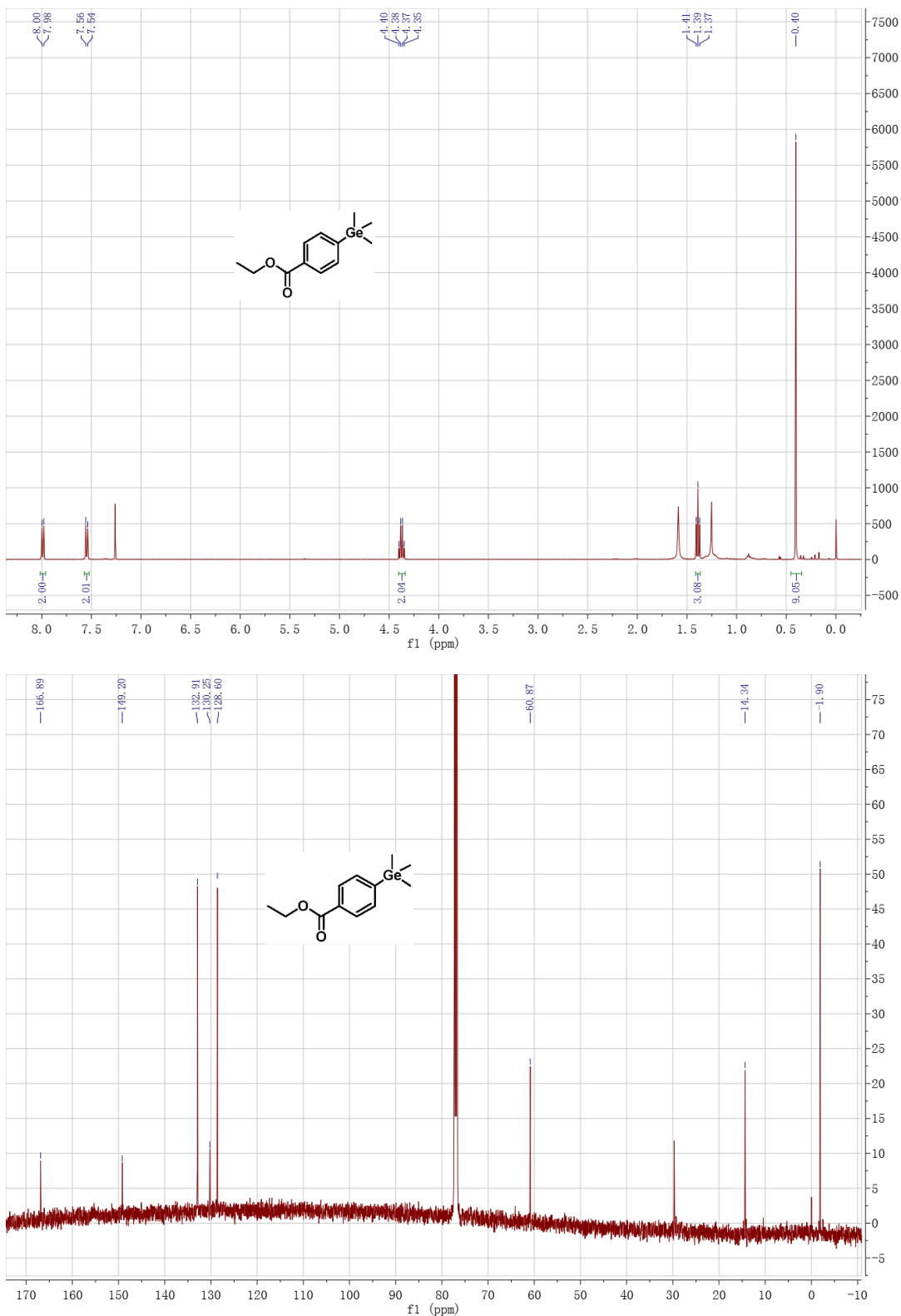
Compound 9c



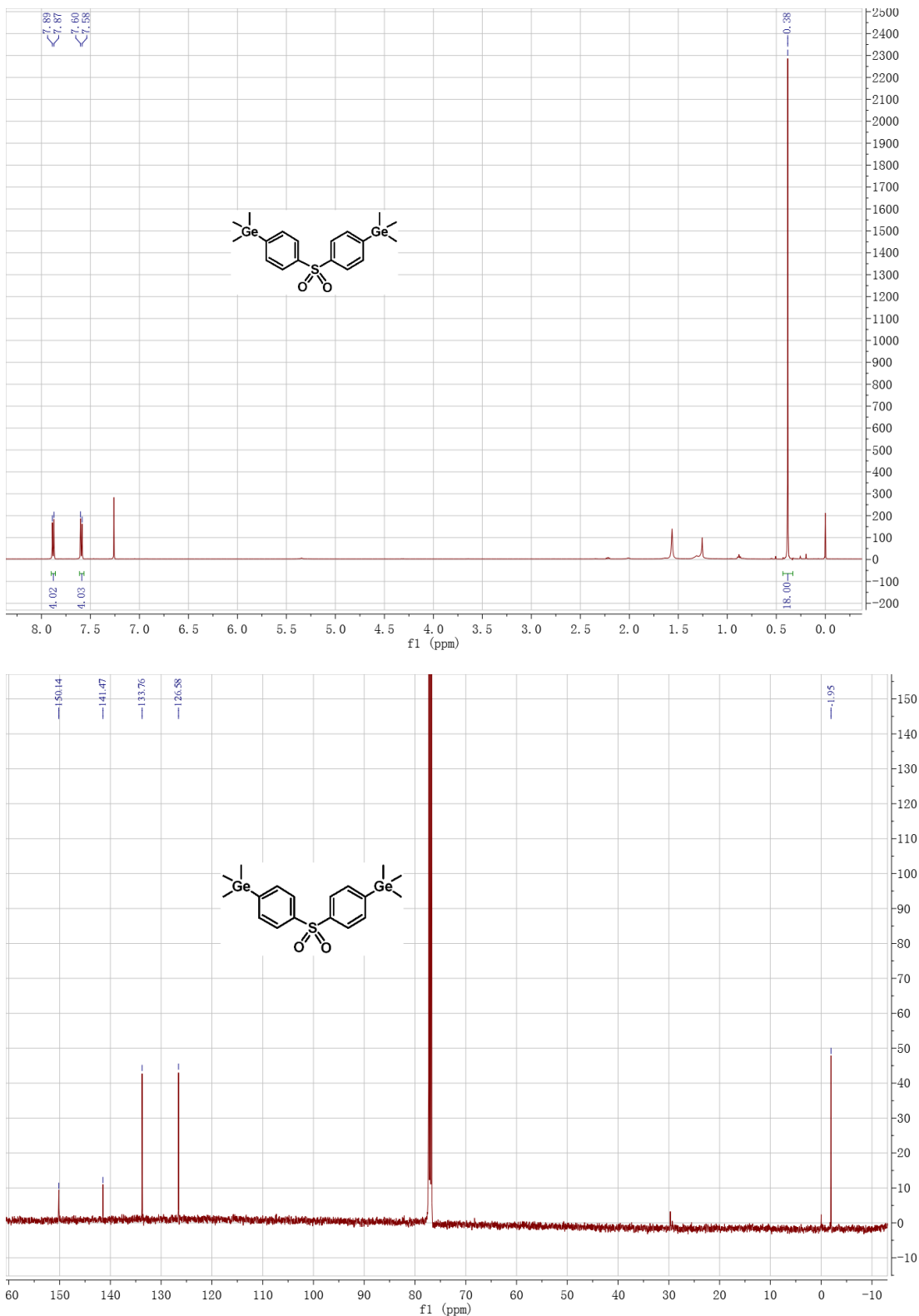
Compound 9b



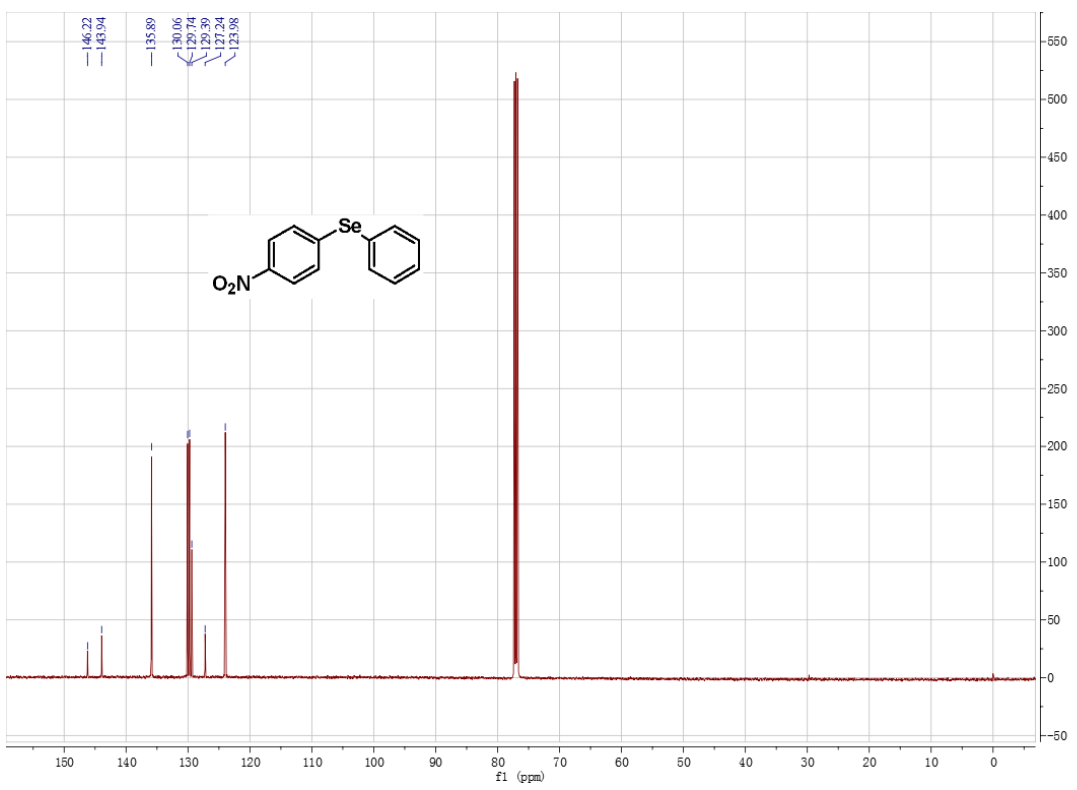
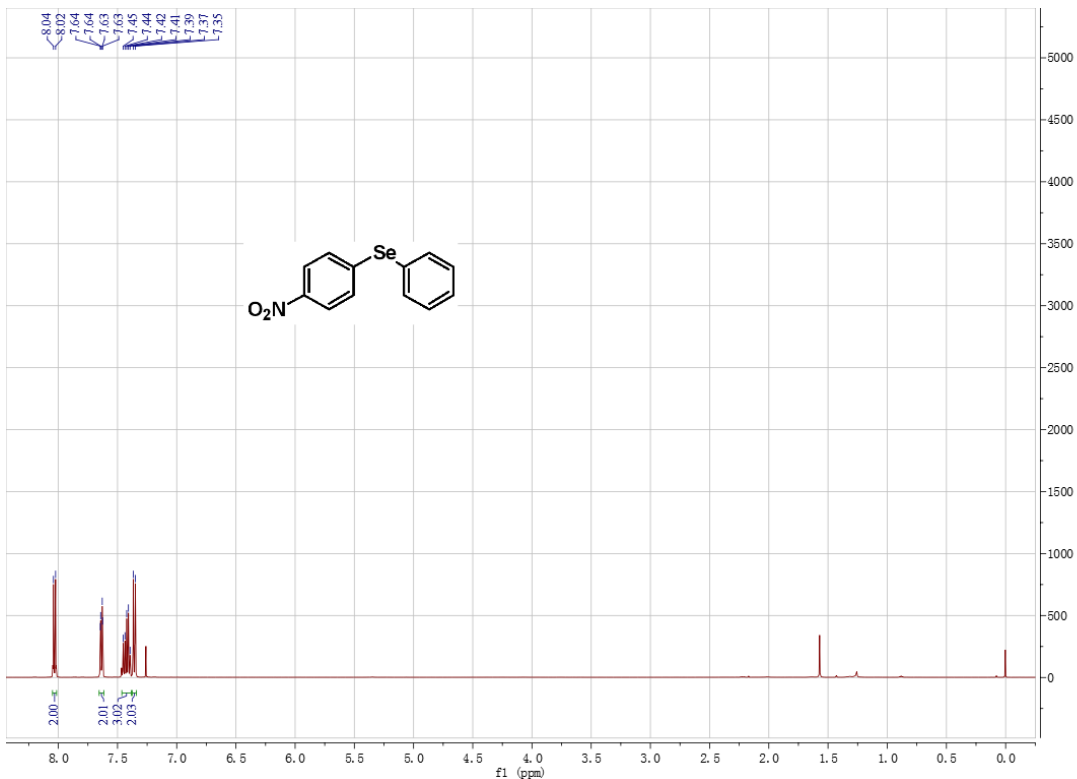
Compound 9e



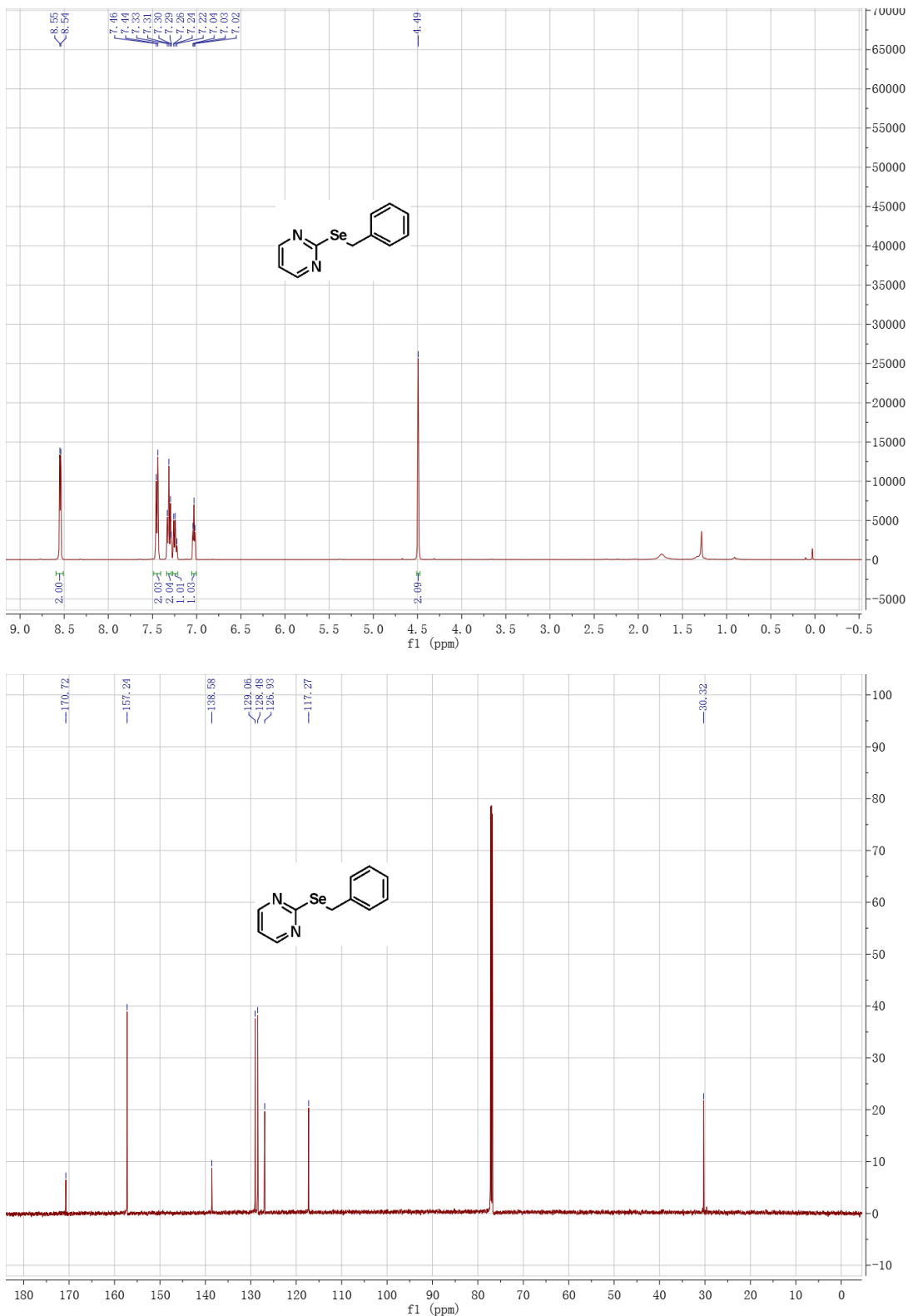
Compound 9d



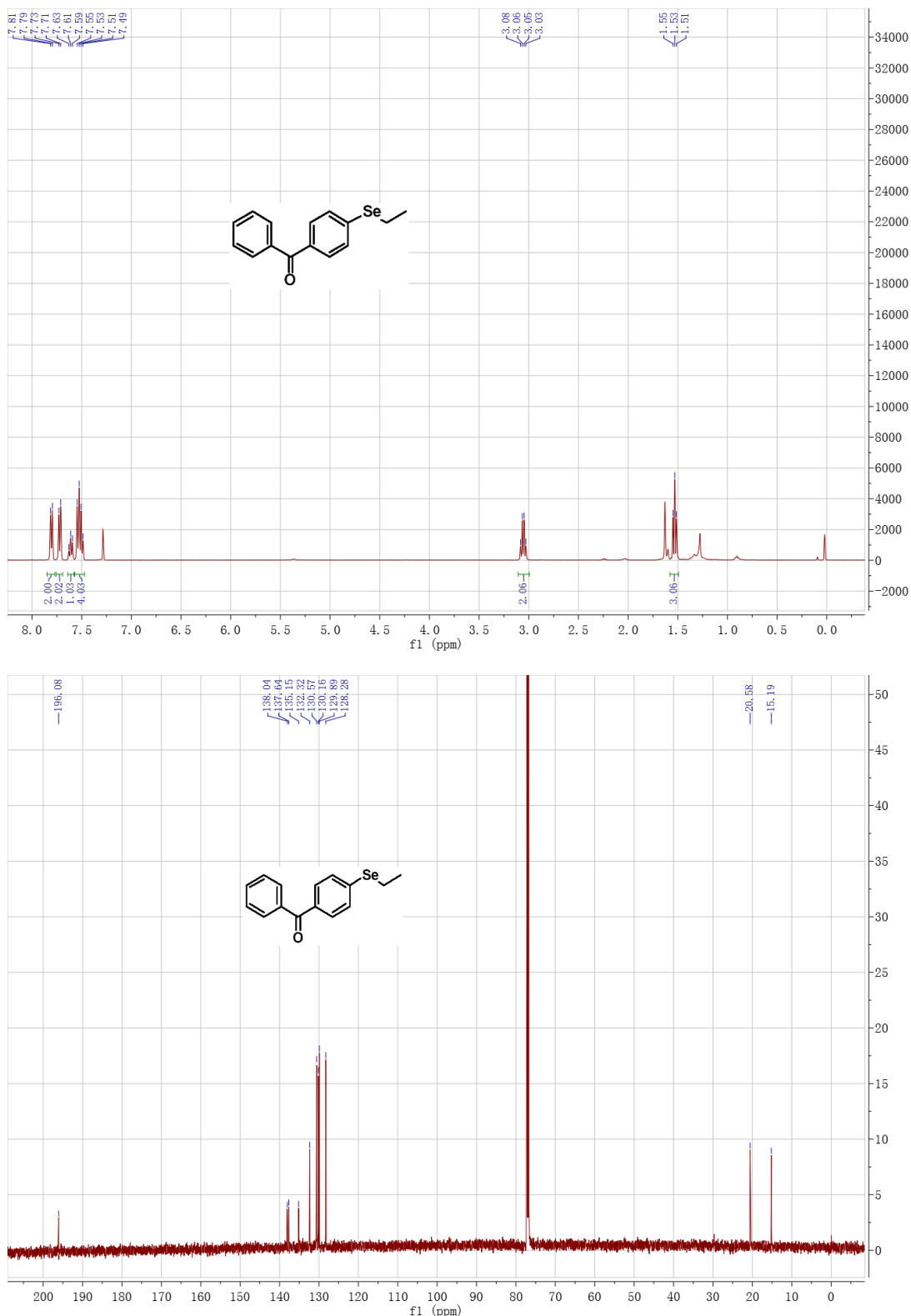
Compound 11a



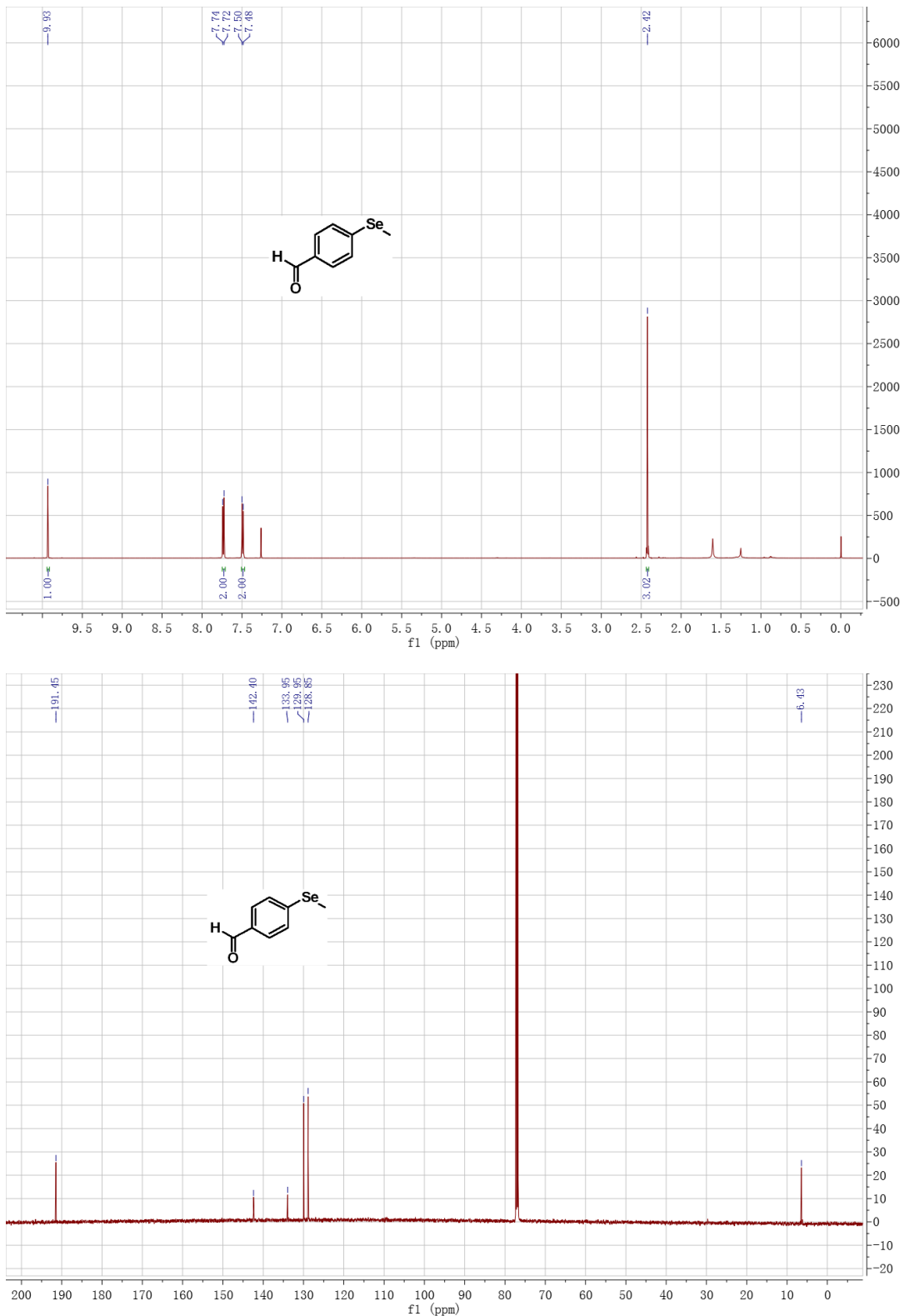
Compound 11d



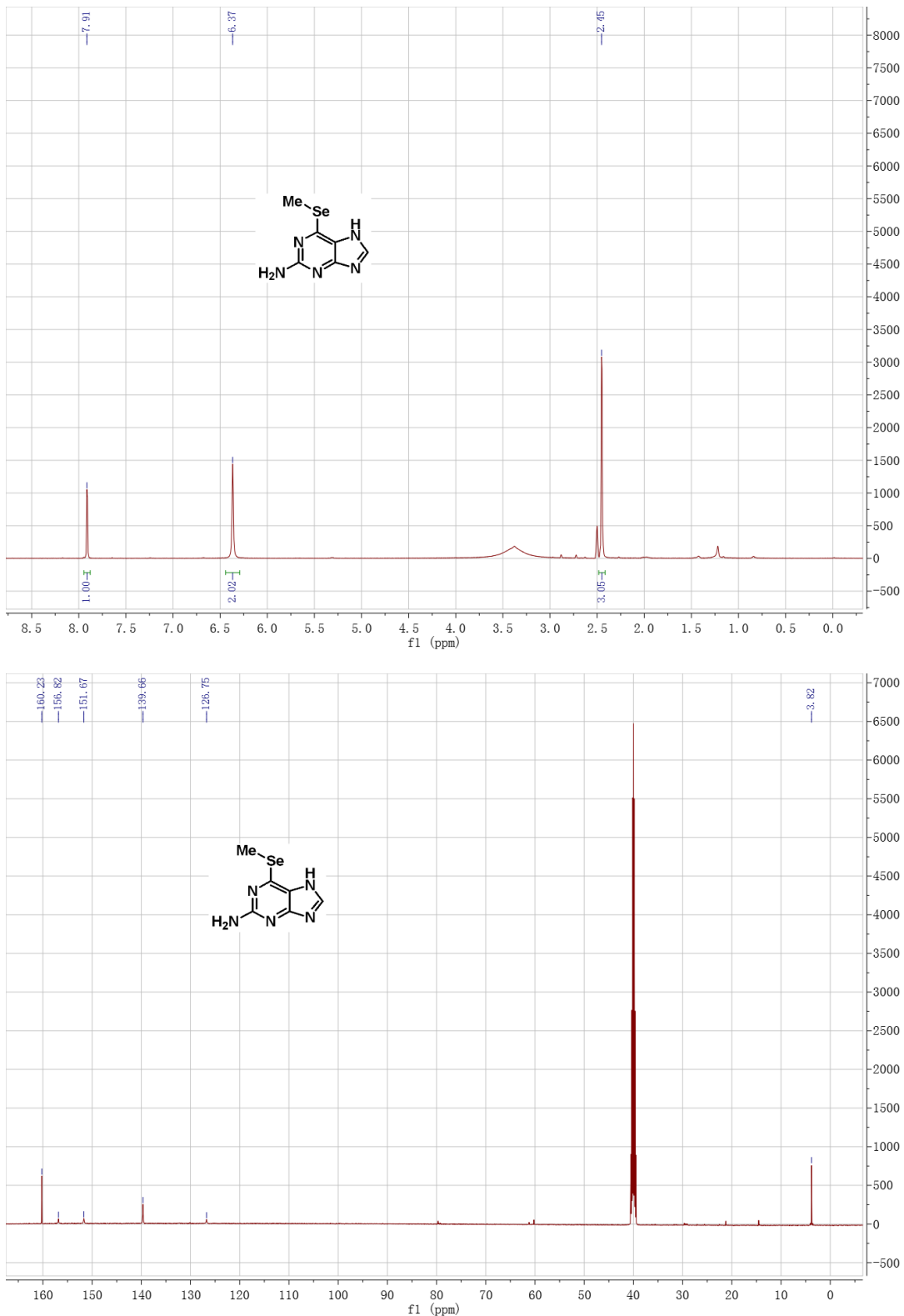
Compound 11b



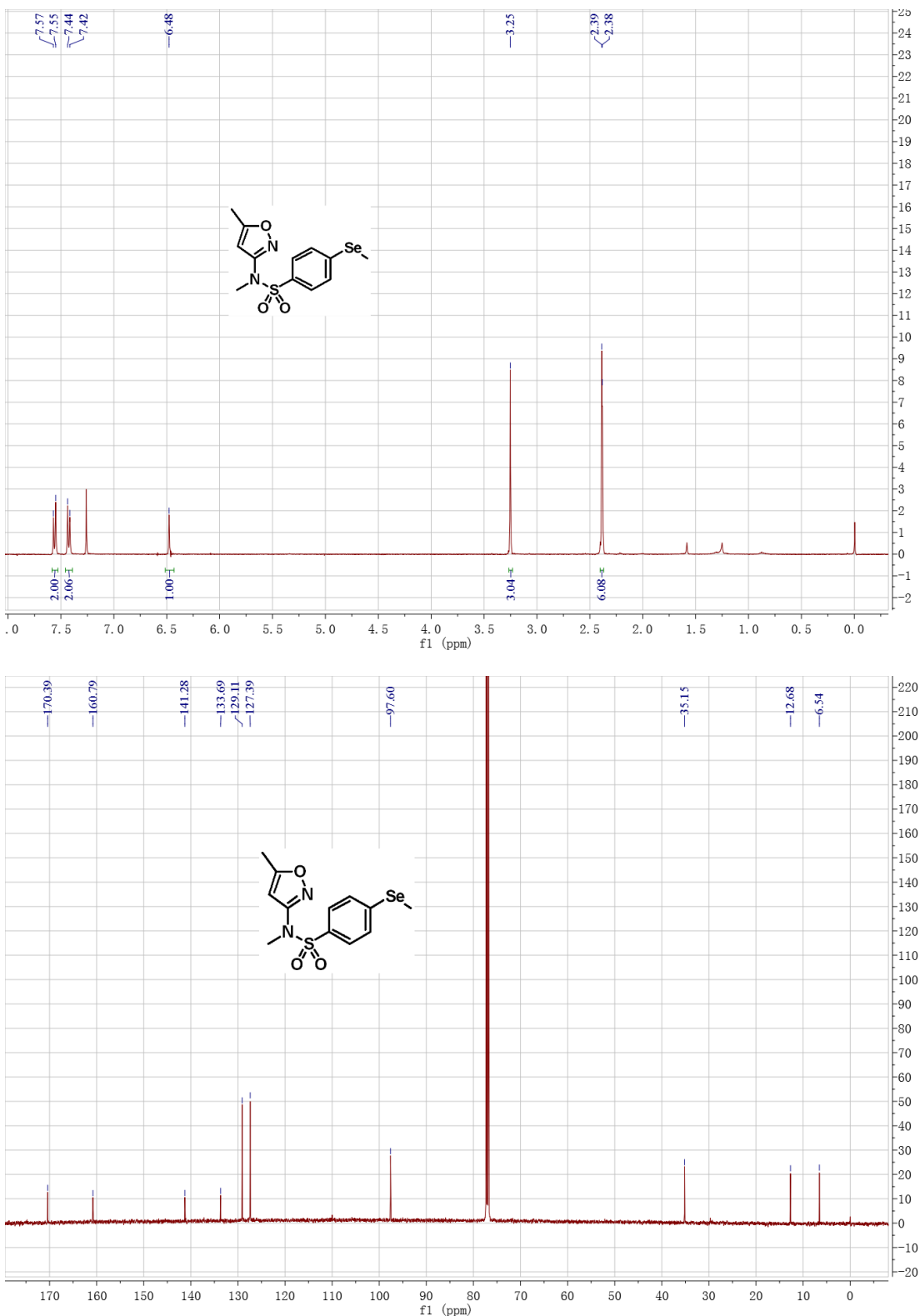
Compound 11c



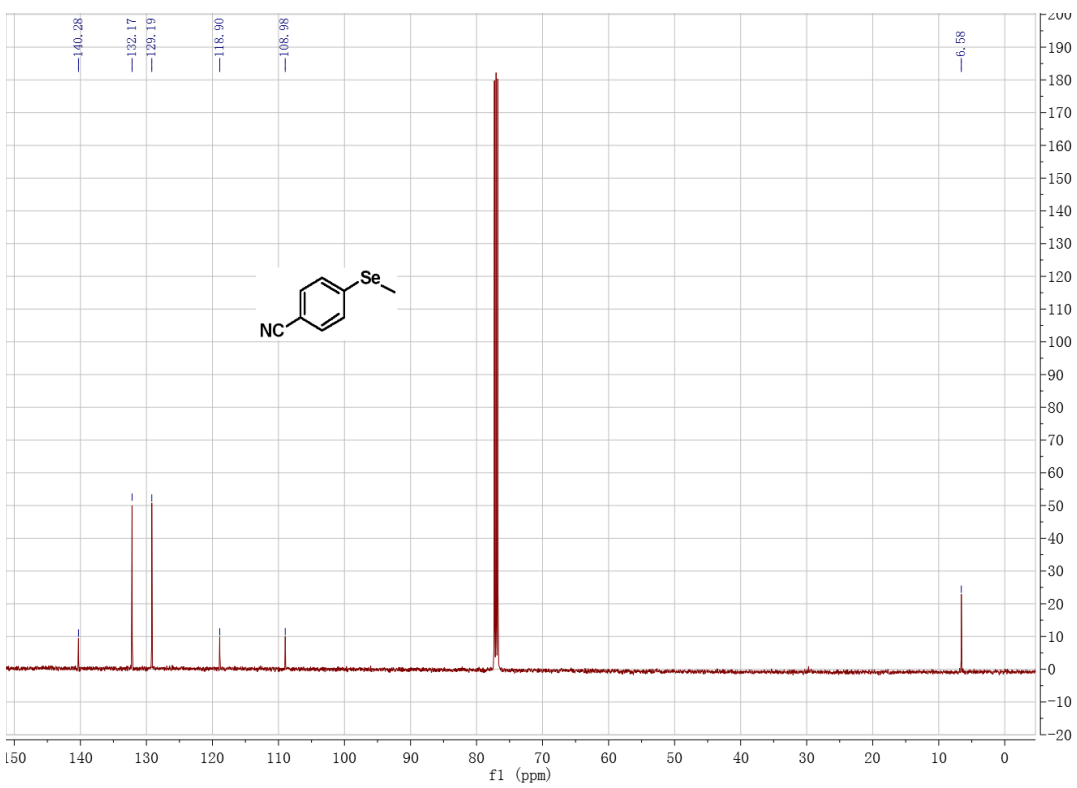
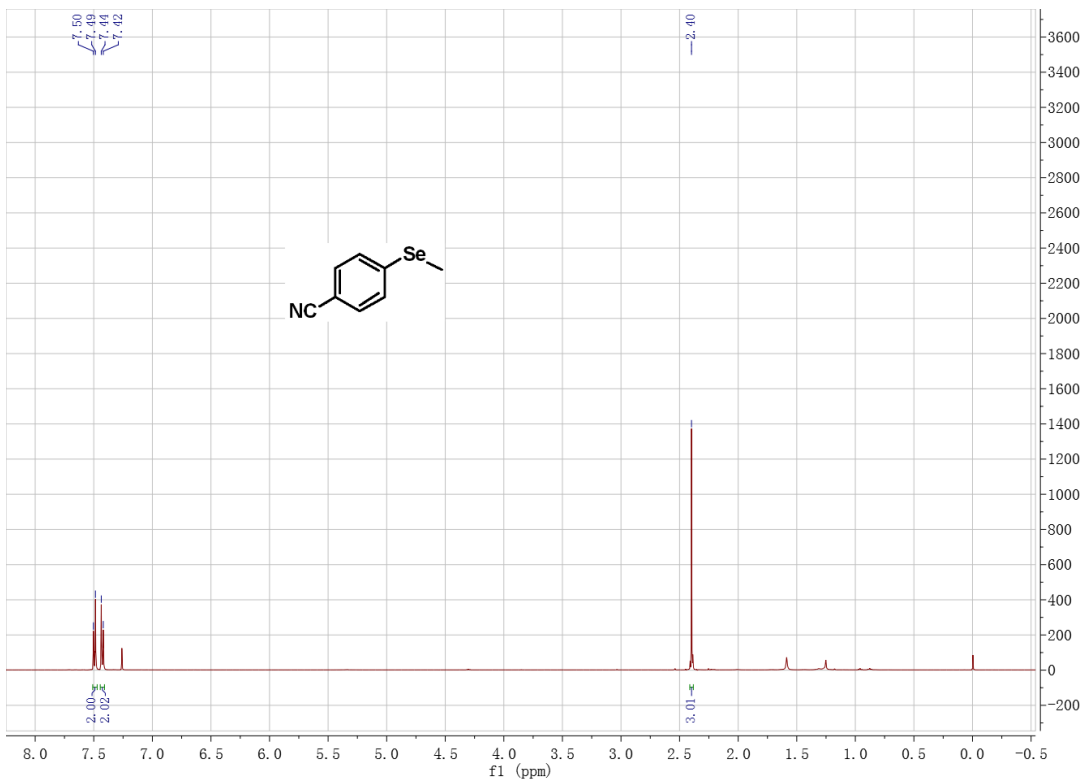
Compound 11e



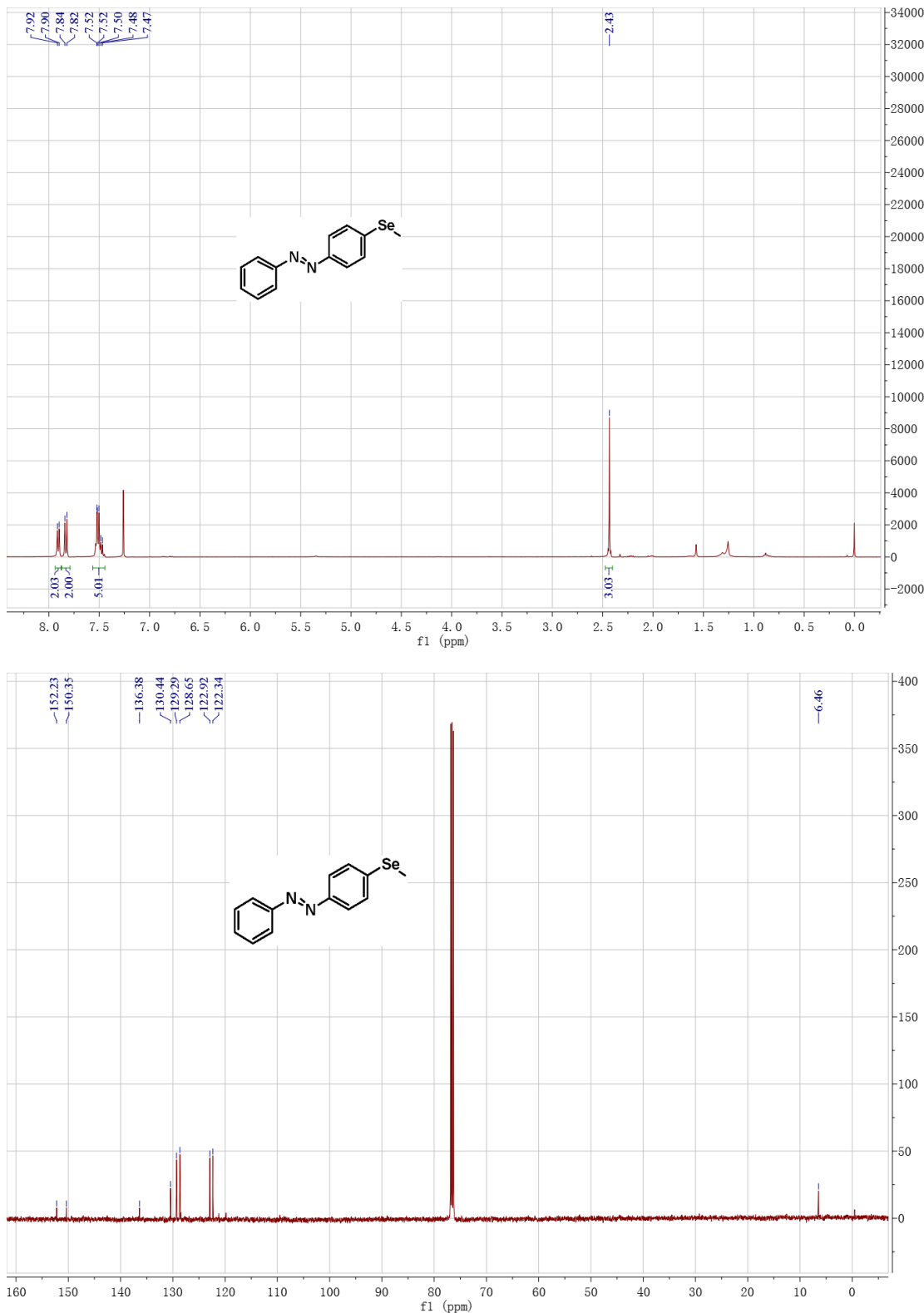
Compound 11f



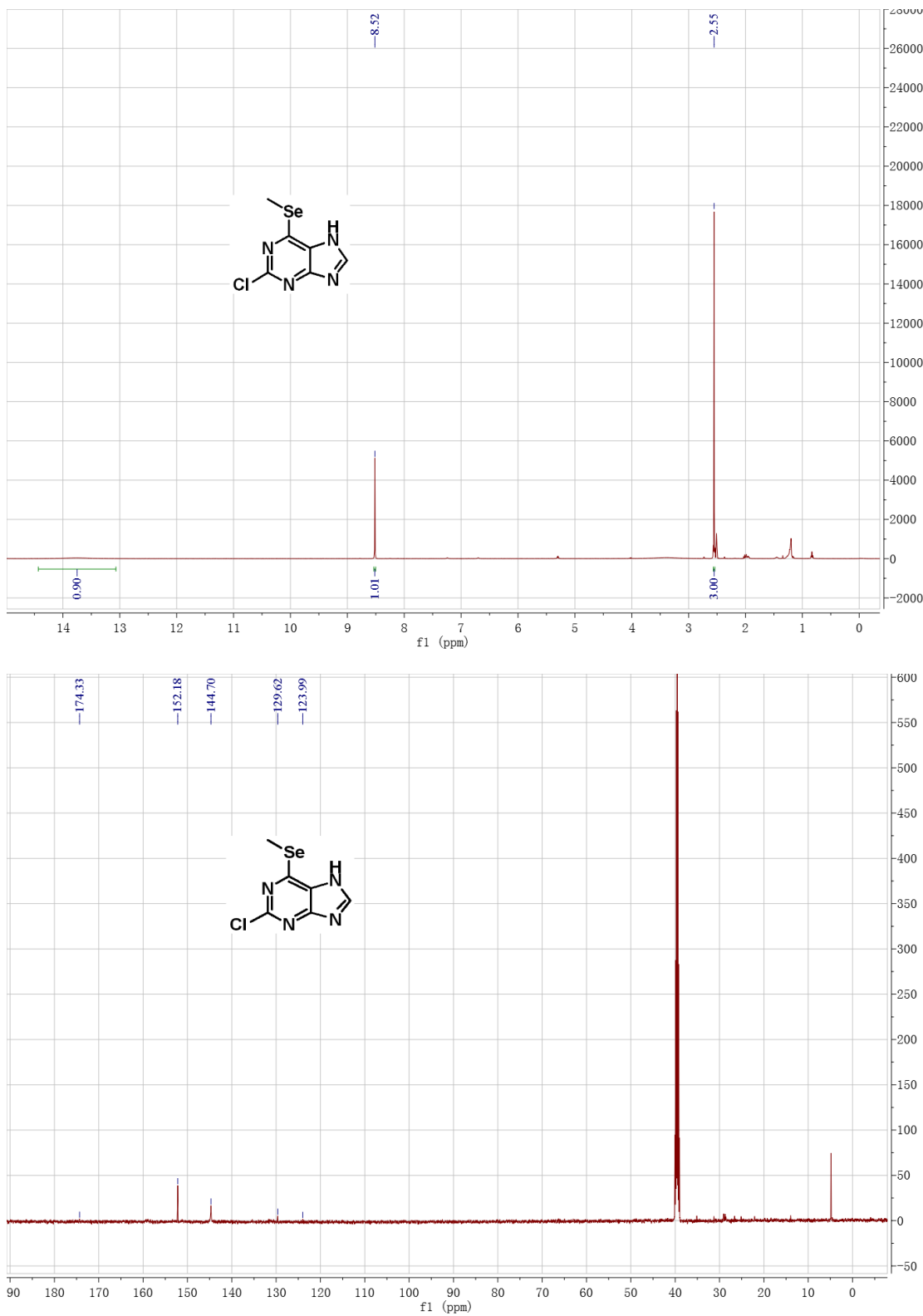
Compound 11g



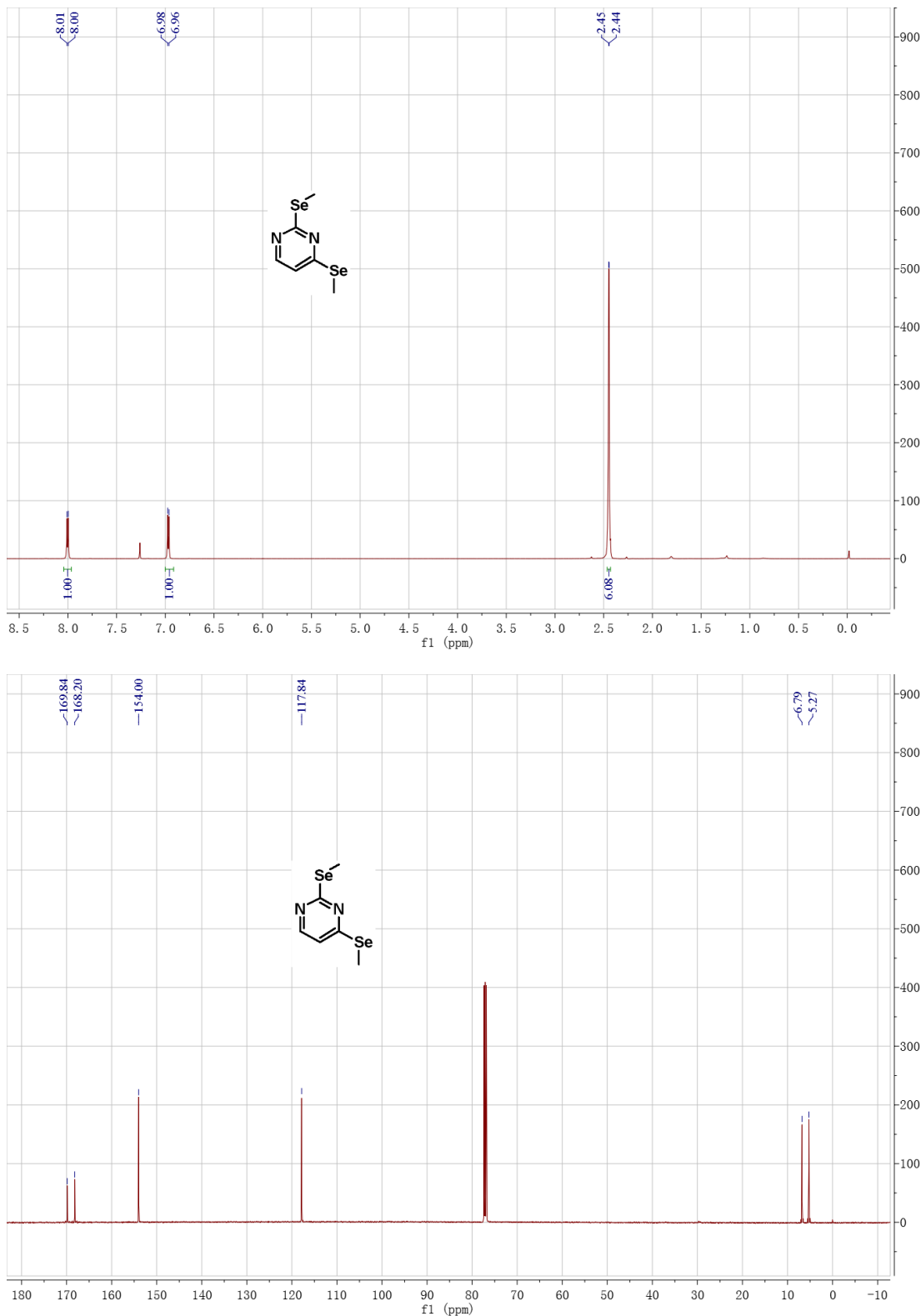
Compound 11h



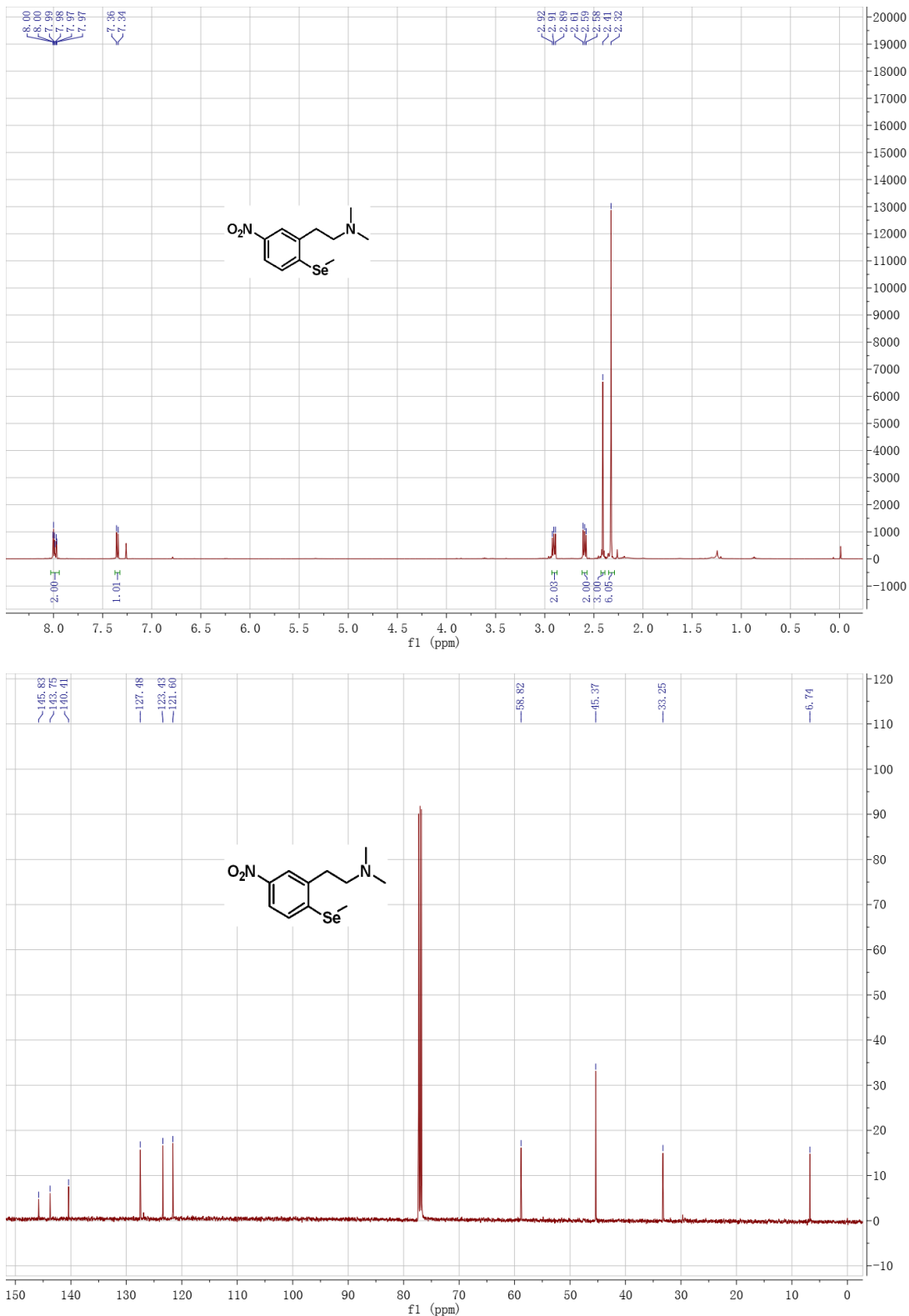
Compound **11i**



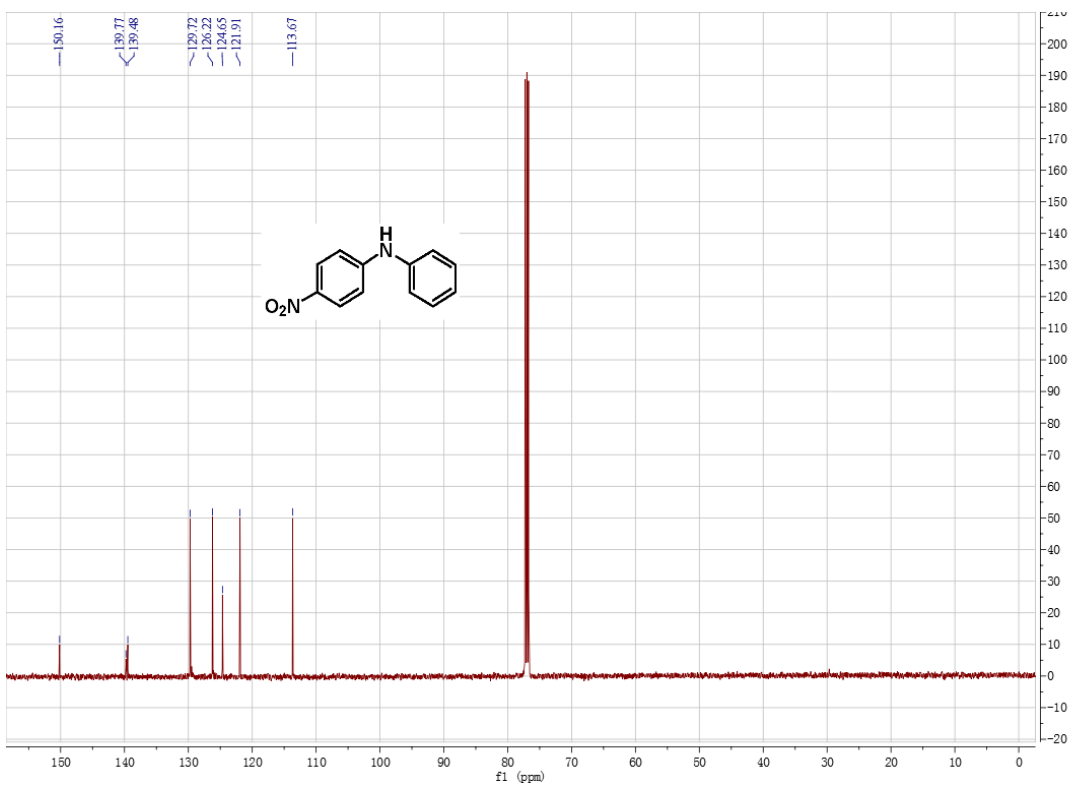
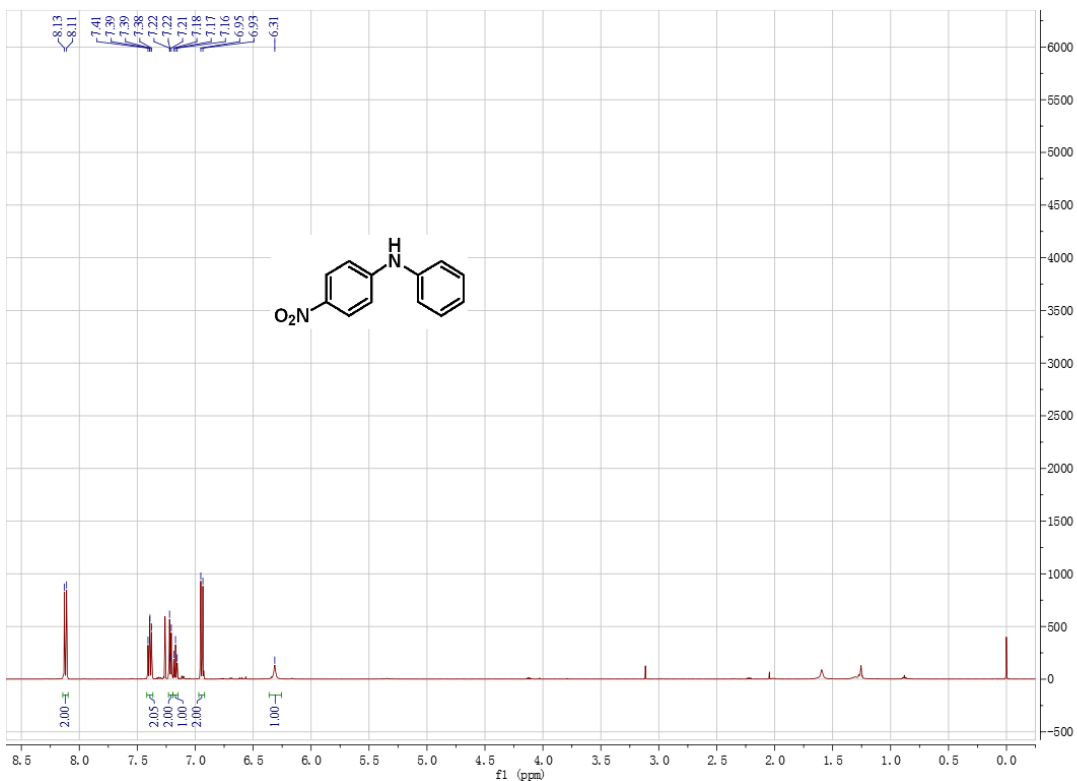
Compound 11j



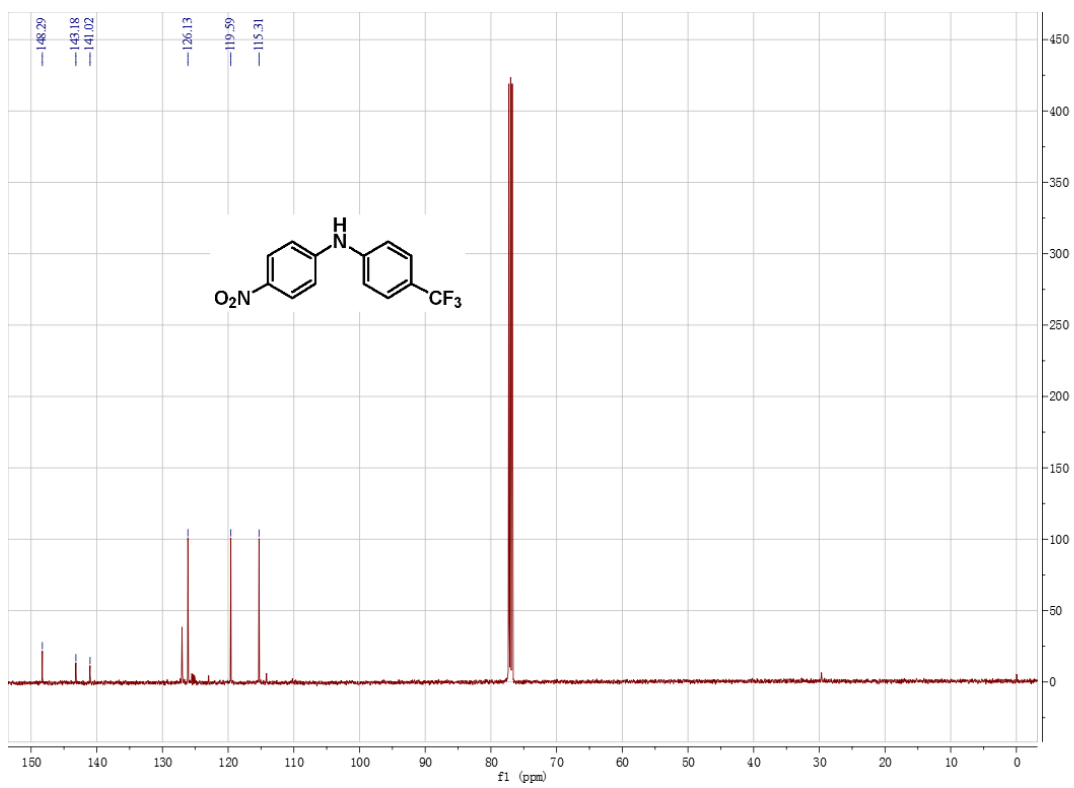
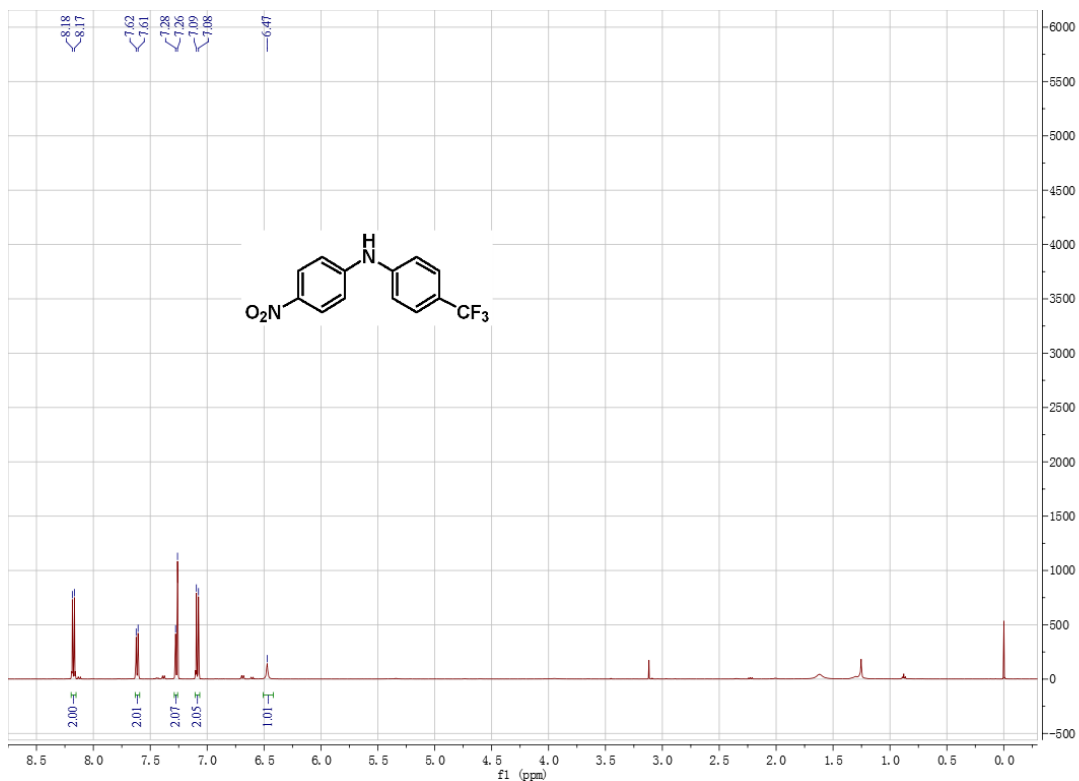
Compound 11k



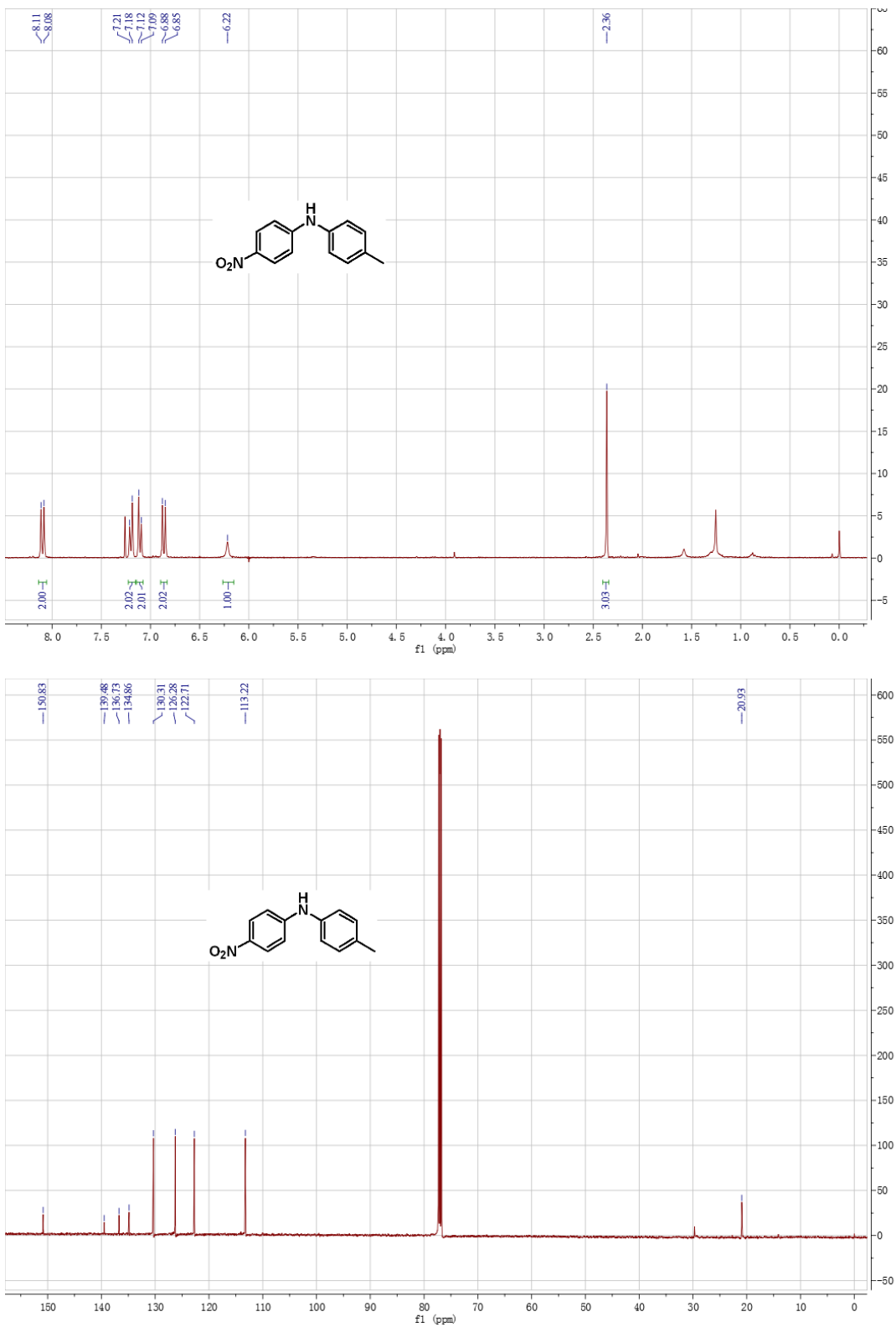
Compound 13a



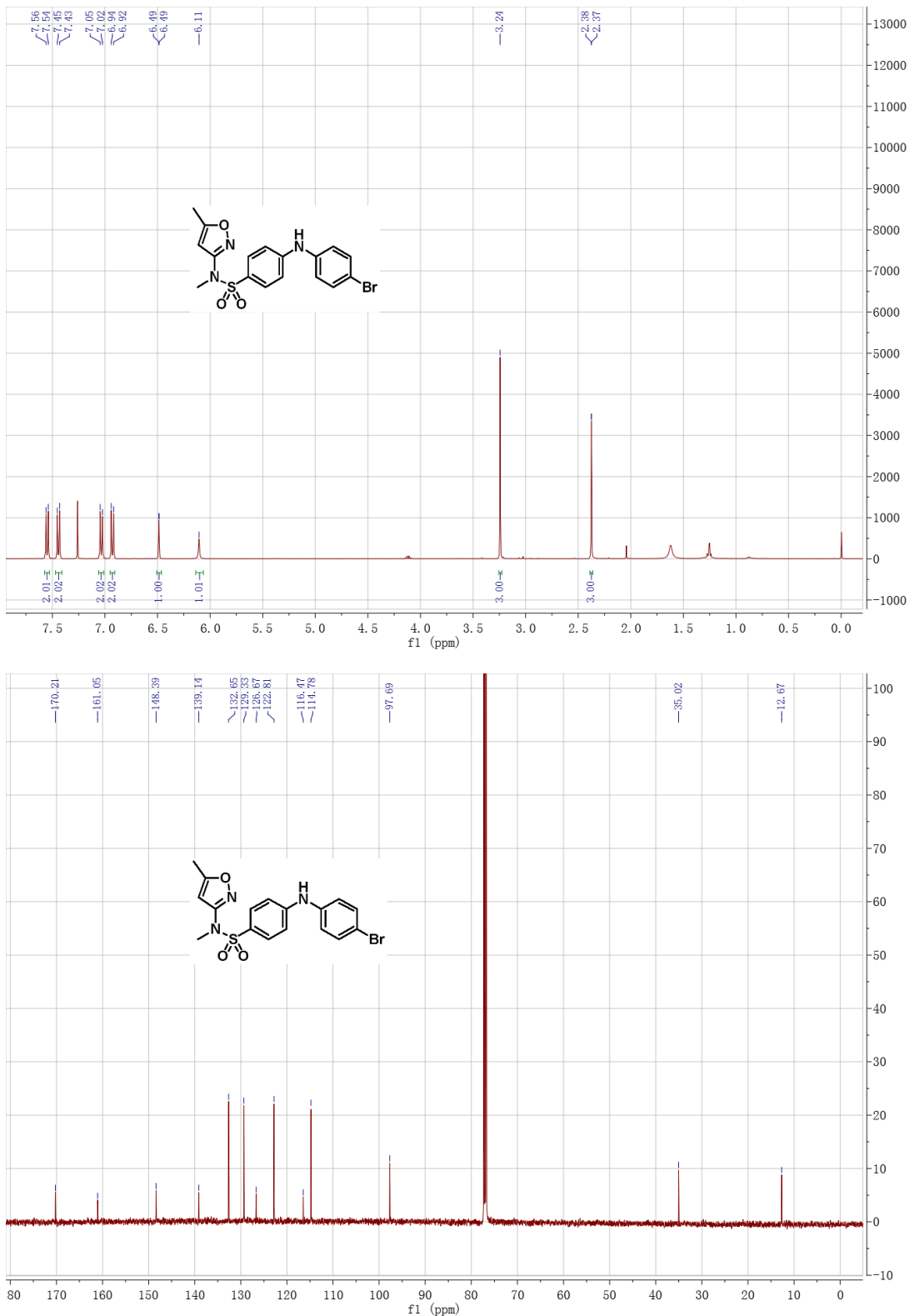
Compound 13b



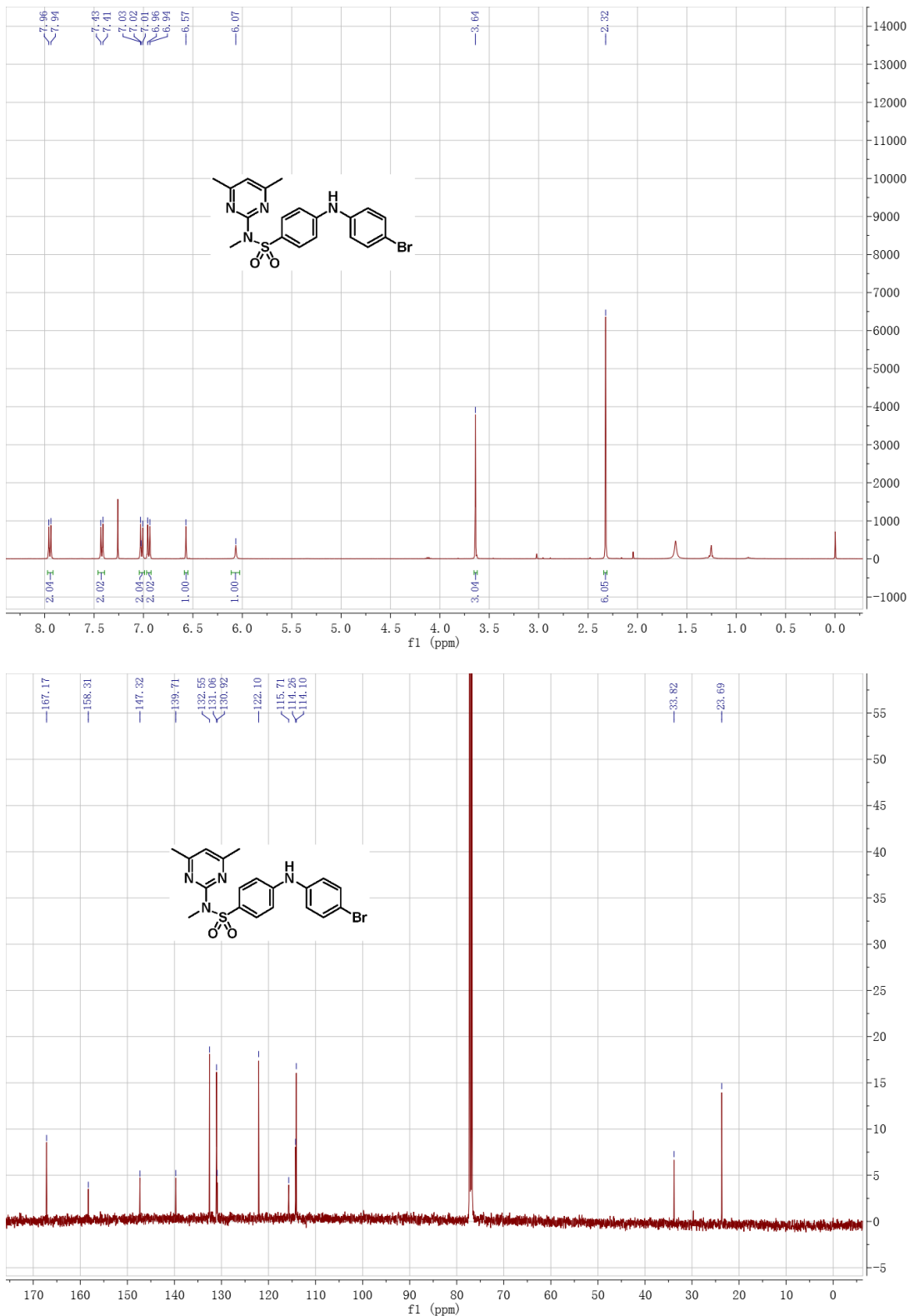
Compound 13c



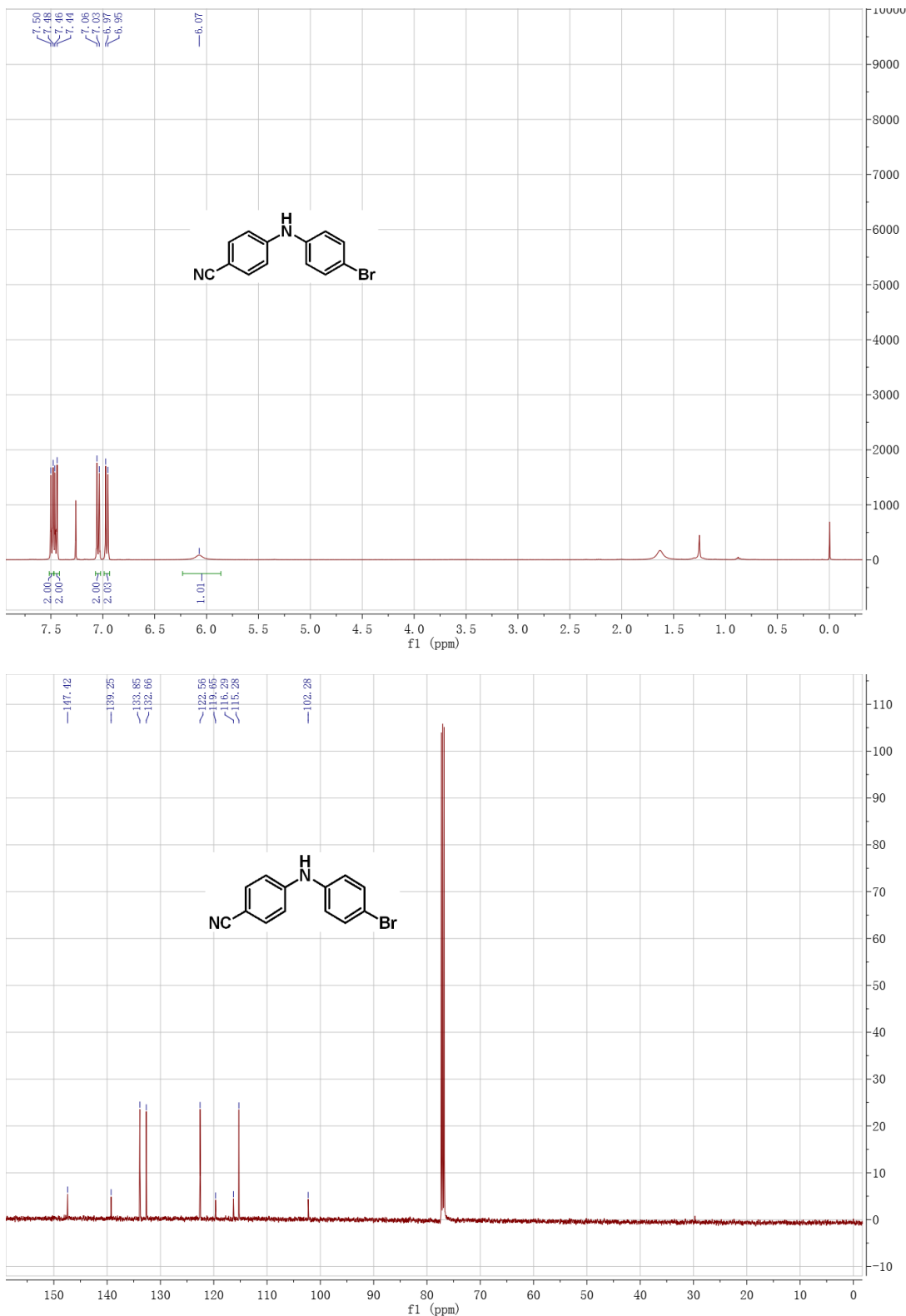
Compound 13e



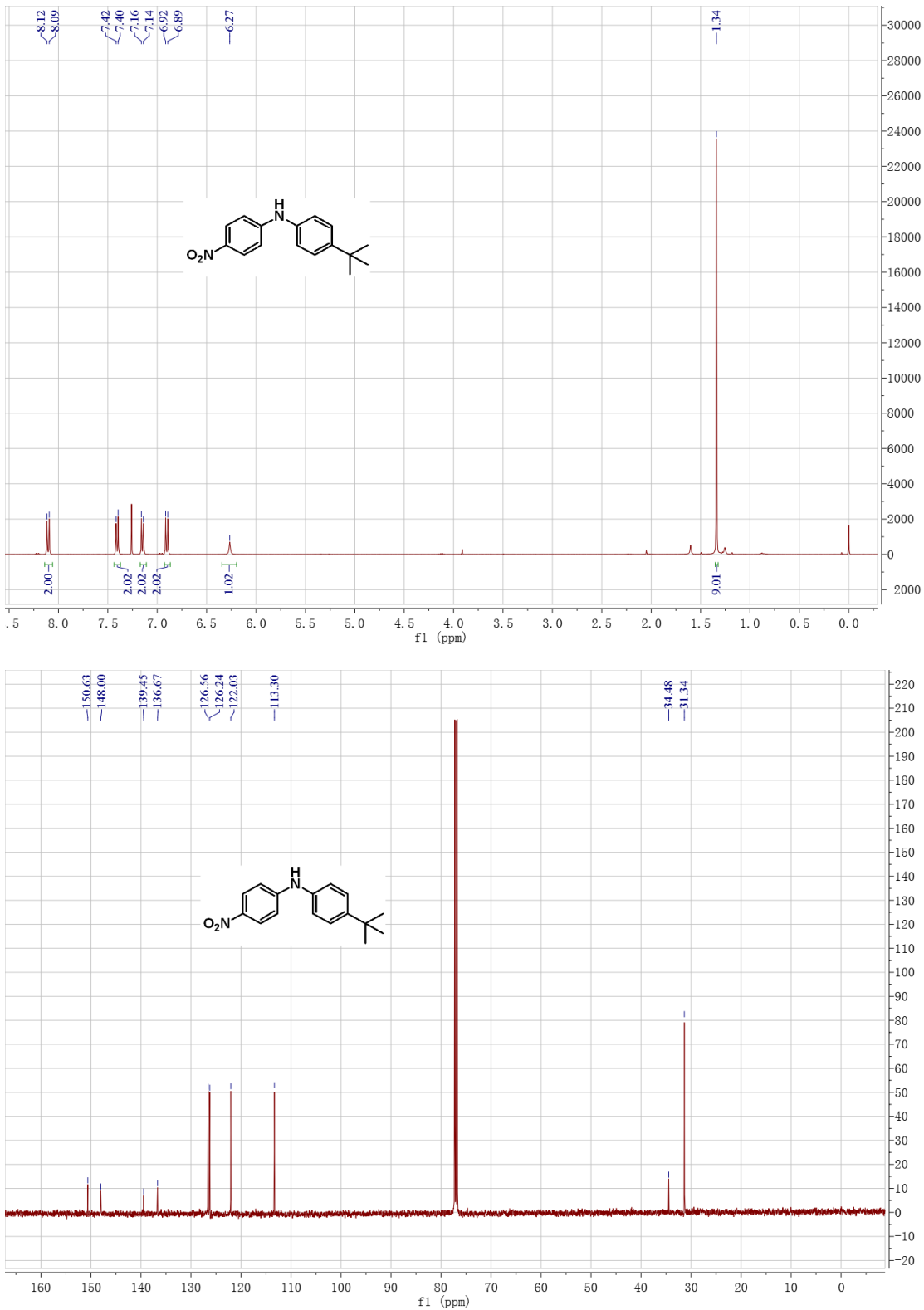
Compound 13f



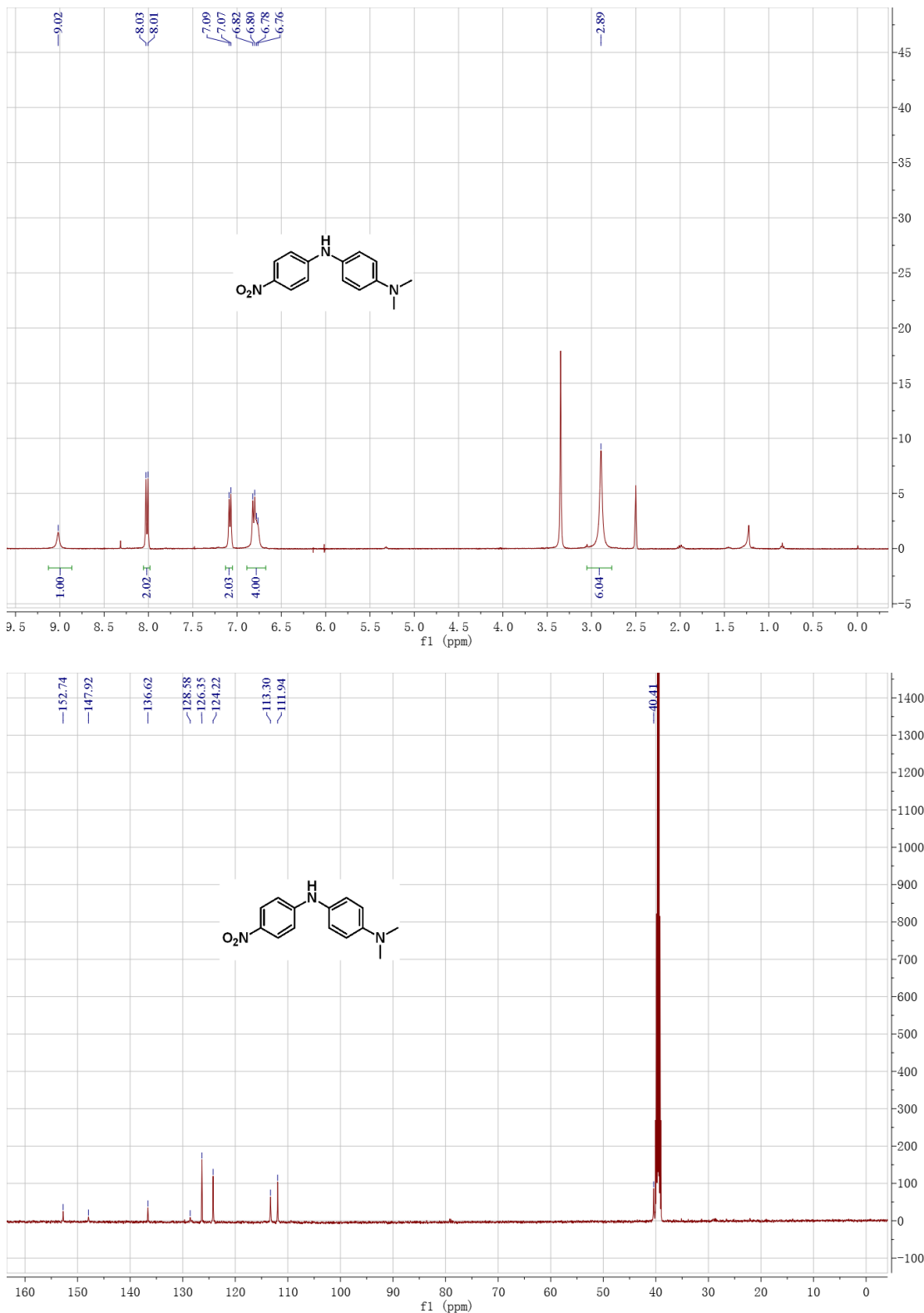
Compound 13d



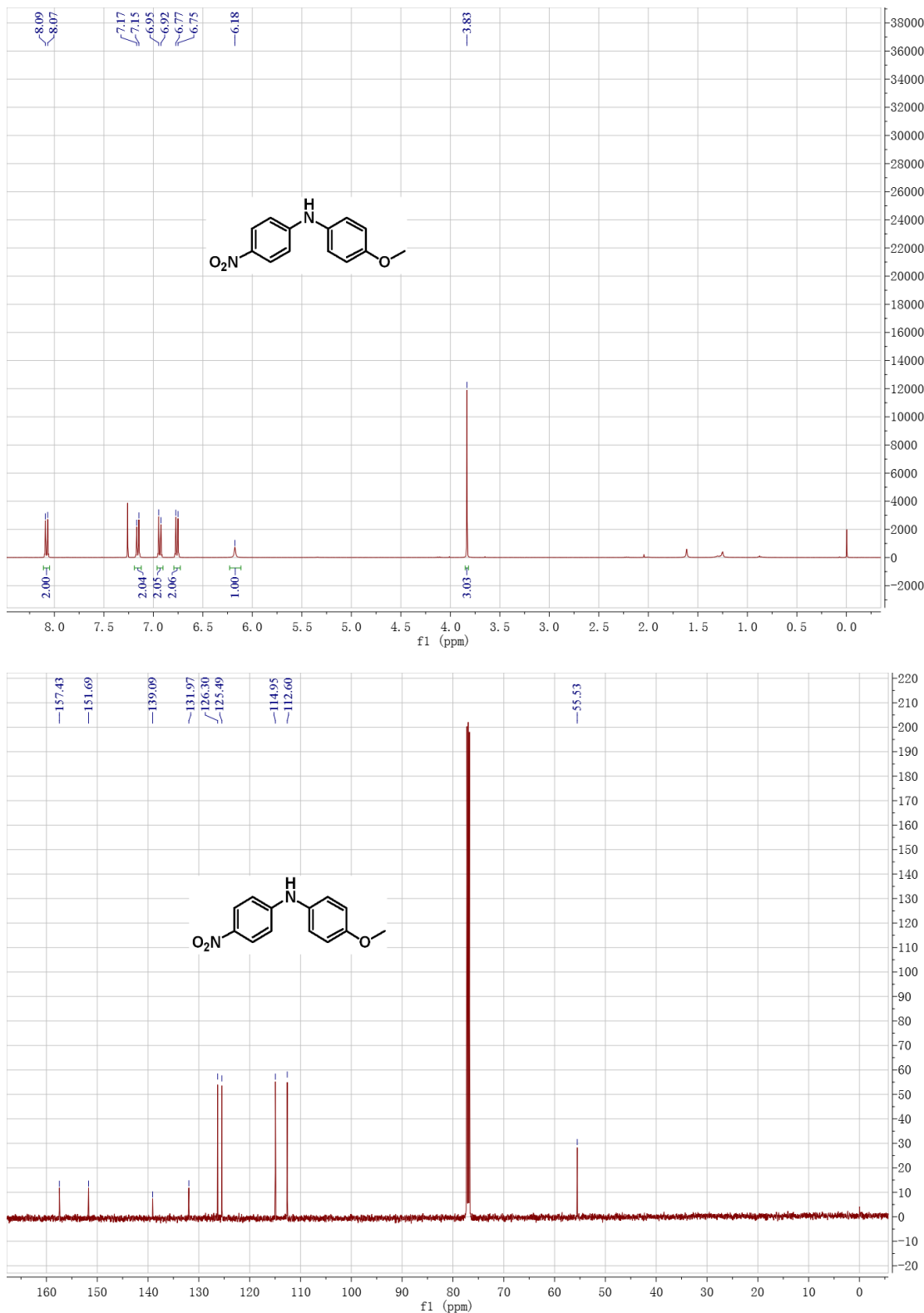
Compound 13g



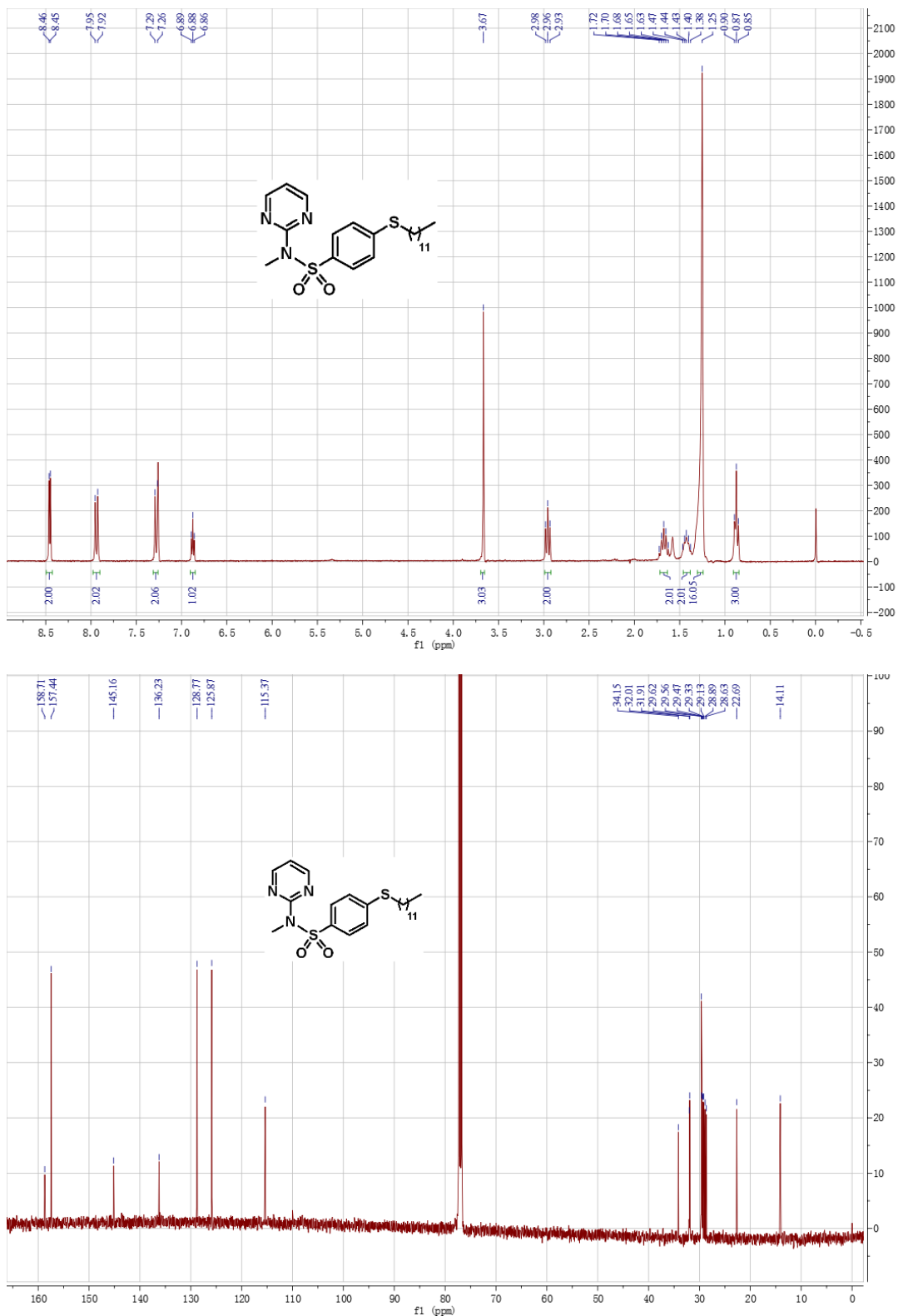
Compound 13h



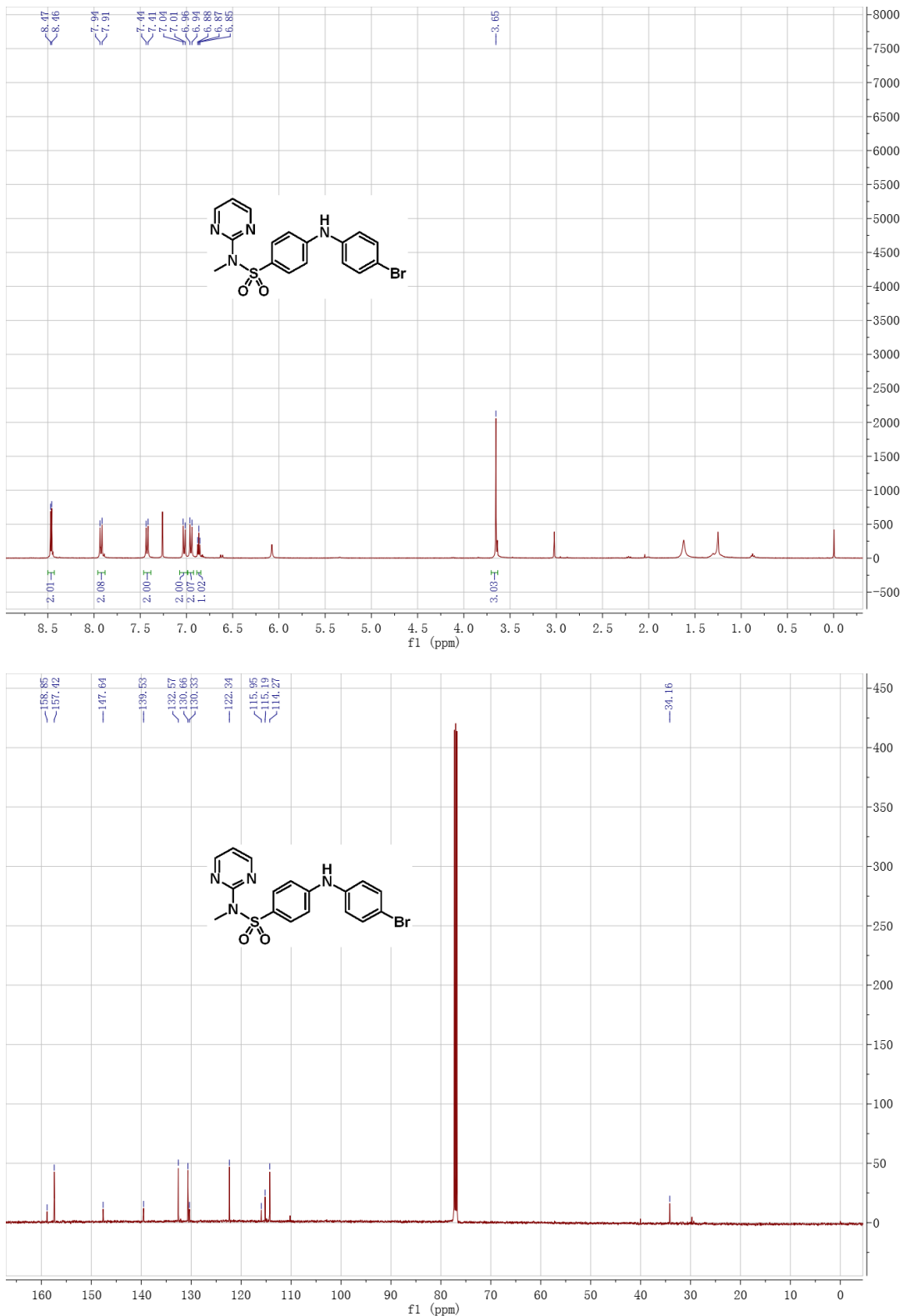
Compound 13i



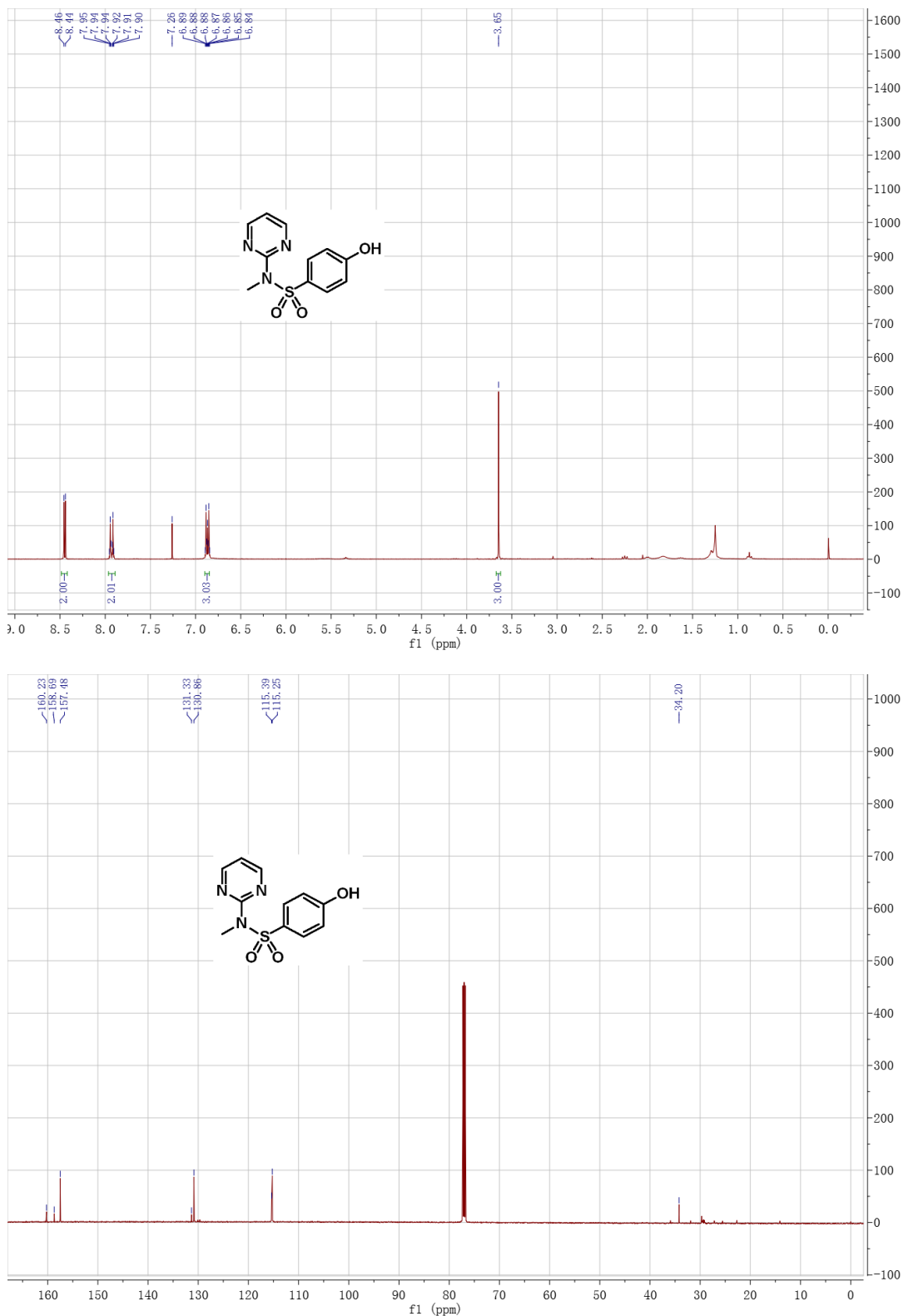
Compound 3mp



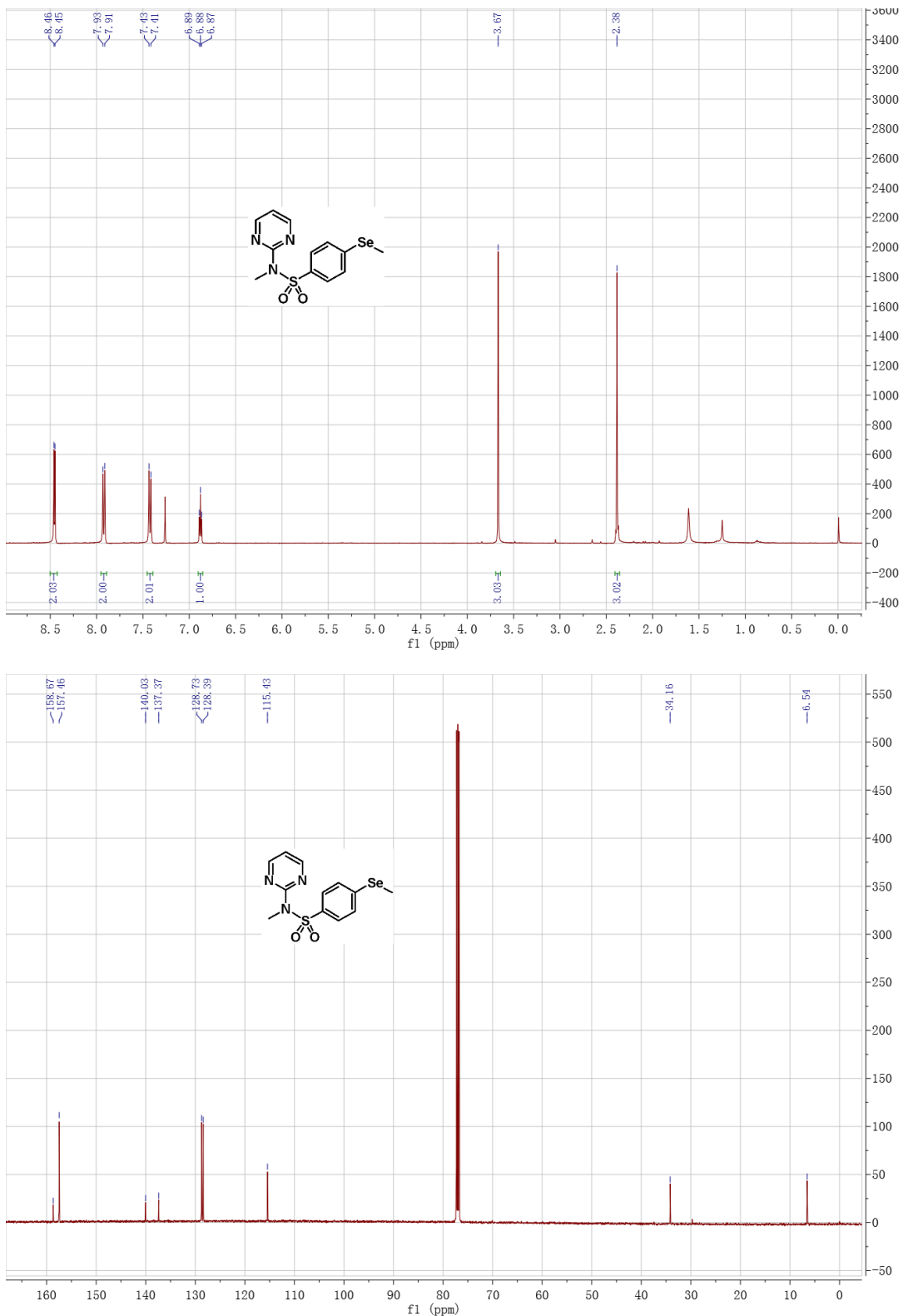
Compound 13h



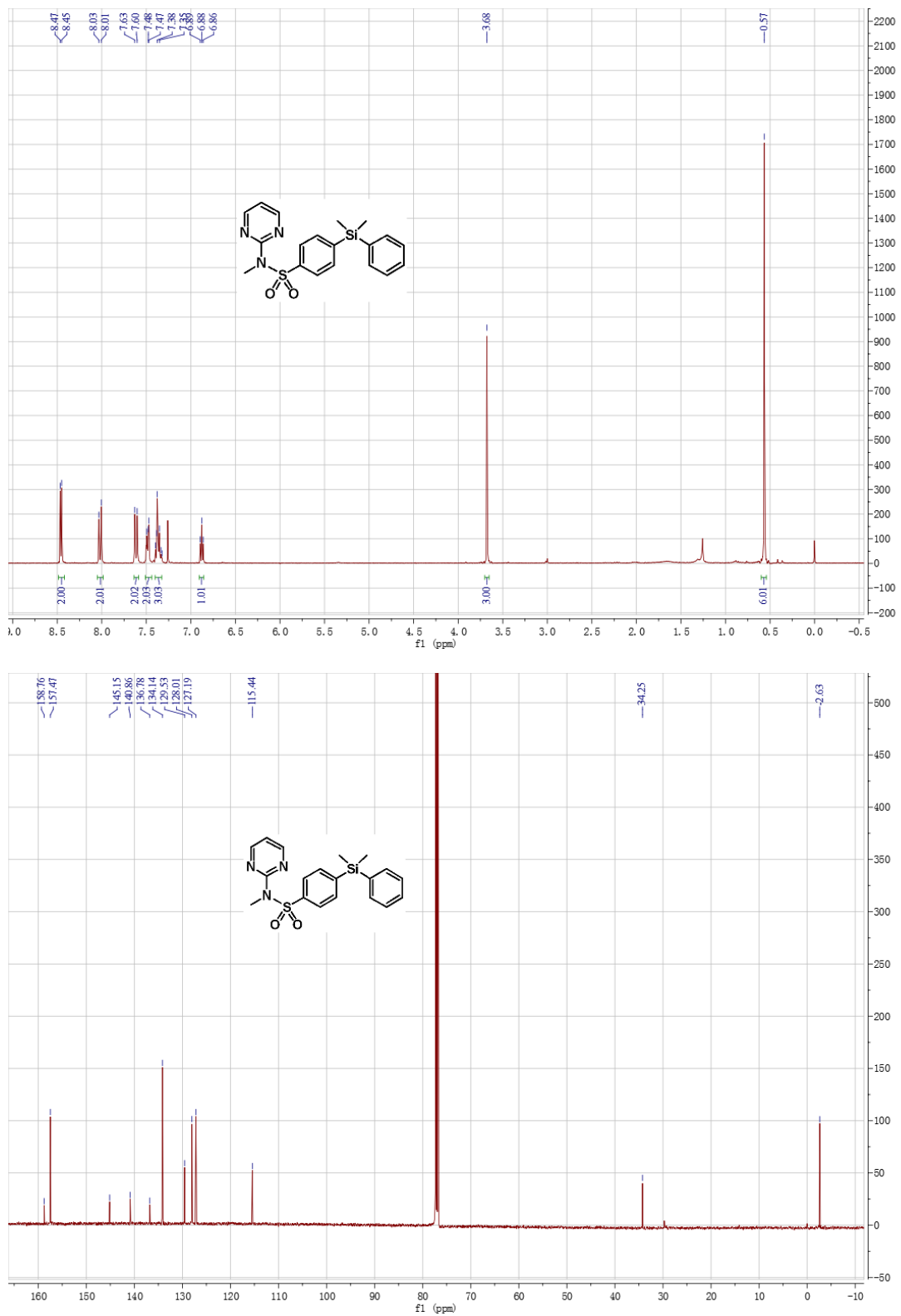
Compound 14a



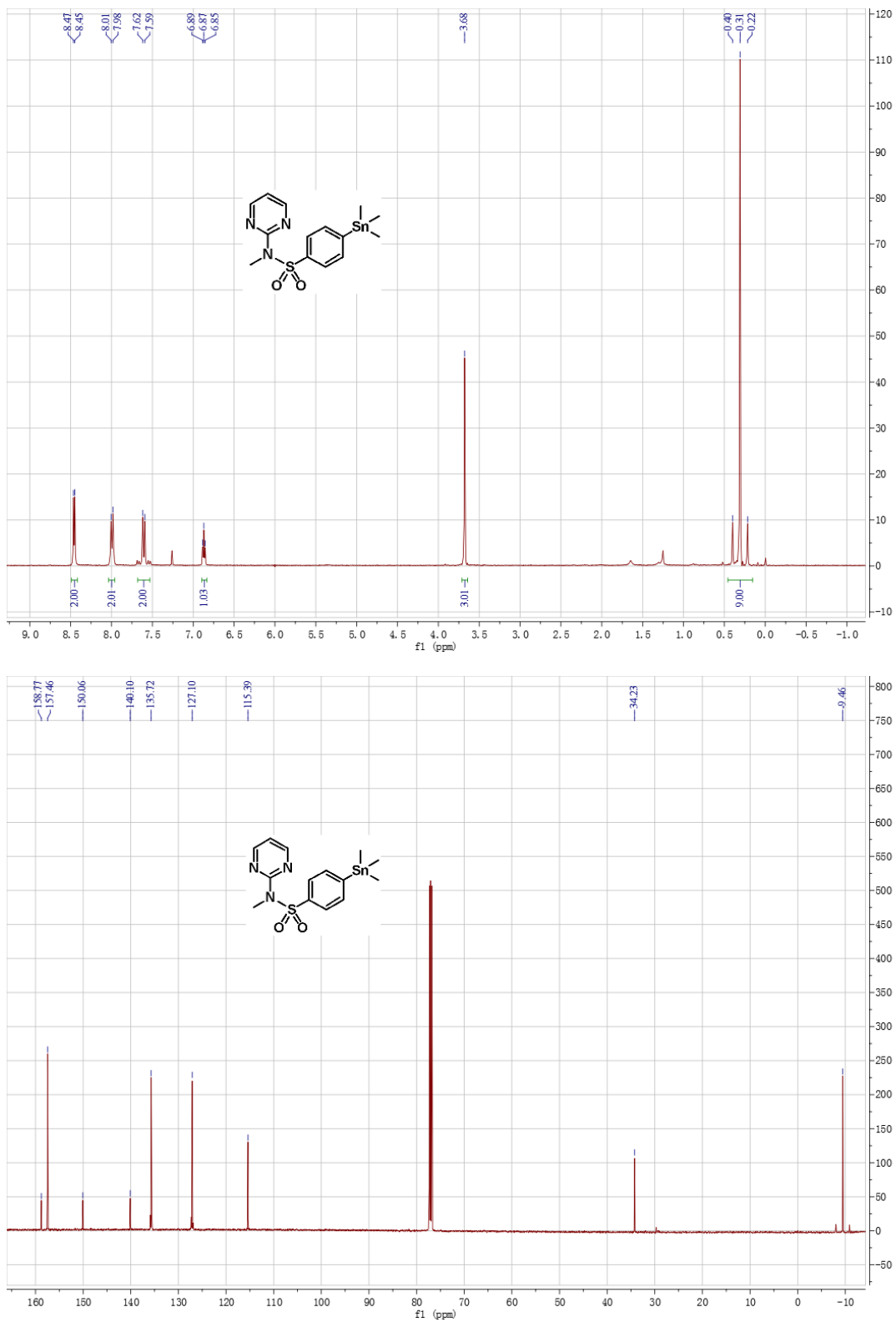
Compound 11h



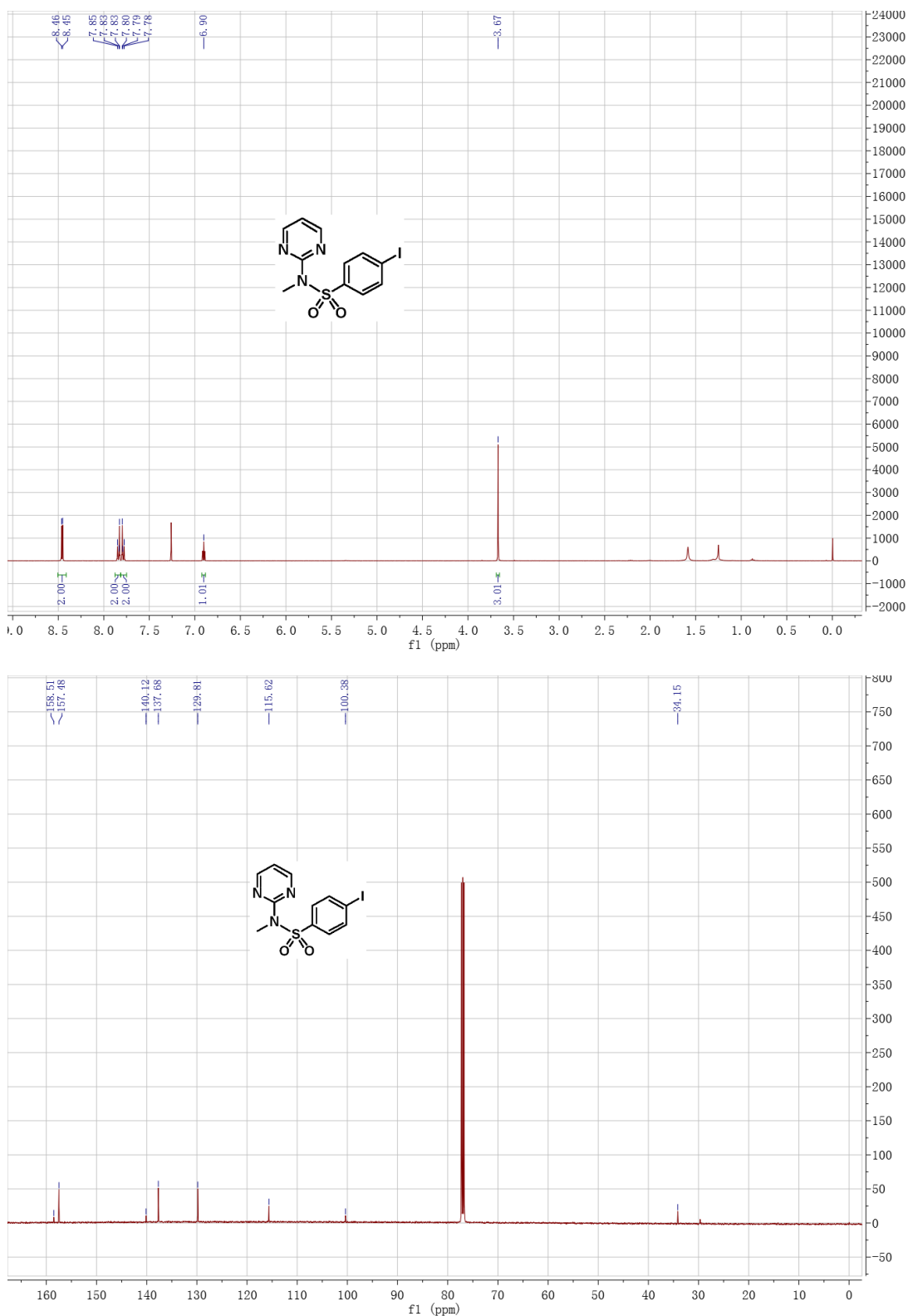
Compound 5j



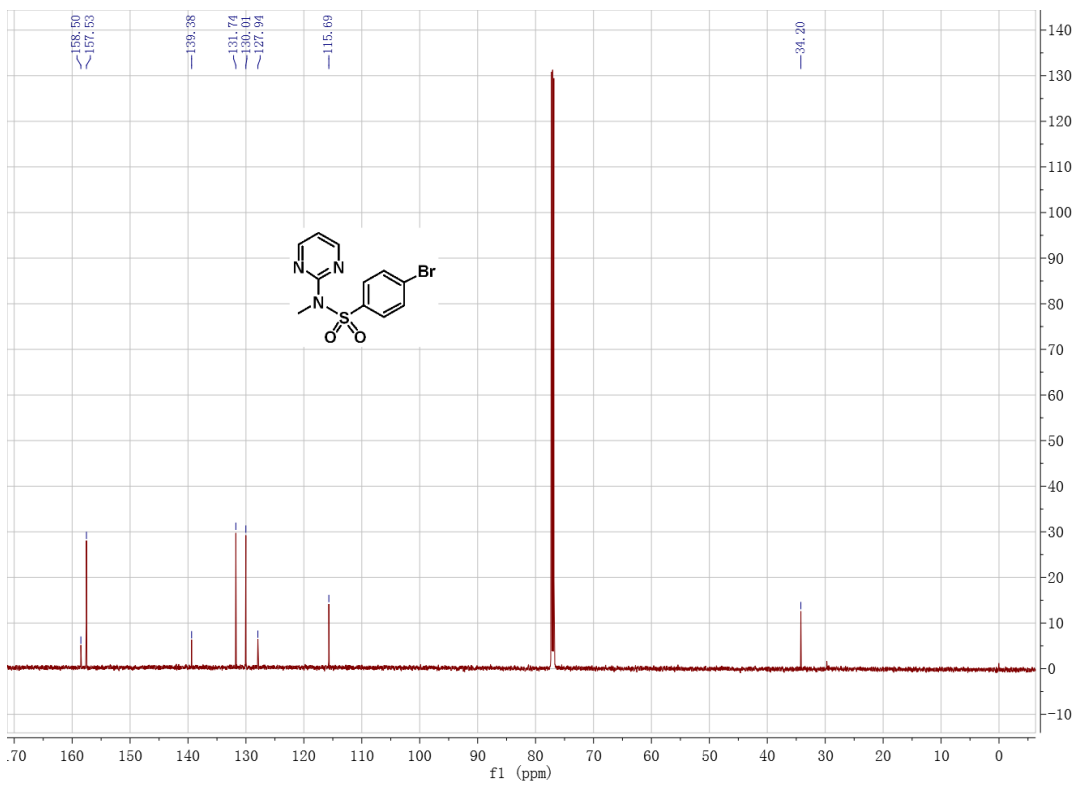
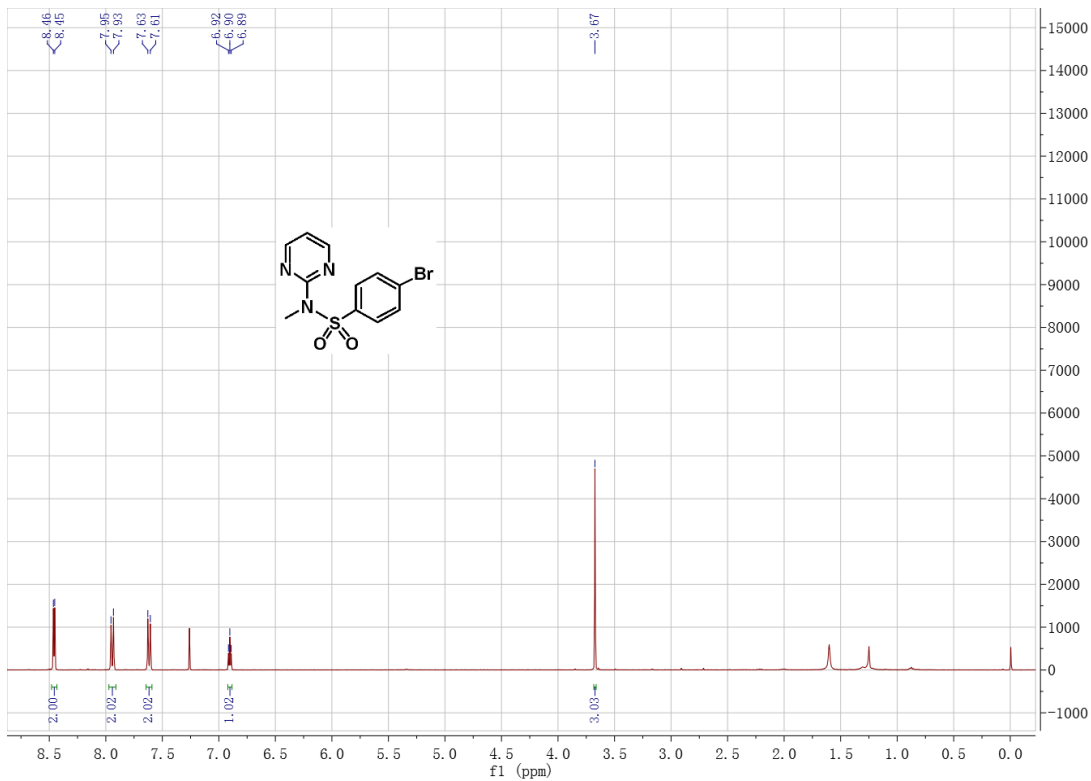
Compound 7o



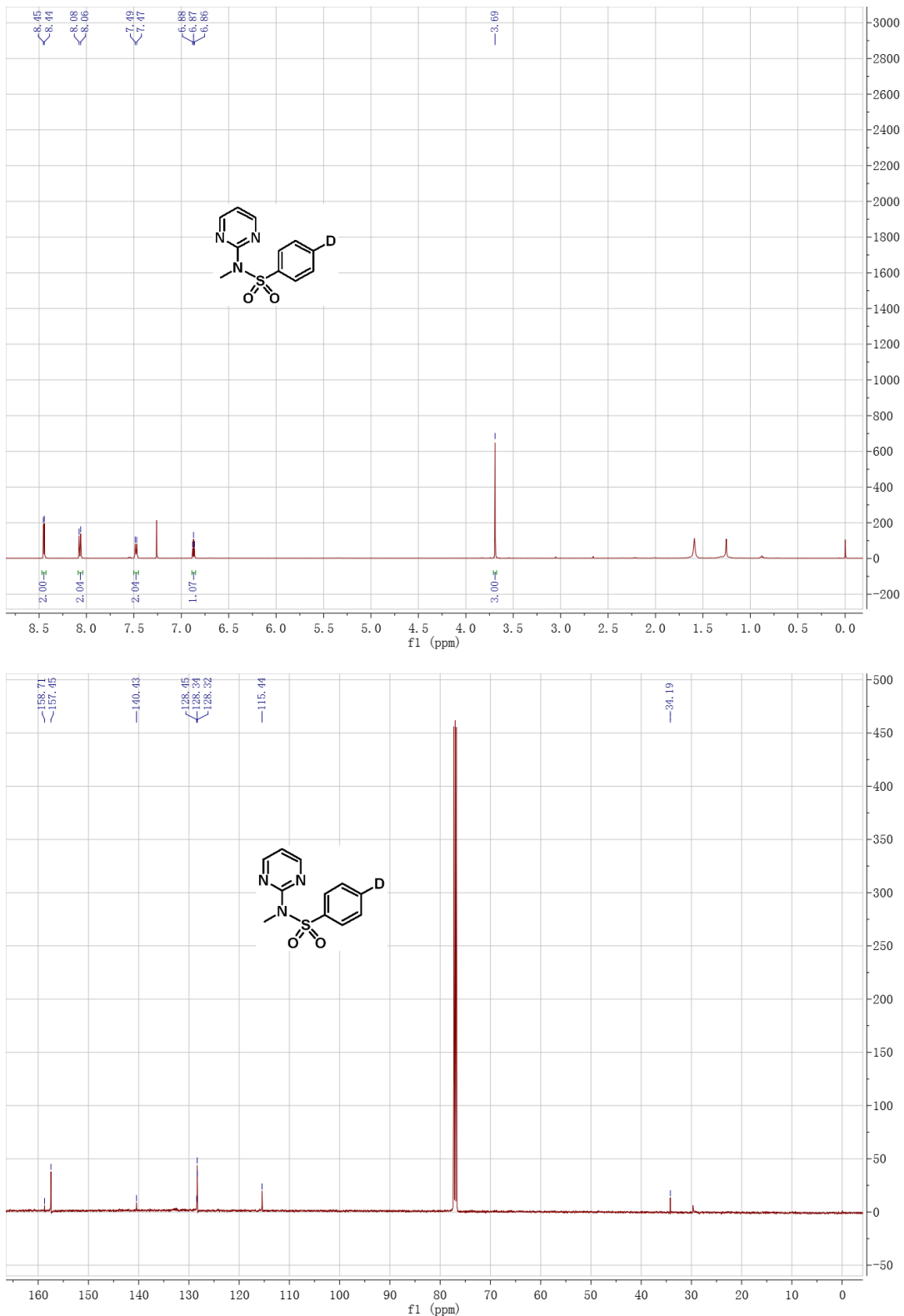
Compound 14b



Compound 14c

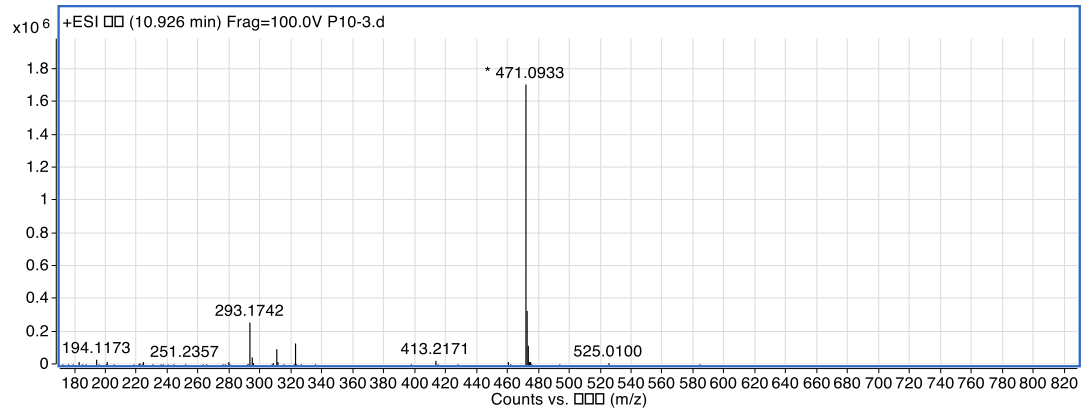


Compound 14d

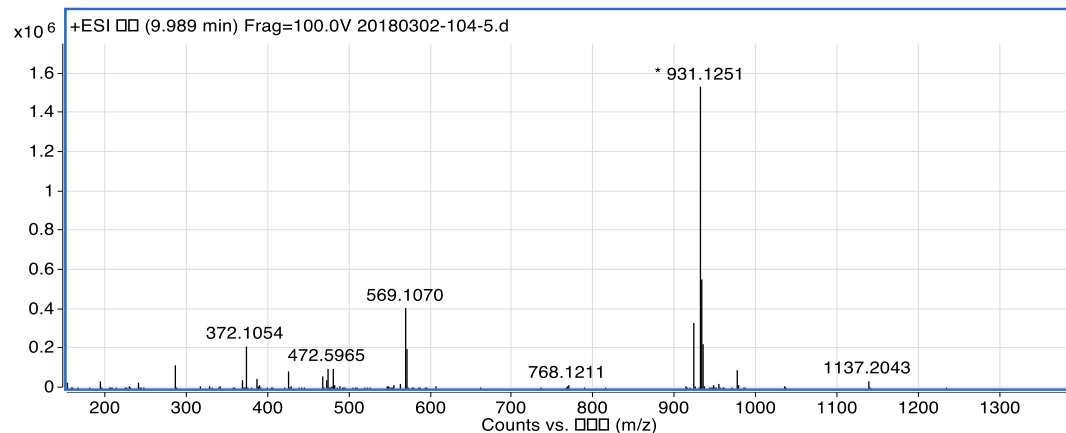


5. Copies of MS Spectrums for Compounds in Fig 5 and Fig 6.

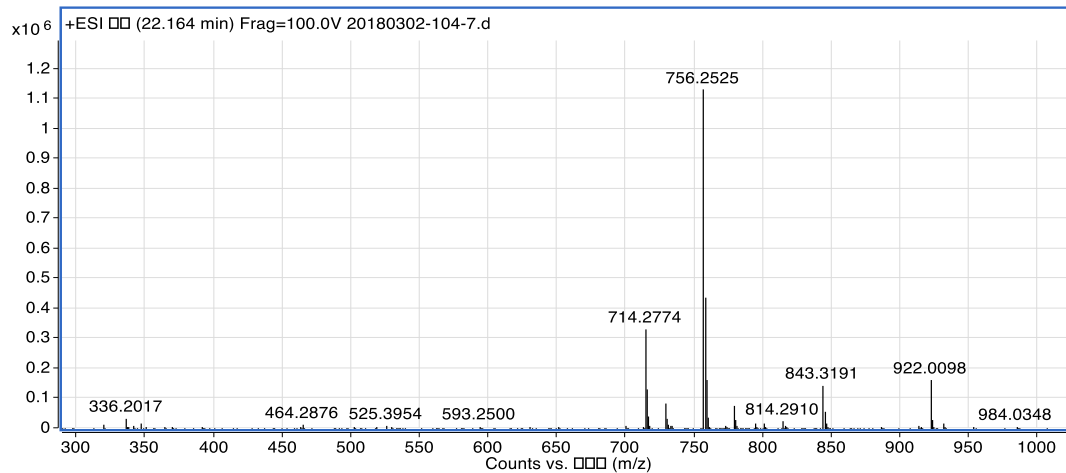
Compound 15a



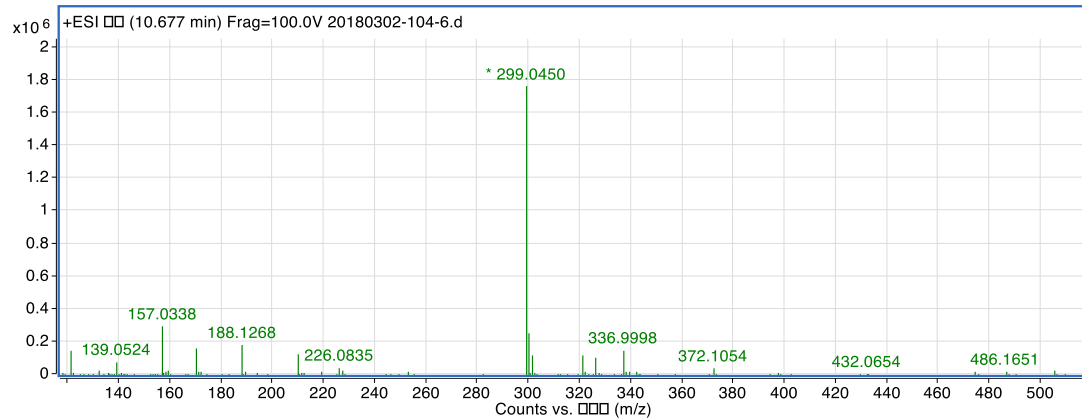
Compound 15b



Compound 15c

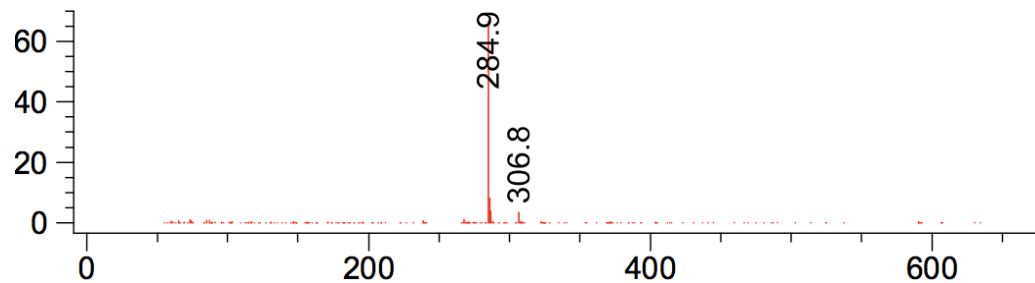


Compound 15f

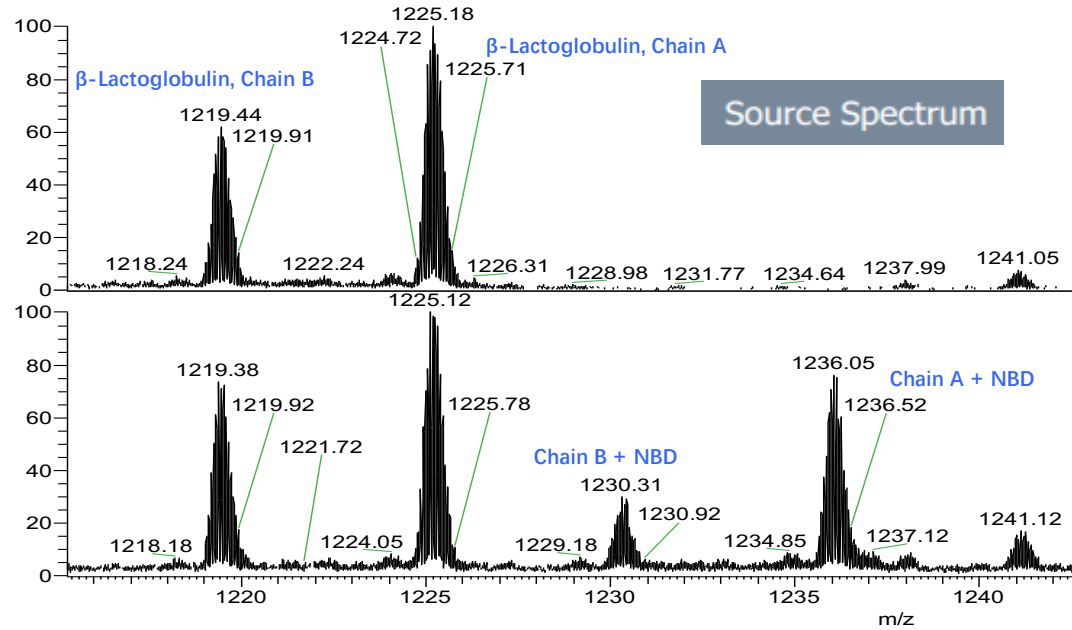


Compound 15e

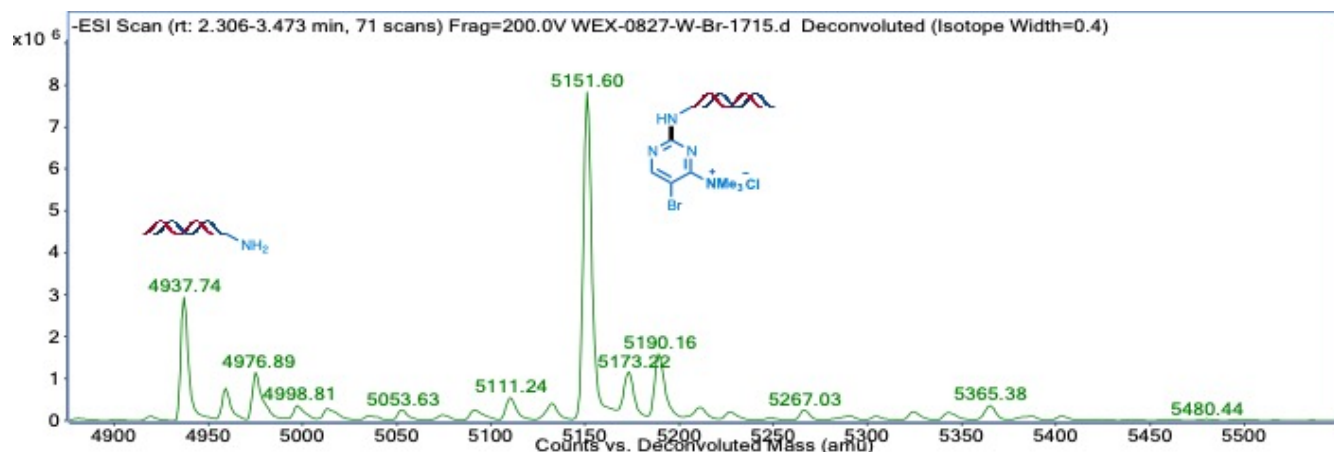
*MSD1 SPC, time=5.317:5.773 of D:\DATA\20180313\DEF_LC



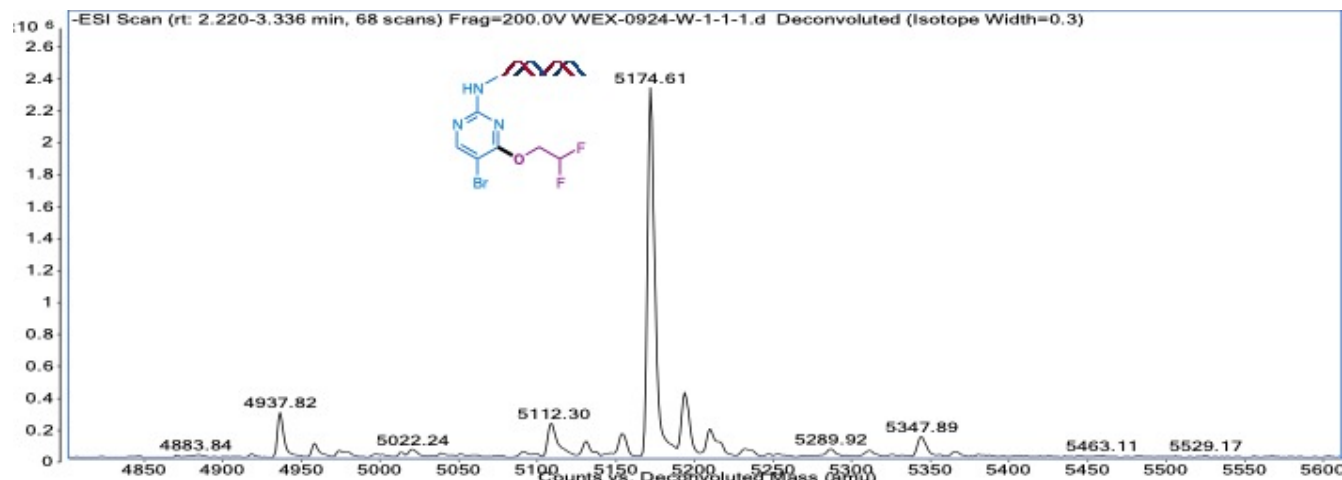
Compound 15d



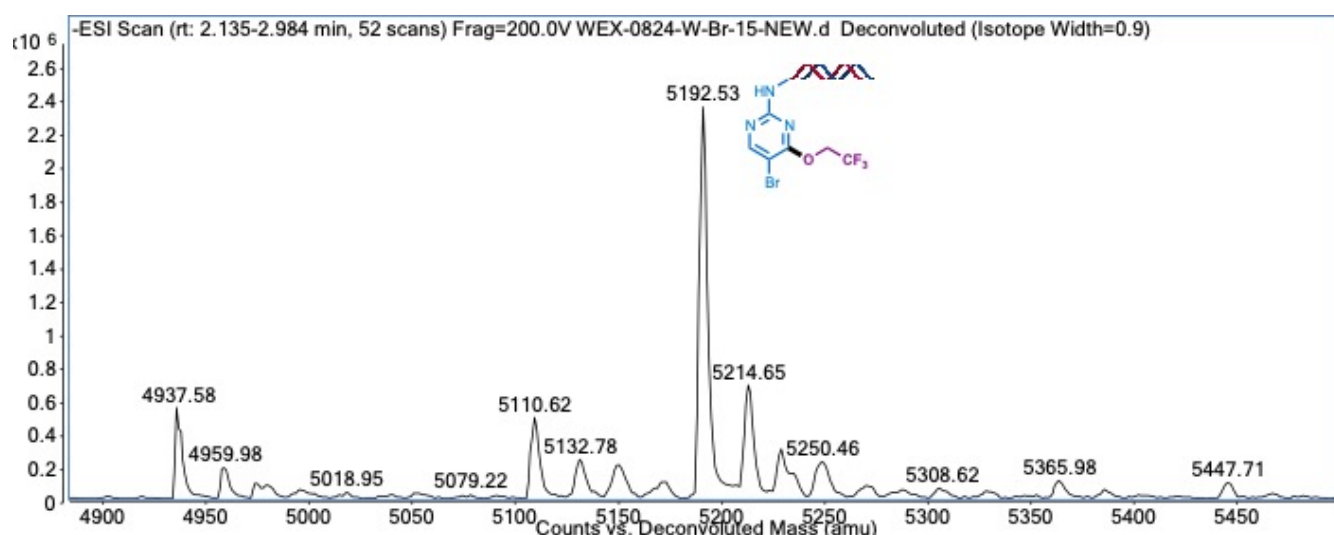
Compound 16a



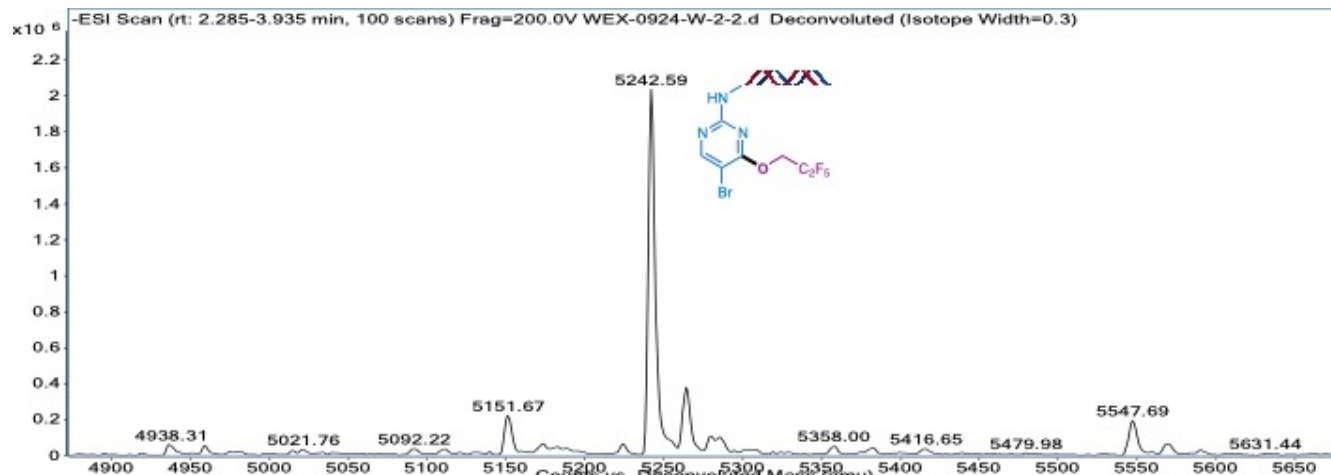
Compound 16b



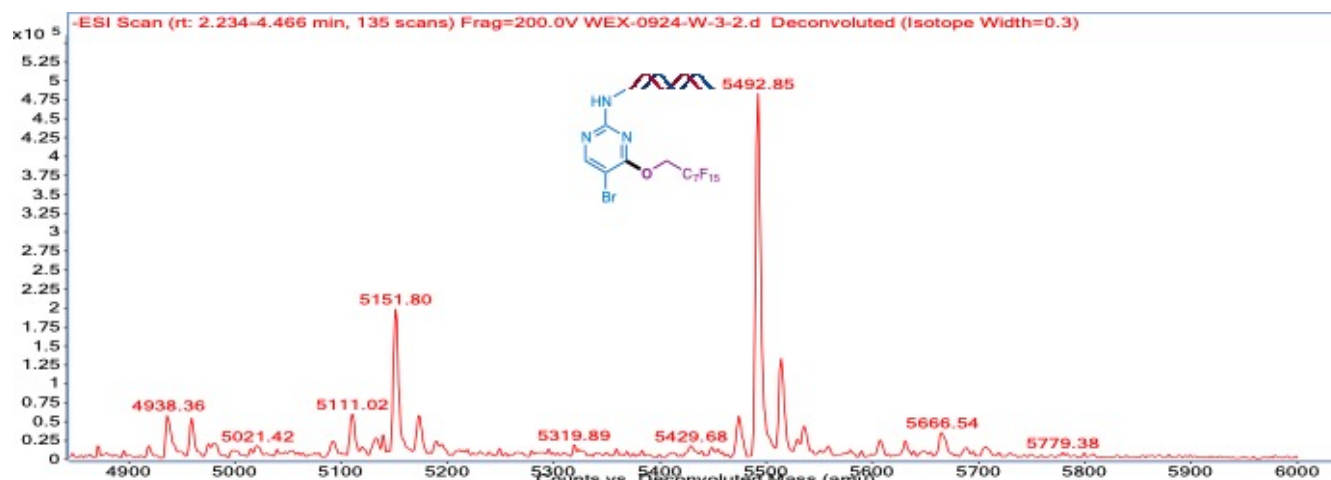
Compound 16c



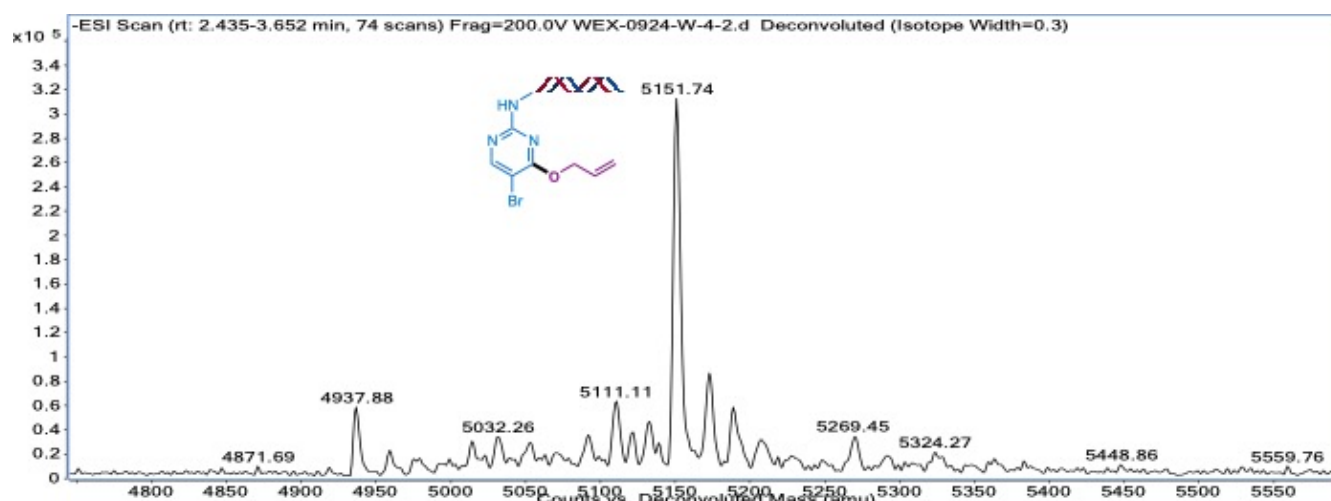
Compound 16d



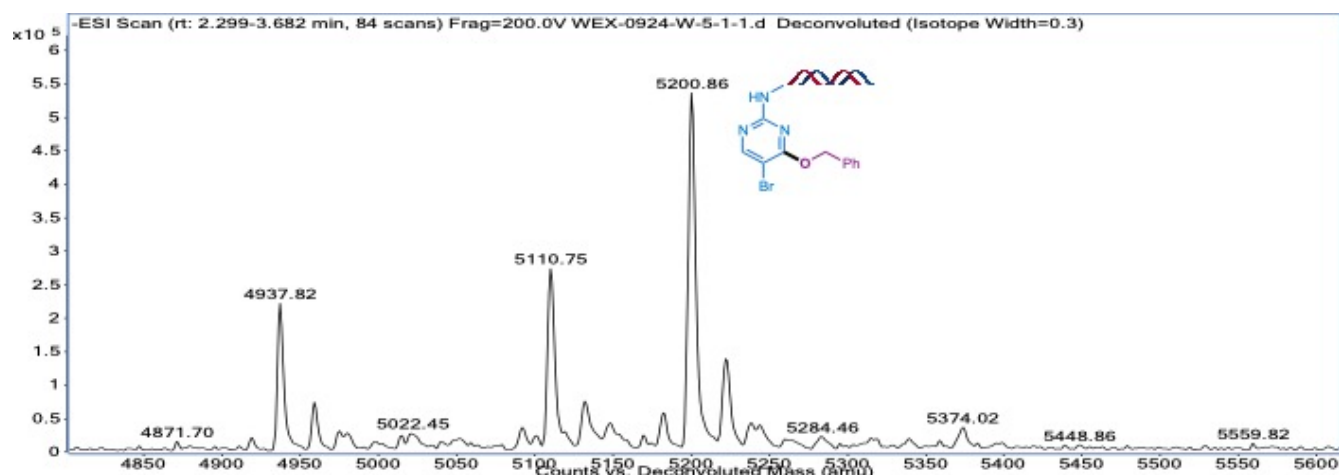
Compound 16e



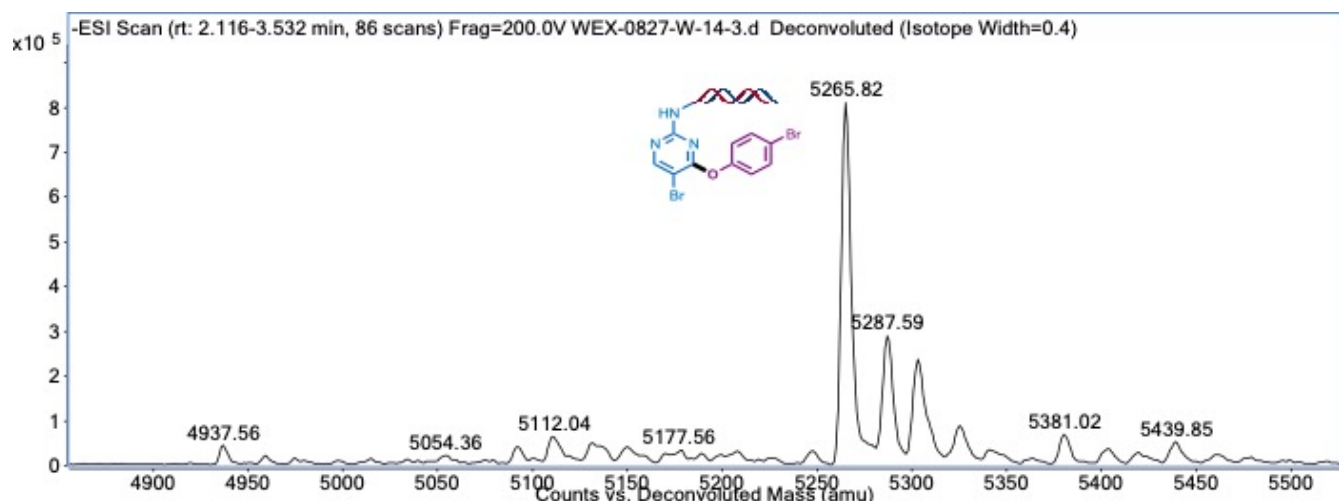
Compound 16f



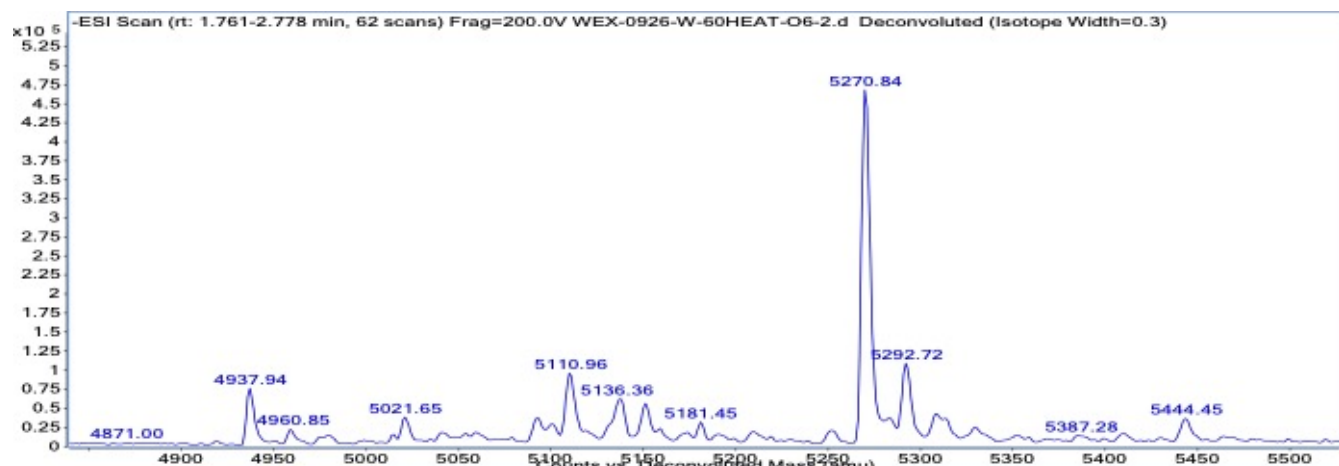
Compound 16g



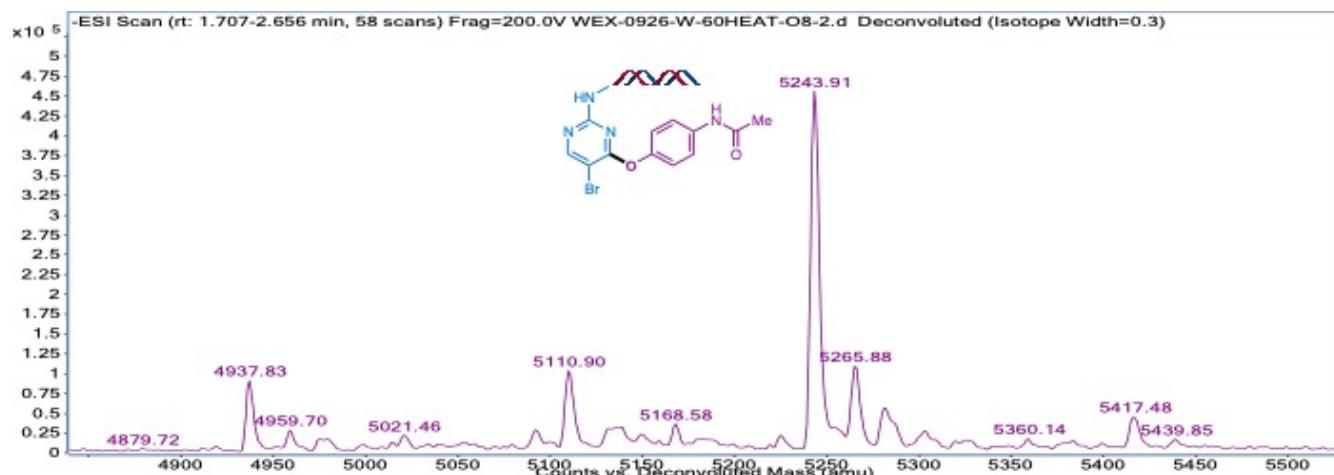
Compound 16h



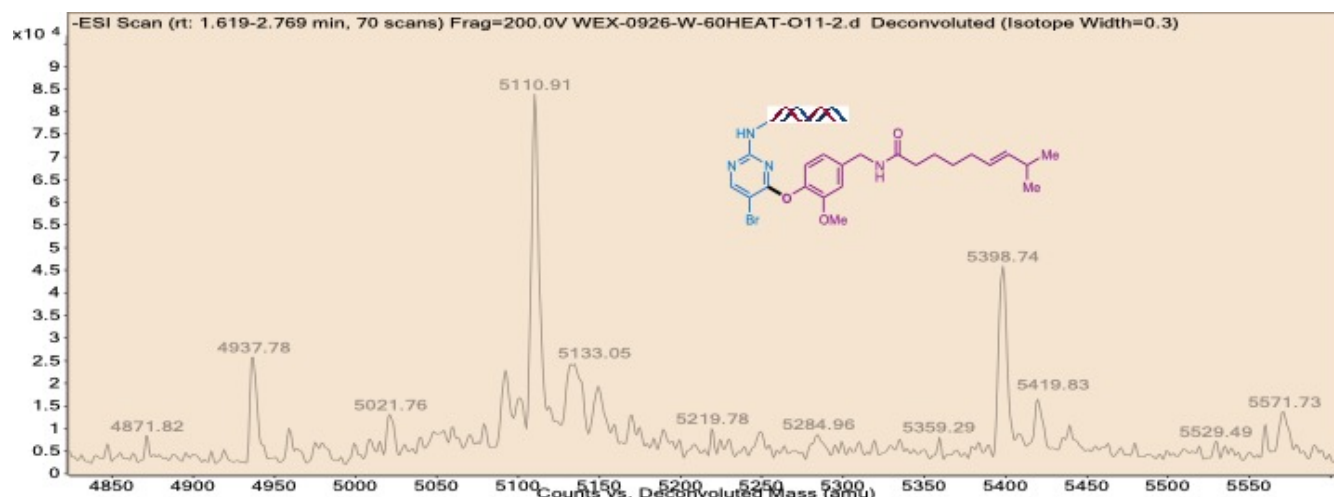
Compound 16i



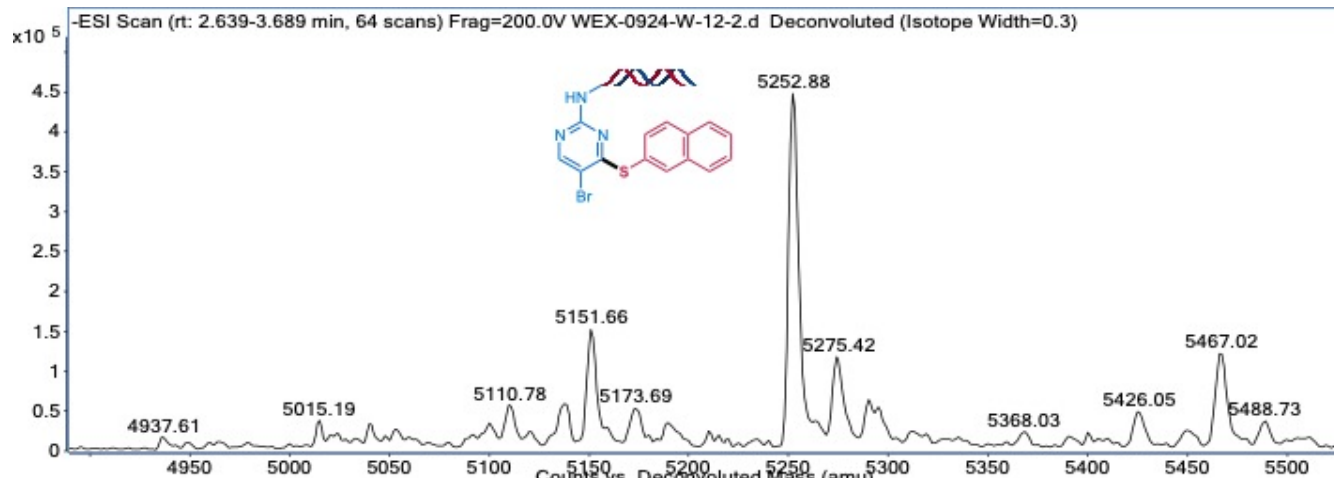
Compound 16j



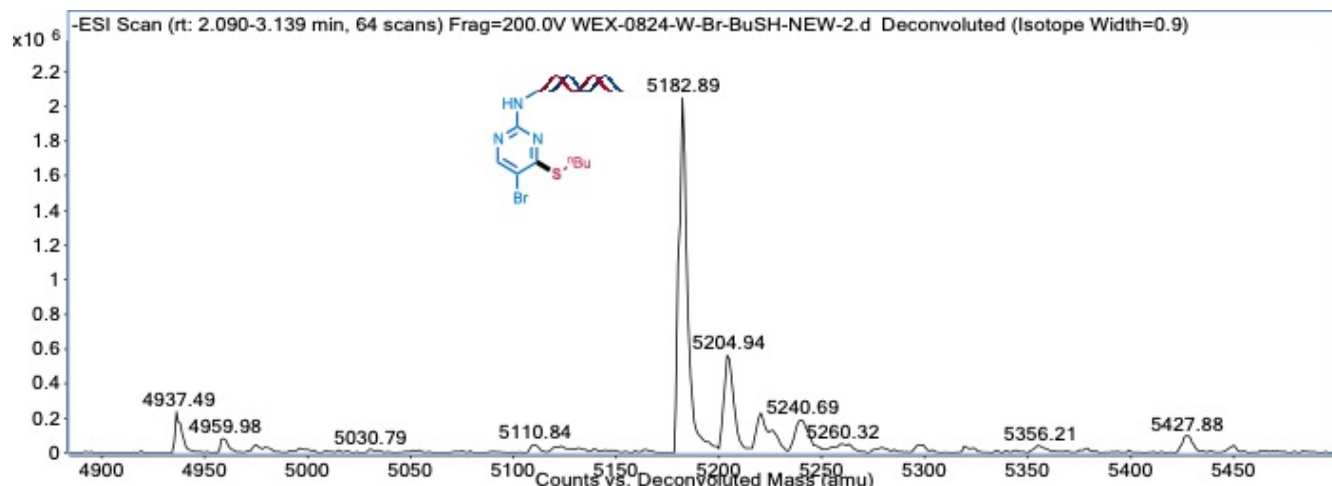
Compound 16k



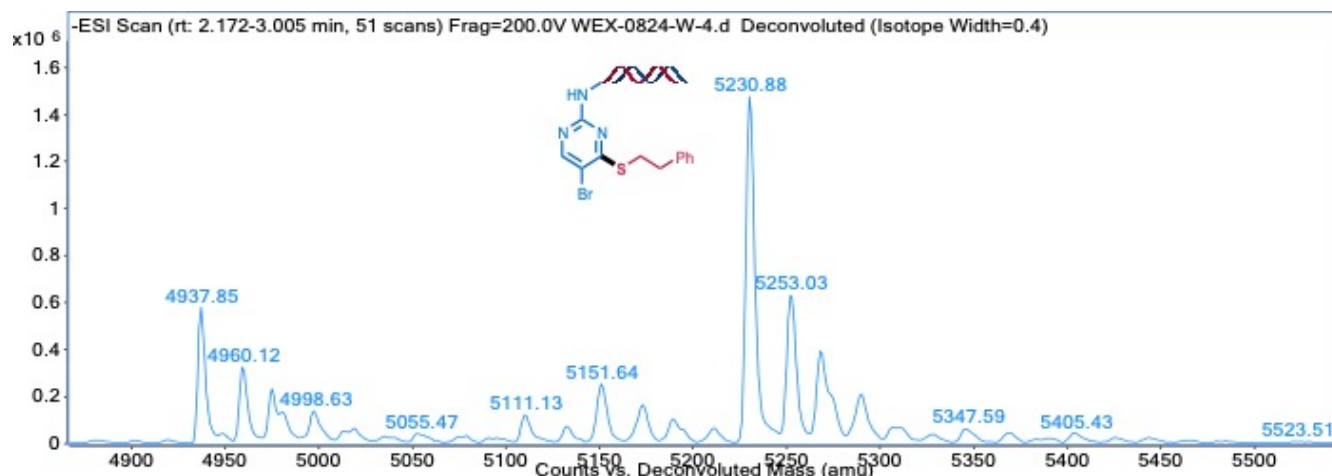
Compound 16l



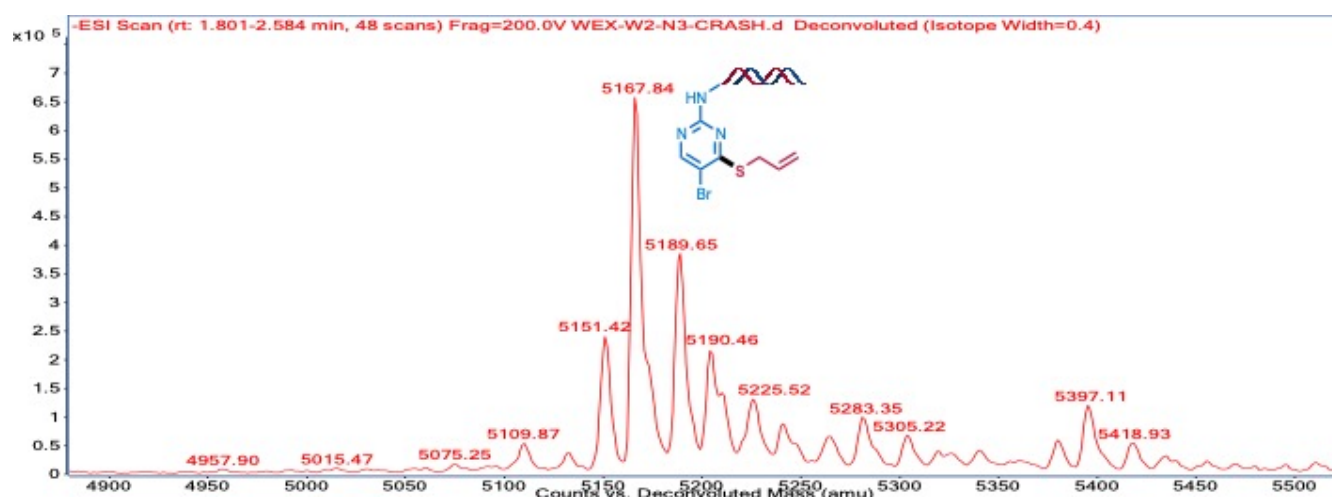
Compound 16m



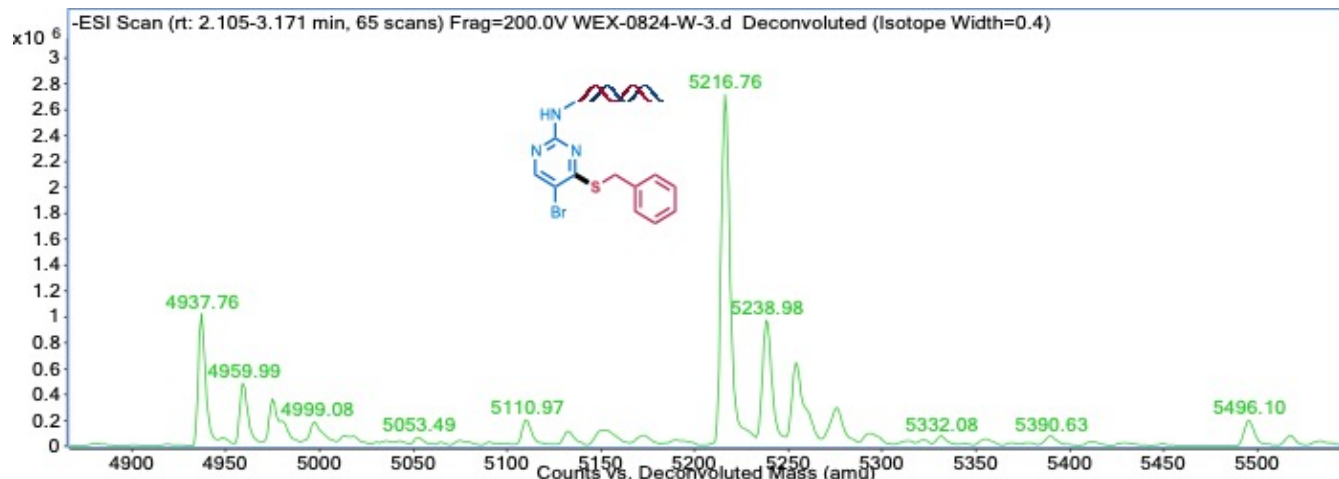
Compound 16n



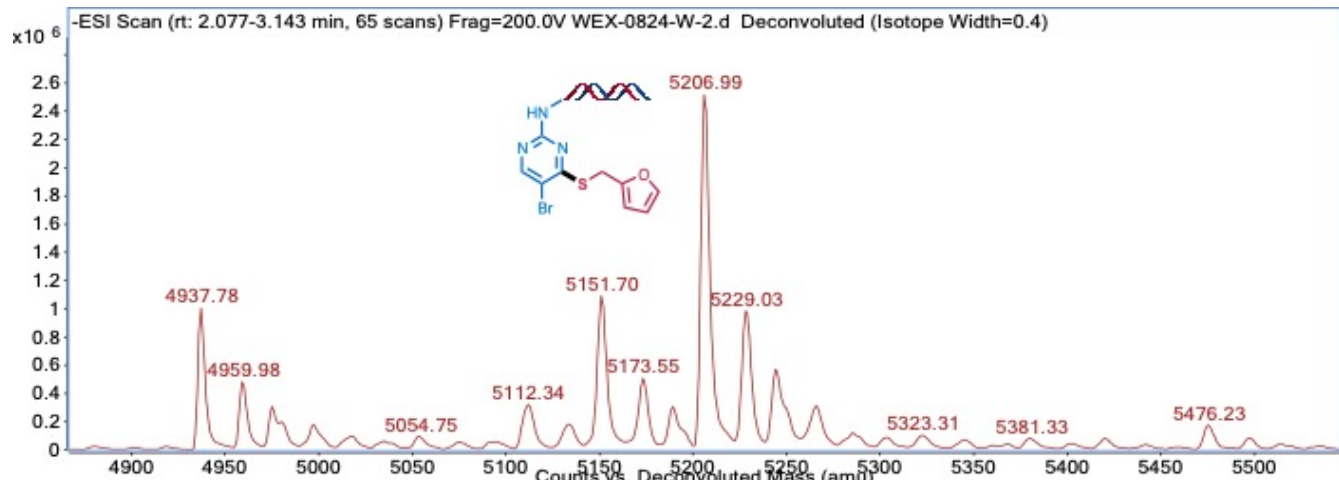
Compound 16o



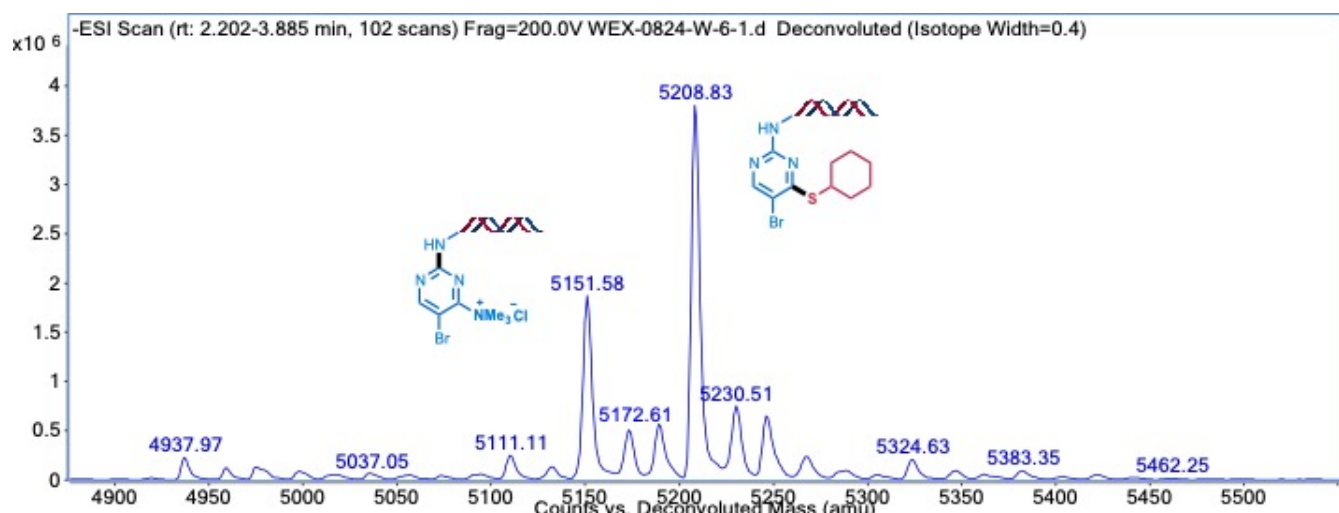
Compound 16p



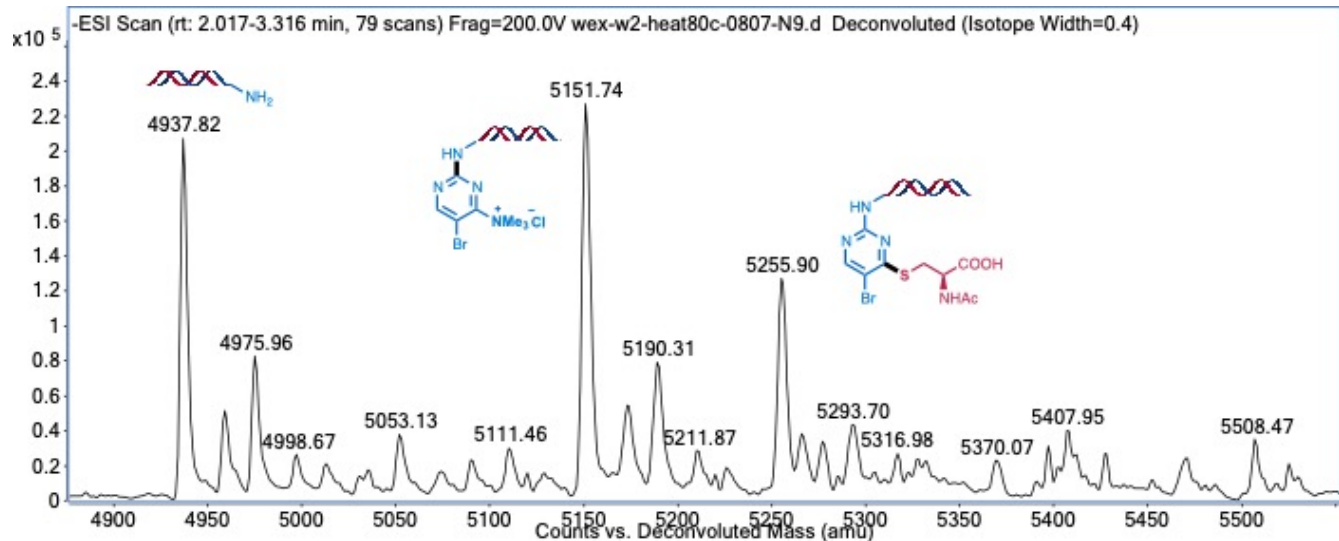
Compound 16q



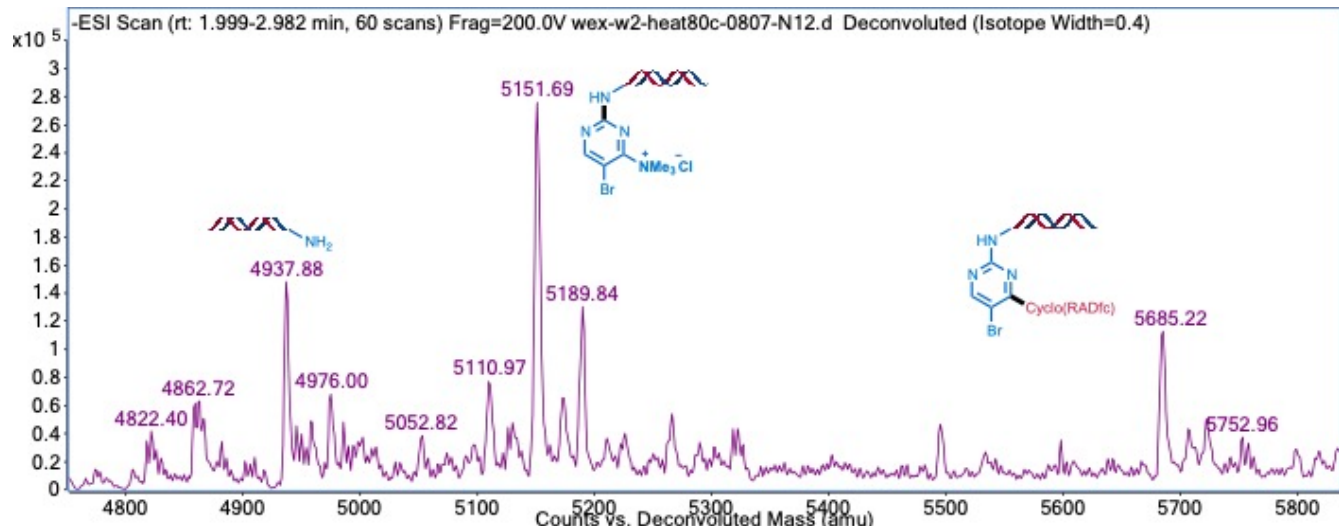
Compound 16r



Compound 16s



Compound 16t



5. Reference

- Wang, D.-Y., Kawahata, M., Yang, Z.-K., Miyamoto, K., Komagawa, S., Yamaguchi, K., Wang, C., and Uchiyama, M. (2016). Stille coupling via C–N bond cleavage. *Nature Communications* 7, 12937.
- Nagao, Y., Miyamoto, S., Miyamoto, M., Takeshige, H., Hayashi, K., Sano, S., Shiro, M., Yamaguchi, K., and Sei, Y. (2006). Highly stereoselective asymmetric pummerer reactions that incorporate intermolecular and intramolecular nonbonded S–O interactions. *J. Am. Chem. Soc.* 128, 9722–9729.
- Irie, T., and Tanida, H. (1980). Neighboring-group participation by hydroxyl oxygen in nucleophilic aromatic substitutions. Smiles rearrangements of (.omega.-hydroxyalkyl)methyl(p-nitrophenyl)sulfonium perchlorates in aqueous alkali. *J. Org. Chem.* 45, 4961–4965.
- Pace, V., Castoldi, L., and Holzer, W. (2012). Highly chemoselective synthesis of aryl allylic sulfoxides through calcium hypobromite oxidation of aryl allylic sulfides. *Tetrahedron Lett.* 53, 967–972.
- Taniguchi, T., Naka, T., Imoto, M., Takeda, M., Nakai, T., Mihara, M., Mizuno, T., Nomoto, A., and Ogawa, A. (2017) Transition-metal-free and oxidant-free cross-coupling of arylhydrazines with disulfides: base-promoted synthesis of unsymmetrical aryl sulfides. *J. Org. Chem.* 82, 6647–6655.
- Tian, H., Zhu, C., Yang, H., and Fu, H. (2014) Iron or boron-catalyzed C–H arylation of substituted phenols at room temperature. *Chem. Commun.* 50, 8875–8877.
- Kondoh, A., Yorimitsu, H., and Oshima, K. (2006). Nucleophilic aromatic substitution reaction of nitroarenes with alkyl- or arylthio groups in dimethyl sulfoxide by means of cesium carbonate. *Tetrahedron* 62, 2357–2360.
- Xu, X.-B., Liu, J., Zhang, J.-J., Wang, Y.-W., and Peng, Y. (2013). Nickel-mediated inter- and intramolecular C–S coupling of thiols and thioacetates with aryl iodides at room temperature. *Org. Lett.* 15, 550–553.
- Kanemura, S., Kondoh, A., Yorimitsu, H., and Oshima, K. (2008). Nickel-catalyzed cross-coupling reactions of alkyl aryl sulfides and alkenyl alkyl sulfides with alkyl Grignard reagents using (Z)-3,3-Dimethyl-1,2-bis(diphenylphosphino)but-1-ene as ligand. *Synthesis* 16, 2659–2664.
- Tobisu, M., Kita, Y., Ano, Y., and Chatani, N. (2008). Rhodium-catalyzed silylation and intramolecular arylation of nitriles via the silicon-assisted cleavage of carbon–cyano bonds. *J. Am. Chem. Soc.* 130, 15982–15989.
- Guo, H., Chen, X., Zhao, C., and He, W. (2015). Suzuki-type cross coupling between aryl halides and silylboranes for the syntheses of aryl silanes. *Chem. Commun.* 51, 17410–17412.
- Hamze, A., Provot, O., Alami, M., and Brion, J. (2006). Platinum oxide catalyzed silylation of aryl halides with triethylsilane: an efficient synthetic route to functionalized aryltriethylsilanes. *Org. Lett.* 8, 931–934.
- McNeill, E., Barder, T. E., and Buchwald, S. L. (2007). Palladium-catalyzed silylation of aryl chlorides with hexamethyldisilane. *Org. Lett.* 9, 3785–3788.
- Chau, N. T. T., Meyer, M., Komagawa, S., Chevallier, F., Fort, Y., Uchiyama, M., Mongin, F., Groos, P. C. (2010). Homoleptic zincate-promoted room-temperature halogen–metal exchange of bromopyridines. *Chem. Eur. J.* 16, 12425–12433.
- Komeyama, K., Asakura, R., and Takaki, K. (2015). A Sn atom-economical approach toward arylstannanes: Ni-catalysed stannylation of aryl halides using Bu₃SnOMe. *Org. Biomol. Chem.* 13, 8713–8716.
- Chen, K., He, P., Zhang, S., and Li, P. (2016). Synthesis of aryl trimethylstannanes from aryl halides: an efficient photochemical method. *Chem. Commun.* 52, 9125–9128.
- Shirakawa, E., Nakao, Y., Murota, Y., and Hiyama, T. (2003). Palladium–iminophosphine-catalyzed homocoupling of alkynylstannanes and other organostannanes using allyl acetate or air as an oxidant. *J. Organomet. Chem.* 670, 132–136.

- Reed, C. D., Launay, G. G., and Carroll, M. A. (2012). Evaluation of tetraethylammonium bicarbonate as a phase-transfer agent in the formation of [18F]fluoroarenes. *J. Fluorine Chem.* 143, 231–237.
- Tang, P., Furuya, T., and Ritter, T. (2010). Silver-catalyzed late-stage fluorination. *J. Am. Chem. Soc.* 132, 12150–12154.
- Fargeas, V. et al. (2003). Nitration of heteroaryltrimethyltins by tetranitromethane and dinitrogen tetroxide: mechanistic aspects, scope and limitations. *Eur. J. Org. Chem.* 1711–1721.
- Jeon, S., Earmme, T., and Jenekhe, S. A. (2014). New sulfone-based electron-transport materials with high triplet energy for highly efficient blue phosphorescent organic light-emitting diodes. *J. Mater. Chem. C*, 2, 10129–10137.
- Komami, N., Matsuoka, K., Yoshino, T., and Matsunaga, S. (2018). Palladium-catalyzed germylation of aryl bromides and aryl triflates using hexamethyldigermane. *Synthesis* 50, 2067–2075.
- Maity, P., Ahammed, S., Manna, R. N., and Ranu, B. C. (2017). Calcium mediated C–F bond substitution in fluoroarenes towards C–chalcogen bond formation. *Org. Chem. Front.* 4, 69–76.
- Sugiura, K., Ushiroda, K., Tanaka, T., Sawada, M., and Sakata, Y. (1990). Porphyrin architectures constructed by CH- π interactions: synthesis and crystal structures of 5,10,15,20-Tetrakis (4-methylchalcogenophenyl) -21H,23H-porphyrins. *Chem. Lett.* 19, 2085–2088.
- Ma, X., Yu, L., Su, C., Yang, Y., Li, H., and Xu, Q. (2017). Efficient generation of C–S bonds via a by-product-promoted selective coupling of alcohols, organic halides, and thiourea. *Org. Chem. Front.* 4, 69–76.
- Lewis, E. S., Yousaf, T. I., and Douglas, T. A. (1987). Methyl transfers. 13. Transfers between aryl selenide anions. An unusual transition-state charge distribution. *J. Am. Chem. Soc.* 109, 2152–2156.
- Dhau, J. S., Singh, A., Singh, A. Dhir, R., Brandao, P., and Felix, V. (2014). Synthesis and characterization of pyrimidyl- and pyrazinylselenium compounds: X-ray structure of 2,5-bis(methylselenenyl)pyrazine. *Inorg. Chim. Acta* 421, 359–363.
- Ding, X., Huang, M., Yi, Z., Du, D., Zhu, X., and Wan, Y. (2017). Room-temperature CuI-catalyzed amination of aryl iodides and aryl bromides. *J. Org. Chem.* 82, 5416–5423.
- Fors, B. P., Davis, N. R., and Buchwald, S. L. (2009). An efficient process for Pd-catalyzed C–N cross-coupling reactions of aryl iodides: insight into controlling factors. *J. Am. Chem. Soc.* 131, 5766–5768.
- Maiti, D., Fors, B. P., Henderson, J. L., Nakamura, Y., and Buchwald, S. L. (2011). Palladium-catalyzed coupling of functionalized primary and secondary amines with aryl and heteroaryl halides: two ligands suffice in most cases. *Chem. Sci.* 2, 57–68.
- Kayama, S., Tani, N., Tabata, H., Oshitari, T., Natsugari, H., and Takahashi, H. (2016). Electronic effects on the amide E/Z-preference of N-benzoyl-carbazole derivatives. *Tetrahedron Lett.* 57, 2395–2398.
- Novak, M., Martin, K. A., and Heinrich, J. L. (1989). S_N2 reactions of a carbon nucleophile with N-Aryl-O-pivaloylhydroxylamines: a model for in vivo reactions of carcinogenic metabolites of aromatic amines. *J. Org. Chem.* 54, 5430–5431.
- McNulty, J. et al. (2007). A pronounced anionic effect in the Pd-catalyzed Buchwald–Hartwig amination reaction revealed in phosphonium salt ionic liquids. *Eur. J. Org. Chem.* 1423–1428.
- Lang, L. et al. (2009). [⁷⁶Br] BMK-I-152, a non-peptide analogue for PET imaging of corticotropin-releasing hormone type 1 receptor (CRHR1). *J. Label Compd. Radiopharm* 52, 394–400.
- Chen, W., Luo, H., Liu, X., Foley, J., and Song, X. (2016). Broadly applicable strategy for the fluorescence based detection and differentiation of glutathione and cysteine/homocysteine: demonstration in vitro and in vivo. *Anal. Chem.* 88, 3638–3646.